NTIA Report TR-07-449

# Propagation Loss Prediction Considerations for Close-In Distances and Low-Antenna Height Applications

**Nicholas DeMinco**


*report series*

U.S. DEPARTMENT OF COMMERCE • National Telecommunications and Information Administration

NTIA Report TR-07-449

# Propagation Loss Prediction Considerations for Close-In Distances and Low-Antenna Height Applications

**Nicholas DeMinco**

**U.S. DEPARTMENT OF COMMERCE**
**Carlos M. Gutierrez, Secretary**

John M. R. Kneuer, Assistant Secretary
for Communications and Information

July 2007

## DISCLAIMER

Certain commercial equipment and materials are identified in this report to specify adequately the technical aspects of the reported results. In no case does such identification imply recommendations or endorsement by the National Telecommunications and Information Administration, nor does it imply that the material or equipment identified is the best available for this purpose.

## CONTENTS

## FIGURES

## TABLES

Page

# PROPAGATION LOSS PREDICTION CONSIDERATIONS FOR CLOSE-IN DISTANCES AND LOW-ANTENNA HEIGHT APPLICATIONS

Nicholas DeMinco[1]

An investigation of different propagation modeling methods to meet the special requirements of a short-range propagation model with low antenna heights was performed, and has resulted in the development of approaches to be taken to accurately model radio-wave propagation loss for these types of scenarios. The basic requirements for the Short-Range Mobile-to-Mobile Propagation Model include: separation distances between the transmitter and receiver from one meter to two kilometers, a frequency range of 150 MHz to 3000 MHz, and antenna heights of one to three meters for both transmitter and receiver sites. It is necessary to develop alternative methods for accurate predictions of propagation loss to provide a propagation model that will simultaneously meet all of these requirements. This will require special considerations that currently available models do not include in their methods of analysis. Several analytical approaches were investigated to develop propagation loss prediction methods that take all of these considerations into account. Analysis efforts have determined that the development of this model will require the use of mutual-coupling predictions and should also include the effects of the surface wave. Conventional far-field antenna patterns and gain of the antennas may also not be valid at close separation distances, since one antenna may not be in the far field of the other antenna. Analysis efforts have also determined that these issues and effects become more significant for the lower frequencies (900 MHz and below). For low antenna heights the effects of the close proximity between the Earth and the antenna produce a strong interaction between the antenna and the ground. The antenna pattern performance is vastly different than if the antenna were in free space.

Key words: antennas; low antenna heights; mobile communications; mutual coupling; propagation modeling; radio-wave propagation

## 1 INTRODUCTION

With the tremendous growth in demand for licensed and unlicensed mobile wireless devices, it is necessary for regulatory agencies to perform electromagnetic compatibility analyses to address the problems of interference between users of the electromagnetic spectrum to accommodate the increasing number and type of these new mobile devices. The evolution of our communications

[1] The author is with the Institute for Telecommunication Sciences, National Telecommunications and Information Administration, U.S. Department of Commerce, Boulder, CO 80305.

infrastructure depends heavily on the use of these licensed and unlicensed mobile communication devices. The growth and prosperity of our economy depends on the successful operation and compatible coexistence of these wireless devices in a crowded electromagnetic spectrum. An accurate and flexible radio-wave propagation model is essential for meeting the needs of both the spectrum management process and the electromagnetic compatibility analysis process.

In an Executive Memorandum from the President dated November 30, 2004, the Department of Commerce was requested to submit a plan to implement recommendations that would ensure that our spectrum management policies are capable of harnessing the potential of rapidly changing technologies. These recommendations included providing a modernized and improved spectrum management system for more efficient and beneficial use of the spectrum. In addition, these recommendations included developing engineering analysis tools to facilitate the deployment of new and expanded services and technologies, while preserving national security and public safety, and encouraging scientific research and development of new technologies. In meeting these recommendations in the area of engineering analyses and technology assessments, it will be necessary to determine the best practices in engineering related to spectrum management, and also address the electromagnetic compatibility analysis process.

In response to this Executive Memorandum, the National Telecommunications and Information Administration/Office of Spectrum Management (NTIA/OSM) tasked the Institute for Telecommunication Sciences (ITS) to determine what radio-wave propagation models currently existed and whether or not they could be used reliably for electromagnetic compatibility analyses and for spectrum management of mobile wireless devices that were very close to each other (distances of one meter to two kilometers) and located at very low antenna heights (one to three meters). ITS reviewed all currently available propagation models in the literature and also those described in the International Telecommunication Union Radiocommunication Sector (ITU-R) Recommendations to determine their applicability. Even though the models that were examined have their own regions of validity with respect to frequency, separation distance, and antenna heights, they were all found to be inadequate for simultaneously meeting the short-range mobile-to-mobile model requirements of: one meter to two kilometer separation distances, one to three meter antenna heights, and a frequency range of 150 MHz to 3000 MHz. Existing radio-wave propagation models are valid only for much higher antenna heights (four meters or greater) and larger separation distances (greater than ten meters). Providing a propagation model that will simultaneously account for close-in distances on the order of one meter, low antenna heights of one to three meters, and frequencies as low as 150 MHz will require special considerations that currently available models do not include in their methods of analysis. It was therefore necessary to initiate an analysis effort to develop alternative models that would be valid in this parameter range. A preliminary analysis effort was initiated for developing alternative radio-wave propagation models that would perform predictions that would be valid for these frequencies, separation distances and low antenna heights typical of the new generation of short-range Mobile-to-Mobile (MTOM) communication devices. The analysis has determined that this requires the use of mutual-coupling predictions and should also include the effects of the surface wave, and the near-field effects of the antennas for these frequencies. The antenna

patterns or gains of the antennas may not be valid at close separation distances, since they may not be in the far-field region of the antennas. Conventional far-field antenna patterns of the antennas may also not be valid at close separation distances, since one antenna may not be in the far field of the other. These issues and effects become more significant for the lower frequencies (900 MHz and below). In addition, the analysis determined that for low antenna heights, the effects of the close proximity of the Earth to the antenna produce a strong interaction of the antenna with ground, changing its impedance and thus affecting the efficiency and gain of the antennas. The antenna impedance is affected when the antenna is within a half-wavelength above the Earth ground. Existing radio-wave propagation models separate the antennas from the propagation loss, and calculate a basic transmission loss that is independent of the antennas. At short separation distances and low antenna heights, it is necessary to develop radio-wave propagation models that include the interaction of the antennas and the radio-wave propagation loss. The effects of the presence of the Earth on the antennas and the propagation loss must also be included.

Investigations of different propagation modeling methods and the special considerations of a short-range propagation model with low antenna heights have resulted in the development of alternative approaches to be taken to accurately model propagation loss in a mobile-to-mobile environment. A hierarchy of approaches were investigated that could be used to develop the short-range MTOM model. These approaches would account for different levels of complexity from very simplistic models where not much information about the scenario was known, to increasingly more sophisticated models that include all of the previously mentioned effects for scenarios where more site-specific information would be available. For example, free-space loss is the least complex and least accurate method, and a mutual-coupling method including all effects is the most complex and most accurate method. A method of intermediate complexity is the complex two-ray theory with complex reflection coefficient and antenna effects included. These methods and others will be discussed in this report. In future efforts, mathematical algorithms for radio-wave propagation models will be developed from the results of this analysis. This report describes the considerations that are involved in developing a model to meet these requirements for the line-of-sight (LOS) scenarios. This initial analysis addressed the LOS propagation environment in an open scenario for vertical polarization. Horizontal polarization will be addressed in future efforts. A future study will cover non-LOS scenarios. Future analysis and measurement efforts to be performed will address LOS and non-LOS scenarios for: the urban/suburban canyon environment, the suburban/residential environment, the parking lot canyon, and the rural environment.

The preliminary analysis effort has determined what technical considerations need to be included in a radio-wave propagation loss prediction model for short-distances and low-antenna heights. Investigations were made of various propagation computation methods and mutual-coupling calculations. This information will be used in future efforts to develop radio-wave propagation models for the short-range MTOM model.

Section 2 describes the fundamental analysis considerations that need to be addressed for short-

range, low-antenna propagation prediction model development. Section 3 describes propagation loss prediction methods that were investigated for use in a short-range, low antenna propagation environment. Section 4 describes the results of this investigation and recommends the approaches to use in the development of a short-range, low-antenna propagation prediction model. Appendix A is a reworked version of a contractor report written by this author, titled "Short-Range Mobile-to-Mobile Propagation Model Study Summary," completed in September 2006. It describes the results of an investigation of what radio-wave propagation loss prediction models currently exist in the literature and ITU-R Recommendations, and discusses why they are inappropriate for simultaneously meeting all of the requirements of the short-range MTOM model.

Appendices B through F contain large numbers of figures that are referred to in various sections of the main body of the report. Due to the large number of figures in each appendix, it would be inappropriate to integrate these into their corresponding sections. Appendix B is referred to in Section 2.3 and contains predicted propagation loss versus distance plots that demonstrate the significance of including the surface wave in propagation loss computations at six combinations of antenna heights and five different frequencies. Appendix C is referred to in Section 2.4 and contains computed antenna elevation patterns for a vertical half-wave dipole at six different frequencies for antenna heights of 1, 2, and 3 meters above average ground demonstrating the effects of the presence of ground. Also shown is the free-space elevation antenna pattern. Appendix D is referred to in Section 3.2 and contains plots of predicted propagation loss versus distance for six combinations of antenna heights and five frequencies that compare the results for the mutual-coupling method with the results of the undisturbed-field method. These plots show that the undisturbed field method achieves very similar results to that of the mutual-coupling method. Appendices E and F are referred to in Section 3.3 and contain plots of predicted propagation loss versus distance for six different frequencies and six combinations of antenna heights that compare four different propagation loss prediction methods: the free-space loss method, two versions of the complex two-ray method, and the undisturbed-field method. Appendix E plots contain the predicted loss out to 30 meters and Appendix F plots contain the predicted loss out to 10 meters with an expanded scale to provide more detail of the short range behavior of the different propagation prediction methods.

# 2 FUNDAMENTAL ANALYSIS CONSIDERATIONS FOR SHORT-RANGE AND LOW-ANTENNA PROPAGATION MODEL DEVELOPMENT

This section describes the analysis considerations used to determine those factors that are important for obtaining an accurate prediction of radio-wave propagation loss in a short-distance environment with low antenna heights that would be valid at frequencies over the 150- to 3000-MHz frequency range. The considerations for the development of the Short-Range MTOM Propagation Model to meet the above requirements at frequencies as low as 150 MHz and make accurate propagation loss predictions will be discussed. Satisfying all three of the above requirements simultaneously for frequencies as low as 150 MHz, increases the complexity needed for the model or group of models to meet the objectives of providing accurate propagation loss predictions. Initially, a literature search was performed where only a small percentage of the references were found to be even partially applicable for the short-range MTOM model, since none of the models and measured data in the currently existing literature references or ITU-R Recommendations can provide an accurate analysis and meet all of these requirements simultaneously. Section A.4 of Appendix A describes the areas where these references and Recommendations can be used for analyses on a limited basis. They can provide propagation loss predictions for only part of the needed frequency band, only the longer distances of the required distance range, and only the higher antenna heights. In addition, they can only be applicable for certain scenarios of the desired environment. Even a combination of these models could not meet all of these requirements of the short-range MTOM model for any significant amount of the frequency band, distances, or antenna heights.

A discussion in Section 2.1 of the determination of reactive near-field region, radiating near-field region, and radiating far-field region distances of an antenna will show how they are based not only on aperture size and frequency, but also on phase error, amplitude error, and the reduction of the higher order terms of near-field reactive region and near-field radiated-field region terms. Computations of far-field region, near-field region and reactive-field region distances for all frequencies based on aperture size will determine what distances are applicable for small antennas.

A discussion of how far out in distance the Earth is flat as a function of frequency in Section 2.2 will show that for distances less than about 5 kilometers, the Earth can be considered flat for radio-wave propagation purposes. The distance to horizon, maximum LOS distance between two antennas, and the first Fresnel zone between two antennas will also be computed as a function of antenna heights in Section 2.2. Six antenna height combinations will be presented for maximum LOS distance between two antennas and the distance to the first Fresnel zone. A discussion of how this first Fresnel zone computation is related to the two-ray breakpoint model, and how it is used to generate a LOS propagation model is described in Section A.3.2 of Appendix A.

The propagation loss computations with and without the surface wave discussed in Section 2.3 will show the significance of the surface wave for six combinations of antenna heights from 150 to 900 MHz over close-in distances.

A description of elevation coverage plots for a dipole antenna as a function of frequency and antenna heights will be presented in Section 2.4 to demonstrate the effects of the Earth on antenna radiation pattern performance. Section 2.5 is a discussion of mutual coupling and how it affects a computation of propagation loss.

## 2.1 Determination of the Far Field, Near Field, and Reactive Field for Typical Antennas

There are three field regions surrounding an antenna: the radiating far-field region also known as the Fraunhofer region, the radiating near-field region also known as the Fresnel region, and the non-radiating reactive near-field region closest to the antenna. The following discussion will describe how to determine these near- and far-field regions for different types of antennas.

In the far-field region of an antenna, the electromagnetic fields exhibit plane wave behavior. The radiating far-field region of an antenna is also characterized as having an angular field distribution that is independent of the radial distance from the antenna. When the transmitter and the receiver are at a separation distance such that the far-field region conditions are satisfied for both of the antennas, then antenna parameters such as gain and radiation patterns can be used to make performance and interference analyses. The radiation pattern of an antenna in the far-field region is independent of distance, r, and hence the angular field distribution of the fields from the antenna will not depend on distance. The electromagnetic fields have a 1/r dependence, and only the transverse components of the electric and magnetic field are present. The ratio of the electric to magnetic field in free space is 377 ohms in the far-field region. Over real ground this ratio can be different from 377 ohms in the far-field region. This ratio can also be different in the near- field region of the antennas. For these reasons it is informative to know where the reactive near- field region, the radiating near-field region, and the far-field region of the antenna occur for different size apertures.

The radiating near-field region of an antenna occurs in a radial distance range that lies between the reactive near-field region and the radiating far-field region of the antenna. Fields exhibit non-plane wave behavior in this region, and their angular field distribution is dependent on the radial distance from the antenna. Even closer to the antenna, the amplitude of the electromagnetic fields in the reactive near-field region dominates over the amplitude of the electromagnetic fields in the radiating near-field region. For an antenna whose maximum dimension is small compared to a wavelength $\lambda$ at the operating frequency, the radiating near-field region may not exist. For most antennas with a maximum aperture dimension of D and where $D>>\lambda$, the radiating near-field region begins at an approximate distance of $r = 0.62 (D^3/\lambda)^{0.5}$, and extends out to the beginning of the far-field region of the antenna [1]. The reactive near-field region starts at the antenna surface and extends out to this distance r. The $D>>\lambda$

condition is not fulfilled for the half-wave dipole and the quarter-wave monopole antennas, so this approximation cannot be used to determine the boundary where the reactive near field begins and the radiated near field ends for such antennas. For a small dipole or monopole antenna, the distance defining where the reactive near-field region ends and the radiating near-field region begins will be $r = \lambda/2\pi$ or $(0.159\lambda)$. This distance of $r = \lambda/2\pi$ is also where the maximum powers in the near-field radiating and near-field reactive regions are equal [1].

The beginning of the far-field region, where the fields exhibit plane-wave behavior, depends on the aperture size with respect to a wavelength. There are three conditions that must be satisfied for distance r to be in the far-field region of an antenna [1]. These conditions are stated as inequalities below.

$$r > \frac{2D^2}{\lambda}$$
$$r >> D \qquad (1)$$
$$r >> \lambda$$

where D is the maximum dimension of the aperture. All three of these conditions must be satisfied simultaneously for an observation point to be in the far-field region of an antenna. These conditions are based on certain criteria for phase and amplitude errors in addition to reduction of $1/r^2$ and $1/r^3$ terms in the near-field region electric and magnetic fields.

The first inequality, $r > 2D^2/\lambda$ is based on achieving a maximum phase difference, from one end of the aperture to the center of the aperture, that is less than a specified amount (the parallel ray approximation), so that the antenna can be considered to be in the far-field region. This depends on the specific antenna type and antenna size in wavelengths, but for most antennas whose maximum dimension is large compared to a wavelength, the maximum phase difference of $\lambda/16$ is used [2]. The maximum phase difference of $\lambda/16$ corresponds to $r=2D^2/\lambda$. Some antennas require a smaller phase difference to get better null performance and sidelobe detail, and therefore the separation distance must be larger [2].

Most of the antennas for mobile-to-mobile communications can be modeled as a monopole or dipole antenna or combination of these antennas. The analysis that follows can be expanded to apply to other antennas. A monopole or dipole antenna can be modeled using a line source in the form of a short current element. Consider a short current element of length z' along the z-axis. The symmetry of this current element about the z-axis allows the simplification of confining the field observation points to the yz plane. The distance R in Figure 1 is then given by:

$$R = \sqrt{y^2 + (z - z')^2} \qquad (2)$$

The field coordinates can be put in terms of a spherical coordinate system using the coordinate transformations.

$$\begin{aligned} r^2 &= y^2 + z^2 \\ z &= r\cos\theta \\ y &= r\sin\theta \end{aligned} \tag{3}$$

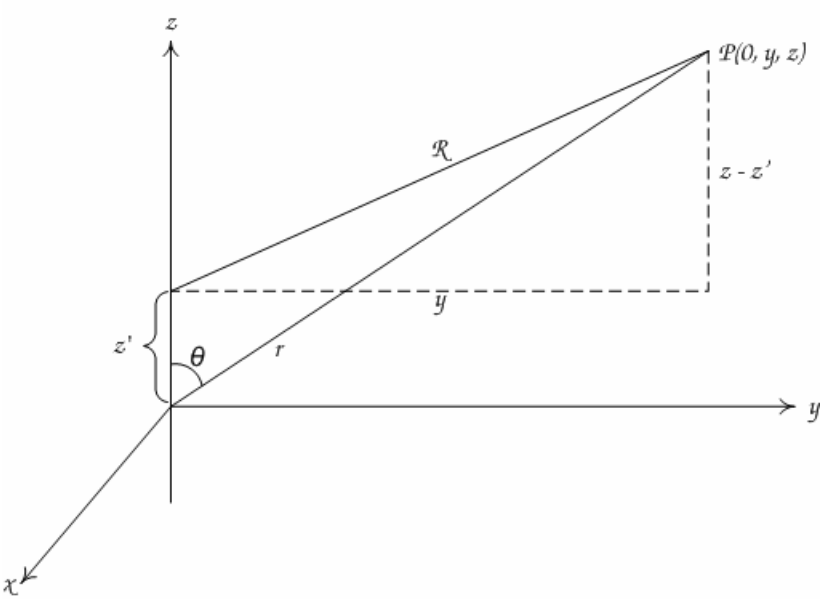

Figure 1. Coordinate system geometry for field calculations.

Using these coordinate transformations the distance R in spherical coordinates is then:

$$R = \sqrt{r^2 - 2\,r\,z'\cos\theta + (z')^2} \tag{4}$$

Expanding this equation using the binomial expansion theorem, the equation for distance R from any point along the length of an antenna aperture to the observation point in terms of the distance r from the center of the antenna aperture is given as [2]:

$$R = r - z'\cos\theta + \frac{(z')^2\sin^2\theta}{2r} + \frac{(z')^3\sin^2\theta\cos\theta}{2\,r^2} + \bullet\bullet\bullet \tag{5}$$

Where z' is the distance along the antenna aperture from the origin, and θ is the angle measured from the z axis (Figure 1). If only the first two terms are used to represent the distance to the far-field region observation point, then the error is represented by the third and fourth terms. The third term is the most significant and attains its maximum value at θ = π/2. The fourth term vanishes at θ = π/2 in addition to the fifth and higher order terms [2]. The reactive near-field

region extends out to distance r, where the fourth term of the equation for radiated field achieves its maximum value of $\pi/8$ [2]. Therefore, the third term represents the maximum total phase error of neglecting the third term in the far-field region approximation. A maximum total phase error of $\pi/8$ radians ($\lambda/16$) is usually acceptable for most antennas with maximum aperture dimensions greater than a wavelength [2]. This $\pi/8$ phase error is also acceptable for small antennas such as very short dipoles and monopoles. For $z' \leq D/2$, and setting $2\pi/\lambda$ times the third term of the above equation equal to $\pi/8$, then $r \geq 2D^2/\lambda$. If the maximum tolerable phase error had been specified as $\pi/16$ ($\lambda/32$), then $r \geq 4D^2/\lambda$.

The second inequality, r>>D, determines the amplitude error associated with assuming the magnitude of R is similar to that of r, where R is the distance from any point along the length of the dipole antenna aperture to the point of observation, and r is the distance from the center of the aperture to the point of observation (Figure 1). The distance R can be described in rectangular coordinates in terms of r from the geometry of Figure 1 as [2]:

$$\begin{aligned} R &= \sqrt{r^2 - 2\,r\,z'\cos\theta + (z')^2} \\ R &= \sqrt{r^2 + (z')^2} \qquad for \quad \theta = \pi/2 \end{aligned} \tag{6}$$

The maximum amplitude error between R and r occurs at $\theta = \pi/2$. If $z' = D/2$, and $r = 5D$, then $R = 5.0249D$. The relative amplitude ratio, r/R is then equal to 0.991, and the relative amplitude error is $(R-r)/r = 0.005$ or one-half percent.

The third inequality $r >> \lambda$ is a requirement to reduce the magnitude of the higher order terms ($1/r^2$ and $1/r^3$) of the electric and magnetic fields of the radiation field of the antenna, so that only the 1/r far-field terms are significant. The $1/r^2$ and $1/r^3$ terms are near-field radiating and reactive field terms, respectively, that decay rapidly with increasing distance from the antenna. This requirement originates from the equations for the electric or magnetic fields of the antenna and satisfies the inequality $\beta r >> 1$, where $\beta = 2\pi/\lambda$ [2]. The equation for the total electric and magnetic fields of a short vertical dipole antenna is [2]:

$$\begin{aligned} E_\theta &= \frac{I\,\Delta z}{4\pi}\, j\omega\mu \left( 1 + \frac{1}{j\beta r} - \frac{1}{(\beta r)^2} \right) \frac{e^{-j\beta r}}{r} \sin\theta \\ E_r &= \frac{I\,\Delta z}{2\pi}\, \eta \left( \frac{1}{r} - \frac{j}{\beta r^2} \right) \frac{e^{-j\beta r}}{r} \cos\theta \\ H_\phi &= \frac{I\,\Delta z}{4\pi}\, j\beta \left( 1 + \frac{1}{j\beta r} \right) \frac{e^{-j\beta r}}{r} \sin\theta \\ \eta &= \sqrt{\frac{\mu}{\varepsilon}} \end{aligned} \tag{7}$$

where $\omega = 2\pi f$, $\mu$ is the permeability of the medium, $\varepsilon$ is the dielectric constant of the medium, and $\eta$ is the intrinsic impedance of the medium = 377 ohms in free space. If $\beta r = 10$, then the $1/r^2$ term is ten percent of the 1/r term, and the $1/r^3$ term is one percent of the 1/r term. The distance requirement to be in the far-field region is then $r > 1.6\lambda$.

$$\beta r = \frac{2\pi}{\lambda} r > 10$$
$$r > 1.6\ \lambda \tag{8}$$

If $\beta r = 20$, then the $1/r^2$ term is five percent of the 1/r term, and the $1/r^3$ term is one-half percent of the 1/r term. The distance requirement to be in the far-field region is then $r > 3.2\lambda$.

A method of plotting these three inequalities $r > 2D^2/\lambda$, $r >> D$ with $r > 5D$, and $r >> \lambda$ with $r > 1.6\lambda$ has been described in [1,3] to determine the distance to the far-field region of any antenna that will satisfy all three equations simultaneously. The results show the distance to the far-field region of an antenna normalized to wavelengths, $r/\lambda$ plotted in terms of aperture electrical size, $D/\lambda$. One author [3] plotted these equations as suggested in [1], and showed the regions of validity in terms of antenna aperture size, $D/\lambda$. Figure 2 shows a plot for the following inequalities plotted as three curves from the equations for all values of the range of $D/\lambda$ where the greater than sign has been replaced by an equals sign. The normalized distance to the far-field region is dominated by the first curve (black) up to a normalized aperture of 0.32. The second curve (red) shows that the normalized distance to the far-field region dominates for normalized apertures between 0.32 and 2.5. The third curve (blue) shows that the normalized distance to the far-field region dominates for all larger normalized apertures greater than 2.5. Amplitude considerations dominate for small apertures, while phase considerations dominate for large apertures.

$$\begin{aligned} r &> \frac{2D^2}{\lambda} && \text{for} && D > 2.50\ \lambda \\ r &> 5D && \text{for} && 0.32\ \lambda \le D \le 2.50\ \lambda \\ r &> 1.6\ \lambda && \text{for} && D < 0.32\ \lambda \end{aligned} \tag{9}$$

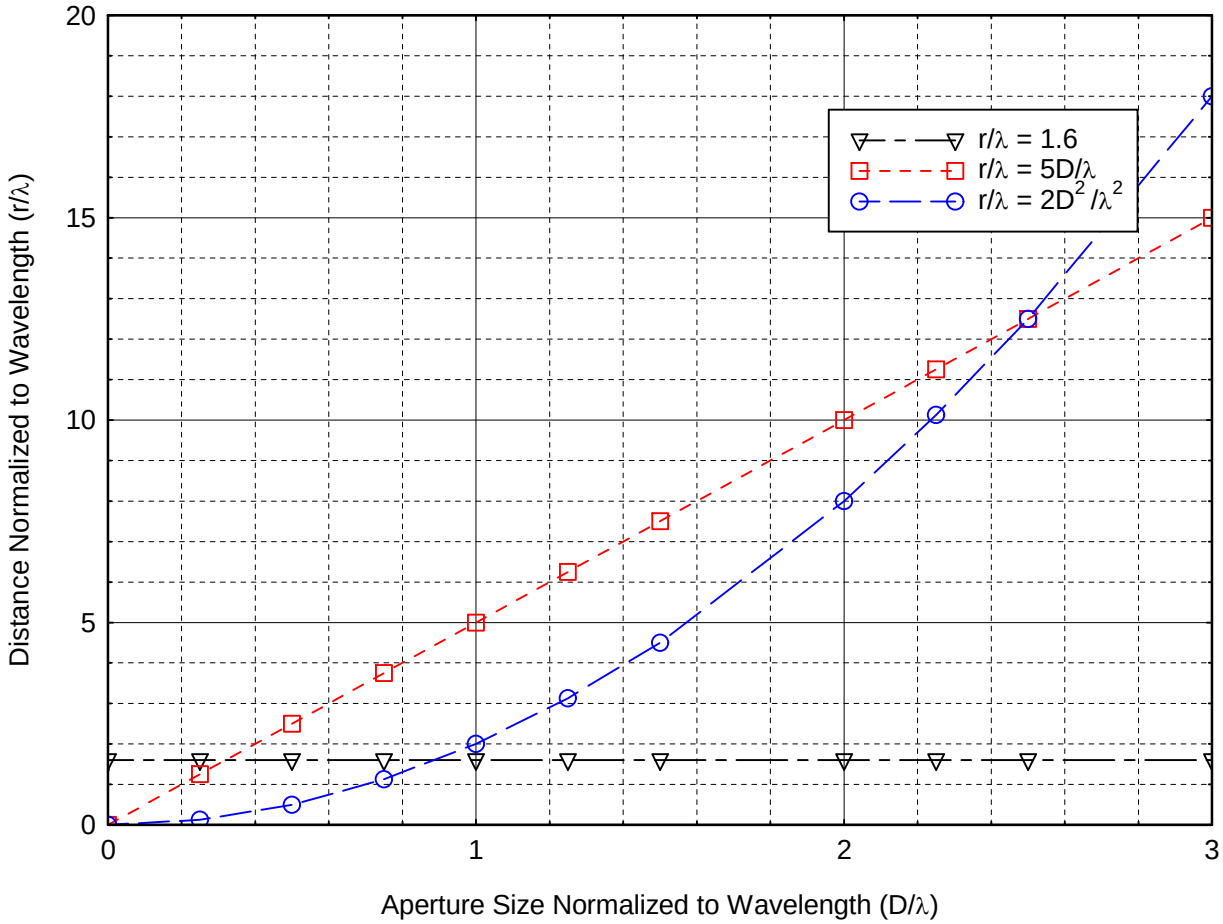


Figure 2. Plotting the three original inequalities to determine far-field distance in wavelengths versus antenna aperture size normalized to wavelengths.

The criteria for the three conditions can be adjusted to suit the application and achieve the desired reduction in relative magnitudes of the higher-order field components and the desired phase and amplitude errors. The regions of validity based on aperture size could change with how one selects the right-hand side of these three inequalities, but if the right-hand sides of these inequalities are each multiplied by the same numerical factor to obtain greater or lesser accuracy, then the regions along the boundaries for the horizontal axis of validity based on aperture size will stay the same. The regions of validity are determined by the intersections of the three equations in this plot, and the areas or regions on the graph that satisfy all three inequalities simultaneously. The distance r must be greater than that specified by all three of the inequalities.

If the right-hand sides of each of these inequalities are each multiplied by a different factor, then the boundaries will change for the regions of validity in terms of aperture size. An example will illustrate this. When the inequalities are multiplied by the different factors, for example: $r>2D^2/\lambda$, $r>3D$, and $r>2\lambda$, these inequalities can be plotted as far-field distance normalized to wavelength along the y-axis, $r/\lambda$, versus aperture size normalized to wavelength along the x-axis,

D/λ, to determine the far-field regions of validity as a function of antenna aperture size as shown in Figure 3. All three inequalities must be satisfied simultaneously for an observation point to be in the far-field region of an antenna, whose maximum aperture size is D. The regions of validity for each inequality are then obtained from the resulting plots of Figure 3 as:

$$\begin{aligned} r &> \frac{2D^2}{\lambda} \quad \text{for} \quad D > 1.50\ \lambda \\ r &> 3D \quad \text{for} \quad 0.67\ \lambda \le D \le 1.50\ \lambda \\ r &> 2.0\ \lambda \quad \text{for} \quad D < 0.67\ \lambda \end{aligned} \tag{10}$$

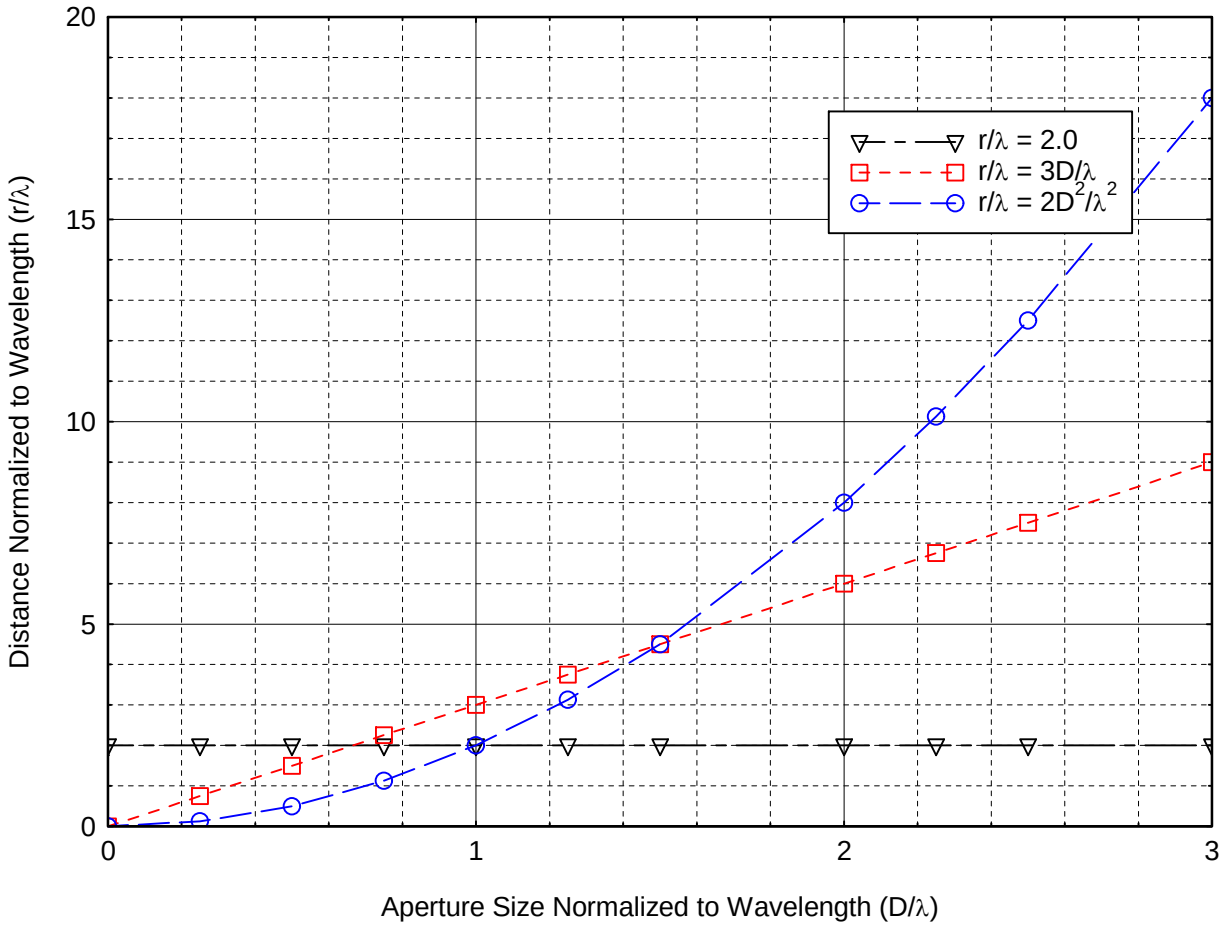


Figure 3. Plotting the three alternate inequalities to determine far-field distance in wavelengths versus antenna aperture size normalized to wavelengths.

The maximum tolerable error for the first expression $r>2D^2/\lambda$ is $\pi/8$ or $\lambda/16$ as before. The maximum relative amplitude error for the second expression r>3D with r=3D and z′=D/2, is (R-r)/r = 0.0136 or about 1.36 percent. For this case R= 3.041D and the relative amplitude r/R = 0.986. The third expression $r>2.0\lambda$ corresponds to $\beta r = 2\pi$, and the $1/r^2$ term is approximately 7.9 percent of the first term. The $1/r^3$ term is approximately 0.63 percent of the first term. The

inequalities can also be solved algebraically to determine the intersection points that divide the regions of validity, and then evaluate the inequalities on either side of the intersection points to determine which inequalities set the distance to the far-field region. Plotting the inequalities as described above is the easier method and more illustrative in determining the regions of validity than solving the equations algebraically. The original criteria described in the original equations above with $r>2D^2/\lambda$, $r>5D$, and $r>1.6\lambda$, will be used for this analysis. This is shown in Figure 2.

For all quarter-wave antennas, since $D<0.32\lambda$, then $r>1.6\lambda$ is the determining inequality in all cases, since it is greater than the other two inequalities, and one graph can be plotted showing the far-field distance versus frequency (Figure 4). The far field for half-wave dipole antennas is determined by the expression $r>5D$, since $0.32\lambda \leq D \leq 2.50\ \lambda$. This is also plotted in Figure 4. Within distances that are in the reactive near-field region and the radiating near-field region, mutual-coupling calculations need to be performed for prediction of propagation loss at these short distances. For small antennas where $D<<\lambda$, the radiating near field region may not exist. For $\lambda/4$ monopoles and $\lambda/2$ dipoles a marginal situation exists, and therefore it is necessary to calculate the boundary between the distance to the reactive near-field and radiating near-field regions as $r=\lambda/2\pi$.

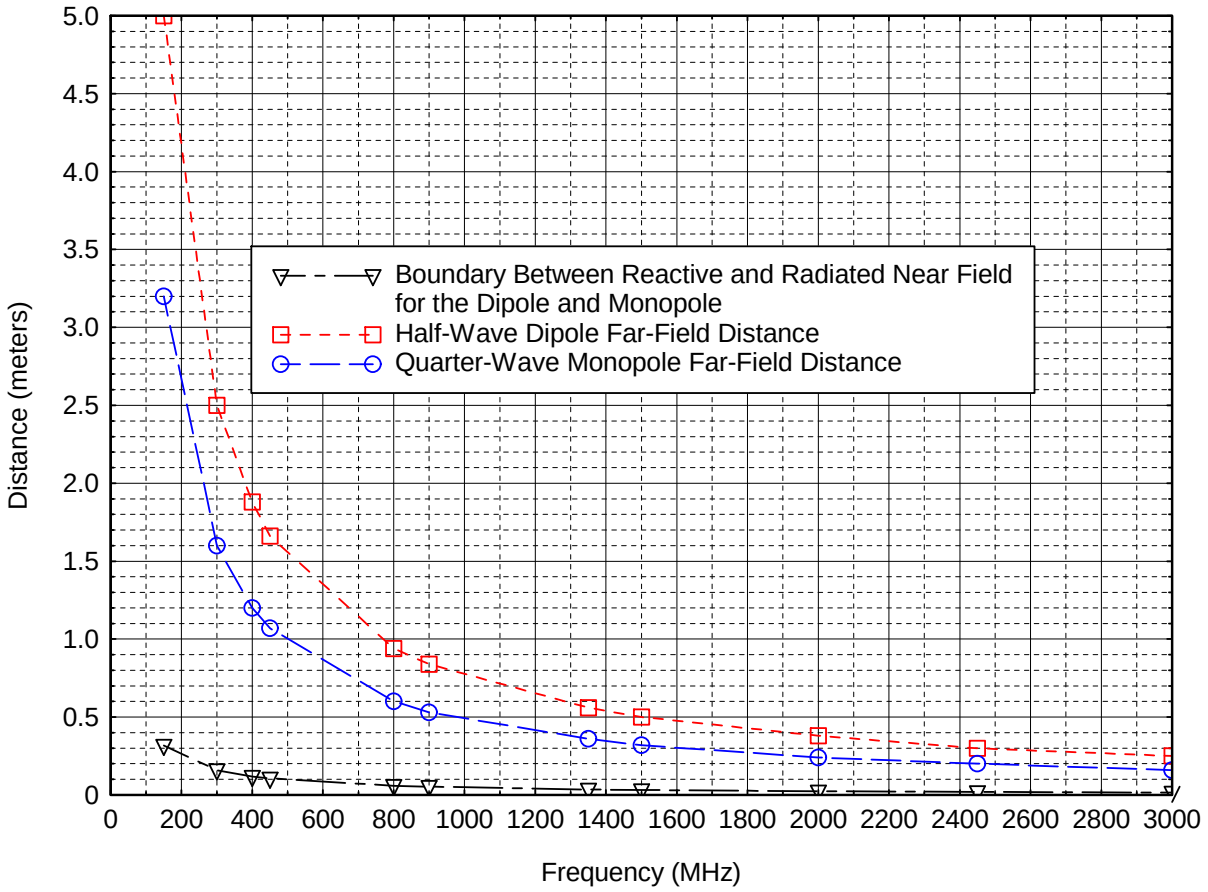


Figure 4. Far-field and near-field boundaries for a half-wave dipole and quarter-wave monopole.

## 2.2 The Flat-Earth Assumption, Distance to Horizon, Maximum Line-of-Sight Distance, and the First Fresnel Zone

The Earth can be considered flat out to a distance d in kilometers given by [4]:

$$d(km) = \frac{80}{[\ f\ (MHz)\ ]^{1/3}} \tag{11}$$

Figure 5 is a plot of this distance versus frequency. It can be seen that the Earth is flat out to over 5 kilometers over the entire frequency range from 150 MHz to 3000 MHz. The flat-Earth assumption for the short-range MTOM propagation model is valid over the entire frequency range, since our maximum distance requirement is 2 kilometers.

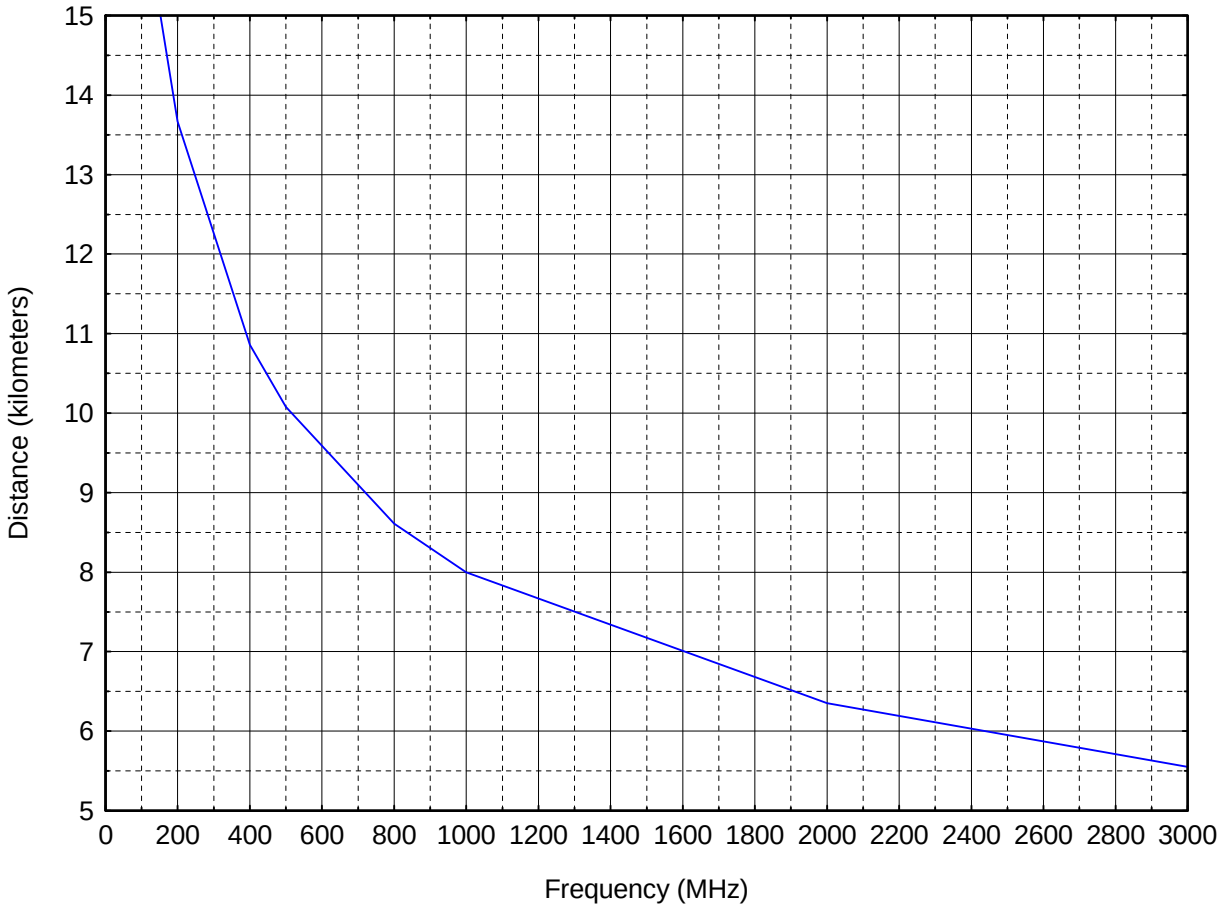


Figure 5. Distance at which the earth can be considered flat versus frequency.

The distance to the horizon over a spherical Earth without terrain is a function of the heights of the transmitter and receiver antennas and the effective Earth's radius, $a_e$= ka, where a is the Earth's radius in meters and k is the effective Earth's radius factor. The distance d in kilometers to the horizon for an antenna height h in meters is given by [5]:

$$d = \sqrt{2kah} \tag{12}$$

It follows that the maximum line-of-sight distance in kilometers between two antennas at heights $h_1$ and $h_2$ in meters is:

$$d = \sqrt{2kah_1} + \sqrt{2kah_2} \tag{13}$$

The maximum line-of-sight distance in kilometers between two antennas at heights $h_1$ and $h_2$ in meters for k= 4/3 is given by:

$$d\,(km) = 4.1215\left(\sqrt{h_1(m)} + \sqrt{h_2(m)}\right) \tag{14}$$

The shortest line-of-sight distance between two antennas occurs when k=2/3. The shortest maximum line-of-sight distance in kilometers between two antennas at heights $h_1$ and $h_2$ in meters for k= 2/3 is given by:

$$d\,(km) = 2.9143\left(\sqrt{h_1(m)} + \sqrt{h_2(m)}\right) \tag{15}$$

Table 1 lists the maximum line-of-sight distances between two antennas for both values of k for the antenna heights of both antennas in the range of 1 to 3 meters. The smallest of these distances is about 6 kilometers, so the line-of-sight condition exists for all antenna heights in this range and within the 2-kilometer range requirements for the model, and the Earth can still be considered flat. This table holds for spherical Earth without terrain. Terrain and building obstructions on the path will reduce the distances and must be treated on a case by case basis using terrain information and other mathematical equations.

Table 1. Maximum Line-of-Sight Distance Between Two Antennas on a Spherical Earth Versus Antenna Heights for Two Values of Effective Earth's Radius

| $h_1$ (meters) | $h_2$ (meters) | d(km) for k= 4/3 | d(km) for k=2/3 |
|---|---|---|---|
| 1 | 1 | 8.24 | 5.83 |
| 2 | 1 | 9.95 | 7.06 |
| 3 | 1 | 11.26 | 7.96 |
| 2 | 2 | 11.66 | 8.24 |
| 3 | 2 | 12.97 | 9.17 |
| 3 | 3 | 14.28 | 10.10 |

The first Fresnel zone over flat Earth in the region of two antennas can be defined as an ellipsoid with the transmit antenna located at one of the foci, and the receive antenna located at the other foci. The first Fresnel zone is where the path length from one antenna to a point on the ellipsoid and then on to the other antenna is $\lambda/2$ longer than the direct path between the antennas. For propagation analysis, a breakpoint can be defined as the distance at which the ground or other object begins to obstruct the first Fresnel zone. At distances less than that distance which has first Fresnel zone clearance, the propagation loss is due to the spherical spreading loss of the

wavefront (free-space propagation) and the vector addition and subtraction of the direct and reflected wave. At distances greater than that distance which has first Fresnel zone clearance, the propagation loss becomes greater. The distance in meters $d_f$ at which the first Fresnel zone becomes obstructed as a function of antenna heights $h_1$ and $h_2$, and wavelength $\lambda$ in meters, is given by [6]:

$$d_f\ (m) = 1/\lambda \sqrt{16\, h_1^2\, h_2^2 - 4\,(h_1^2 + h_2^2)(\lambda/2)^2 + (\lambda/2)^4} \qquad (16)$$

Table 2 lists the distance $d_f$ as a function of the antenna heights and wavelength.

Table 2. Distance $d_f$ in Meters of the First Fresnel Zone Clearance as a Function of Antenna Heights and Frequency/Wavelength

| $h_1$ (m) | $h_2$ (m) | $d_f$ (m) f=150 MHz $\lambda$ = 2m | $d_f$ (m) f=300 MHz $\lambda$ = 1m | $d_f$ (m) f=450 MHz $\lambda$= .667m | $d_f$ (m) f=900 MHz $\lambda$= .333m | $d_f$ (m) f=1500 MHz $\lambda$= .200m | $d_f$ (m) f=1800 MHz $\lambda$= .167m | $d_f$ (m) f=3000 MHz $\lambda$= .100m |
|---|---|---|---|---|---|---|---|---|
| 1 | 1 | 1.5 | 3.75 | 5.83 | 11.93 | 19.95 | 23.95 | 39.98 |
| 2 | 1 | 3.35 | 7.69 | 11.78 | 23.92 | 39.94 | 47.94 | 79.97 |
| 3 | 1 | 5.12 | 11.58 | 17.71 | 35.90 | 59.92 | 71.92 | 119.96 |
| 2 | 2 | 7.50 | 15.75 | 23.82 | 47.96 | 79.95 | 95.94 | 159.98 |
| 3 | 2 | 11.46 | 23.73 | 35.80 | 71.98 | 119.95 | 143.93 | 239.97 |
| 3 | 3 | 17.50 | 35.75 | 53.81 | 108.02 | 179.95 | 215.92 | 359.98 |

The distance at which the first Fresnel zone becomes obstructed represents a breakpoint for the curve that describes LOS propagation loss. It is related and similar to the breakpoint for the two-ray theory. The two-slope/breakpoint method can be matched with the two-ray LOS model, and the distance to the first Fresnel zone is the location of the breakpoint. The shape of the envelope of the two-ray theory matches that of the two-slope/breakpoint model. The distance of the breakpoint from the transmitter is equal to the maximum distance that has first Fresnel zone clearance. At distances less than the breakpoint for the two-ray theory, the signal strength or propagation loss oscillates due to the constructive and destructive interference between the direct and reflected waves. At distances greater than the breakpoint, the signal decreases or the loss increases at a much faster rate than before the breakpoint. This information can be used to construct a double regression model that can represent the propagation loss for a line-of-sight scenario. A discussion of how this double regression model can be used to fit measured data can be found in Appendix A.

## 2.3 The Significance of the Surface Wave for Loss Computations

Since the short-range MTOM model must include very short distances and very low antenna heights, propagation is predominantly via the ground wave. The ground-wave signal includes the direct line-of-sight space wave, the ground-reflected wave, and the Norton surface wave that diffracts around the curved Earth or propagates along the surface of a flat Earth. The Earth can be considered flat for all practical purposes in the Short-Range MTOM model. The Norton surface wave will be referred to as simply the surface wave in this report. Propagation of the ground wave depends on the relative geometry of the transmitter and the receiver location and the antenna heights. The radio wave propagates primarily as a surface wave when both the transmitter and the receiver are near the Earth in terms of wavelength, because the direct and ground-reflected waves in the space wave will cancel each other and the surface wave will then be significant. The surface wave is predominantly vertically polarized, since the ground conductivity effectively shorts out most of the horizontal electric field component. What is left of the horizontal field component of the surface wave is attenuated at a rate many times the vertical component of the electric field of the surface wave. When one or both of the antennas are elevated above the ground to a significant height with respect to a wavelength, the space wave predominates. The surface wave propagates along and is guided by the Earth's surface. This is similar to the way that an electromagnetic wave is guided along a transmission line. Charges are induced in the Earth by the surface wave. These charges travel with the surface wave and create a current in the Earth. The Earth carrying this current can be represented by a lossy capacitor (a resistance shunted by a capacitive reactance). The characteristics of the Earth as a conductor can therefore be represented by this equivalent parallel RC circuit, where the Earth's conductivity can be simulated with a resistor and the Earth's dielectric constant by a capacitor. As the surface wave passes over the surface of the Earth, it is attenuated as a result of the energy absorbed by the Earth due to the power loss resulting from the current flowing through the Earth's resistance. Energy is taken from the surface wave to supply losses in the ground, and the attenuation of this wave is directly affected by the ground constants of the Earth along which it travels [7].

Figures B-1 through B-30 of Appendix B show a comparison of the computed propagation loss with and without the inclusion of the surface wave over short distances for six different combinations of transmitter and receiver antenna heights, $h_1$ and $h_2$, at frequencies up to 900 MHz. These plots were obtained using the undisturbed-field method and can also be computed using the algebraic expressions for the total electromagnetic field and converting to transmission loss using an equation described later in this report that determines propagation loss as a function of electric-field strength and frequency. Since the losses in Figures B-1 through B-30 represent the ratio of received power to transmitted power, this is a numeric ration less than one, and as a result the loss values in dB are negative. The mutual-coupling method also uses this convention with a received-power to transmitted-power ratio, so the losses are also in negative dB. The undisturbed-field method includes a surface wave and hence makes accurate predictions of propagation loss for the short distances and antennas located close to the ground. The surface

wave is still present but small at frequencies up to 450 MHz. Above 450 MHz the difference between the curves with and without the surface wave is less than or equal to 1 dB. At 900 MHz the effects of the surface wave are negligible. The surface wave at these higher frequencies in the VHF band actually subtracts from the direct and reflected waves, because it is out of phase with these two waves over most of the path. The net result is a slight increase in propagation loss. A plot at 30 MHz is also shown for comparison where the surface wave is in phase with the direct and reflected waves and they add together, and as a result the addition will reduce the propagation loss. These plots were obtained using the undisturbed-field method, and can be computed from the total electromagnetic field using equations to determine transmission loss. This equation that determines propagation loss as a function of electric field strength and frequency is described later in this report. Notice that the surface wave is more significant for the low antenna heights of one meter for all frequencies, because the surface wave increases with decreasing antenna height. Although the surface wave is generally considered negligible at frequencies at and above 150 MHz for most applications, the surface wave can have a significant effect at these higher frequencies, because of the very short distance requirements that can be as small as one meter for the short-range MTOM model. In addition, the surface wave is also stronger when one or both of the antennas are close to the ground. Therefore, the surface wave should be included for propagation predictions at frequencies at and below 450 MHz. Both the undisturbed-field and mutual-coupling methods to be discussed later in this report include the surface wave in their loss computations.

### 2.4 The Effects of the Earth on Antenna Patterns at Low Heights Above Earth

For low antenna heights, the effects of the close proximity of the Earth to the antenna produce a strong interaction of the antenna patterns with the ground. The antenna pattern performance is vastly different than if the antenna were in free space. If the antenna is within a half wavelength of the ground, the antenna input impedance is also affected, which will affect efficiency and gain. The main beam is generally tilted up in elevation from the horizontal position that it would have had in free space. This causes the antenna to have less low elevation angle coverage. Figures C-1 through C-6 of Appendix C show the elevation antenna patterns for a vertical half-wave dipole at six frequencies for antenna heights of 1, 2, and 3 meters over average ground. Also shown in each figure is the free-space antenna pattern. The antenna patterns over ground are quite different from the free-space antenna patterns and have an increased lobing effect as the frequency increases and the antenna height increases**.**

### 2.5 Mutual Coupling

Two antennas will always have a mutual coupling present between them, which becomes quite strong when the antenna separation distances are small. In addition, when the antennas are in close proximity to Earth or a large ground plane, there will also be a strong interaction with the antenna images created by the Earth or ground plane. This can have a major influence on the antenna gain, impedance, and radiation patterns. The fields from one antenna will induce

currents in the other antenna, which will in turn cause radiation from the other antenna and induce currents in the original antenna. A mutual coupling will exist between the two antennas and the images formed by the presence of a ground plane or the Earth. In many cases involving close antenna separations, the mutual coupling between the antennas must be considered when computing propagation loss between the antennas. However, there are scenarios where this effect can be neglected, which will be discussed in the next sections.

# 3 METHODS OF COMPUTING PROPAGATION LOSS FOR SHORT DISTANCES AND LOW-ANTENNA HEIGHTS

Several methods were compared in an effort to determine how accurately they can predict propagation loss for low antenna heights and short distances. These methods under consideration included the mutual-coupling method, the undisturbed-field method, and the complex two-ray method. The mutual-coupling method was the most accurate method for prediction of propagation loss. Therefore, the loss prediction method that performs mutual-coupling computations between closely spaced antennas over real ground was used for the initial analysis as a reference and compared to other methods. It was necessary to investigate other methods that could accurately predict propagation loss and compare their results to the mutual-coupling method to see where the simpler methods could replace the mutual-coupling method, because the mutual-coupling method is difficult to implement for a large number of computations of different antenna heights, separation distances, and frequencies. One alternative method for computing propagation loss was the undisturbed-field method, which was much easier to implement than the mutual-coupling method, and could still maintain a high degree of accuracy for propagation loss prediction. The complex two-ray method was compared to both the mutual-coupling and undisturbed-field methods to determine under what conditions it could be used, but it was found to not be accurate for close-in distances and low-antenna heights.

A discussion in Section 3.1 of the simple two-ray method and the complex two-ray method will show why these formulas are informative, but inadequate to determine electric fields and propagation loss at close-in distances, but the complex two-ray method can be used at longer distances.

Section 3.2 is a discussion of computation methods that will take into account the necessary factors that need to be considered for close-in antenna separations and low-antenna heights. The results of mutual-coupling method computations between two antennas will show where propagation loss can be determined accurately by using this method. These mutual-coupling computations will be compared in Section 3.2 to an alternative computation method that uses the undisturbed electric field and a propagation formula to determine the propagation loss versus distance and frequency. It will be shown that the undisturbed-field method can compute propagation loss with accuracy close to that of the mutual-coupling method by comparison of computations over a wide variety of antenna heights, separation distances, and frequencies.

Section 3.3 will compare the undisturbed-field method to the complex two-ray method and the free-space loss method to determine under what conditions of antenna heights, separation distances and frequencies that the simpler methods can be used. Section 3.3 will also discuss the problem with using the free-space term in the power-law propagation formula at distances that are too close for the lower frequencies.

### 3.1 Conventional Two-Ray Methods that Only Predict Propagation Loss Approximately

A simple two-ray method for predicting radio-wave propagation loss where antenna patterns are not taken into account and the reflection coefficient is set equal to -1.0 does not represent real-world conditions. This method will predict an unrealistic propagation loss versus frequency with very deep nulls and significant lobing structure. The simple two-ray method does not include the effects of antenna patterns. A better two-ray method is one that incorporates the far-field radiation patterns of the antennas and uses the actual reflection coefficient as a function of frequency, incidence angle and ground constants, even though the gains are not valid in the near-field region of the antenna for close-in distance separations. This will be referred to here as the complex two-ray method. Figure 6 compares the simple two-ray method with the complex two-ray method for a frequency of 900 MHz with $h_1$ equal to three meters and $h_2$ equal to one meter with a half-wavelength dipole at the transmitter and receiver antenna locations. The relative dielectric constant of average ground is 15.0 and the conductivity is 0.005 Siemens/meter. Since the losses for both of the two-ray methods are presented as the ratio of received power to transmitted power, the losses are a numeric ratio less than one, and as a result the losses in dB are negative. Notice how much these curves differ, and how the simple two-ray method exaggerates the nulls. Even though the complex two-ray method can make a better prediction of propagation loss than the simple two-ray model, it still does not take into account the significant effects for the short ranges and low antenna heights. More sophisticated methods that do factor in all of the significant effects that are present are discussed in Section 3.2. Comparisons between the complex two-ray method and the more sophisticated methods (based on mutual-coupling and undisturbed-field methods) will show where the complex two-ray method is not adequate at short distances, but can be used as a simpler method at longer distances for LOS scenarios.

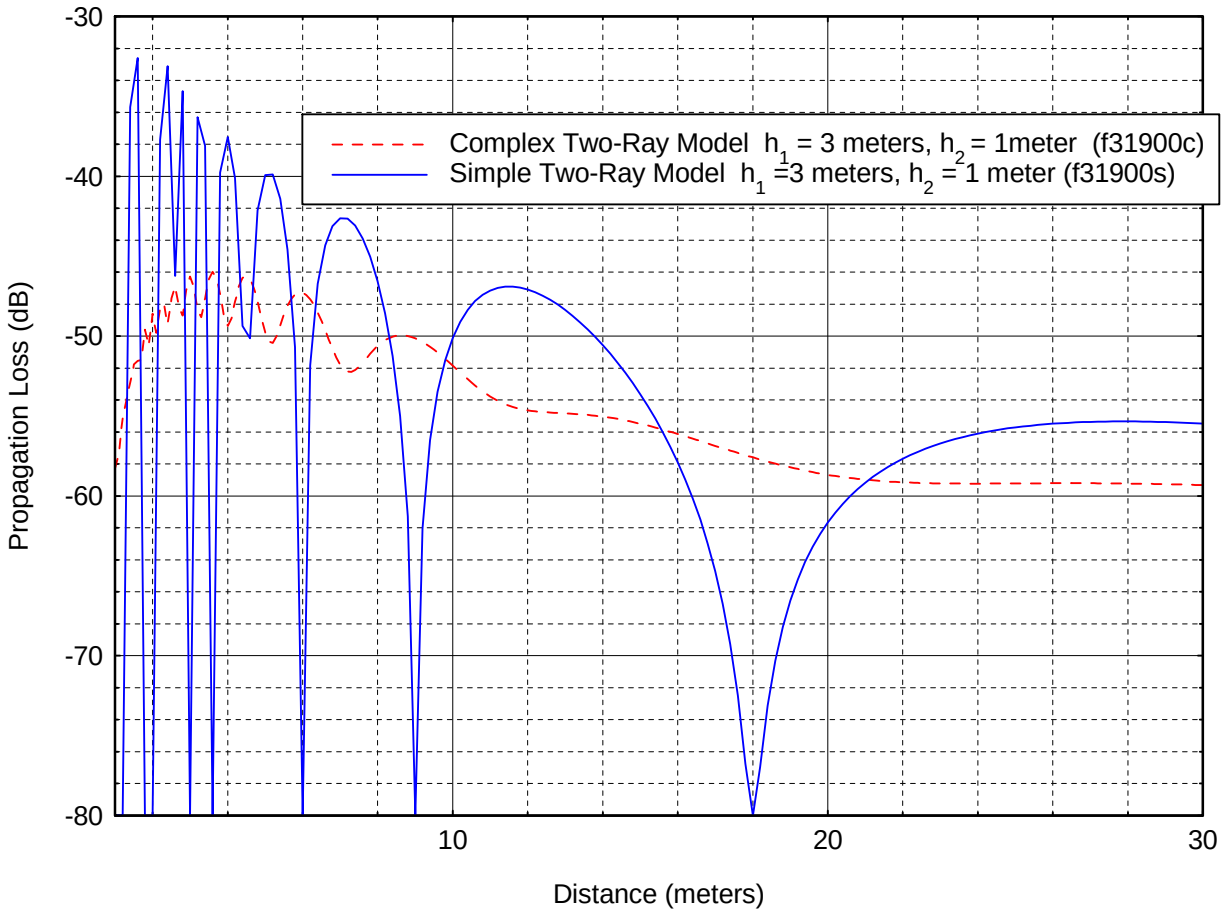


Figure 6. Comparison of simple two-ray model with complex two-ray model at 900 MHz.

### 3.2 Sophisticated Propagation Loss Prediction Methods that Include All Effects

For an even more accurate propagation loss prediction, sophisticated prediction methods would factor in a near-field antenna response when the distances are in the near-field radiation region, and factor in a far-field region antenna radiation pattern when distances are in the far-field region. Two sophisticated methods for propagation loss prediction that factor in these effects were investigated.

One involves a mutual-coupling computation between two antennas for a prediction of propagation loss. The other involves computation of the undisturbed-electric field, and then determining the loss based on the amplitude of this electric field as a function of distance. The complex two-ray method will be compared to these two sophisticated prediction methods. The undisturbed-field method includes near-field effects, the complex two-ray method, antenna near-field and far-field response, the mutual coupling between the transmitter antenna and its image, and the surface wave. Near-field effects include the change in current distribution due to the

presence of the antenna image. Antenna near-field response distinguishes itself as being due to the difference in pattern response of the antenna from the response that it would have in the far-field region of the antenna. This near-field or far-field pattern response influences the transfer of energy from one antenna to another antenna and also affects the propagation loss. This method involves computing the electric field produced at different distances and heights in the environment of real ground from a transmitting antenna at different heights. This computation was performed using the Numerical Electromagnetics Code (NEC) to determine the electric fields at different antenna heights and antenna separation distances at different frequencies over an average ground. This electric field is then used in the equation that relates electric field to a propagation loss as a function of frequency, and the antenna gain magnitudes are factored out to result in a transmission loss to be used in a propagation model. These computation results can then be used to generate a set of equations for building a propagation model. This method also includes the interaction of the antenna with the propagation loss, which must be included for short-distance scenarios. Existing radio-wave propagation models separate the antenna from the propagation loss and calculate a basic transmission loss, which is not correct for short distances.

The equation that computes a propagation loss can be derived using some simple relations and mathematical expressions. The relationship between received power, $p_r$, in watts by an antenna with an effective capture area, $a_e = \lambda^2 g_r / 4\pi$, in square meters, which is immersed in an electric field in root-mean-square (RMS) volts/meter is:

$$p_r(watts) = \frac{e(volts/m)^2}{\eta(ohms)} a_e = \frac{e(volts/m)^2}{\eta(ohms)} \bullet \frac{\lambda(meters)^2 g_r}{4\pi} \tag{17}$$

where $g_r$ is the numerical gain of the receiver antenna, and $\lambda$ is the wavelength in meters at the operating frequency. The impedance $\eta = 120\pi$ ohms. Rearranging and solving for $e^2$ and converting units:

$$\begin{aligned} e(volts/m)^2 &= \frac{480\pi^2 p_r(watts)(f(Hz))^2}{c^2 g_r} \\ (1.0 \times 10^{-12}) e(\mu volts/m)^2 &= \frac{480\pi^2 p_r(watts)(1.0 \times 10^{12})(f(MHz))^2}{(3.0 \times 10^8)^2 g_r} \end{aligned} \tag{18}$$

Taking the logarithm of both sides and rearranging the equation:

$$\begin{aligned} -120.00 + E(dB\mu V/m) &= 36.76 + P_r(dBw) + 120.00 + 20 \log f(MHz) - 169.54 - G_r(dB) \\ E(dB\mu V/m) &= 107.22 + P_r(dBw) + 20 \log f(MHz) - G_r(dB) \\ P_r(dBw) &= E(dB\mu V/m) - 107.22 - 20 \log f(MHz) + G_r(dB) \end{aligned} \tag{19}$$

The received power can also be expressed in terms of the transmitter power, $P_t$ (dBkw), propagation loss, L(dB), transmitter gain, $G_t$ (dB), and receiver gain, $G_r$ (dB).

$$P_r\,(dBw) = P_t(dBkw) + 30.00 + G_t(dB) - L\,(dB) + G_r(dB) \tag{20}$$

Setting the two equations for $P_r$ (dBw) equal to each other, and solving for the propagation loss L(dB):

$$L(dB) = 137.22 + P_t(dBkw) + G_t(dB) - E(dB\mu V/m) + 20 \log\ f(MHz) \tag{21}$$

The transmitter antenna gain $G_t$ (dB) used in the undisturbed-field computations is for a half-wave dipole and is 2.15 dB. This needs to be entered into this equation to compute the transmission loss L(dB). The final equation for the undisturbed-field method is:

$$L(dB) = 139.37 + P_t(dBkw) - E(dB\mu V/m) + 20 \log\ f(MHz) \tag{22}$$

The second method includes all of the features of the undisturbed-field method, and adds the effects of a mutual coupling between transmitter and receiver antennas, in addition to the mutual coupling of the image antennas created by the interaction with the Earth ground. This method includes how the mutual-coupling effects of one antenna influence the current distribution on the other antenna. It will be referred to as the mutual-coupling method. It is an intensive computational method requiring lots of computation time and setup time to produce the results. The impedance of the antennas must be rematched at each distance and each set of antenna heights. These computations were performed using the Numerical Electromagnetics Code (NEC). Many iterative runs are required for each scenario and configuration at all separation distances, antenna heights, and frequencies. The input files for each scenario are run in NEC first to determine the impedance of the antennas for all configurations, so that the antennas can be conjugate matched for accurate predictions of mutual-coupling loss. When all scenarios and configurations have been run, then the input files are all rerun to determine the induced current, $I_{ind}$, in the receiver antenna for a specific input power, $P_{input}$, at the transmitter antenna, and a real part of the receiver antenna impedance, $R_L$ . The mutual-coupling loss, M, in dB is then:

$$M\ (dB) = 10 \log\left(\frac{0.5\, I_{ind}\,(amps)^2\ R_L(ohms)}{P_{input}(watts)}\right) \tag{23}$$

It will be shown in the computation results for a variety of antenna heights, distances, frequencies, and ground constants that the first method of the undisturbed-field method is almost equivalent to the second method using mutual coupling except for very short distances where mutual impedances have a significant effect. Even at the very short distances where the difference in the predictions of propagation loss is a maximum, the propagation losses computed by the two methods differ by less than two dB and are typically less than one dB for distances greater than two meters. The worst cases for the difference in the two predictions occurs when there is a difference in transmitter and receiver antenna heights, and is approximately two dB when the antenna heights differ by two meters and the transmitter to receiver separations are

small (less than 2 meters). Figures D-1 through D-30 in Appendix D are plots of propagation loss predicted by these two methods for six combinations of antenna heights and five frequencies across the desired frequency range of 150 MHz to 3000 MHz. The losses in these figures represent the ratio of received power to transmitted power, which is a ratio that is always less than one, and as a result the loss values are negative. These curves indicate that the differences in the two computation methods are small and can be neglected in most scenarios. As a result, the undisturbed-field method will be used for the final model derivation in preference to the mutual-coupling method, and the propagation loss will be compensated for in those limited scenarios where the difference approaches the maximum of two dB. The undisturbed-field method was chosen over the mutual-coupling method, because of its simplicity and reduced computation time for many combinations of frequencies, antenna heights, distances, and ground constants. If the error between the two methods is considered to be too large for a particular scenario, then the mutual-coupling method can be used for these short distances.

### 3.3 Comparisons of the Undisturbed-Field Method with the Complex Two-Ray Method and Free-Space Propagation Loss

The undisturbed-field method will now be compared to the complex two-ray method and free-space loss method to show why the complex two-ray method or the free-space loss method are not adequate to predict propagation loss for the desired scenarios when the distances are small (less than 10 meters). The undisturbed-field method includes more significant effects than the other methods and therefore is more accurate than all of the methods except the mutual-coupling method. Figures E-1 through E-36 in Appendix E compare these methods for six combinations of antenna heights and six frequencies from 150 to 3000 MHz. The mutual-coupling method is more accurate than the undisturbed-field method, but based on the results of the analysis in Section 3.2 the two methods yield very similar results for most scenarios and the differences are small and can either be neglected or the difference can be compensated for in the model. The mutual-coupling method requires rather complex procedures for many different combinations of parameter values and distances, but the undisturbed-field method is many orders of magnitude faster for many different combinations of parameters and distances. The undisturbed-field method should be the method of choice whenever possible for best accuracy. However, it would be convenient to use the complex two-ray method for larger distances instead of the undisturbed-field method, where possible, to simplify the development of the radio-wave propagation model. It can be observed from Figures E-1 through E-36 that the complex two-ray method achieves adequate accuracy for loss predictions for longer distances.

The complex two-ray method described previously in Section 3.5 was run in two modes. One mode incorporated the far-field patterns of a dipole antenna at both the transmitter and receiver locations. The other mode incorporated a far-field dipole antenna pattern at the transmitter and an isotropic radiator far-field pattern at the receiver antenna. In both modes the gain magnitude was normalized out, so that the complex two-ray model would predict a pseudo basic transmission loss for both modes independent of the antenna gain magnitudes, but not independent of the antenna pattern characteristics. These two modes that were used to compute

propagation loss for the complex two-ray method produced different results, which demonstrates an interesting effect for close-in antenna separations and the computation of transmission loss. Transmission loss for close-in antenna separations is not independent of the antennas and their near-field and mutual-coupling characteristics, and therefore a basic transmission loss can only be defined for larger antenna separations. Basic transmission loss is generally only defined for larger antenna separation distances, since other propagation models are confined to larger separation distances where the effects discussed here are not present.

Figures E-1 through E-36 show that at the lower frequency of 150 MHz the complex two-ray method can be used at distances above 10 meters with an error of less than 1 dB, but at higher frequencies the complex two-ray model can only be used at distances of greater than 20 meters for an error less than 1 dB. Each scenario of different antenna heights and frequencies can be examined more closely to determine a closer distance for each case, so that the complex two-ray method can be used more often to save computation time. The free-space loss tends to represent an average propagation loss, but its large error does not make it suitable for most cases.

Examination of the expanded scale plots of Figures F-1 through F-36 in Appendix F shows that when the transmitter and receiver antenna heights are equal, the curves tend to follow each other, but there is still a significant error in the prediction of propagation loss for short distances when using the complex two-ray method or free-space method. When the transmitter and receiver antenna heights are not equal, the curves from the predictions are vastly different. For these cases of different transmitter and receiver antenna heights, the undisturbed-field method tends to predict a propagation loss that is between the predictions made by the two complex two-ray method predictions. In many cases it appears to be an average of the two complex two-ray predictions. The undisturbed-field method is the best prediction method for transmitter-to-receiver separation distances of less than 20 meters and should be used for those situations. Figures E-1 through E-36 and F-1 through F-36 can be used to determine when it is safe to use the complex two-ray method at distances less than the 20 meters to save time in calculations. More comparison curves of the undisturbed-field method and the complex two-ray model can be plotted at additional frequencies to determine a finer resolution for determining the minimum distance where the two-ray method can be used in place of the undisturbed-field method.

# 4 CONCLUSIONS AND RECOMMENDATIONS

Investigations of different propagation modeling methods and the special considerations of a short-range propagation model with low-antenna heights have resulted in the development of alternative approaches to be taken to accurately model propagation loss in a mobile-to-mobile environment. This initial analysis addressed the line-of-sight propagation environment in an open scenario for vertical polarization. Non-LOS propagation will be addressed in future efforts. Horizontal polarization will also be addressed in future efforts. Other analysis efforts to be performed will address the urban/suburban canyon (LOS and non-LOS), the parking lot canyon (LOS and non-LOS), the general non-LOS propagation environment, the suburban residential environment, the rural environment, and an indoor environment. The results of the investigation into a propagation model that will meet the requirements of the Short-Range MTOM Propagation Model for LOS scenarios, show that for distances less than 10 meters at the frequencies near 150 MHz, and for distances less than 20 meters for all other frequencies, a model that is appropriate for short distances and low-antenna heights will achieve accurate predictions.

None of the models and measured data in the existing literature or ITU-R Recommendations will provide an accurate analysis and meet all of the requirements simultaneously. Some of these models use a free-space loss term in the power-law propagation formula. During the analysis it was discovered that using the free-space loss term in the power-law propagation formula at distances that are too close for the lower frequencies will result in inaccurate predictions. These methods were all found to be inadequate for the short-range mobile-to-mobile model requirements of one meter to two kilometer separation distances, one to three meter antenna heights, and a frequency range of 150-3000 MHz. It has been determined by analysis that alternate methods must be used in the development of radio-wave propagation models that are appropriate to assess the electromagnetic compatibility between the new generation of mobile wireless devices. The challenging scenarios with very close separation distances and very low antenna heights are typical of these mobile wireless devices. A loss computation method that performs mutual-coupling computations between closely spaced antennas over real ground was used for the initial analysis and compared to other methods. This mutual-coupling method includes the effects of the near- and far-field regions of the antennas as well as a mutual-coupling interaction between the antennas and the antenna images with ground, and is considered the most accurate method for prediction of propagation loss, but is rather difficult to implement for a wide variety of antenna heights, antenna separations, frequencies and ground constants. Therefore, an alternative method, the undisturbed-field method, was also investigated which included all of the significant effects of the mutual-coupling model. The propagation model to be implemented for distances in the range of 1-20 meters will be based on this undisturbed-field method that includes compensation for the antenna near-field response and far-field response, ground constants, close-antenna spacing, and geometries created by the different antenna heights. For distances less than two meters, the mutual-coupling method will be used if the accuracy of the undisturbed-field method is not considered accurate enough. For longer distances, greater than 20 meters, a previously described complex two-ray method that includes antenna parameters and the complex reflection coefficient will be used. In future propagation

modeling efforts, mathematical algorithms will be developed from the results of the current analysis effort described in this report. Measurements to be performed at a future date will verify the future propagation modeling efforts. Propagation prediction methods for the other propagation environments mentioned in the first paragraph of this section will also be addressed in future analysis efforts.

## 5 REFERENCES

[1] W. L. Stutzman and G. A. Thiele, *Antenna Theory and Design,* New York: John Wiley & Sons, 1998, Second Edition.

[2] C.A. Balanis, *Antenna Theory Analysis and Design,* New York: John Wiley & Sons, 1997, Second Edition.

[3] R. Bansal, "The far-field: How far is far enough?," *Applied Microwaves & Wireless*, Vol. 11, No. 11, pp. 58-60, Nov. 1999.

[4] A. Picquenard, *Radio-Wave Propagation*, New York: John Wiley & Sons, 1974, p. 80.

[5] R. E. Collin, *Antennas and Radio-Wave Propagation*, New York: McGraw-Hill Book Company, 1985, p.349.

[6] M. J. Feuerstein, et al., "Path loss, delay spread, and outage models as a function of antenna heights for microcellular system design," *IEEE Trans. on Vehicular Technology*, Vol. 43, No. 3, pp. 487-498, Aug. 1994.

[7] F.E. Terman, *Electronic and Radio Engineering*, New York: McGraw-Hill Book Co., 1955.

# APPENDIX A: SHORT-RANGE MOBILE-TO-MOBILE PROPAGATION MODEL STUDY SUMMARY

This appendix is a reworked version of a white-paper report written but not officially published for the sponsor of this work effort, the Office of Spectrum Management (NTIA/OSM) in September 2006. It is referred to several times in the main body of this report and is too voluminous to integrate into the report at those reference points without creating a loss of continuity problem in the main report. The inclusion of this report in an unabridged state prevents the loss of valuable information of an extensive and detailed study effort investigating currently available radio-wave propagation prediction models. This appendix describes a significant and important work effort and investigation detailing why currently available propagation models will not simultaneously meet all of the specific requirements of the sponsor, and why it is necessary to develop new propagation models. When this report was originally written during the initial phase of the study, the low frequency limit was 30 MHz, but was later changed to 150 MHz. This appendix describes what propagation models currently exist and where they can be used for analyses on a limited basis, providing only a part of the needed frequency band, a portion of the required distance range, and only higher antenna heights. This appendix is the result of a supplemental study effort to determine what propagation prediction models currently exist, and virtually none of this information is contained in the main body of the report. The main body of the report constitutes an investigation of how to address the short-range and low-antenna height sponsor requirement, which the currently available models in the literature do not address. Some of the information in this appendix is applicable to the longer distance and higher antenna height requirements of the sponsor.

## A.1 INTRODUCTION

An investigation of currently available models was performed to determine if they could be used to meet the requirements of the Short-Range Mobile-to-Mobile (MTOM) propagation model. The basic requirements for the Short-Range (MTOM) Propagation Model include: separation distances between the transmitter and receiver from one meter to 2 kilometers, a frequency range of 30 MHz to 3000 MHz, and antenna heights of one to three meters for both transmitter and receiver sites. The development of a radio-wave propagation model that will meet these requirements will demand special consideration that currently available models do not include in their methods of analysis. Each of these requirements includes conditions and constraints that have to be accounted for to make accurate propagation loss predictions. Satisfying these requirements simultaneously increases the complexity needed for a model or group of models to meet the requirements. Section A.4 describes the areas where these currently existing models can be used for analyses on a limited basis, providing only part of the needed frequency band, a portion of the required distance range, and higher antenna heights, and be applicable for the desired environment. Even a combination of these models could not meet the requirements for

any significant amount of the frequency band, distance range, or antenna height range of the short-range MTOM model. This appendix describes available propagation models that can be used and what alternative radio-wave propagation models need to be developed to meet the short-range MTOM model requirements.

The interdecile (10% and 90%) range of the propagation loss computed by the model needs to be specified as a function of frequency. An environment description must be included to provide a model that will accurately predict radio-wave propagation loss. The environments considered for model development will be similar to those four listed in Table 1 of International Telecommunication Union- Radiocommunication Sector (ITU-R) Recommendation ITU-R P.1411-2 [A-1] with the addition of a fifth environment to include the short range indoor environment as described in Recommendation ITU-R P.1238 [A-2]. In addition to the normal models included in the first three environments of ITU-R P.1411-2, it will be necessary to include a narrow street mode that takes into account the waveguide mode of propagation for situations where the normal mode would be inadequate. Use of the waveguide mode of propagation is more accurate for narrow street or corridor conditions. The models used in these two ITU-R recommendations will require extensive modifications and additions to meet the short-range mobile-to-mobile propagation model requirements. This will be described further in this appendix.

Initially, a literature search was performed, which resulted in 125 references. After a thorough review of all of these references, only 32 of them were found to be even partially applicable for use in our short-range MTOM propagation model development, since none of the existing models in the references could provide all of the requirements simultaneously.

There is a hierarchy of model approaches that could be used to develop the short-range MTOM model. These approaches can range from the simple slope and breakpoint techniques obtained from regression fits to measured data which are site-general and provide a rough approximation of the propagation loss, to a more complex site-specific approach that uses ray-tracing techniques with actual scenario geometries. The site-specific approach is much more accurate, but requires more information about the scenario and environment. Environment descriptions will be discussed in the next section. A model approach in between the simple site-general and site-specific approaches would include algebraic formulas derived from the site-specific rigorous analysis, but simplified for easy use in specific but different scenarios.

The development of a model that will provide loss predictions for close-in distances as short as one meter requires the use of mutual coupling predictions and possibly the inclusion of a surface wave. The radiation patterns may not be valid at close separation distances, since they may not be used in the far field, and could be in the near field or induction field of the antenna. This situation gets more significant for the lower frequencies of 900 MHz and below.

For low antenna heights, the effects of the close proximity of the Earth to the antenna produces a strong interaction of the antenna patterns with the ground. The antenna pattern performance is vastly different than if the antenna were in free space. The use of a free-space antenna gain will

not be valid. If the antenna is within a half wavelength of the ground the antenna input impedance is affected, and will affect the efficiency and gain of the antennas. Providing a propagation model that will simultaneously account for close-in distances on the order of one meter, low antenna heights of one to three meters, and frequencies as low as 30 MHz, will require special considerations that currently available models do not include in their methods of analysis. This makes it necessary to develop alternative models to meet the requirements of the short-range MTOM model.

Section A.2 contains a discussion of the environment descriptions to be included in the short-range MTOM propagation model. Section A.3 contains a review of all of the currently available radio-wave propagation models to determine their limitations and applicability to the short-range MTOM propagation model. Section A.4 contains a discussion of what can be used from available models and what needs to be developed for the short-range MTOM propagation model. Section A.5 contains a discussion of the conclusion for the investigation of currently available radio-wave propagation models and their applicability to the short-range MTOM propagation model.

## A.2 ENVIRONMENT DESCRIPTIONS

The environments that will be included in the short-range MTOM propagation model will include: urban high-rise, urban/suburban low-rise, residential, rural, and the indoor environment.

### A.2.1 Urban High-Rise Environment

The urban high-rise environment is a typical urban canyon representative of a downtown area in a city, and is characterized by streets lined with tall buildings of several floors each. Since the buildings will be quite tall with respect to the antenna heights of one to three meters, propagation over the rooftops of the buildings may not make a significant contribution to the signal in comparison to those signals due to the direct path (if present) and those resulting from diffraction and reflection around the sides of the building walls. The significance of diffraction over the tops of the buildings needs to be determined. Long path delays could result from the rows of tall buildings. Doppler shifts of the reflected waves could result from the large numbers of moving vehicles and pedestrians. The width of the urban canyon (corridor) resulting from the combined width of the street and sidewalks between the walls of the high-rise can be narrow or wide. Wide and narrow urban canyons will need to be treated separately.

### A.2.2 Urban/Suburban Low-Rise Environment

The urban/suburban low-rise environment is a typical street environment in a town or city where the building heights are generally less than three stories, so diffraction over rooftops with one to

three meter antenna heights may be significant. This is different from the original scenario of ITU-R P.1411-2 [A-1] in that at least one of those antenna heights can be much higher for the original scenario, but both antenna heights will be low for the short-range MTOM model. Moving vehicles on the street can create reflections and shadowing resulting in some small doppler shifts, but the changing multipath environment that is produced as vehicles and people move about is more significant. The environment to be used in the short-range MTOM model will have low antennas at both ends. Long delays may or may not be present. As with the urban high-rise environment, the width of the corridor resulting from the combined width of the street and sidewalks between the walls of the buildings along the street can be narrow or wide. It will be necessary to treat wide and narrow corridors with two different models.

### A.2.3 Residential Environment

The residential environment is characterized by one and two story buildings typical of a residential neighborhood in suburbia. The streets are generally only two lanes wide with room for cars parked on each side of the street. Trees and shrubs could be present with foliage attenuation in light or dense amounts. Automobile and pedestrian traffic could be light or heavy.

### A.2.4 Rural Environment

The rural environment consists of small buildings widely dispersed and surrounded by large open fields, woods, or gardens. Both heavy and light foliage could be present and terrain would also become a factor. The vehicle traffic could be light or heavy.

### A.2.5 Indoor Environment

The indoor environment is characterized by a signal that may be due to a combination of a signal from a direct path and one or more signals from reflection or diffraction paths. Only one or all of these signals from different paths may exist. The indoor environment could be inside a large or small building with varying amounts and sizes of objects that could reflect or diffract energy. The walls, floor, and ceiling can also reflect signals. Receiver/transmitter mobility and objects or persons moving about in the room make the propagation loss a time varying phenomenon. Signals arriving at the receiver from different paths due to direct, reflected, and diffracted rays experience changes in amplitude and phase and add together vectorially, creating deep fades in the total received signal.

## A.3 DISCUSSION OF AVAILABLE MODELS

A review of currently available radio-wave propagation models was performed to determine their limitations and applicability. Currently available models include those discussed in the

ITU-R Recommendations and those described in the technical literature. All models were examined to determine their ranges of validity for distance, antenna heights, frequency, and environment.

### A.3.1 Survey of Models Available from the ITU-R Recommendations[2]

An examination of the applicable ITU Recommendations resulted in several that could be applied to these requirements, but each of these could meet the modeling requirements only on a limited basis, providing only part of the needed frequency band and a portion of the required distance range, and were generally applicable for higher antenna heights, and may not have met environment requirements. A limited number of environments were available. A combination of these models would not meet the requirements for any significant amount of the frequency band, distance range, or antenna height range. Only the ITU-R Recommendations that met some of the requirements were considered. The ITU-R Recommendations examined include: ITU-R P. 1411-2 [A-1], ITU-R P.1238-3 [A-2], ITU-R P.1546-1 [A-3], ITU-R P.1546-2 [A-4], and ITU-R P.833 [A-5].

Recommendation ITU-R P.1546-1 has propagation loss curves for antenna heights down to ten meters, and an interpolation procedure for both transmitter and receiver antenna heights down to one meter. The frequency range for this Recommendation is 30 MHz to 3000 MHz, which will meet the frequency requirements of the short-range mobile-to-mobile propagation model. The distances covered by the propagation loss curves are one kilometer to 1000 kilometers, but cannot be interpolated to distances below one kilometer. The interpolation of heights to the one to three meter range were compared to other propagation models that are considered accurate for this antenna height range. A preliminary investigation has shown that as much as twelve decibel (dB) error occurs when the ten-meter propagation loss values are interpolated down to antenna heights of two meters. The propagation-loss curves provide field-strength values exceeded 50%, 10%, and 1% of the time for time variability. Propagation-loss curves are also provided for 50% location variability. This Recommendation will have limited applicability for distances greater than one kilometer, since there is no interpolation procedure for distances less than one kilometer, and the antenna height interpolation below ten meters does not compare well with other propagation models that are valid in this low-antenna height range of one to three meters. This model is only applicable for a clear unobstructed environment. This Recommendation will not be adequate for the short-range mobile-to-mobile propagation model.

Since ITU-R P. 1546-1 [A-3] cannot be interpolated down to antenna heights of one to three meters with accuracy, and is not applicable for distances less than one kilometer, then it cannot

2 This information was current at the date this white paper was originally written and submitted to sponsor (September 2006). ITU Recommendations may be updated each time the Study Group 3 meets. New revisions of the Recommendations are not covered by this appendix.

be used at all, since the minimum antenna height before interpolation is 10 meters and outside our requirement range, and the short-range MTOM model requires distances down to one meter. There are no environments specified in this Recommendation, such as streets or canyons. Comparisons with the Irregular Terrain Model (ITM) and a known and validated ground-wave propagation model (GW87) show a 12 dB error for loss predictions.

A new algorithm proposed as a revision to [A-3] by ITU members in a contribution from the United Kingdom [A-4] does show some improvement, but on page 12 in this contribution, the comparisons in Figures 11 and 12 with measured data still show major deviations of propagation loss predictions for longer distances as great as 20-30 dB, which would probably be more severe at shorter distances. The deviation also appears to get worse with increasing frequency (UHF and above). Figure 4 of this contribution shows better agreement with measured data using a diffraction model. The use of the ITU Recommendation ITU-R P.1546-1 with the revision added with the new ITU contribution is not recommended for the short distances and one to three meter antenna heights of the short-range MTOM communications model.

Recommendation ITU-R P.1238-3 [A-2] has a simple formula and procedure for site-general indoor scenarios. The frequency range is 900 MHz to 100 GHz. Antenna heights are not used in the model and hence are not a factor. The minimum distance is specified as greater than one meter, and the maximum distance is specified as 1 km. The formula also includes a floor penetration factor for propagation between floors. The minimum distance of one meter is greater than the distance that specifies the condition of being in the far-field at 900 MHz for a short whip antenna, and is well within the far-field distance at frequencies above 900 MHz. This Recommendation cannot be used for frequencies below 900 MHz and distances greater than one kilometer. It is also limited to indoor propagation, but could be used to satisfy the indoor requirements for frequencies greater than or equal to 900 MHz. An indoor model for frequencies below 900 MHz will need to be developed. Recommendation ITU-R P.1238-3 contains propagation prediction methods for planning indoor communications for 900 MHz to100 GHz. Other references could supply numbers for frequencies below 900 MHz, or a similar model for indoor propagation. The basic model that is used for indoor propagation in this Recommendation is:

$$L_t = 20 \log f + N \log d + L_f(n) - 28 \qquad \text{(A-1)}$$

where
$L_t$ is the total loss in dB.
N is the distance power loss coefficient.
f is the frequency in MHz.
d is the separation distance in meters between the base station and the portable unit. (Maximum distance is one kilometer. Minimum distance is greater than one meter.)
$L_f$ is the floor penetration loss factor in dB.
n is the number of floors between base station and portable.

A table for values of N, the power loss coefficient, appears in the Recommendation. A floor penetration loss table is included. Shadow fading statistics can be factored in. The technique contained in this Recommendation is very similar to other references that appear in the literature.

Recommendation ITU-R P.1411-2 [A-1] is for outdoor propagation-loss predictions. The frequency range for this Recommendation is 300 MHz to 100 GHz, but it appears that the range of validity of the various models in this Recommendation is for frequencies less than 30 GHz. Atmospheric effects will not be necessary for frequencies less than 3 GHz. The model can be used for 300 MHz to 3000 MHz, but an alternative model will be needed to cover the lower part of the frequency range of 30 MHz to 300 MHz. A minimum distance is not specified for line-of-sight (LOS), but the maximum distance is 1 kilometer. The minimum distance for LOS in this Recommendation also needs to be determined. It is expected that a different model for close-in distances will need to be developed. The minimum distance for LOS depends on the separation being adequate to be in the far-field region of the antennas, which is a function of frequency and aperture size. A model that is valid at distances less than the distance to the far-field region of the antennas would consider mutual coupling and other phenomena. For LOS, the specification for frequency mentions three separate models for three separate frequency categories: UHF (300 MHz to 3000 MHz), SHF up to 15 GHz (3,000 MHz to 15,000 MHz), and millimeter wave frequencies (15 GHz to 100 GHz). For LOS, the antenna height ranges of validity are not specified, but since this LOS model is the same as [A-6], then the base-station antenna heights are 6.6 and 3.3 meters, and the mobile antenna height is 1.5 meters. Further examination of this Recommendation and the valid antenna height range needs to be made.

In Recommendation ITU-R P.1411-2 the non-LOS distance range is specified as 20 meters to 5000 meters, and the frequency range is specified as 800 to 2000 MHz. For non-LOS, the receiver antenna height is in the range of one to three meters for low antennas held by a pedestrian or located in a vehicle, but the antenna height range for the base station is 4 to 50 meters. This Recommendation considers base-station antenna heights both above and below the building roof level, and defines four physical operating environments previously described in addition to a clutter environment representing vehicle and pedestrian traffic. When one antenna is above the rooftops, an analysis that considers propagation via diffraction over rooftops is used. When the antennas are located below the rooftops, then an analysis within street canyons that considers propagation via diffraction around building corners and reflection from building walls is used. These models need to be compared to other models that appear in the literature. Another model needs to be developed for the frequency range of 30 MHz to 300 MHz for the same environments that this Recommendation covers. The environment descriptions are suitable for the short-range MTOM model. The LOS model is identical to that which appears in reference [A-6], but there is nothing to specify the minimum distance for this reference, except that the minimum distance for [A-6] is 10 meters.

Recommendation ITU-R P.833-4 [A-5] contains formulas and graphs for vegetation attenuation for frequencies between 30 MHz and 30 GHz. The specific attenuations will depend on the particular type of vegetation in the environment. The receiver antenna is at a height of 1.6 and

2.4 meters, and the transmitter antenna is as high as 25 meters. A more detailed model is needed to cover more vegetation environment types with both antennas at heights of one to three meters.

### A.3.2 Survey of Models Available in the Current Literature

A survey was performed of available propagation models and measured data in the current literature to determine their applicability to the short-range MTOM propagation model. The literature search of relevant work in mobile communications originally started with 125 references. After reviewing and filtering all of the available references, only the most specific and relevant information related to the short-range MTOM was retained, resulting in 32 references that will be described here. As with the ITU-R Recommendations, many of the references in the literature met the requirements only partially and as a result, modifications would have to be made to the models in these references, or new models would have to be created to meet the short-range MTOM model requirements. Many of these analyses and measurements were conducted at around 900 and 1900 MHz for the cellular and PCS communications. There are no models or measured data available for urban environments above or below these frequencies. The behavior for frequencies in the 1900 to 3000 MHz band is probably close to that at 1900 MHz, and the behavior in the 700 MHz to 800 MHz range is probably similar to that at 900 MHz. However, new analytical models will need to be developed, and new measurements will have to be performed for frequencies in the 150 MHz to 300 MHz band, since the ITU-R Recommendation P.1411-3 will cover 300 MHz to 3000 MHz, but the minimum base station antenna height of four meters for ITU-R P.1411-3 is just outside of the required range, so new models may need to be developed for the 300 to 3000 MHz range. It may be necessary to develop models and perform measurements at 3000 MHz to determine if behavior at 1900 MHz can be extrapolated to 3000 MHz. In the following discussions of the literature references, the original symbols for propagation loss and other variables will be used as they actually appear in each of the references, and they will be defined in the discussion for each of the equations in which they are used. The path propagation loss referred to in each reference is the basic transmission loss between two isotropic antennas.

[A-6] contains a simple breakpoint model for LOS propagation and another model for out-of-sight (OOS) propagation and both agree with measurements. The OOS propagation model uses a turning-corner-loss for the non-LOS scenario. The measurements were performed at 1956 MHz using a direct sequence BPSK spread-spectrum signal with transmitter antenna heights of 6.6 and 3.3 meters and a receiver antenna height of 1.5 meters. The minimum distance of applicability was 10 meters. The measured data was collected in both an urban and suburban environment, with the major difference being that of the building heights (30 and 15 meters, respectively) and traffic density. The LOS model equations are identical to that in Recommendation ITU-R P.1411-2 and consist of a plot of two sloping lines with a single break point. Separate equations were given that represent the upper ($L_u$) and lower ($L_l$) bounds for path propagation loss that were found to bracket the measured data. These equations are:

$$
\begin{aligned}
L_u &= L_b + 20\log\frac{d}{R_b} \quad for \quad d \le R_b \\
L_u &= L_b + 40\log\frac{d}{R_b} \quad for \quad d > R_b \\
L_l &= L_b + 20 + 25\log\frac{d}{R_b} \quad for \quad d \le R_b \\
L_l &= L_b + 20 + 40\log\frac{d}{R_b} \quad for \quad d > R_b \\
R_b &= \frac{4\,h_t\,h_r}{\lambda} \\
L_b &= 20\log\frac{\lambda^2}{8\pi h_t h_r}
\end{aligned}
\tag{A-2}
$$

where
$L_u$ is the upper bound for path propagation loss in dB.
$L_l$ is the lower bound for path propagation loss in dB.
$L_b$ is the breakpoint loss in dB.
$R_b$ is the breakpoint distance in meters.
d is the distance from the transmitter in meters.
$\lambda$ is the wavelength in meters at the operating frequency.

The measured data verifies the ITU-R P.1411-2 LOS model for transmitter antenna heights of 6.6 meters and a receiver antenna height of 1.5 meters, but no data is shown for the 3.3 meter transmitter antenna height.

The out-of-sight (OOS) model was developed assuming that the reflected rays are dominant over the diffracted rays. The OOS model combines all significant reflected signals to represent the multipath environment using summations. Good agreement with measured data is obtained using this summation method. The resultant equation uses free-space loss combined with the addition of a turning-corner attenuation loss, and slopes from the measured data. The average path loss for OOS propagation is given by:

$$
L_{oos} = 20\log\left(\frac{\lambda}{4\pi\,d_1}\right) + A + 10\,B\log\left(\frac{d_2 + d_1}{d_1}\right) \tag{A-3}
$$

where $L_{oos}$ is the path loss in the OOS street.

A is the turning corner attenuation and is equal to the loss immediately after turning the corner minus the loss just before turning the corner. The loss before and after turning the corner is determined from a summation of all of the significant reflected signals that represents the multipath loss environment before and after turning the corner.

B is the slope in the OOS street and is determined by the slope of the multipath loss computed for A, $d_1$ is the distance to the corner, and $d_2$ is the distance along the OOS street.

There are eight figures in this reference with methods of determining A and B for specific combinations of $d_1$ and $d_2$, and street widths. This is an older reference and much has been done to improve predictions since then. References discussed later show refinement in measurements and modeling.

[A-6] describes the phenomenon for a single frequency, at transmitter heights that are at 6.6 meters. The results for 3.3 meters are not shown, but may be available. This paper also states that when the antennas are below the rooftops, then a 2D ray-tracing technique is accurate enough and a 3D ray tracing algorithm is not necessary. This model verifies the LOS model in ITU-R Recommendation ITU-R P.1411-2 [A-1], but not the non-LOS model of the same ITU Recommendation.

[A-7] treats line-of-sight propagation only. It starts out with a two-ray theory, but mostly fits slopes to measured data. A breakpoint model is defined with two slopes and a single breakpoint. A regression analysis was performed to fit measured data to predictions. The work was performed for 900 and 1900 MHz in urban, suburban and rural environments. The transmitter antenna heights were 3.2, 8.7, and 13.7 meters, and the receiver antenna height was 1.6 meters. The minimum distance for the analysis was 10 meters, but the measurements started at a minimum separation distance of 3.6 meters. The rural measurements were used to test the applicability of the two-ray model. The measurements in the urban and suburban areas permitted observation of the channeling effects of the corridor along the street propagation path. This paper gives justification for the single breakpoint model for LOS regions that have two slopes separated by a breakpoint. On a logarithmic scale the slope before the breakpoint is less than 2 and after the breakpoint is greater than 2. A typical slope before the breakpoint is 1.6, and 3.7 after the breakpoint. The breakpoint distance defines the size of a microcell. In this reference it was discovered that for the scenario geometry used for the measurements, the antenna patterns of the transmitter and receiver significantly affected the measurements for distances less than ten meters, which is why it is difficult to take measurements at short distances. It was found that the shape of the envelope of the two-ray theory matches that of the two-slope/breakpoint model, and that the distance of the breakpoint from the transmitter was equal to the maximum distance that has first Fresnel zone clearance. Good agreement was obtained between measurements and predictions with the two-slope/breakpoint model. The breakpoint model will be described further in references [A-8, A-9]. The antenna patterns of the transmitter and receiver significantly affect the measurements for distances less than ten meters. For these limited frequencies of 900 and 1900 MHz, some useful data can be used for modeling. The two-ray loss model is given by:

$$P_r = P_t\left(\frac{\lambda}{4\pi}\right)^2\left[\frac{1}{r_1}e^{-jkr_1} + \Gamma(\alpha)\frac{1}{r_2}e^{-jkr_2}\right]^2$$
$$\Gamma(\theta) = \frac{\cos\theta - a\sqrt{\varepsilon_r - \sin^2\theta}}{\cos\theta + a\sqrt{\varepsilon_r - \sin^2\theta}} \qquad \text{(A-4)}$$

where
$r_1$ is the distance between the transmitter and receiver along the direct path.
$r_2$ is the distance between the transmitter and receiver along the reflection path.
$\theta$ is the incidence angle wrt the normal to the ground and is equal to 90 -$\alpha$.
$\alpha$ is the incidence angle wrt the ground.
$\varepsilon_r$ is the complex ground constant and equal to $\varepsilon$ - j60$\sigma\lambda$.
$\varepsilon$ is the relative dielectric constant of the ground.
$\sigma$ is the conductivity of the ground in mhos per meter.
$\lambda$ is the wavelength in meters
a is equal to $1/\varepsilon_r$ for vertical polarization and 1 for horizontal polarization.

The horizontal distance d (the breakpoint distance) at which the first Fresnel zone just touches the ground is:

$$d = 1/\lambda\sqrt{(\Sigma^2 - \Delta^2)^2 - 2(\Sigma^2 + \Delta^2)(\lambda/2)^2 + (\lambda/2)^4}$$
$$d = 1/\lambda\sqrt{16h_1^2 h_2^2 - 4(h_1^2 + h_2^2)(\lambda/2)^2 + (\lambda/2)^4} \qquad \text{(A-5)}$$

where
$\Sigma = h_1 + h_2$.
$\Delta = h_1 - h_2$.
$h_1$ is the transmitter antenna height in meters.
$h_2$ is the receiver antenna height in meters.
d is approximately equal to $4\, h_1\, h_2/\lambda$ .

The non-LOS conditions in suburban and urban environments are discussed in [A-8], which is a companion paper to [A-7] which treated LOS conditions. The work was performed at 900 and 1900 MHz in urban and suburban environments using low antenna heights of 3.2, 8.7, and 13.4 meters for the transmitter antennas, and 1.6 meters for the receiver antenna heights. The minimum measurement distances range from 30 to 50 meters. Extensive non-LOS and LOS data for these environments, frequencies, and antenna heights are presented in the report, and the results of regression fits to the measured data are presented with slopes and standard deviations. This paper analyzes diffraction around corners and states that it is valid to use diffraction as the total propagation phenomenon only when the antennas are well below the rooftops. Data on received signal as a function of antenna height along with regression slopes are also shown in the report. Non-LOS paths included zig-zag and staircase patterns through urban and suburban

environments. The height gain for the low base-station antennas along non-LOS paths is found to be linear with height for a suburban environment, but in an urban environment there is almost no height gain when low antennas are used. Good use can be made of the multiple regression slopes in this paper. Extensive LOS and non-LOS graphical data are available from the figures in the paper. A two-slope regression with breakpoint is used for LOS. A single-slope regression is used for non-LOS. Tables with numerous slopes and standard deviations for regression curve fits are in this paper, and regression equations can be created from this data.

The measured data from [A-7] and [A-8] are examined in more detail in [A-9], and this reference goes on to refine the models for LOS and non-LOS for many scenarios. The frequencies studied were 900 and 1900 MHz. The transmitter antenna heights were 3.2, 8.7, and 13.4 meters, and the receiver antenna height was 1.6 meters. The distance range includes 30 meters to approximately 3 kilometers. New formulas which are much simpler than previous formulas, were developed for low antenna heights and short distances in a wide variety of scenarios. This study was performed because the other existing models, such as the Walfisch-Bertoni model, were only useful with high base-station antennas above the rooftops and were not accurate for low antenna heights. A significant portion of the signal energy still propagates over the rooftops via diffraction and this component of the signal must be included in the equations to obtain accurate models for the high antenna heights, so these models would be different for low antenna heights. These simplified formulas could be used for the short-range MTOM model at the original frequencies of 900 and 1900 MHz, and for low antenna heights, but modeling at other frequencies outside these ranges will need to be performed. Also, a short-range model is needed for distances of less than 30 meters and greater than one meter.

The following simplified algebraic equations for path propagation loss, $P_L(R_K)$, result from this refinement of the original data analysis.

The equation for the low-rise scenario for all non-LOS routes is given by:

$$\begin{aligned} P_L(R_K) = {} & [139.01 + 42.59 \log f_G] \\ & - [14.97 + 4.99 \log f_G]\, sgn(\Delta h) \bullet \log(1 + |\Delta h|) \\ & + [40.67 - 4.57\, sgn(\Delta h) \bullet \log(1 + |\Delta h|)] \bullet \log R_K \\ & + [20 \log(\Delta h_m / 7.8) + 10 \log(20 / r_h)] \end{aligned} . \qquad \text{(A-6)}$$

The equation for the high-rise scenario for the lateral non-LOS route with $h_m$ = 1.6 m is given by:

$$P_L(R_K) = 135.41 + 12.49 \log f_G - 4.99 \log h_b + (46.84 - 2.34 \log h_b) \bullet \log R_K . \qquad \text{(A-7)}$$

The equation for the high-rise scenario for the combined non-LOS staircase plus lateral route with $h_m$ = 1.6 m is given by:

$$P_L(R_K) = 143.21 + 29.74 \log f_G - 0.99 \log h_b + (47.23 + 3.72 \log h_b) \bullet \log R_K \,. \qquad \text{(A-8)}$$

The equation for the low-rise plus high-rise scenario for the LOS route with $R_K<R_{BK}$ is given by:

$$\begin{aligned} P_L(R_K) &= 81.14 + 39.40 \log f_G - 0.09 \log h_b \\ &\quad + (15.80 - 5.73 \log h_b) \bullet \log R_K \end{aligned} \,. \qquad \text{(A-9)}$$

The equation for the low-rise plus high rise scenario for the LOS route with $R_K>R_{BK}$ is given by:

$$\begin{aligned} P_L(R_K) &= [48.38 - 32.10 \log R_{BK}] + 45.70 \log f_G \\ &\quad + [25.34 - 13.90 \log R_{BK}] \log h_b \\ &\quad + [32.10 + 13.90 \log h_b] \log R_K + 20 \log (1.6/ h_m) \end{aligned} \,. \qquad \text{(A-10)}$$

where
$P_L(R_K)$ = the path propagation loss in dB at distance $R_K$ between the transmitter and the mobile.
$\Delta h = h_b - h_{BD}$ = relative height of transmitter to average building height in meters ($-8 \leq \Delta h \leq 6$).
$R_k$ = mobile distance from the transmitter in kilometers ($0.05 < R_k < 3.0$).
$f_G$ = frequency in GHz.
$\Delta h_m$ = height of the last building relative to the mobile in meters.
$r_h$ = distance of the mobile from the last rooftop in meters.
$h_b$ = transmitting antenna height from ground level in meters.
$h_m$ = mobile antenna height from ground level in meters.
$\lambda$ = the wavelength in meters.
$R_{BK}$ = breakpoint distance converted to kilometers = $4h_bh_m/1000\lambda$.
$\text{sgn}(\Delta h) = +1$ for $\Delta h \geq 0$, otherwise $\text{sgn}(\Delta h) = -1$.

In this reference a measurement-based propagation model is developed that is valid for base station heights that are near to or below the heights of the surrounding buildings for low building heights and at lamppost heights for high-rise environments. Of particular interest to the short-range MTOM model is the measured data and modeling for the transmitter antenna height of 3.2 meters in conjunction with the receiver antenna height of 1.6 meters. Data is available in this reference for the dependence of propagation loss as a function of transmitter antenna height. These algebraic models could be compared to the newly developed models at the low antenna heights along with any new measured data.

[A-10] describes a further analysis of the data in [A-7 to A-9] to determine the dependence of propagation loss or received signal strength on base station antenna height. Much of the data in this reference and [A-9] state the antenna heights with respect to the average building height in the environment, but the antenna heights are still those stated in [A-7 to A-9]. The frequencies

of interest are still 900 and 1900 MHz, and the minimum distances range from 30 to 50 meters. The analysis is based on the theory that a significant portion of the signal is that from diffraction over rooftops. For the short-range MTOM model we are primarily interested in the lowest antenna height used for a base station transmitter antenna. A theoretical model is developed for the effects of base station antenna height and is found to provide good agreement with measured data. The signal components propagating over the rooftops of the buildings are modeled as diffracting over absorbing screens, where an absorbing screen simulates the rooftop of each building. The result is the range loss exponent n as a function of antenna height, $h_{BS}$, with respect to building height $h_{rt}$ ($\Delta h = h_{BS} - h_{rt}$ over a range of -8 to +6). This data will provide information in determining just how significant the over-the-rooftops component of the diffraction signal is for the lowest transmitter antenna height of 3.2 meters. This theoretical model is further simplified in [A-11]. The dependence of path loss and received signal as a function of antenna height is also useful information for our model.

A simplified model is described in [A-11] for path loss prediction in urban and suburban environments with base station antenna heights above, near, and below roof level for urban and suburban environments. This simplified model was derived from a more complex model that required multiple dimension integration and was not suitable for easy use as a system planning tool for predicting propagation loss. This model included free-space wave front spreading, multiple diffraction past rows of buildings, diffraction from rooftop to street level, and building shadowing, which this reference states are the most important processes for propagation in urban and suburban environments. With low base station antennas and small cells (microcells), building height and the width of streets have a very significant effect on radio propagation. When compared with numerous measurements, good agreement was obtained for the propagation loss predictions. The simplified version of this model was developed to meet the requirements of system planning for prediction of propagation loss and interference assessment. This model has been verified at 900 and 1900 MHz, and at low antenna heights (transmitter at 3.2 meters and receiver at 1.6 meters) by comparison with measured data. A simplified version of the complex theoretical model was developed for three cases: near, above, and below roof level. This model could provide a good comparison with newly developed models and other measured data. It was developed from approximations to the complex theoretical mathematical models, but the models discussed in previous references were derived from measured data using regression curve fits to the data or algebraic algorithms fitted to the data. The minimum valid distance range is 30 to 50 meters, since it is based on data in [A-9].

The simplified equations for the path propagation loss, L, are described below. A mobile receiver antenna is assumed to be at a height of 1.5 m.

For base station antenna heights near roof level:

$$L = -10\log\left(\frac{\lambda}{2\sqrt{2}\pi R}\right)^2 - 10\log\left[\frac{\lambda}{2\pi^2 r}\left(\frac{1}{\theta} - \frac{1}{2\pi+\theta}\right)^2\right] - 10\log\left(\frac{d}{R}\right)^2. \qquad \text{(A-11)}$$

For base station antenna heights above roof level:

$$L = -10\log\left[\frac{\lambda}{4\pi R}\right]^2 - 10\log\left[(2.35)^2\left(\frac{\Delta h_b}{R}\sqrt{\frac{d}{\lambda}}\right)^{1.8}\right] - 10\log\left[\frac{\lambda}{2\pi^2 r}\left(\frac{1}{\theta} - \frac{1}{2\pi+\theta}\right)^2\right]. \quad \text{(A-12)}$$

For base station antenna heights below roof level:

$$L = -10\log\left(\frac{\lambda}{2\sqrt{2}\pi R}\right)^2 - 10\log\left[\frac{\lambda}{2\pi^2 r}\left(\frac{1}{\theta} - \frac{1}{2\pi+\theta}\right)^2\right] - 10\log\left[\left(\frac{d}{2\pi(R-d)}\right)^2 \frac{\lambda}{\sqrt{(\Delta h_b)^2 + d^2}} \bullet \left(\frac{1}{\phi} - \frac{1}{2\pi+\phi}\right)^2\right]. \quad \text{(A-13)}$$

where
R = the transmitter to receiver distance in meters.
$\varphi = -\tan^{-1}(\Delta h_b/d)$.
$\Delta h_b = h_{bs} - h_{BLD}$ in meters.
$h_{bs}$ = the base station antenna height in meters.
$h_{BLD}$ = the average building roof height.
d = the average separation between buildings center-to-center in meters.
$\Delta h_m = h_{BLD} - h_m$ in meters.
$h_m$ = the mobile antenna height in meters.

$$r = \sqrt{(\Delta h_m)^2 + x^2} \quad \text{in meters} \quad \text{(A-14)}$$

$\theta = \tan^{-1} \Delta h_m/2$.
x = w/2 in meters.
w = street width in meters.
M = number of buildings
$\lambda$ = wavelength in meters.
R = Md = the transmitter to mobile separation distance in meters.

The data in [A-9] are analyzed further in [A-12] which determines that microcellular propagation is far from being isotropic, but is in fact anisotropic. A suburban or urban environment with rectangular street grids has a propagation characteristic that is diamond shaped rather than circular. The path loss formulas presented in this paper are for a slightly different environment (residential/commercial-low-rise) than those presented in [A-9] (low-rise and high-rise), so some of the formula coefficients are different. The path loss formulas in [A-12] were used to plot and identify the diamond-shaped contours typical of this anisotropic coverage for this low-rise environment with low antenna heights. These models have been validated at 900 and 1900 MHz. The transmitter antenna heights range from 3 to 13 meters, and the receiver antenna height

is at 1.6 meters. A lateral route is a non-LOS route where the base station antenna is in the middle of the block and the receiver moves down an adjacent perpendicular street path. A lateral-like route is a non-LOS route where the base station is in the backyard and the receiver moves down a parallel street. The ST Route is a zig-zag path pattern through neighborhood streets having the aerial-view appearance of a staircase. The path propagation loss $P_L(R_K)$ for a transmitter-to-mobile separation distance $R_K$ for each of the following scenarios is given by the following equations. The equation for the lateral route is given by:

$$\begin{aligned} P_L(R_K) &= [127.39 + 31.63 \log f_G] \\ &- [13.05 + 4.35 \log f_G] \, sgn(\Delta h) \bullet \log(1 + |\Delta h|) \\ &+ [29.18 - 6.70 \, sgn(\Delta h) \bullet \log(1 + |\Delta h|)] \bullet \log R_K \end{aligned} \quad \text{(A-15)}$$

The equation for the lateral-like route is obtained by subtracting 3 dB from the above equation for the lateral route formula.

The equation for the combined staircase route is given by:

$$\begin{aligned} P_L(R_K) &= [138.31 + 38.88 \log f_G] \\ &- [13.74 + 4.58 \log f_G] \, sgn(\Delta h) \bullet \log(1 + |\Delta h|) \\ &+ [40.06 - 4.35 \, sgn(\Delta h) \bullet \log(1 + |\Delta h|)] \bullet \log R_K \end{aligned} \quad \text{(A-16)}$$

The equation for the low-rise plus high-rise LOS route for $R_K < R_{BK}$ is given by:

$$P_L(R_K) = 81.14 + 39.40 \log f_G - 0.09 \log h_b + (15.80 - 5.73 \log h_b) \bullet \log R_K . \quad \text{(A-17)}$$

The equation for the low-rise plus high-rise LOS route for $R_K > R_{BK}$ is given by:

$$\begin{aligned} P_L(R_K) &= [48.38 - 32.10 \log R_{BK}] + 45.70 \log f_G \\ &+ [25.34 - 13.90 \log R_{BK}] \bullet \log h_b \\ &+ [32.10 + (13.90 \log h_b) \bullet \log R_K + 20 \log(1.6/h_m)] \end{aligned} \quad \text{(A-18)}$$

where
$\Delta h = h_b - h_{BD}$ = relative height of transmitter to average building height in meters ($-8 \leq \Delta h \leq 6$).
$R_k$ = mobile distance from the transmitter in kilometers ($0.05 < R_k < 3.0$).
$f_G$ = frequency in GHz.
$\Delta h_m$ = height of the last building relative to the mobile in meters.
$h_b$ = transmitting antenna height from ground level in meters.
$h_m$ = mobile antenna height from ground level in meters.
$\lambda$ = the wavelength in meters.
$R_{BK}$ = breakpoint distance converted to kilometers = $4h_bh_m/1000\lambda$.
$sgn(\Delta h) = +1$ for $\Delta h \geq 0$, otherwise $sgn(\Delta h) = -1$.

From the above equations it can be seen that for non-LOS paths the loss depends on the height of the base station antenna relative to the average building height, but for LOS paths the loss depends directly on the height of the base station. These equations supply additional data and modeling information for the short-range MTOM model development, since some of the environments are slightly different from those discussed in Reference [A-9]. The minimum distances of 30 to 50 meters, and the frequencies of 900 and 1900 MHz are the same as in [A-9].

Wide-band measurements at 1900 MHz are described in [A-13] with base station antenna heights of 3.7, 8.5, and 13.3 meters and a receiver antenna height of 1.7 meters to simulate a typical microcellular scenario. The minimum distance considered was 10 meters. Models are presented for LOS and non-LOS propagation that were derived from single and double regression models. These models are from different authors than the previously described references, but the approach is similar. The data from these independent measurements can be used as yet another source to compare with propagation models. The double regression model has a breakpoint distance that has first Fresnel zone clearance for LOS topographies. This paper also states that for a LOS scenario with a simple case of a direct path and a single ground reflection between the transmitter and receiver, the distance power law model describes the mean path loss. When the transmitter to receiver separation distances are less than the first Fresnel zone distance, the mean path loss exponent is 2, and for distances beyond the first Fresnel zone distance the exponent is approximately 4. Data in this reference provides more accurate loss exponents for both regions.

As stated previously, the distance $d_f$ at which the first Fresnel zone becomes obstructed is given by:

$$d_f = 1/\lambda \sqrt{(\Sigma^2 - \Delta^2)^2 - 2(\Sigma^2 + \Delta^2)(\lambda/2)^2 + (\lambda/2)^4} \; . \qquad \text{(A-19)}$$

This reference also relates the two-ray model to the double slope or distance power law model. The path propagation loss PL(d) for the distance power law model is simply stated as:

$$PL(d) = PL(d_0) + 10\, n \log(d/d_0) \quad dB$$
$$PL(d_0) = 10 \log\left(\frac{4\pi d_0}{\lambda}\right)^2 \quad dB \qquad . \qquad \text{(A-20)}$$

A close-in reference distance of one meter is used for $d_0$ for the reference loss computation. This model uses a free-space loss for $PL(d_0)$ which is not correct for lower frequencies below 900 MHz and when the path does not have first Fresnel zone clearance. These models are based on the dual slopes that result when the path loss in decibels is plotted versus the logarithm of distance. This paper shows that this dual slope technique can be used to accurately characterize the measured path loss for the LOS case, only when no more than two rays are involved. This paper also demonstrates that a model, where only the antenna heights and frequency are used to determine the Fresnel zone breakpoint can predict microcellular propagation as well as the minimum mean square error (MMSE) fit to the data. The breakpoint can be related to Fresnel

zone theory. If a propagation path has first Fresnel zone clearance, then the propagation loss is due totally to the spherical spreading loss of the wave front, which is free-space loss. The Fresnel zone model is only valid for LOS scenarios where there is a direct signal path between the transmitter and receiver. A double regression model works well for LOS cases, while a single regression model works well for non-LOS. Two forms of the double regression model are used: one where the breakpoint is the first Fresnel zone clearance distance, and the other where the breakpoint is determined by the MMSE best fit to the data. Simple algebraic formulas are presented for LOS and non-LOS scenarios.

For LOS a double regression formula is used, and for non-LOS a single regression formula is used. Two methods are presented for the LOS. For LOS method 1, the breakpoint is fixed at the first Fresnel zone clearance distance, $d_f$ , and the path propagation loss $PL_1(d)$ is computed from:

$$\begin{aligned} PL_1(d) &= 10\, n_1 \log d + P_1 \qquad for \quad 1 < d < d_f \\ PL_1(d) &= 10\, n_2 \log (d/\, d_f) + 10\, n_1 \log d_f + P_1 \qquad for \quad d > d_f \end{aligned} \quad . \tag{A-21}$$

where $P_1 = PL(d_0)$ is the free-space propagation loss at $d_0 = 1$ meter, and $P_1 = 38$ dB at 1900 MHz.

For LOS method 2, the breakpoint is determined to be that value of distance and loss that results in the MMSE for all data by statistical analysis of the data. The path propagation loss, $PL_2$ (d), is given by:

$$\begin{aligned} PL_2(d) &= 10\, n_1^* \log d + P_1 \qquad for \quad 1 < d < d_b \\ PL_2(d) &= 10\, n_2^* \log (d/\, d_b) + 10\, n_1^* \log d_b + P_1 \qquad for \quad d > d_b \end{aligned} \quad . \tag{A-22}$$

where $d_b$ is the statistically determined breakpoint distance. The values of $d_b$, $n_1$*, and $n_2$* are those which minimize the MMSE for the data. MMSE = $\sigma^2$, where $\sigma$ is the standard deviation of the data.

For non-LOS, a single regression is used that minimizes the MMSE. Tables of $n_1$, $n_2$, $n_1$*, $n_2$ *, $d_f$, $d_b$, and $\sigma$ are given for LOS and non-LOS in this reference. This reference provides independent measured data from other authors at 1900 MHz and at low antenna heights with 3.7 meters for the transmitter antenna and 1.7 meters for the receiver antenna. Single and double regression curve fits to the data are used for the model. The propagation loss for these models can be compared to other models in previous references for similar scenarios.
Local spatial averages of local mean attenuation for microcellular data are used in [A-14] to curve fit in non-LOS environments and obtain the anisotropic diamond-shape patterns for microcellular coverage contours. These contours are described extensively as complex mathematical functions, and then further simplified in the form of a simple fitting function described below. The frequency is 894 MHz, the transmitter antenna height is at 1.8 meters, and the receiver antenna height is 9.1 meters. This paper mentions that the sides of the diamond shaped contours are concave, which suggests that the coupling into cross streets is primarily due

to diffraction around corners rather than reflections from buildings. The reasoning is that if the reflections were the dominant mechanism, then the attenuation at a point for contours plotted on an xy grid would be a function of x+y, which would make the sides of the diamond contour straight and not concave. Diffraction causes the attenuation to be proportional to a product of two functions, one a function of only x and the other a function of only y, where both are decreasing functions of the independent variable, which leads to the concave shapes. The diamonds are not smooth or uniform due to the environment. This reference makes use of the data in [A-15] that was collected in urban, suburban, and rural environments. Since the receiver antenna height was at 9.1 meters and the transmitter antenna height was at 1.8 meters, this data is out of our range, but the authors have an interesting interpretation of non-LOS propagation with their concave diamond-shaped coverage contours. A minimum mean square error analysis of predictions compared to measurements determines the coefficients of the fitting function to the data in the x and y coordinates. The fitting function L(z) with coefficients A, B, and C are determined for z, where z can be either the x or y coordinate, and is of the form:

$$L(z) = \frac{1}{A + Bz^2 + Cz^4}. \qquad \text{(A-23)}$$

This paper provides an alternative way of presenting the coverage analysis as an anisotropic diamond-shape pattern instead of circles, even though the receiver antenna height is too high for the short-range MTOM model.

A LOS multi-ray model for microcellular and mobile communications is contained in [A-15]. Calculations were performed using a two-ray theory for open environments, and two-ray theory plus the addition of four specular wall-reflected rays for the urban canyon environment. Antenna heights are approximately three meters for the transmitter antenna height and approximately two meters for the receiver antenna height. The measurements were taken at 900 MHz and 11 GHz. It was stated in this reference that the addition of the four rays reflected from the walls adequately represents the microcell radio-wave propagation in the urban canyon environment, but this is an older reference. It was later discovered by other authors that diffraction around and over the rooftops of buildings is also important.

Path loss and delay spread measurements are shown in [A-16] to agree with the double regression LOS model (two slopes) that has its breakpoint at a distance that has first Fresnel zone clearance. The behavior of delay spread as a function of distance is also characterized. Delay spread and propagation losses are both statistically quantified. Base station antenna heights include 3.7, 8.5, and 13.3 meters, and mobile receiver antenna heights are 1.7 meters. The frequency is 1900 MHz.

There are measurements and predictions in [A-17] for LOS wideband propagation loss at 1800 MHz using low antenna heights where both the receiver and the transmitter are at a height of 1.7 meters. Measurement distances range from 40 meters to one kilometer. The measurement scenarios include both rural and urban environments. Power delay profiles are also presented. RMS delay spread was calculated from the power delay profiles. The data was fitted to a straight line for the standard path loss exponent model mentioned previously, where the

exponent was calculated to be 2.8 with a reference distance of five meters, which is in good agreement with previous work at Virginia Tech where the exponent was found to be 2.7 [A-16]. Free space loss is assumed up to a distance of five meters. This data and model information is useful since the antenna heights are at 1.7 meters and the distances are short. These authors are the same as for [A-13].

[A-18] contains propagation models and measurements for short distances ranging from two to 12 meters at 5300 MHz. The transmitter antenna heights ranged from two to 3.5 meters, and the receiver antenna height was fixed at 1.8 meters. This reference is one of the few references of all of the 125 references reviewed that simultaneously has very short ranges and low antenna heights for both modeling and measured data. The measurements were performed for three scenario environments: open roadway with trees, roadway with buildings on the sides, and a parking lot with cars. For all of these scenarios there was a strong LOS component with very little or no shadowing, and the vehicles were located in prescribed driving lanes, so a well-defined geometry existed for the MTOM path. When the predicted path gain (propagation loss) versus distance was compared to the measured data for these paths, the two-ray model was found to estimate the shape of the curve and predict the location and depth of the fades. The extra noise or variability of the signal was then modeled as a zero-mean complex Gaussian process, where the mean power was derived from measurements. This is interesting data for low antenna heights and extremely short distances even though it is outside of our frequency range, but it is expected that propagation at 3000 MHz for these scenarios would be similar. The authors maintain that the two-ray model can reliably estimate the shape of the loss curve as well as the location and depth of the fades for the open roadway scenario. For the scenario containing a roadway with buildings, a four-ray model better estimated the loss. The parking lot scenario is also of interest for the short-range MTOM.

Measurements and model predictions at 1800 MHz are described in [A-19] for both low and high antenna heights. Ray-based algorithms are compared to slope intercept models and the COST 231 model. The data is for one to three story buildings (3 to 9 meters high) where the antennas are at or above the rooftop levels. The modeling is site specific in that the actual dimensions and locations of the buildings are used in the analysis. It was found that, for antennas at or above rooftop levels the ray-based algorithm results in good agreement with measurements, with an average difference of one dB and a standard deviation of four or five dB. For antennas below the rooftops, it was found that additional ray paths must be included to achieve the accuracy attained with the higher antennas. These additional ray paths involve reflections at buildings near the base station and diffraction rays at the vertical edges of the buildings. When the base station is below the rooftops, and if the rays diffracted over the rooftops are the only ones used in the calculations, then the predicted signal levels are too low and the losses are too high, so it is necessary to include the rays reflected from the buildings and the rays diffracted around the buildings. There is a large resource of measured data in this reference in the form of signal strength versus distance covering the distance range of 100 to 400 meters.

The importance of system simulation is described in [A-20] where an integration of radio propagation models with models of the transmitters, receivers, and signals presents a complete

systems performance prediction for specific systems such as: code division multiple access (CDMA), time division multiple access (TDMA), Global System for Mobile Communication (GSM), and digital audio/television. Examples are given for each of these and the authors describe how signal impairments such as path loss, shadowing, multipath propagation, frequency-selective fading, flat fading, time dispersion, and delay spread are used to simulate the radio channel. This reference emphasizes how each of these systems have different responses to these effects.

The indoor radio propagation problem is described in [A-21] and provides some simple models for prediction in the 400 MHz to 2400 MHz frequency range. The models are similar to the power loss exponent versus distance expressions found in the other indoor propagation modeling loss references. Results of measured data from other references is presented at 433, 869, and 2450 MHz. Many effects that influence radio propagation in the indoor environment are discussed and include: presence of the human body when holding equipment, directional characteristics of antennas, misalignment of polarization, diffraction, reflection, and multipath. The simple exponent formula for path propagation loss, PL (in dB), used in this reference is:

$$PL = -27.55 + 20 \log(fd) + PL_{fs} + 10\, n \log d \ . \qquad \text{(A-24)}$$

where
f = the frequency in MHz.
d = the distance in meters.
$PL_{fs}$ = the free-space loss at one meter distance in dB.
The value of n is typically 4, but can range up to 9.

This is similar to the ITU and other indoor radio-propagation model references, and provides measured data at additional frequencies of 433, 869, and 2450 MHz for comparison with propagation models.

Radio propagation models and measurements in the 900 MHz, 1300 MHz and 1900 MHz bands are described in [A-22] for the indoor environment and outdoor microcellular environment. Some of the data cited in this reference use low antenna heights. This reference describes how these wireless systems are usually interference limited rather than noise limited. Knowledge of the propagation environment for computing link budgets is necessary to determine coverage areas and power transfer between potential interferers and receivers. Interference from co-channel and adjacent channel transmitters will determine the performance and capacity of microcellular systems. The received signal envelope statistical characteristics are described, as well as how they impact performance. If no direct LOS path exists between the transmitter and receiver, then the cumulative distribution function (CDF) of the received signal envelope is described by a Rayleigh distribution function. When a direct LOS path exists between the transmitter and receiver, then the CDF of the received signal envelope is described by a Rician distribution function. Power law equations with a statistical variation are given for both indoor and outdoor microcellular propagation that calculates the local average signal. The slope of the function (path-loss exponent) is computed using linear regression of the measured data. The

variation (standard deviation) about the best-fit mean path-loss model is computed as the minimum mean square error of the measured data. Power-delay profiles, mean excess delay, root-mean-square (rms) delay spread, and excess delay spread for indoor channels are discussed, which are essential performance parameters for system design. Penetration of signals into buildings is discussed. For microcell propagation, the authors reference the paper by Blackard et al. [A-16] where wideband measurements indicate that the first Fresnel zone is an accurate MMSE breakpoint for a dual regression path loss in LOS, and where different loss exponents are used before and after the breakpoint; this is similar to previous references. An equation is given for the first Fresnel zone clearance distance as in other references previously described. In addition, a table is presented that compares results with exponents, breakpoints, and standard deviations for the case where the breakpoint is determined by the first Fresnel zone, and the case where the breakpoint is that which minimizes the MMSE. This information also is from [A-16] which is a preliminary to [A-13], the final journal paper that contains more details.

For the indoor model, the familiar formula for path propagation loss, PL(d) is:

$$PL(d) = PL(d_0) + 10\,n \log(d/d_0) + X\sigma\,. \qquad \text{(A-25)}$$

where
$PL(d_0)$ is the free-space propagation loss in dB at a reference distance $d_0$ in meters.
d is the distance between the transmitter and the mobile in meters.

There are two tables with values of exponent n and standard deviaton Xσ for different environments, and Table 4 on page 18 of [A-22] has floor attenuation factors for multiple floors.

Propagation modeling for the city environment is described in [A-23] for the UHF (300 to 3000 MHz) and X (5200 to 10900 MHz) frequency bands for both regularly distributed rows of buildings on flat terrain and an array of randomly distributed buildings on irregular terrain. For the regularly distributed buildings on flat terrain, a 2D multi-slit waveguide model is used for LOS conditions and a two-dimensional multi-diffraction model is used for non-LOS conditions. A statistical parametric model is used for randomly distributed buildings on irregular terrain that includes single and multiple scattering effects of buildings and diffraction around buildings. Instead of using the conventional two-ray model for LOS conditions and multiple reflections from the walls, a multi-slit waveguide model was proposed in this reference. It was found that the conventional two-ray model plus reflections from the walls resulted in good predictions for wide urban canyons (wide streets). The waveguide model was better for narrow streets. As the street width is increased, the multi-slit waveguide model predictions approach the two-ray model predictions. Wide streets are characterized by $a>h_b$ where a is the street width between buildings and $h_b$ is the average building height, and $a^2 > h_t h_r$ where $h_t$ and $h_r$ are the transmitter and receiver antenna heights. Extensive and simplified deterministic and statistical models are presented for both the conventional two-ray model and the waveguide model techniques. This paper also quotes some of the earlier work by Bertoni, Xia, and Maciel [A-7 and A-10].

The equation for the path propagation loss, L for the 2D waveguide loss model for a long distance (r>>a) from the source is:

$$L = +32.1 - 40\log|\Gamma_g| - 20\log\frac{\left(1-(M|\Gamma_n|)^2\right)}{\left(1+(M|\Gamma_n|)^2\right)} + 17.8\log r - 20\log\left(|\Gamma_n| + |D_{mn}|\right) + 8.6\left(\left|\ln M|\Gamma_n|\right|\left[\frac{(\pi n - \phi_n)}{a}\right]\frac{r}{\rho_n a}\right) \quad \text{(A-26)}$$

where
$\Gamma_g$ is the reflection coefficient of the ground.
$\Gamma_n$ is the reflection coefficient of the walls.
$\varphi_n$ is the phase of the reflection coefficent of the walls.
$D_{mn}$ is the diffraction coefficient for each ray diffracted from the wall's edge.
a is the width of the waveguide wall (street width between buildings).
r is the distance along the street.
$\rho_n$ is a propagation parameter along the waveguide (street):

$$\rho_n = \sqrt{k^2 - (n\pi/a)^2} \quad \text{(A-27)}$$

where
k is $2\pi/\lambda$.
n is the number of reflections.

$$M = \frac{L_{avg}}{L_{avg} + l_{avg}} \quad \text{(A-28)}$$

where
M is the parameter of discontinuity of the multi-slit waveguide.
$L_{avg}$ is the average of the unbroken lengths of buildings along the street.
$l_{avg}$ is the average of the gaps between the buildings along the street.

Out of the four waveguide propagation model references, this is the best reference to use for narrow urban street propagation for 30 to 3000 MHz, since the other references verified model performance over this frequency range, and this reference contains the simplest formula obtained from the complex derivation.

The original derivation of the 2D multi-slit waveguide model for LOS conditions for the 902-928 MHz band for the microcellular urban and suburban environment is described in [A-24]. Results of VHF (30 to 300 MHz) and UHF (300 to 3000 MHz) measurements are compared to theoretical predictions for the urban environment. The predictions of path loss characteristics are analyzed for various street widths, average building heights, and electrical impedance properties of the building walls. These results then are compared with measured data. Extensive

equations are presented. The waveguide model can better explain the attenuation past the breakpoint than the loss exponent model where the loss exponent n varies from 4 to 7. This model agrees with the one cited in [A-22].

A rigorous derivation of a two-dimensional waveguide slit model for UHF (300 to 3000 MHz) and L-band (390 to 1550 MHz) for urban areas is contained in [A-25]. Comparisons between predictions and measurements are made. Simplified formulas are presented for easy computations. This approximate and simplified expression is not as accurate as the more general ones presented in [A-22 and A-23].

The original theoretical derivation in [A-26] describes both the 3D and the 2D multi-slit waveguide model with comparisons to different data than [A-21] at VHF/UHF frequencies. These equations are in a much more complex form than those of the other references [A-22 to A-24].

A recent book on radio-wave propagation [A-27] includes many of the basic principles in the development of models for analysis as well as the treatment of measured data. Much of this information is included in the author's paper references described previously, but is explained in more detail in the book. Some of the information applies to low antennas in a tall building environment, where the primary propagation paths are around the sides of the buildings rather than over the tops of the buildings. Prediction in this case requires only a two-dimensional data base of the building footprints for the ray-tracing models, which is important for saving time in model development and execution time. In an analysis using two-dimensional ray tracing over a floor or ground, the rays arriving at the subscriber location directly and via multiple reflections are determined first. Sections of the book describe microcell propagation with base station heights of 3.2, 8.7, and 13.4 meters, and a receiver height of 1.6 meters for LOS and nonLOS conditions with equations for all cases. These models are similar to those in journal papers and could be used for 900 to 1900 MHz. The basic two-ray model is presented with its application above flat Earth. The process of breakpoint distance derivation and two-slope regression fit are explained in detail. A multi-ray model is presented where twice-reflected images and six more rays are added in an urban canyon. There are additional equations for a mobile-to-mobile link over a three-story building as well as for LOS links. Propagation through trees is discussed. The concepts of small area average, fast fading, and shadow fading (which is the same as log normal fading) are described. A technique for separating shadow fading from range dependence is presented, which is important for modeling purposes. Slope and intercept models are developed for prediction of propagation loss versus distance.

Indoor propagation is described in [A-28] and provides simplified equations for propagation loss prediction with statistics added in to account for dispersion and loss experienced by radio waves as they pass through walls, equipment, furniture, curtains, doors, ceilings, and people. It is an old reference, but it is instructive in the basic concepts to take into consideration when predicting propagation indoors. Comparisons are made between predictions and measured data. This paper is useful since it contains propagation data at 49.83 MHz. The author uses a fourth power in the distance model for propagation loss, and then adds certain modifications to account for different scenario conditions. The fourth power in distance model is:

$$P_r = P_t\, g_t\, g_r \left( \frac{h_t\, h_r}{d^2} \right)^2 \qquad \text{(A-29)}$$

where
$P_r$ is the received power.
$P_t$ is the transmitted power.
$g_t$ is the transmitter antenna gain.
$g_r$ is the receiver antenna gain.
$h_t$ is transmitter antenna height.
$h_r$ is transmitter antenna height.
d is the separation distance between the transmitter antenna and the receiver antenna.

An informative overview of what has been done in predictions and measurements for wireless personal communications up to 1994 is described in [A-29]. The macrocell environment with high base station antennas is discussed as well as the microcell environment with low antennas. An extensive bibliography is included with numerous references. Site specific as well as non-site specific analyses are considered. Indoor and outdoor propagation are discussed without many equations. Measurements in a rural environment were used to confirm the use of a two-ray model.

A more recent overview (up to June 2003) of what has been done in the area of propagation model predictions for mobile communications is described in [A-30]. Many of the models previously discussed are referenced in this paper. Both indoor and outdoor model environments are treated. A comparison of the models is included in the form of a table, and could be used for judging the applicability of one model over another for the limited instances where they could be applied to the short-range MTOM model.
[A-31] contains a large amount of measured data for the indoor radio-wave propagation environment.

Prediction of radio channel behavior for wireless systems beyond the second generation is described in [A-32]. Radio channel parameters are usually described in terms of statistical variations, but third and later generation wireless systems require statistical information about the delay spread and angle-of-arrival of the multipath signals. Rake receiver design for wideband code-division multiple-access systems depends on the statistics of multipath components in terms of the number of rays and their lifetime. Smart antennas and other complex antenna designs used in third generation and later systems need information about the angle-of-arrival of the multipath signals. To avoid expensive and time consuming measurements, it is advantageous to have computer software designed specifically for the prediction of area coverage, propagation loss, delay spread, angle-of-arrival, etc. The software should incorporate ray-tracing techniques using geometric optics and uniform theory of diffraction, and must account for building and terrain data for an appropriate site specific analysis to provide confidence in the prediction of these performance parameters. This paper describes the use of these ray-tracing codes to predict channel statistics. The authors describe how it is possible to

make statistically useful predictions of radio-channel characteristics using these ray-tracing techniques and accounting for reflections from the buildings and ground, diffraction at building edges, and non-specular scattering at building surfaces. Comparisons of predictions using these ray-tracing codes with measurements have shown that the small-area average power over a region can be computed with a mean error of 1 dB and a standard deviation of 8 dB. These same computer codes can be used to predict time delay spread and angle-of-arrival of the individual rays, because the ray-tracing codes with the data base of the environment give all the physical parameters of the ray paths. The statistical distributions of delay spread and angle-of-arrival obtained with these computer codes compare well with measurements. This is the latest work by these authors in attempting to describe the urban and suburban radio-wave propagation environment.

## A.4 WHAT CAN BE USED FROM AVAILABLE MODELS AND WHAT NEEDS TO BE DEVELOPED?

Existing models and measured data for both indoor and outdoor radio-wave propagation that could be used for developing the short-range MTOM model will be discussed here with an emphasis on outdoor propagation, since outdoor radio-wave propagation is a priority for the short-range MTOM model. There is a hierarchy of model approaches that could be used to develop the short-range MTOM model. These approaches can range from the simple slope and breakpoint techniques obtained from regression fits to measured data which are site-general and provide a rough approximation of the propagation loss, to a more complex site-specific approach that uses ray-tracing techniques with actual scenario geometries. The site-specific approach is much more accurate, but requires more information about the scenario and environment. A model approach in between the simple site-general and site-specific approaches would include algebraic formulas derived from the site-specific rigorous analysis, but simplified for easy use for a selection of different specific scenarios.

### A.4.1 Indoor Propagation

ITU Recommendation ITU-R P.1238 [A-2] can be used for frequencies at and above 900 MHz, but an indoor model for frequencies below 900 MHz will have to be developed. This model can be used out to distances of one kilometer. The minimum distance of slightly greater than one meter is greater than the distance that specifies the far-field at 900 MHz, but the distance to the far-field region will increase with decreasing frequency and the model will not be valid below 900 MHz. Other models available in the literature are very similar to this ITU model. These other references could provide some measured data at lower frequencies. [A-21] can provide additional measured data and modeling parameters at 433, 869, and 2450 MHz. [A-20] can provide indoor models and measured data at 900, 1300, and 1900 MHz, and this data has specified low antenna heights. [A-22] contains power law equations with statistical variations. Power-delay profiles, mean excess delay, rms delay spread, and excess delay spread for indoor

channels are discussed. These are essential parameters for modeling an indoor environment. [A-28] describes indoor propagation loss and provides similar equations to other references in addition to statistics to account for dispersion and loss experienced by radio waves as they pass through walls, equipment, furniture, curtains, doors, ceilings, and people. This paper contains data at the low VHF frequency of 49.83 MHz. [A-30] contains data and similar models for the indoor environment at frequencies from 850 MHz to over 4000 MHz. [A-31] is like [A-22], but with added shadowing considerations created by objects in the indoor environment. In addition to having to develop models at lower frequencies, investigations will have to be made for very close-in distances since near-field considerations and mutual coupling calculations will have to be taken into account. The surface wave at these distances also may affect the amount of signal propagating from transmitter to receiver.

### A.4.2 Outdoor Propagation

ITU Recommendation ITU-R P.1411[A-1] can be used for outdoor predictions in the 300 to 3000 MHz frequency range, but an alternative model will need to be developed for frequencies in the 150 to 300 MHz frequency range. A minimum distance is not specified for the LOS model, but the maximum distance is one kilometer, which falls short of our two kilometer requirement. The minimum distance needs to be determined, and is usually a function of the distance to be in the far-field region, mutual coupling, and possibly surface wave effects. The LOS antenna heights are not specified in this recommendation. The non-LOS distance range is specified as 20 to 500 meters, and the frequency range is 800 to 2000 MHz. Both of these models in ITU-R P.1411 do not meet all of the requirements of the short-range MTOM model, but could be used in their regions of validity. The receiver antenna height is for low antennas held by a pedestrian or in a vehicle, but the base station antenna height ranges from 4 to 50 meters. The base station antenna height is just out of the required range, but [A-6] uses the identical LOS model with transmitter antenna heights of 6.6 and 3.3 meters, a receiver antenna height of 1.5 meters, and a minimum distance of 10 meters, so the model could be valid for the required frequencies, antenna heights, and distances. The frequency for this reference is 1956 MHz. This model [A-6] and the associated measured data verifies the LOS model in ITU-R P.1411, but not the non-LOS model. A model for attenuation in foliage needs to be developed, since ITU-R P.833-4 has one antenna height that is too high for the short-range MTOM model. These are quasi-stationary models and do not take motion of transmitter or receiver into account.

The models and measured data in [A-7] begin with two-ray theory, but mostly fit slopes to measured data using a regression analysis. This work is an improvement over previous efforts and was performed at 900 and 1900 MHz. The lowest transmitter antenna height was at 3.3 meters and the receiver antenna height was at 1.6 meters. In the scenario geometry used for the measurements, the antenna patterns of the transmitter and receiver antennas significantly affect the measurements for distances less than ten meters, which is why it is difficult to take measurements at short distances. It was found that the shape of the envelope of the two-ray theory matches that of the two-slope/breakpoint model. The distance of the breakpoint from the transmitter was equal to the maximum distance that has first Fresnel zone clearance. The

measured data and models in this reference could be used for LOS analysis in the 900 and 1900 MHz frequency band. The non-LOS modeling in this frequency band is described by the same authors in [A-8]. The lowest transmitter antenna height was 3.2 meters and the receiver antenna height was 1.6 meters. The non-LOS paths included zig-zag and staircase patterns through urban and suburban neighborhoods. This paper analyzes diffraction around corners and states that it is valid to use diffraction as the total propagation phenomenon only when the antennas are below the rooftops. Good use can be made of the multiple regression slopes in this reference for non-LOS propagation [A-8]. Extensive LOS and non-LOS graphical data are available from the figures in the paper. A two-slope regression with breakpoint is used for LOS, and single-slope regression is used for non-LOS. Tables with numerous slopes and standard deviations for regression curve fits are contained in this paper, and equations can be created from this data.

[A-9] is a later attempt at refining the interpretation of the data in [A-7] and [A-8], and the results were the development of simpler LOS and non-LOS models. These simplified models could be used for the short-range MTOM model at the 900 to 1900 MHZ frequencies and for low antenna heights, but models at other frequencies outside of this range will need to be developed. A short-range model will need to be developed for distances less than 30 meters. Of particular interest to the short-range MTOM model is the measured data and modeling for the transmitter height of 3.2 meters in conjunction with the receiver antenna height of 1.6 meters. These models could be compared to the results of newly developed models at the low antenna heights and compared to measured data. [A-10] further investigates the measured data of [A-7 to A-9] and addresses the problem of just how significant the over-the-rooftops component of the diffraction signal is for the lowest transmitter antenna height. This theoretical model agrees well with measured data, and is further simplified in [A-11]. [A-11] is a further refinement of the models and measured data for 900 and1900 MHz of [A-7 to A-9] with the transmitter height antenna at 3.2 meters and the receiver antenna height at 1.6 meters. This model was developed from approximations to the complex theoretical mathematical models, but the models described in previous references were derived from measured data using regressive curve fits to the data, or algebraic algorithms derived from the data. A simplified version of the complex theoretical model was developed for three cases: near, above, and below roof level. This model could provide a good comparison with newly developed models and other measured data. Models in previously discussed references were derived from measured data and other regression curve fits to that data or algebraic algorithms fitted to the data. The minimum valid distance is in the 30 to 50 meter range, since this model is based on the data of [A-7 to A-9]. [A-12] analyzes the data from [A-7 to A-9] and determines that microcellular propagation is far from being isotropic, but is in fact anisotropic. A suburban or urban environment with rectangular street grids has a propagation characteristic that is diamond shaped rather than circular. These new equations can provide additional data for our short-range MTOM model, since some of the environments are slightly different from those discussed in [A-9] even though the minimum distances are the same.

[A-13] describes models developed by different authors than in the previously described references, but their approach is very similar. They use the distance power law for a LOS model with a dual slope which can be used to accurately characterize the measured path loss for the LOS case only when no more than two rays are involved. For other situations, a double

regression formula is used for LOS, and a single regression formula is used for non-LOS. Two separate methods are used for LOS. One method fixes the breakpoint at the first Fresnel zone distance and the other method uses the value of distance and loss that results in the minimum mean square error for all data. This reference provides independent measured data from other authors at 1900 MHz at low antenna heights and some single and double regression curve fits to the data.

[A-17] contains measurements and predictions for wideband propagation at 1800 MHz using low antenna heights where both antennas are at 1.7 meters. These authors are the same as [A-13]. [A-17] contains interesting data for low transmitter antenna heights of 2 to 3.5 meters and receiver antenna heights of 1.7 meters at extremely short distances of 2 to 12 meters at 5300 MHz. Even though the frequency range for this data is outside that for the short-range MTOM model, the propagation at 3000 MHz may be similar. This reference maintains that the two-ray model can reliably estimate the shape of the loss curve as well as the location and depth of the fades for the open roadway scenario. The parking lot scenario is also of interest.

[A-19] describes a site specific model where actual dimensions of the neighborhood and buildings are used with ray-based algorithms. This reference mentions that additional ray paths need to be included for accurate modeling, including those ray paths that involve reflections at buildings near the base station and diffraction rays at the vertical edges of the buildings.

[A-22] contains additional data at 900, 1300, and 1900 MHz with low antenna heights for the microcellular environment. Power law equations with statistical variation that calculates the local average signal are given for both indoor and outdoor microcellular propagation. Linear regression of the measured data is used to compute the slope (exponent) of the function.
Out of the four references [A-23 to A-27] for waveguide urban street models, [A-23] is the best one to use for narrow urban street radio-wave propagation for 30 to 3000 MHz, since this author's other references have verified model performance over this frequency range, and [A-23] has the most simplified form of the equations.

[A-29] is a book that contains much of the information from the journal papers of the author H.L. Bertoni and his coworkers, but gives more information on building models in addition to a technique for separating shadow fading from signal variation due to changes in distance. The book mentions that for the case of tall buildings in a low antenna environment, loss prediction requires only a two-dimensional data base of the building footprints.

[A-32] is a very recent reference that describes the requirements for computer software designed specifically for the prediction of area coverage, propagation loss, delay spread, angle-of-arrival, etc. The software should incorporate ray-tracing techniques using Geometric Optics (GO) and Uniform Theory of Diffraction (UTD), and must account for building and terrain data for an appropriate site-specific analysis to provide confidence in predicting these performance parameters. This paper describes the use of these ray-tracing techniques to predict channel statistics. The authors describe how it is possible to make statistically useful predictions of radio-channel characteristics using these ray-tracing techniques accounting for reflections from the buildings and ground, diffraction at building edges, and non-specular scattering at building

surfaces. These computer programs can be used to predict time delay spread and angle-of-arrival of the individual rays, because the ray-tracing codes with the environment data bases give all of the physical parameters of the ray paths. This is the latest work by these authors in attempting to describe the urban and suburban radio-propagation environment. This type of modeling is in the site-specific category and requires a significant effort to implement.

## A.5 CONCLUSION

The development of models requiring close-in distances on the order of one meter, low antenna heights of one to three meters, and frequencies as low as 30 MHz will require special consideration that currently available models do not include in their methods of analysis. Each of these requirements has conditions and constraints that have to be provided for to make accurate propagation loss predictions. Satisfying all three of these requirements simultaneously increases the complexity needed for a model or group of models to meet the objectives of providing accurate propagation loss predictions. None of the models and measured data in the currently existing literature references or ITU-R Recommendations can provide an accurate analysis and meet all of these requirements simultaneously. Section A.4 of this report described the areas where these references and Recommendations are appropriate to be used for analyses on a limited basis, providing only part of the needed frequency band, a portion of the required distance range, and the higher antenna heights, and will be applicable for the desired environment. Even a combination of these models will not meet the requirements for any significant amount of the frequency band, distance range, or antenna height range of the short-range MTOM model.

The development of a model that will provide loss predictions for close-in distances as short as one meter requires the use of mutual coupling predictions and possibly the inclusion of a surface wave. The antenna patterns of the antennas will not be valid at close separation distances since they will not be in the far field of the antennas, and will be in the near field or induction field of the antenna. This situation gets more significant for the lower frequencies of 900 MHz and below.

For low antenna heights the effects of the close proximity of the Earth to the antenna produces a strong interaction between the antenna patterns and the ground. The antenna pattern performance is vastly different than if the antenna were in free space. The use of a free-space antenna gain will not be valid. If the antenna is within a half wavelength of the ground, the antenna input impedance is affected, and will affect the efficiency and gain of the antennas.

At short distances of one meter and simultaneously having a close proximity to Earth of one to three meters, the surface wave component of the ground wave is significant even at frequencies up to 450 MHz.

Providing a propagation model that will simultaneously meet all these requirements will require special consideration that currently available models do not include in their methods of analysis. Thus, it is necessary to develop alternative models to meet the requirements of the short-range MTOM model.

## A.6 REFERENCES


[A-1] ITU-R (International Telecommunication Union-Radiocommunication Sector), Propagation Data and Prediction Methods for the Planning of Short-Range Outdoor Radiocommunication Systems and Radio Local Area Networks in the Frequency Range 300 MHz to 100 GHz, Recommendation ITU-R P.1411-2, International Telecommunication Union, Geneva, Switzerland, 2003.

[A-2] ITU-R, Propagation Data and Prediction Methods for the Planning of Indoor Radiocommunication Systems and Radial Local Area Networks in the Frequency Range 900 MHz to 100 GHz, Recommendation ITU-R P.1238-3, International Telecommunication Union, Geneva, Switzerland, 2003.

[A-3] ITU-R, Method for Point-to-Area Predictions for Terrestrial Services in the Frequency Range 30 MHz to 3,000 MHz, Recommendation ITU-R P.1546-1, International Telecommunication Union, Geneva, Switzerland, 2003.

[A-4] ITU-R, Proposed Revision to Recommendation ITU-R P.1546-2, International Telecommunication Union, Geneva, Switzerland, 2005.

[A-5] ITU-R, Attenuation in Vegetation, Recommendation ITU-R P.833-4, International Telecommunication Union, Geneva, Switzerland, 2003.

[A-6] V. Erceg et al., "Urban/suburban out-of-sight propagation modeling," *IEEE Communications Magazine*, pp. 56-61, June 1972.

[A-7] H.H. Xia et al., "Radio propagation characteristics for line-of-sight microcellular and personal communications," *IEEE Trans. Ant. Prop.*, AP-41, No. 10, pp. 1439- 1447, Oct. 1993.

[A-8] H.H. Xia et al., "Microcellular propagation characteristics for personal communications in urban and suburban environments," *IEEE Trans. Vehic. Technol.*, No. 3, Vol 43, pp. 743-752, Aug. 1994.

[A-9] D. Har, H.H. Xia, and H.L. Bertoni, "Path-loss prediction model for microcells," *IEEE Trans. Vehic. Technol.*, Vol. 48, No. 5, pp. 1453-1462, Sep.1999.

[A-10] L.R. Maciel, H.L. Bertoni, and H.H. Xia, "Unified approach to prediction of propagation over buildings for all ranges of base station antenna height," *IEEE Trans. Vehic. Technol.*, Vol. 42, No. 1, pp. 41-45, Feb.1993.

[A-11] H.H. Xia, "A simplified analytical model for predicting path loss in urban and suburban environments," *IEEE Trans. Vehic. Technol.*, Vol. 46, No. 4, pp. 1040-1046, Nov.1997.

[A-12] D. Har and H.L. Bertoni, "Effect of anisotropic propagation modeling on microcellular system design," *IEEE Trans. Vehic. Technol.*, Vol. 49, No. 3, pp. 1303-1313, May 2000.

[A-13] M.J. Feuerstein et al., "Path loss, delay spread, and outage models as functions of antenna height for microcellular system design," *IEEE Trans. Vehic. Technol.*, Vol. 43, No. 3, pp. 487-498, Aug. 1994.

[A-14] A.J. Goldsmith and L.J. Greenstein, "A measurement-based model for predicting coverage areas of urban microcells," *IEEE Journal on Selected Areas in Communications*, Vol. 11, No. 7, pp. 1013-1023, Sep. 1993.

[A-15] A.J. Rustako, Jr et al., "Radio propagation at microwave frequencies for line-of-sight microcellular mobile and personal communications," *IEEE Trans. Vehic. Technol.*, Vol 40, No. 1, pp. 203-210, Feb. 1991.

[A-16] K.L. Blackard et al., "Path loss and delay spread models as functions of antenna height for microcellular system design," Proceedings, *IEEE Vehicular Technology Conference*, Denver, CO, May 10-13, 1992, Vol. 1, pp.333-337.

[A-17] N. Patwari et al., "Peer-to-peer low antenna outdoor radio wave propagation at 1.8 GHz," Proceedings, *IEEE Vehicular Technology Conference*, Houston, TX, May 16-20, 1999, Vol. 1, pp. 371-375.

[A-18] A. Domazetovic et al., "Propagation models for short-range wireless channels with predictable path geometries," *IEEE Trans. Comm.*, Vol. 53, No. 7, pp. 1123-1126, Jul. 2005.

[A-19] L. Piazzi and H.L. Bertoni, "Achievable accuracy of site-specific path-loss predictions in residential environments," *IEEE Trans. Vehic. Technol.*, Vol. 48, No. 3, pp. 922-930, May 1999.

[A-20] K. Kalbasi and P. Washkewicz, "Propagation modeling for wireless design," *Communication Systems Design Magazine*, pp. 25-32, Feb. 1997.

[A-21] L.J.W. van Loon, "Mobile in-home UHF radio propagation for short-range devices," *IEEE Ant. Prop. Magazine*, Vol. 41, No. 2, pp. 37-40, Apr. 1999.

[A-22] T.S. Rappaport and S. Sanhu, "Radio-wave propagation for emerging wireless personal-communication systems," *IEEE Ant. and Prop. Magazine*, Vol. 36, no. 5, pp. 14-24, Oct.1994.

[A-23] N. Blaunstein, “Prediction of cellular characteristics for various urban environments,” *IEEE Ant. Prop. Magazine*, Vol. 41, No. 6, pp. 135 -144, Dec.1999.

[A-24] N. Blaunstein, R. Giladi, and M. Levin, “Characteristics prediction in urban and suburban environments,” *IEEE Trans. Vehic. Technol.*, Vol. 47, No. 1, pp. 225-234, Feb. 1998.

[A-25] N. Blaunstein, “Average field attenuation in the nonregular impedance street waveguide,” *IEEE Trans. Ant. Prop.*, Vol. 46, No. 12, pp. 1782-1789, Dec.1998.

[A-26] N. Blaunstein and M. Levin, “VHF/UHF wave attenuation in a city with regularly distributed buildings,” *Rad. Sci.*, Vol. 31, pp. 313-323, 1996.

[A-27] H.L. Bertoni, *Radio Propagation for Modern Wireless Systems*, New Jersey, Prentice Hall, 1999.

[A-28] T. Ishii, “RF propagation in buildings,” *RF Design Magazine*, pp. 45-49, Jul. 1989.

[A-29] H.L. Bertoni et al., “UHF propagation predictions for wireless personal communications,” *Proc. of the IEEE*, Vol. 82, No. 9, pp. 1333-1359, Sep.1994.

[A-30] T. Sarkar et al., “A survey of various propagation models for mobile communication,” *IEEE Ant. Prop. Magazine*, Vol. 45, No.3, pp. 51-82, Jun. 2003.

[A-31] T.S. Rappaport, “Factory radio communications,” *RF Design Magazine*, pp. 67-73, Jan. 1989.

[A-32] H.L. Bertoni, S.A. Torrico, and G. Liang, “Predicting the radio channel beyond second-generation wireless systems,” *IEEE Ant. and Prop. Magazine*, Vol. 47, No.4, pp. 28-40, Aug. 2005.

## APPENDIX B: PROPAGATION LOSS VS. DISTANCE WITH AND WITHOUT THE SURFACE WAVE

Appendix B contains a large number of figures that are referred to in the main body of the report, and it would be inappropriate to integrate this many figures into the corresponding section of the report. Appendix B is referred to in Section 2.3 and contains predicted propagation loss versus distance plots that demonstrate the significance of including the surface wave in propagation loss computations at six combinations of antenna heights and five different frequencies. These plots are a result of analytic computations described is Section 2.3. These plots show that the surface wave can have a significant effect on propagation loss prediction at frequencies at and below 450 MHz.

The numbers in parentheses in the figure legends, in this appendix and elsewhere in the report, e.g., n119se1f, are identifiers for the data set.

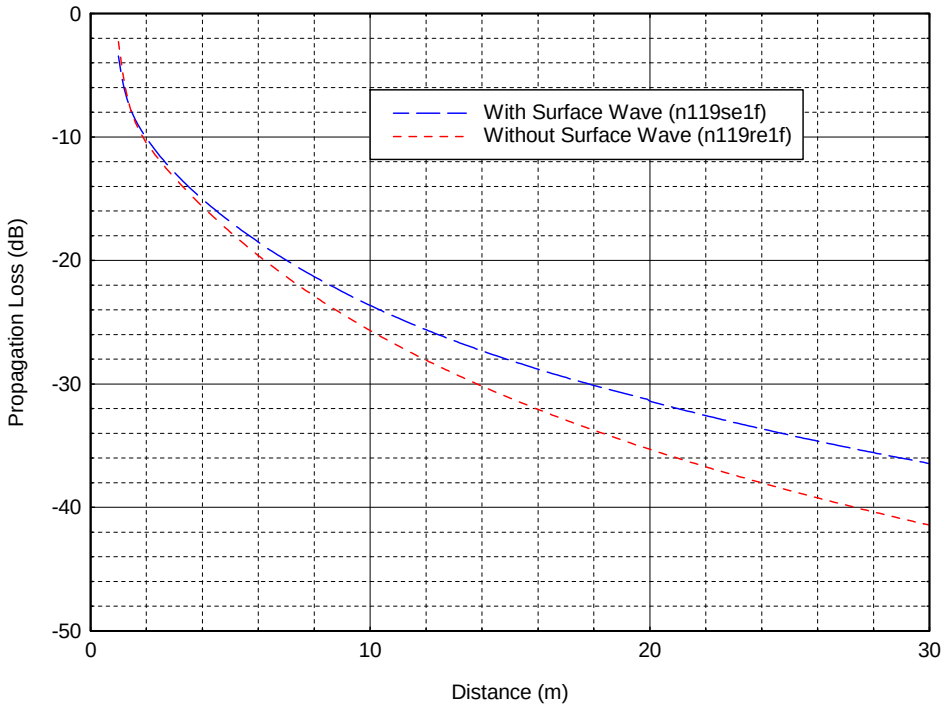


Figure B-1. Propagation loss vs. distance with and without the surface wave at 30 MHz for antenna heights $h_1$=1m and $h_2$=1m.

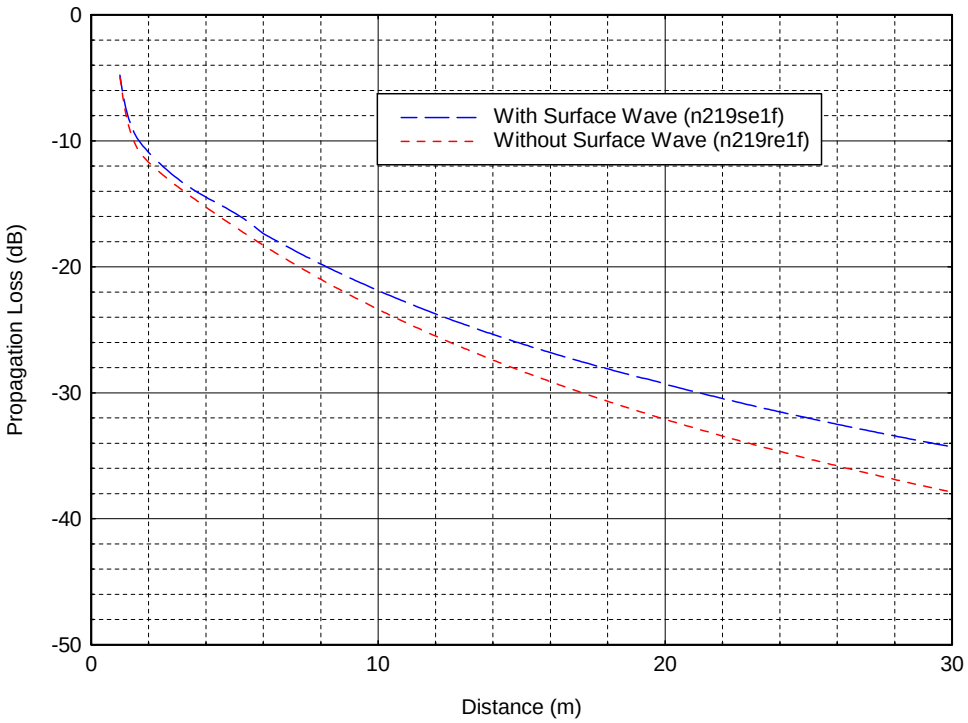


Figure B-2. Propagation loss vs. distance with and without the surface wave at 30 MHz for antenna heights $h_1$=2m and $h_2$=1m.

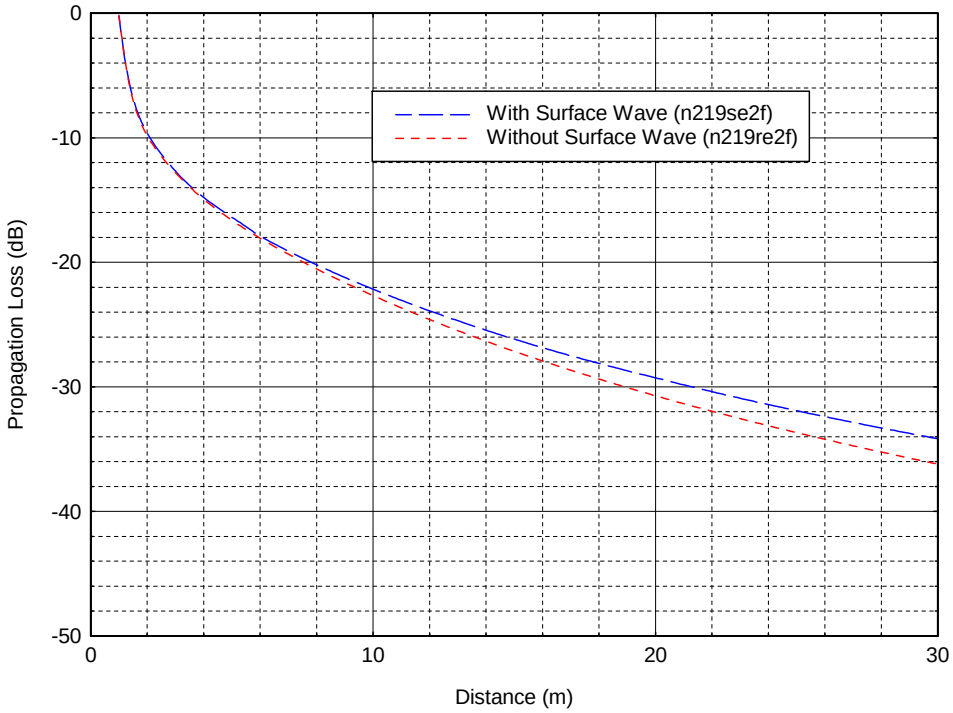


Figure B-3. Propagation loss vs. distance with and without the surface wave at 30 MHz for antenna heights $h_1$=2m and $h_2$=2m.

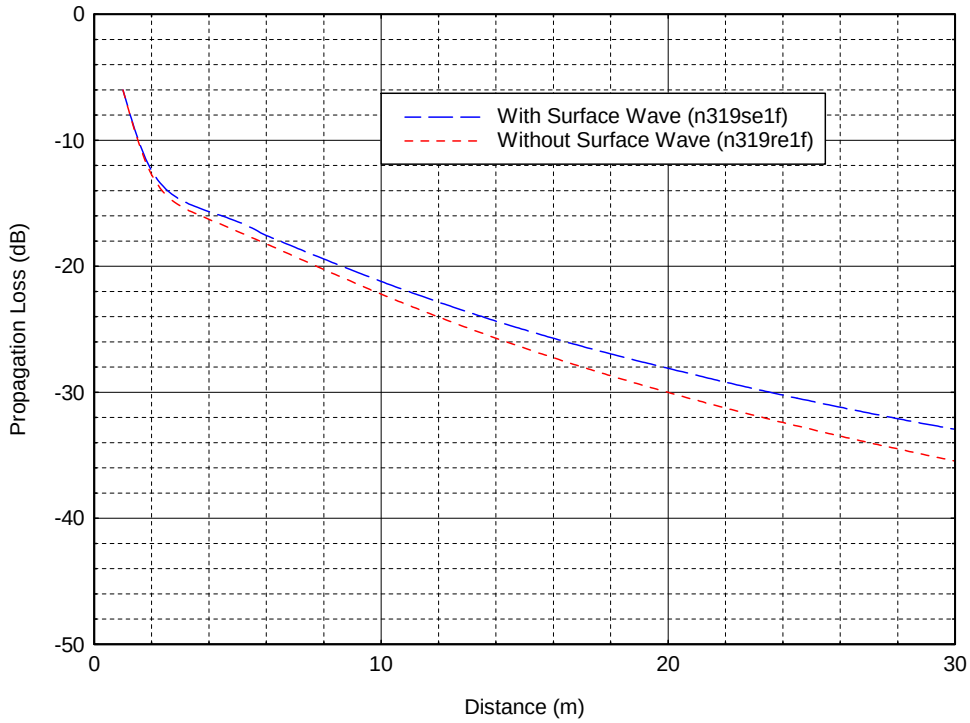


Figure B-4. Propagation loss vs. distance with and without the surface wave at 30 MHz for antenna heights $h_1$=3m and $h_2$=1m.

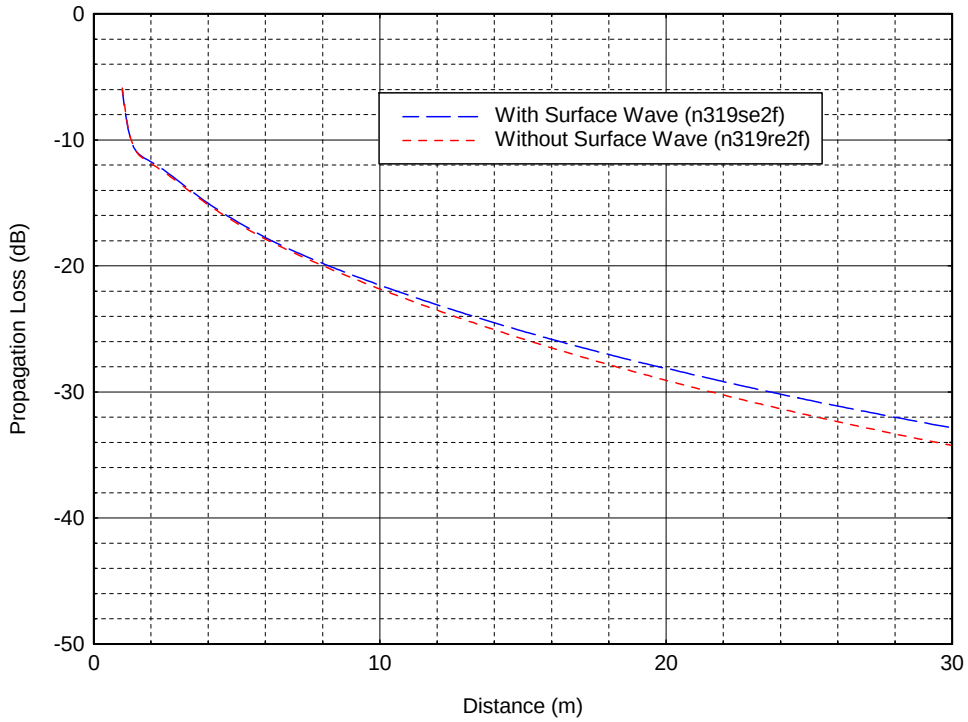


Figure B-5. Propagation loss vs. distance with and without the surface wave at 30 MHz for antenna heights $h_1$=3m and $h_2$=2m.

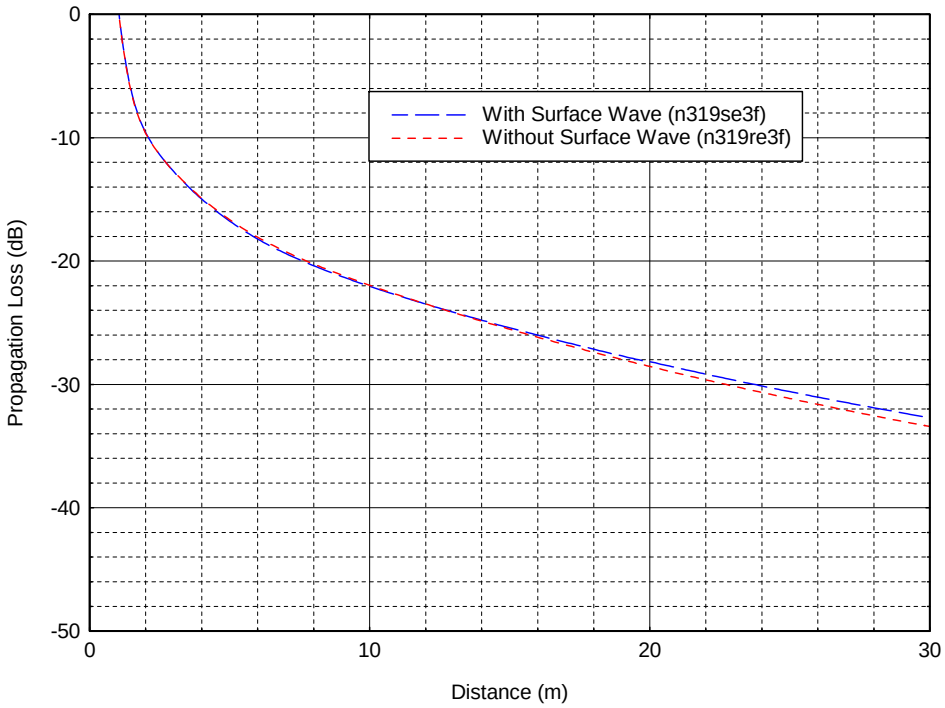


Figure B-6. Propagation loss vs. distance with and without the surface wave at 30 MHz for antenna heights $h_1$=3m and $h_2$=3m.

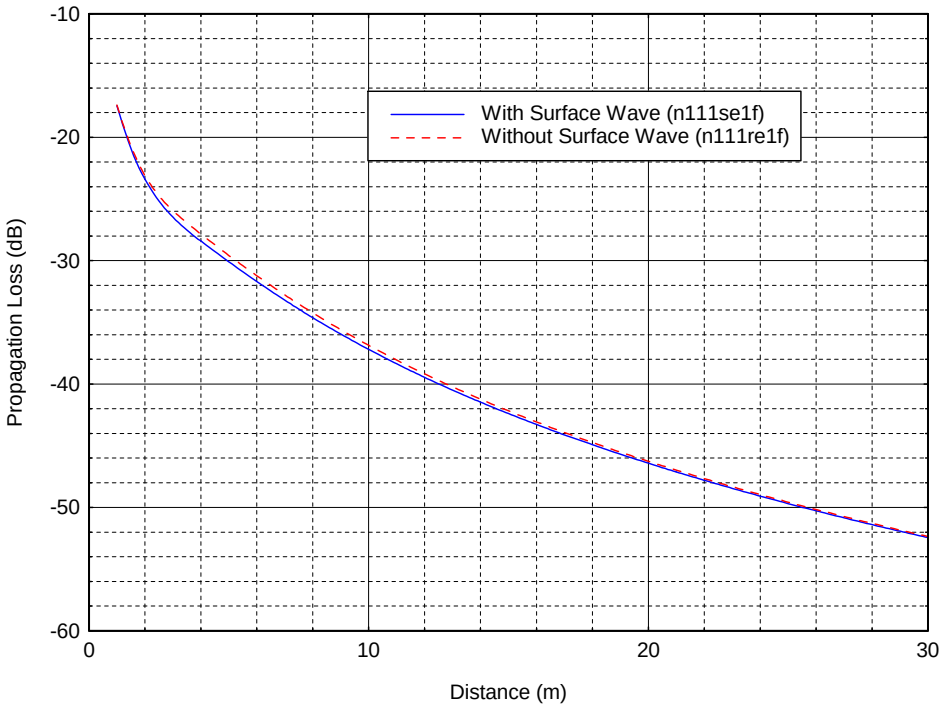


Figure B-7. Propagation loss vs. distance with and without the surface wave at 150 MHz for antenna heights $h_1$=1m and $h_2$=1m.

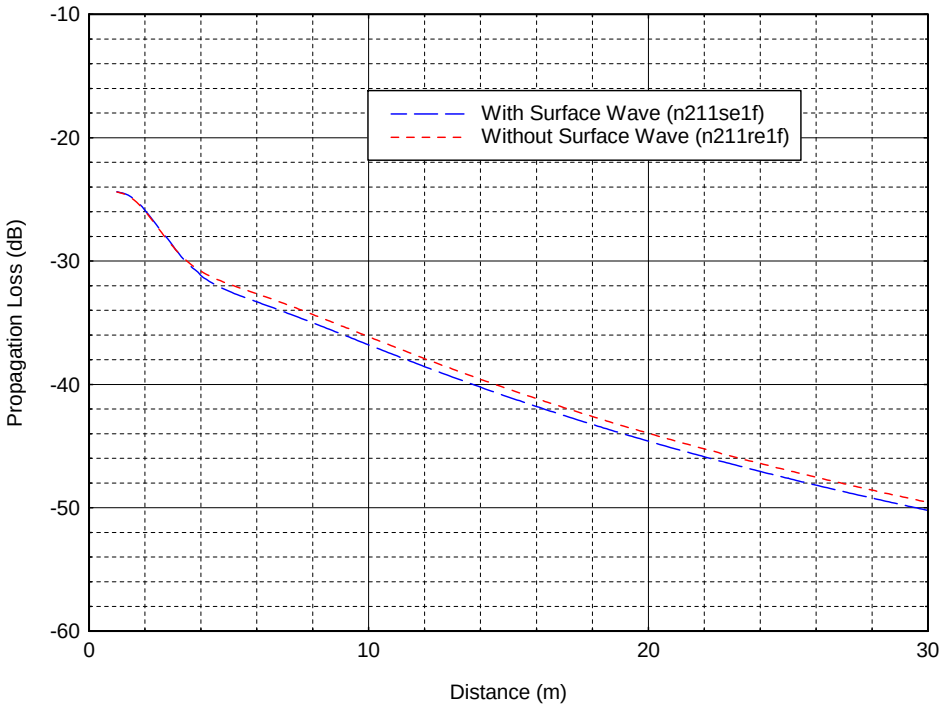


Figure B-8. Propagation loss vs. distance with and without the surface wave at 150 MHz for antenna heights $h_1$=2m and $h_2$=1m.

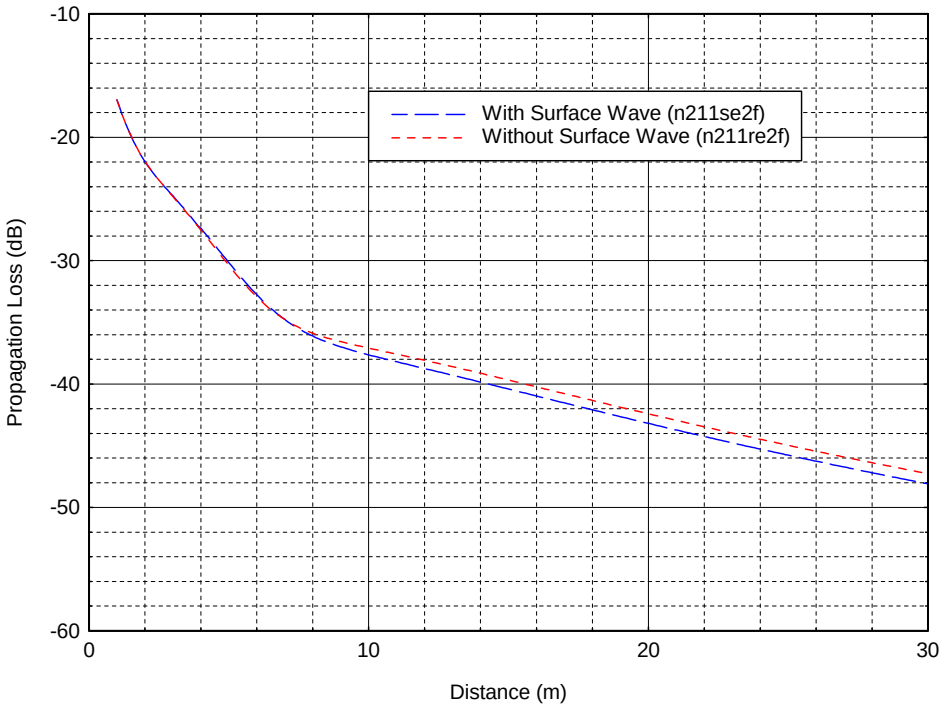


Figure B-9. Propagation loss vs. distance with and without the surface wave at 150 MHz for antenna heights $h_1$=2m and $h_2$=2m.

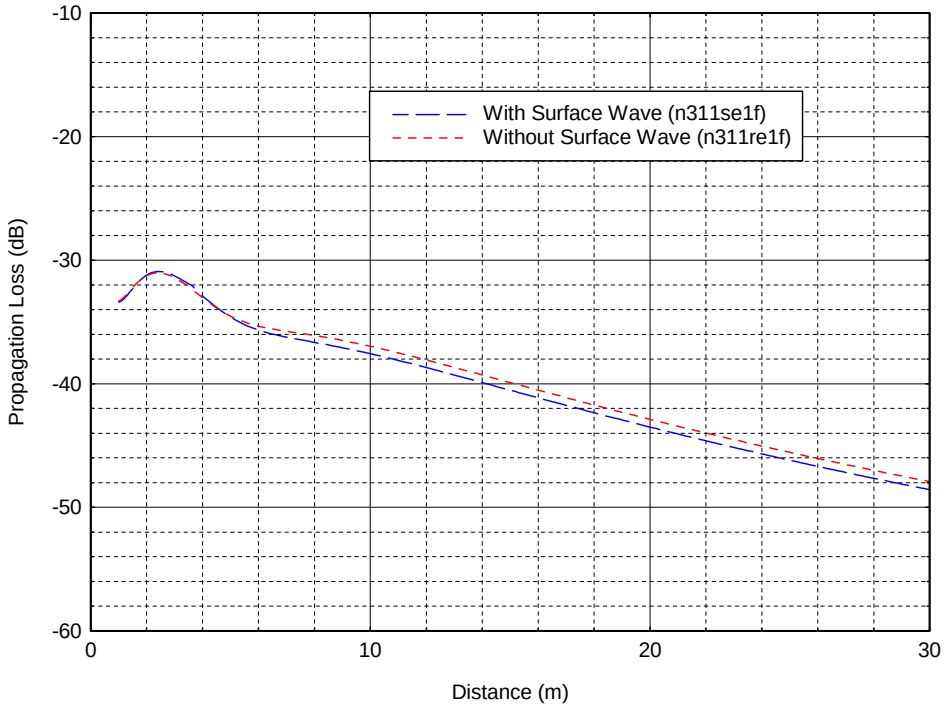


Figure B-10. Propagation loss vs. distance with and without the surface wave at 150 MHz for antenna heights $h_1$=3m and $h_2$=1m.

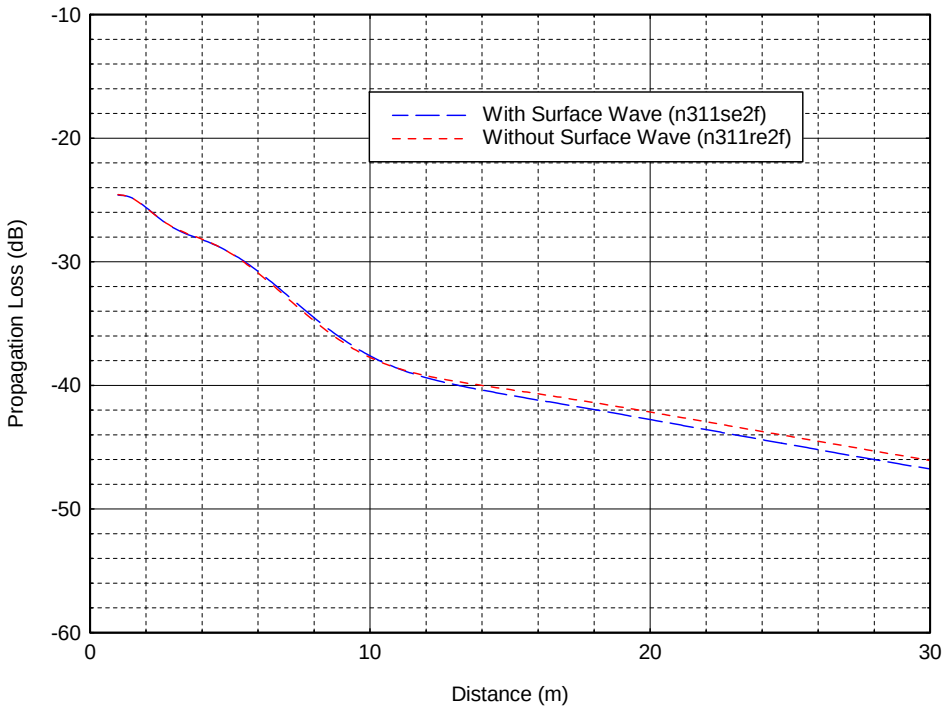


Figure B-11. Propagation loss vs. distance with and without the surface wave at 150 MHz for antenna heights $h_1$=3m and $h_2$=2m.

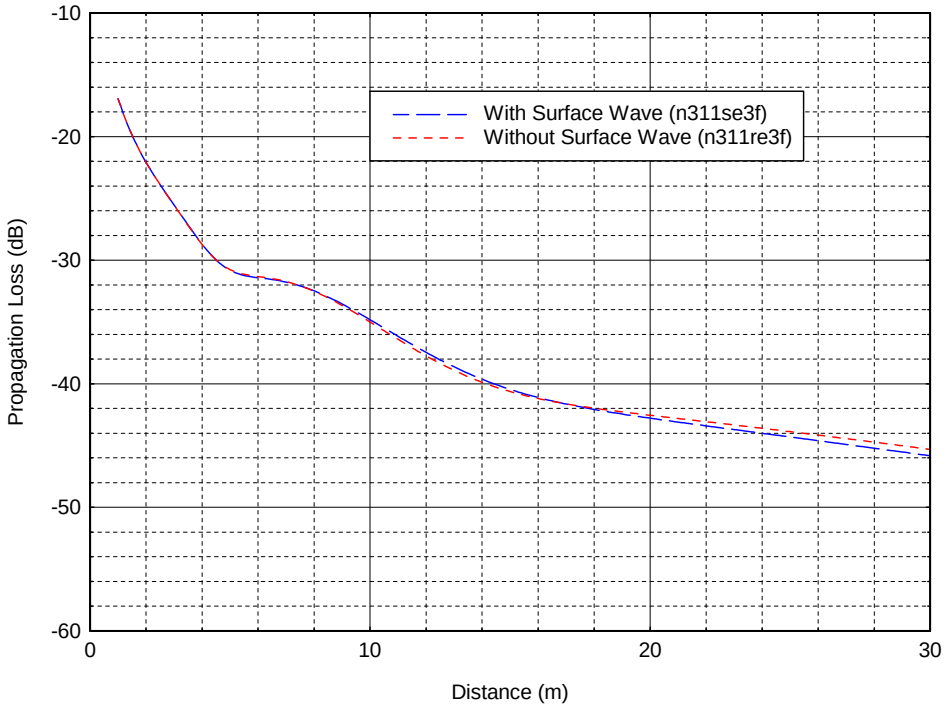


Figure B-12. Propagation loss vs. distance with and without the surface wave at 150 MHz for antenna heights $h_1$=3m and $h_2$=3m.

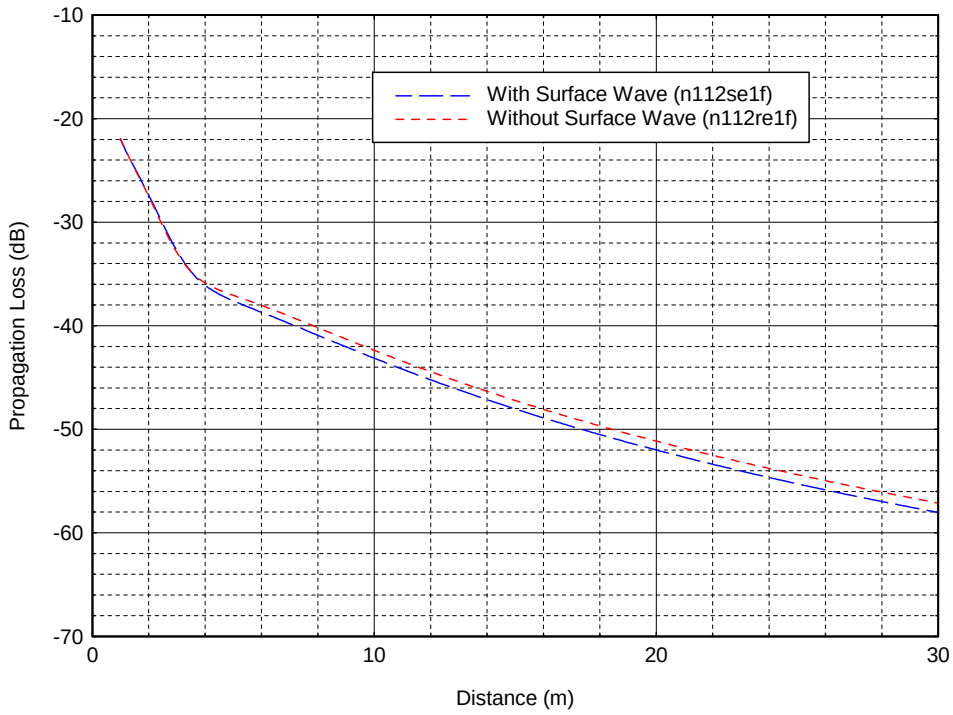


Figure B-13. Propagation loss vs. distance with and without the surface wave at 300 MHz for antenna heights $h_1$=1m and $h_2$=1m.

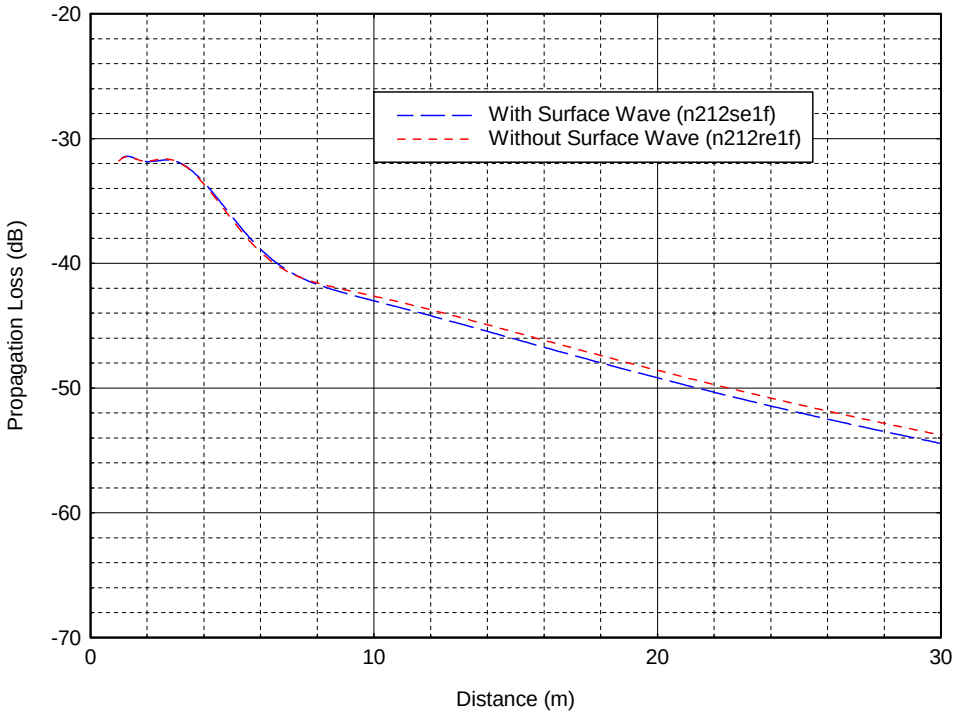


Figure B-14. Propagation loss vs. distance with and without the surface wave at 300 MHz for antenna heights $h_1$=2m and $h_2$=1m.

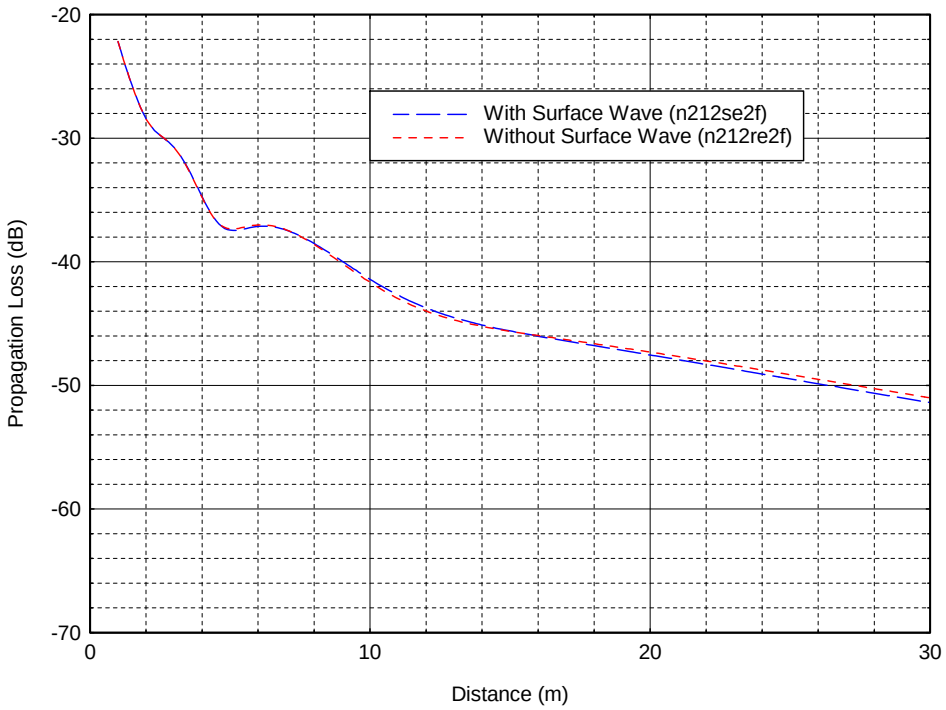


Figure B-15. Propagation loss vs. distance with and without the surface wave at 300 MHz for antenna heights $h_1$=2m and $h_2$=2m.

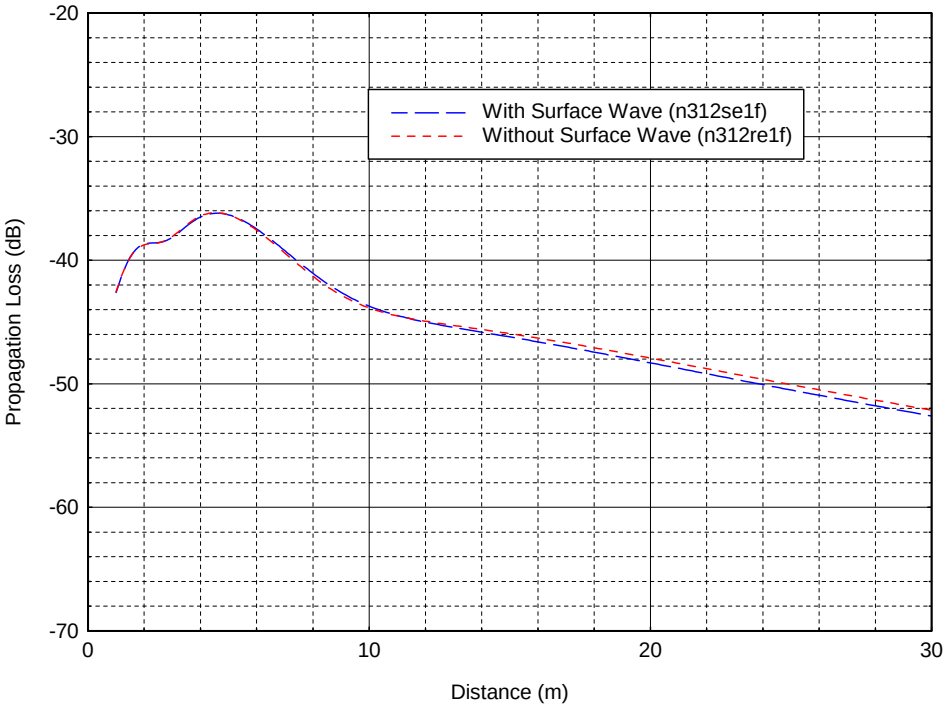


Figure B-16. Propagation loss vs. distance with and without the surface wave at 300 MHz for antenna heights $h_1$=3 and $h_2$=1.

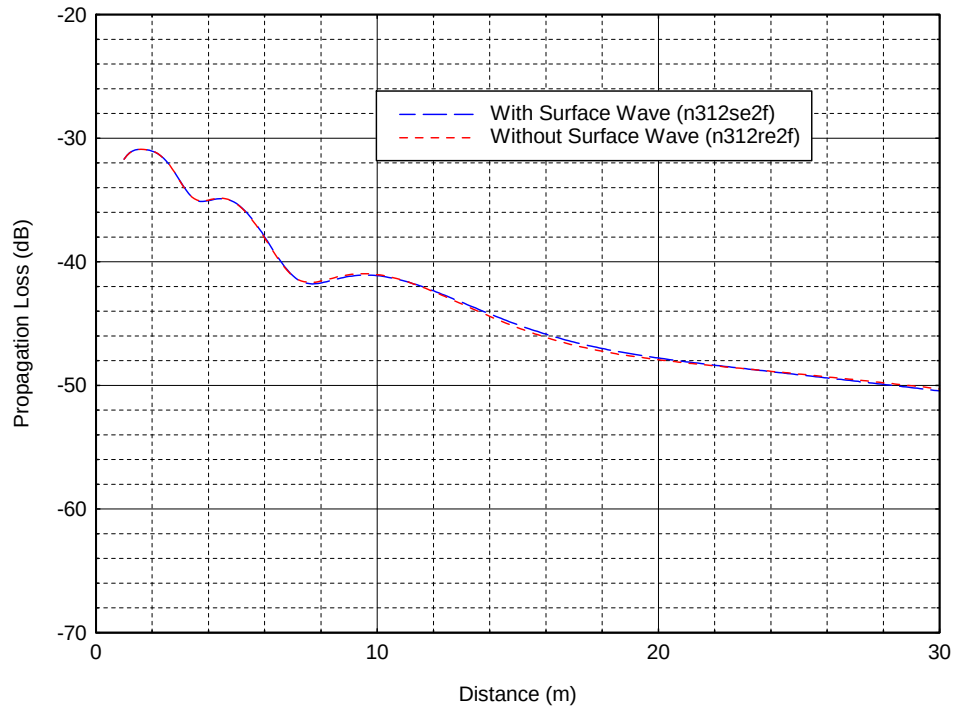


Figure B-17. Propagation loss vs. distance with and without the surface wave at 300 MHz for antenna heights $h_1$=3m and $h_2$=2m.

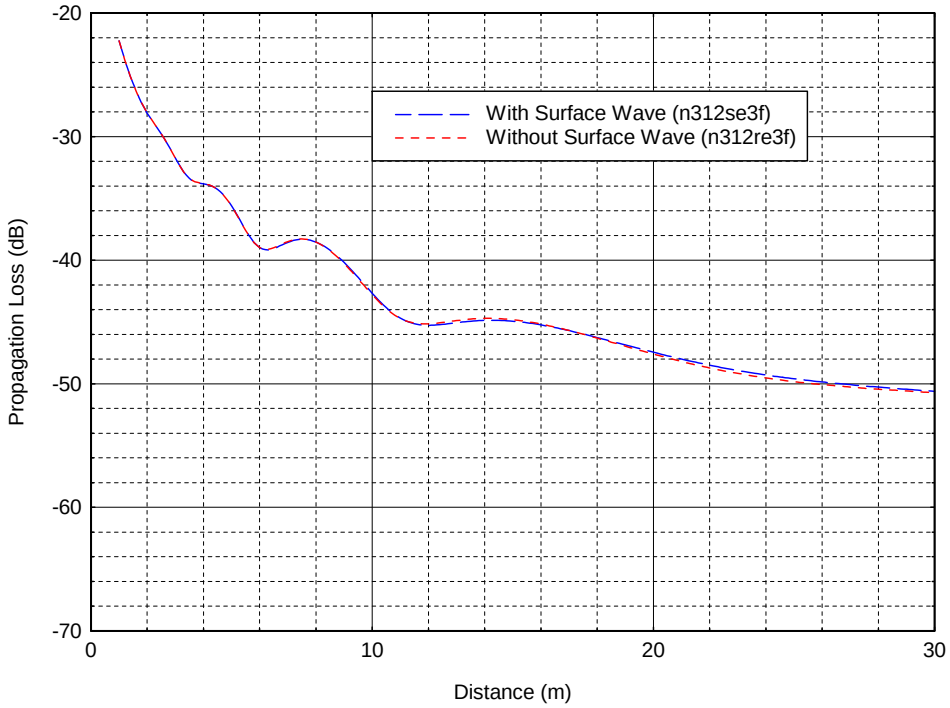


Figure B-18. Propagation loss vs. distance with and without the surface wave at 300 MHz for antenna heights $h_1$=3m and $h_2$=2m.

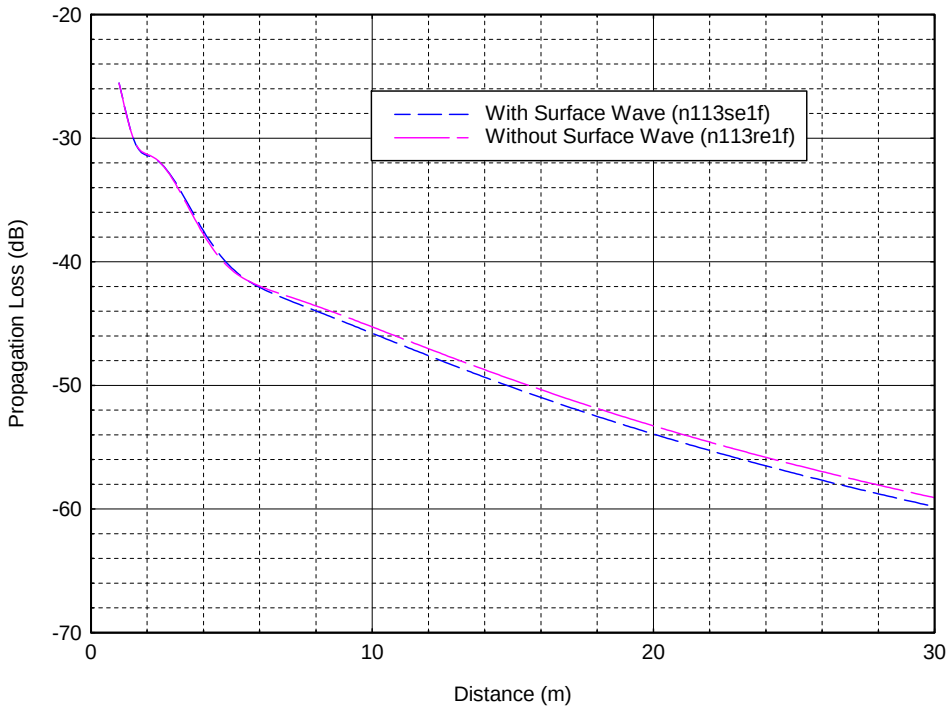


Figure B-19. Propagation loss vs. distance with and without the surface wave at 450 MHz for antenna heights $h_1$=1m and $h_2$=1m.

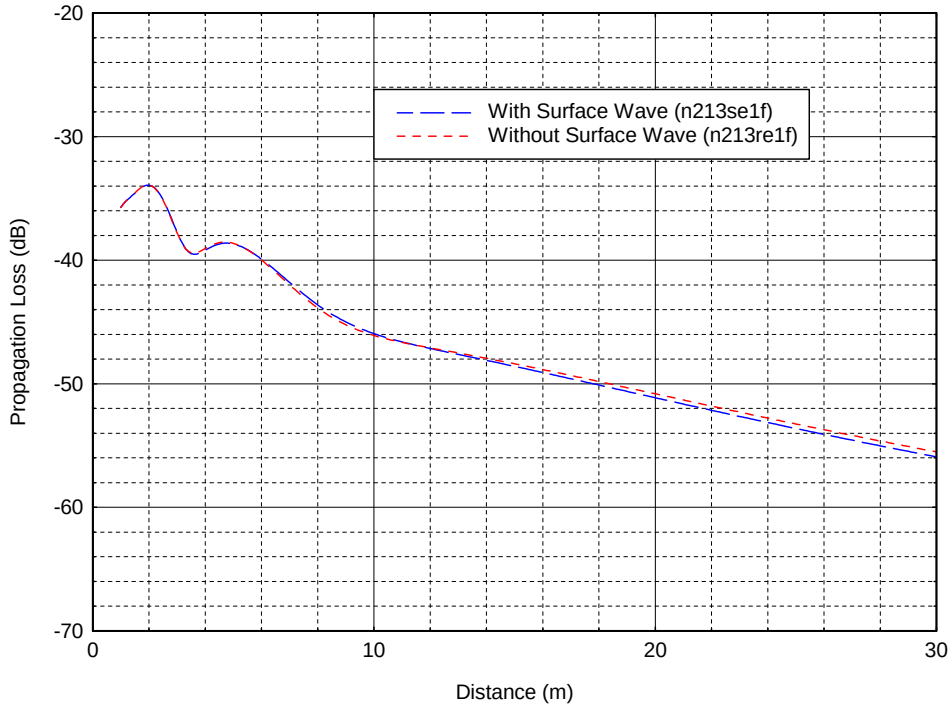


Figure B-20. Propagation loss vs. distance with and without the surface wave at 450 MHz for antenna heights $h_1$=2m and $h_2$=1m.

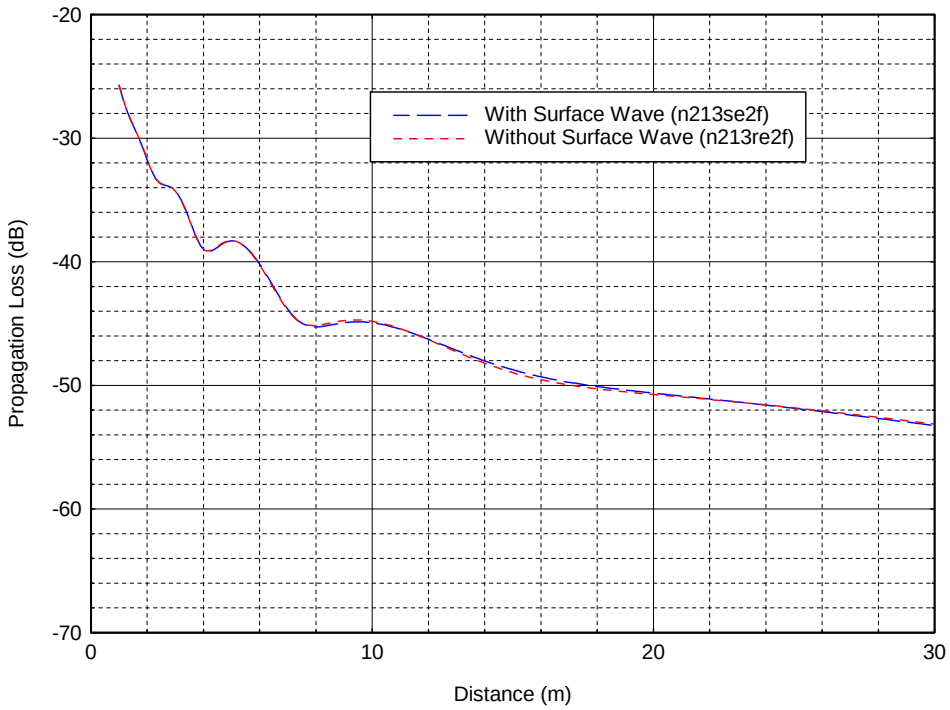


Figure B-21. Propagation loss vs. distance with and without the surface wave at 450 MHz for antenna heights $h_1$=2m and $h_2$=2m.

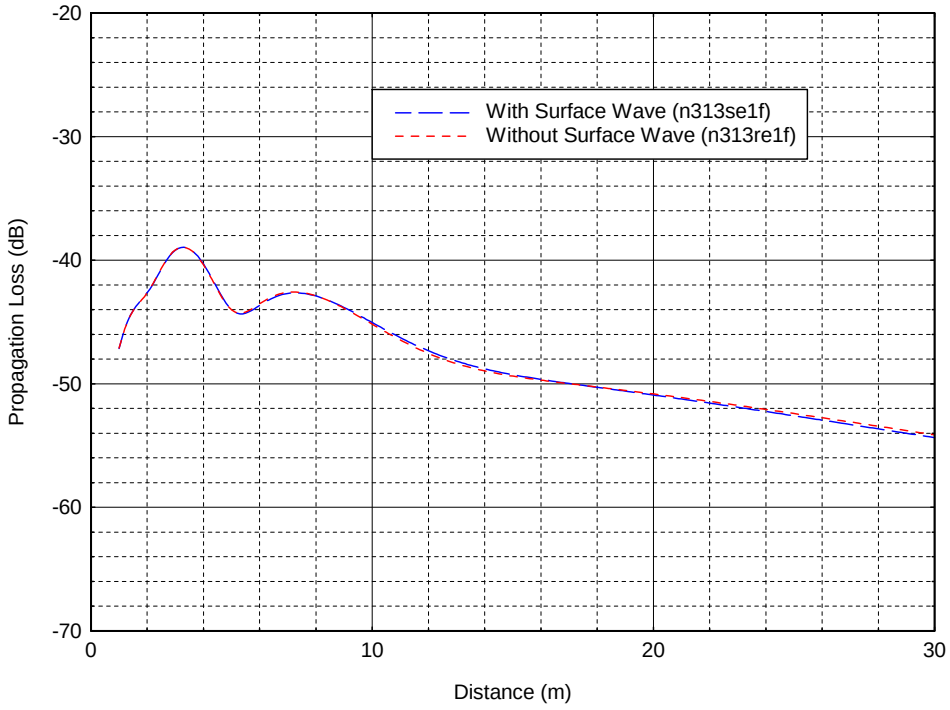


Figure B-22. Propagation loss vs. distance with and without the surface wave at 450 MHz for antenna heights $h_1$=3m and $h_2$=1m.

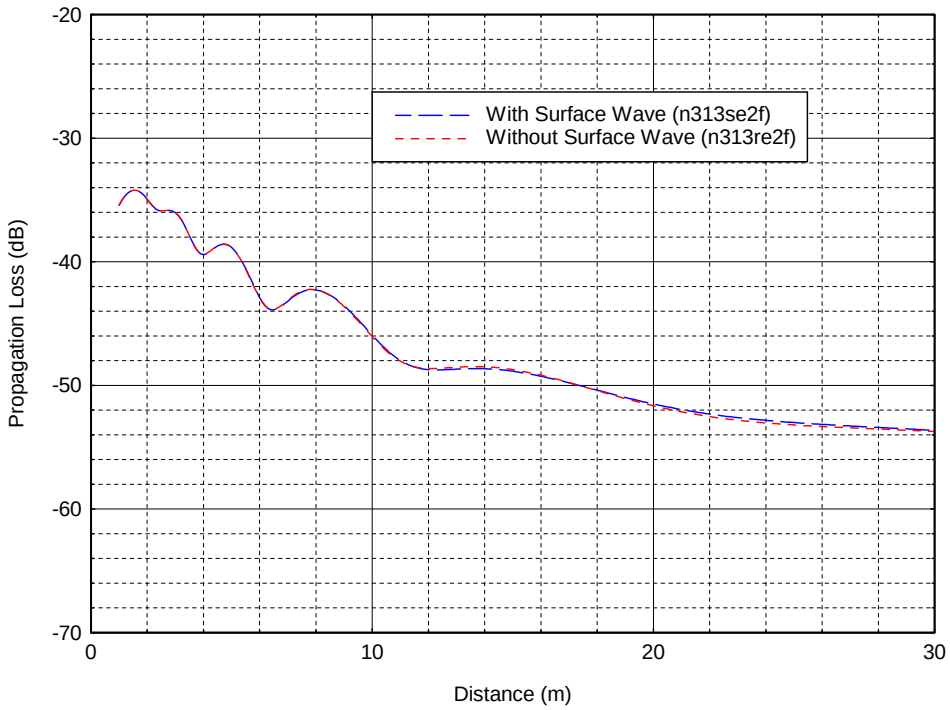


Figure B-23. Propagation loss vs. distance with and without the surface wave at 450 MHz for antenna heights $h_1$=3m and $h_2$=2m.

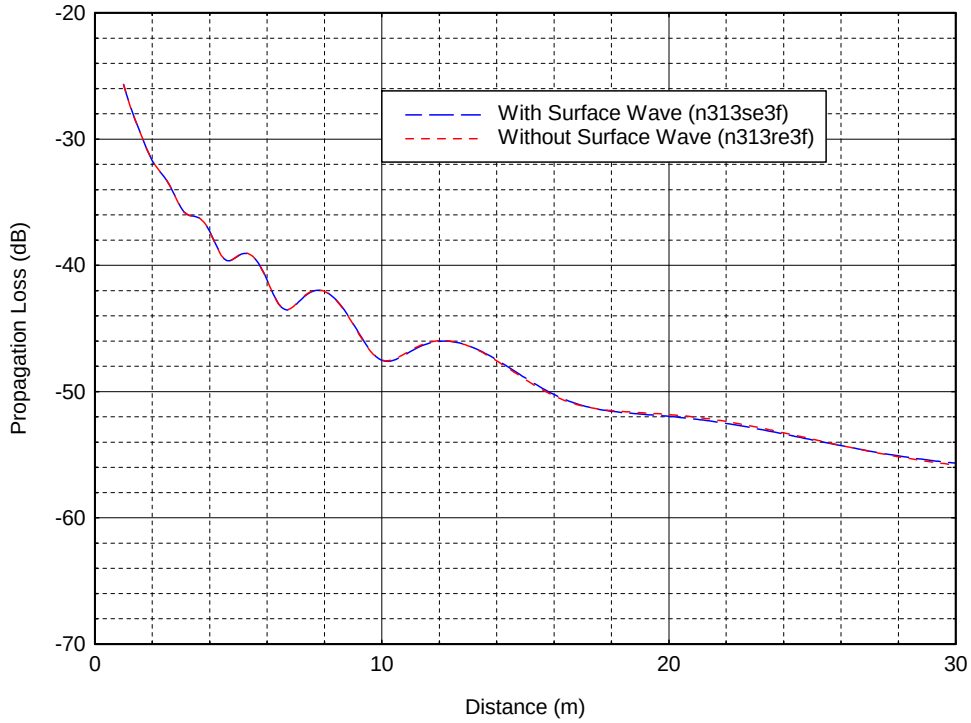


Figure B-24. Propagation loss vs. distance with and without the surface wave at 450 MHz for antenna heights $h_1$=3m and $h_2$=3m.

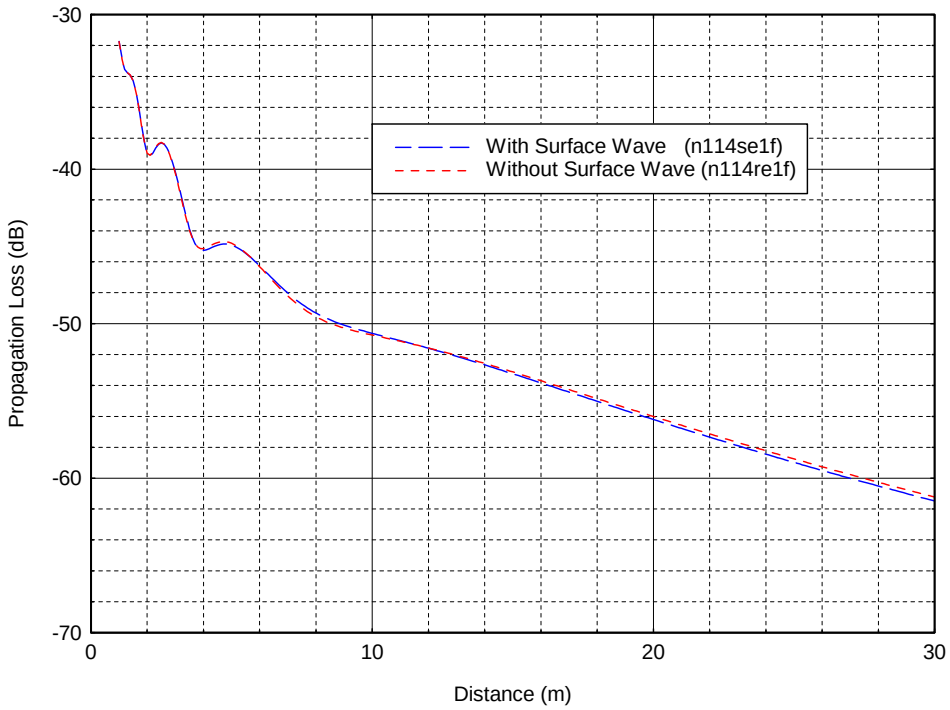


Figure B-25. Propagation loss vs. distance with and without the surface wave at 900 MHz for antenna heights $h_1$=1m and $h_2$=1m.

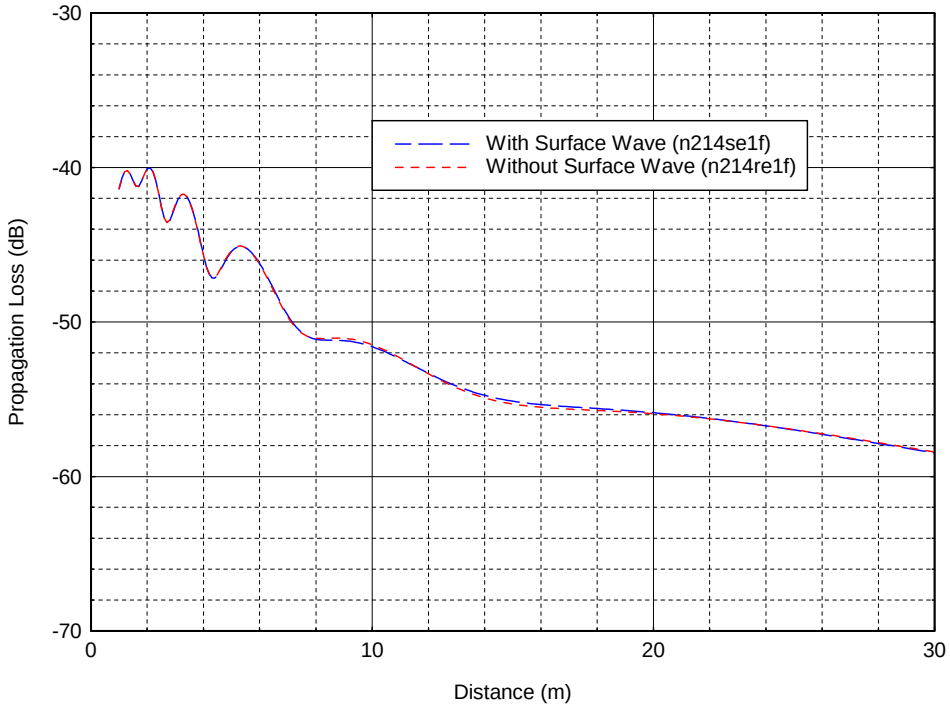


Figure B-26. Propagation loss vs. distance with and without the surface wave at 900 MHz for antenna heights $h_1$=2m and $h_2$=1m.

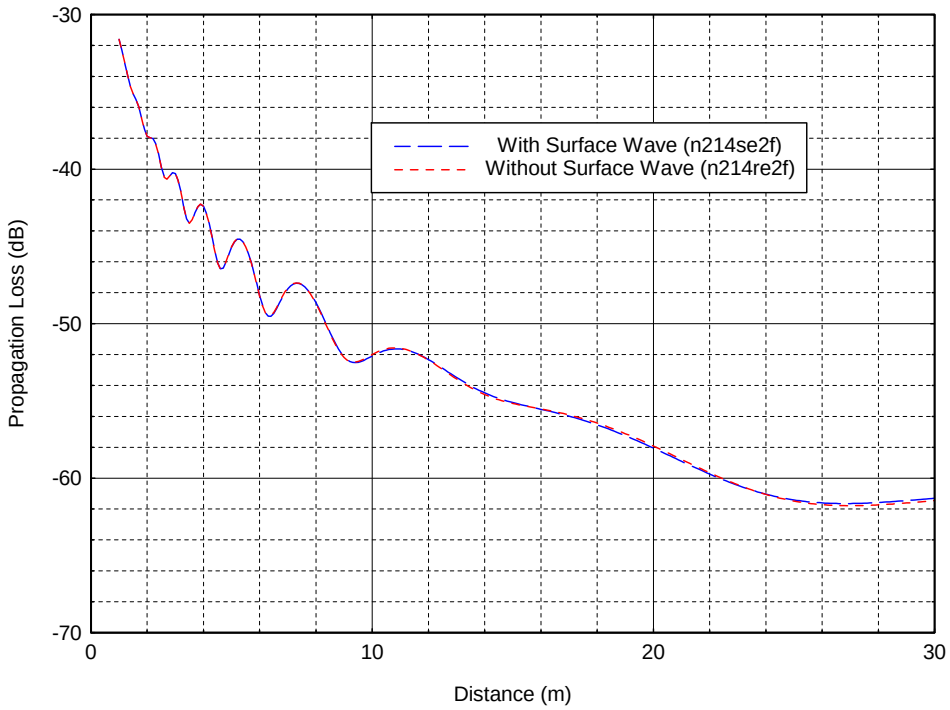


Figure B-27. Propagation loss vs. distance with and without the surface wave at 900 MHz for antenna heights $h_1$=2m and $h_2$=2m.

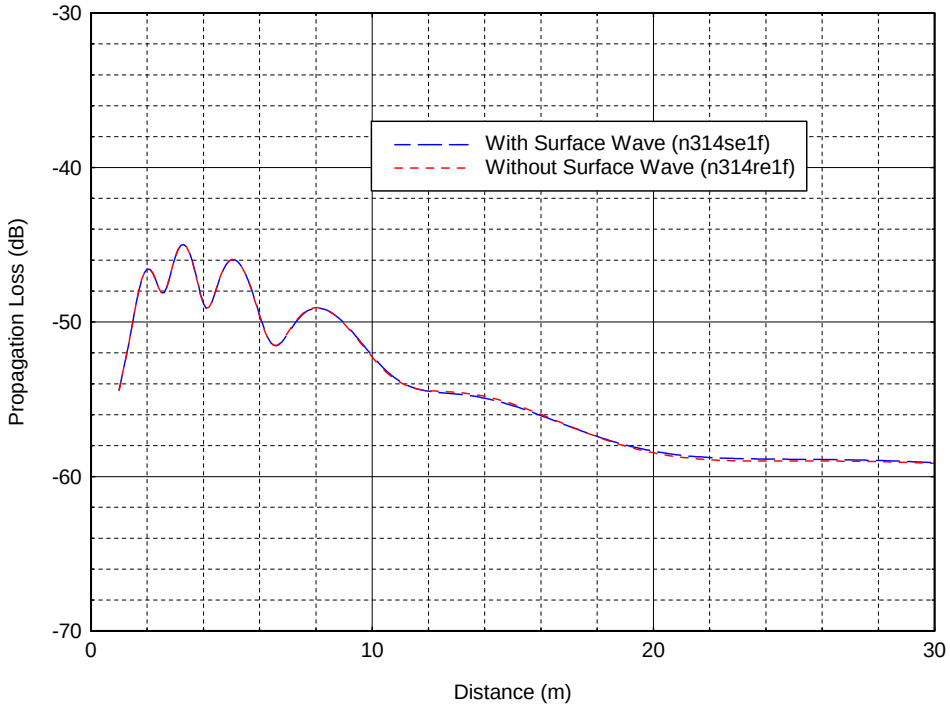


Figure B-28. Propagation loss vs. distance with and without the surface wave at 900 MHz for antenna heights $h_1$=3m and $h_2$=1m.

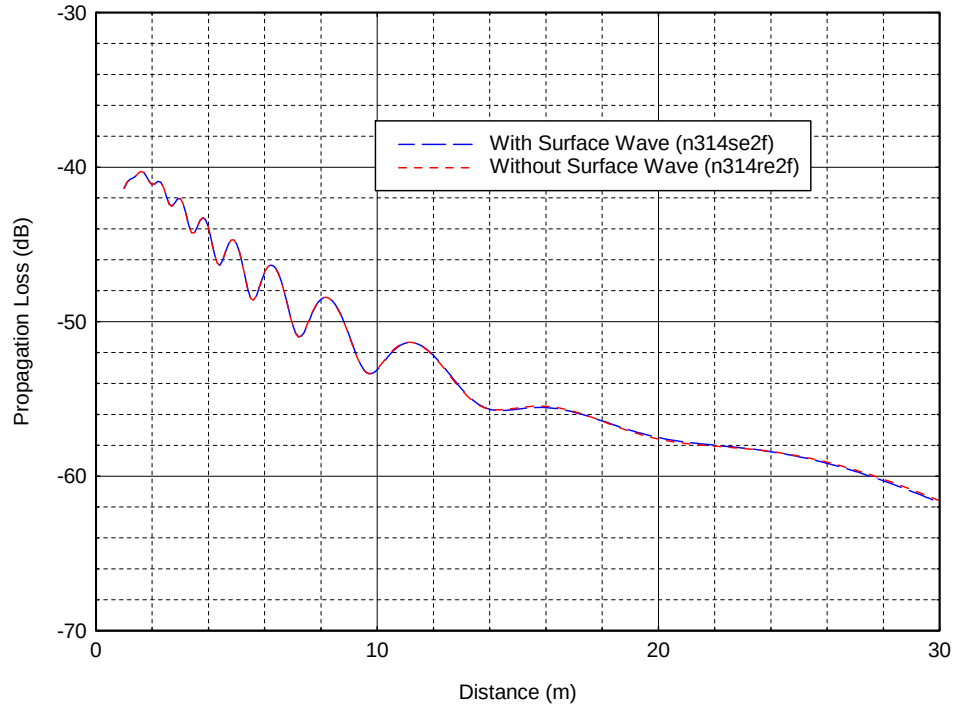


Figure B-29. Propagation loss vs. distance with and without the surface wave at 900 MHz for antenna heights $h_1$=3m and $h_2$=2m.

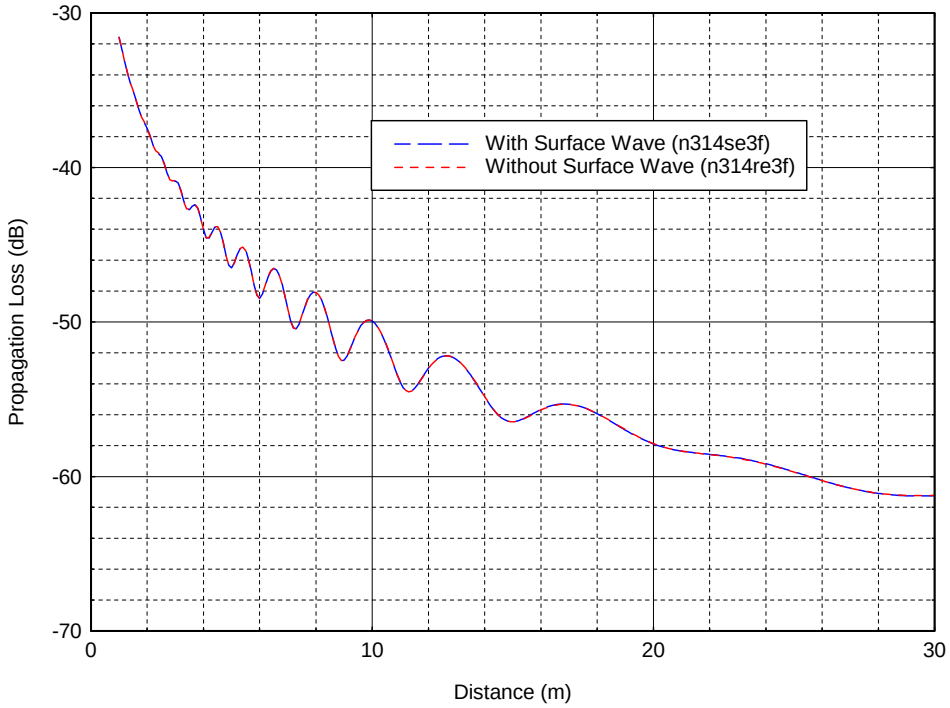


Figure B-30. Propagation loss vs. distance with and without the surface wave at 900 MHz for antenna heights $h_1$=3m and $h_2$=3m.

## APPENDIX C: ANTENNA ELEVATION PATTERNS FOR A VERTICAL HALF-WAVE DIPOLE AT DIFFERENT FREQUENCIES AND HEIGHTS ABOVE AVERAGE GROUND

Appendix C contains a large number of figures that are referred to in the main body of the report, and it would be inappropriate to integrate this many figures into the corresponding section of the report. Appendix C is referred to in Section 2.4 and contains computed antenna elevation patterns for a vertical half-wave dipole at six different frequencies for antenna heights of 1, 2, and 3 meters above average ground demonstrating the effects of the presence of ground. These plots are the results of analytic computations described in Section 2.4. Also shown is the free-space elevation antenna pattern. These figures show that the ground has a very significant effect on the antenna patterns, and the free-space antenna pattern is very different than the pattern that results for an antenna in a real environment over ground.

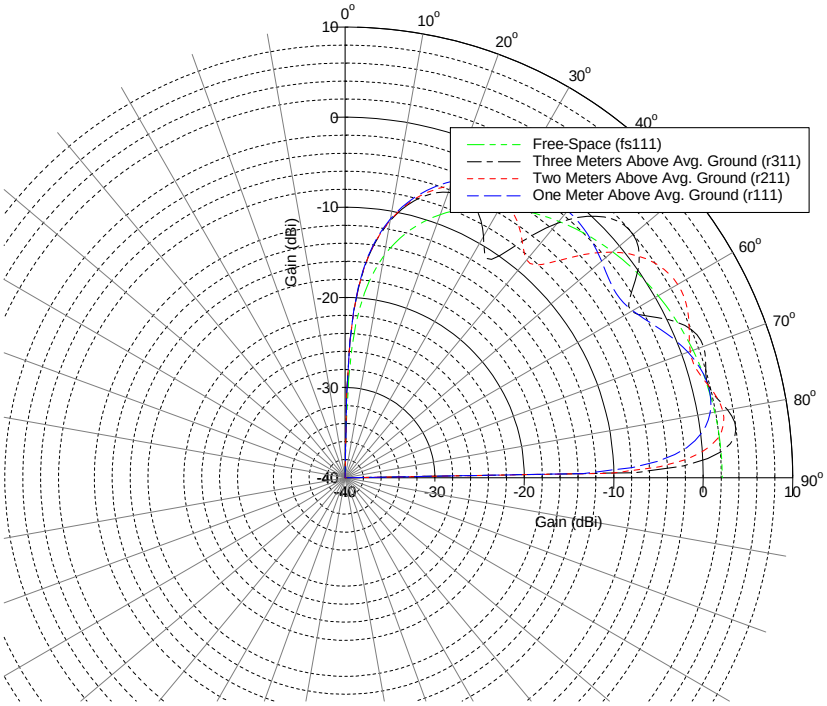


Figure C-1. Elevation patterns for vertical half-wave dipole at 150 MHz.

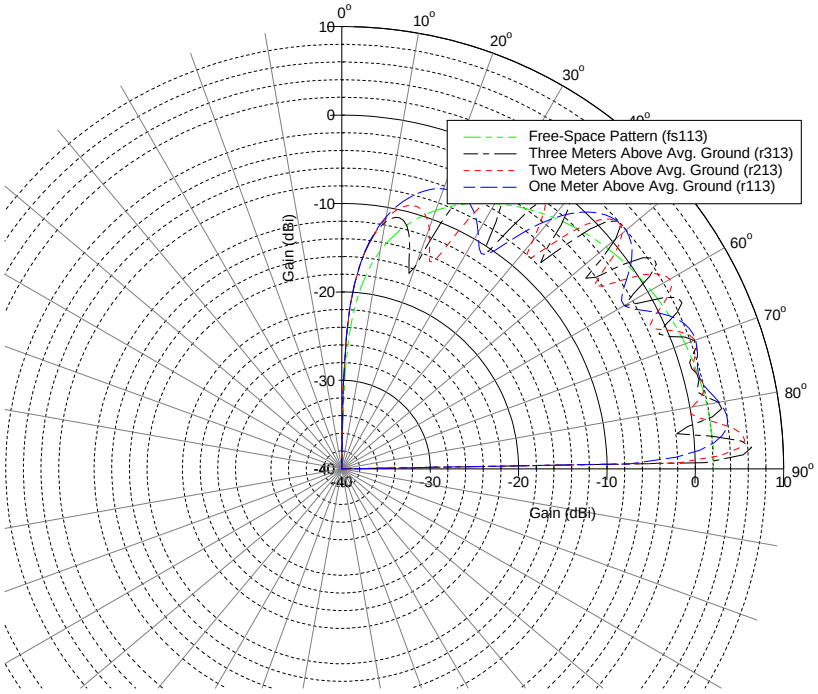


Figure C-2. Elevation patterns for vertical half-wave dipole at 450 MHz.

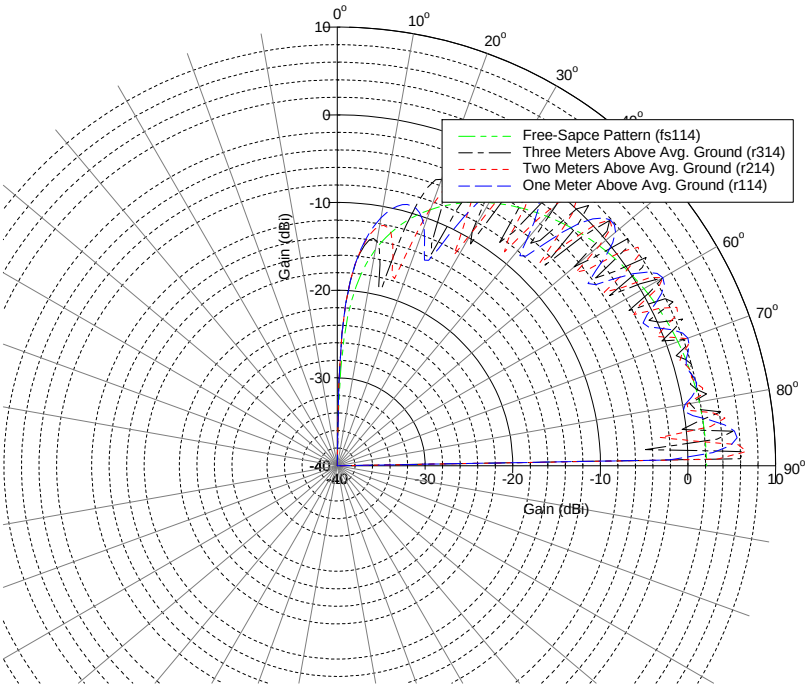


Figure C-3. Elevation patterns for vertical half-wave dipole at 900 MHz.

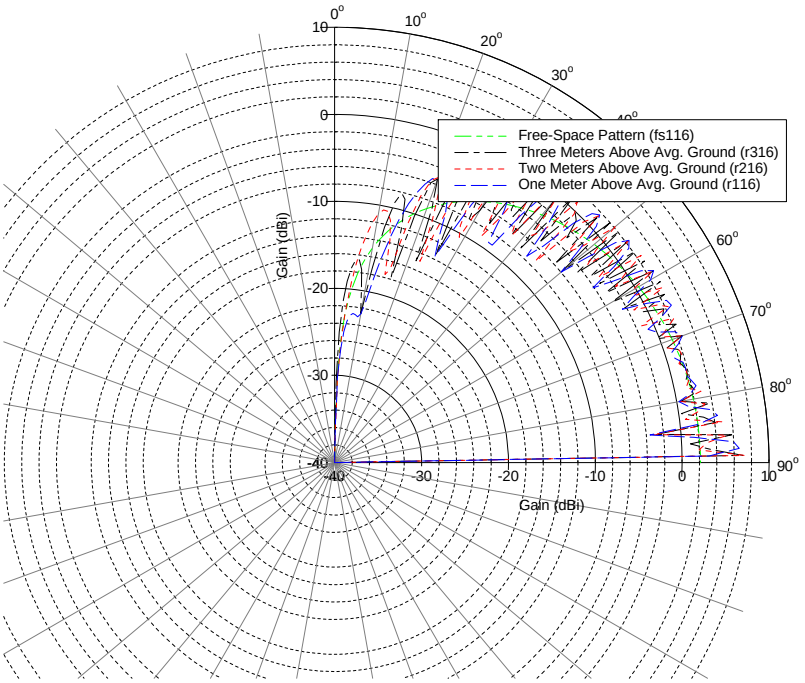


Figure C-4. Elevation patterns for vertical half-wave dipole at 1750 MHz.

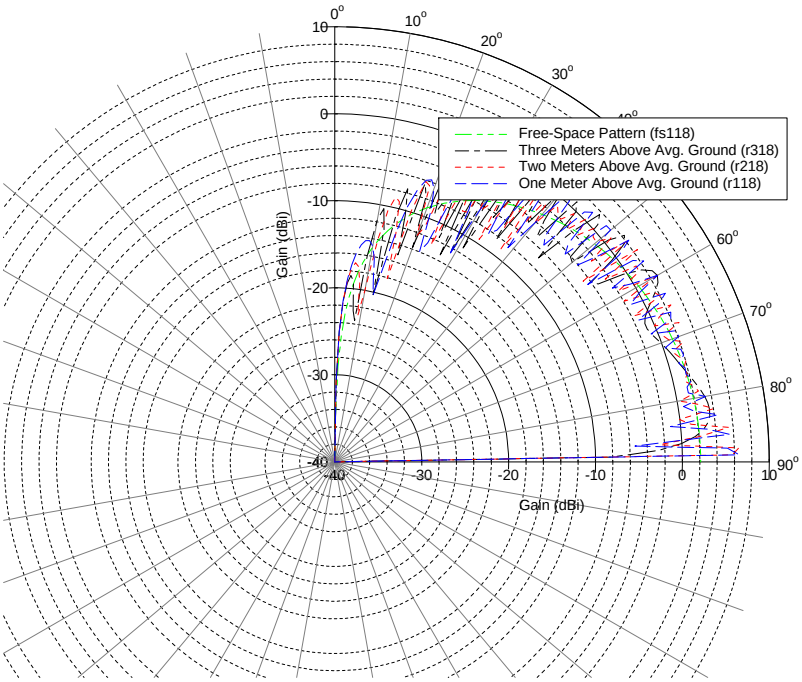


Figure C-5. Elevation patterns for vertical half-wave dipole at 3000 MHz.

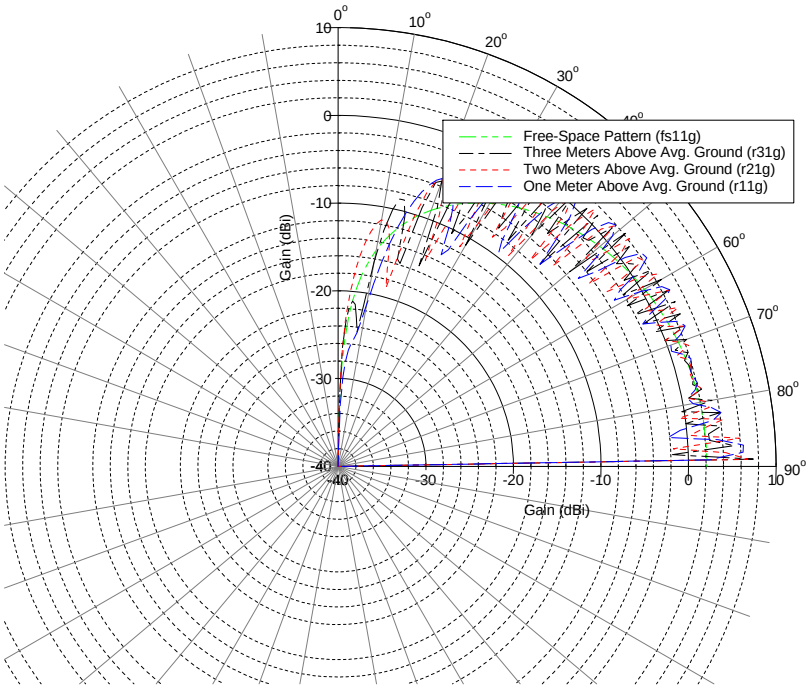


Figure C-6. Elevation patterns for vertical half-wave dipole at 1590 MHz.

## APPENDIX D: COMPARISON OF THE MUTUAL-COUPLING METHOD WITH THE UNDISTURBED-FIELD METHOD

Appendix D contains a large number of figures that are referred to in the main body of the report, and it would be inappropriate to integrate this many figures into the corresponding section of the report. Appendix D is referred to in Section 3.2 and contains plots of predicted propagation loss versus distance for six combinations of antenna heights and five frequencies that compare the results for the mutual-coupling method with the results of the undisturbed-field method. These plots are the results of analytic computations described in Section 3.2. These plots show that the undisturbed field method achieves very similar results to that of the mutual-coupling method except for the very short distances of 2 meters or less. For these short distances, the error is less than 2 dB. The undisturbed-field method is a much simpler and faster computation technique than the mutual-coupling method, so it is advantageous to use the undisturbed-field method as much as possible.

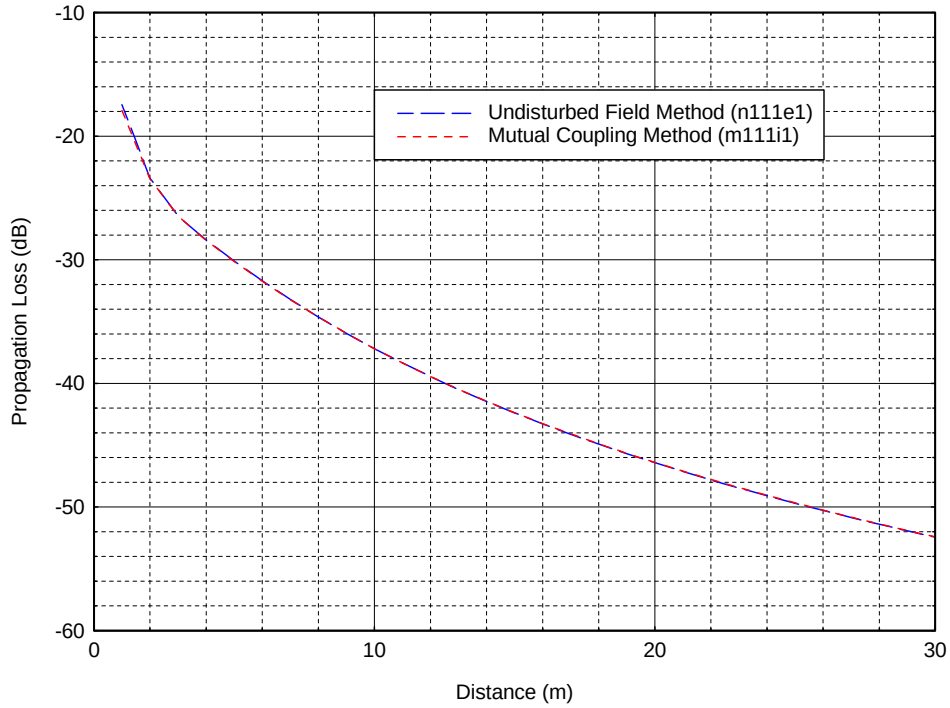


Figure D-1. Comparison of mutual-coupling method with undisturbed-field method at 150 MHz for antenna heights $h_1$=1m and $h_2$=1m.

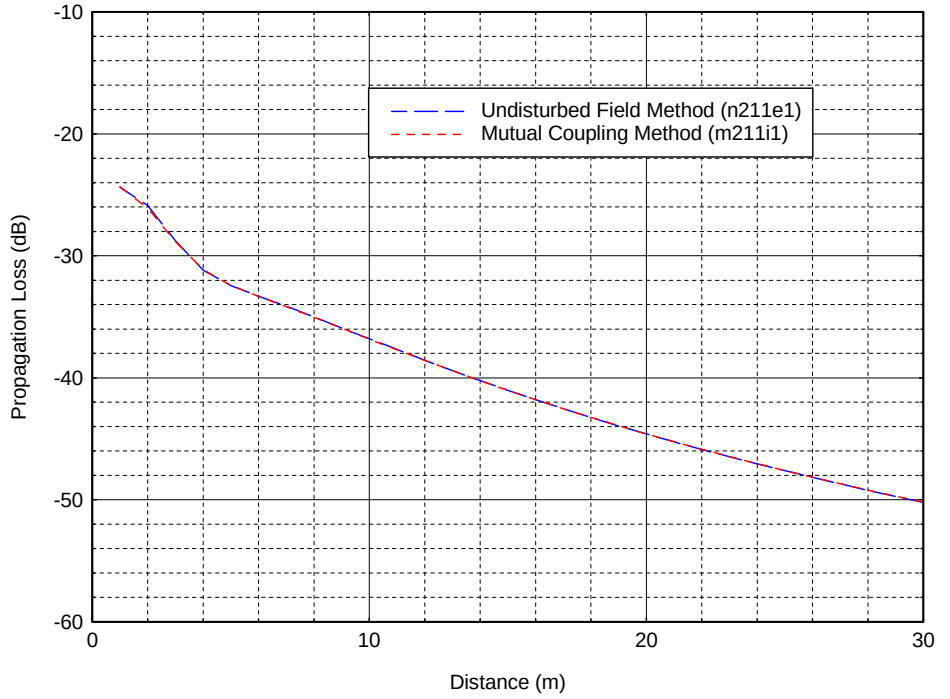


Figure D-2. Comparison of mutual-coupling method with undisturbed-field method at 150 MHz for antenna heights $h_1$=2m and $h_2$=1m.

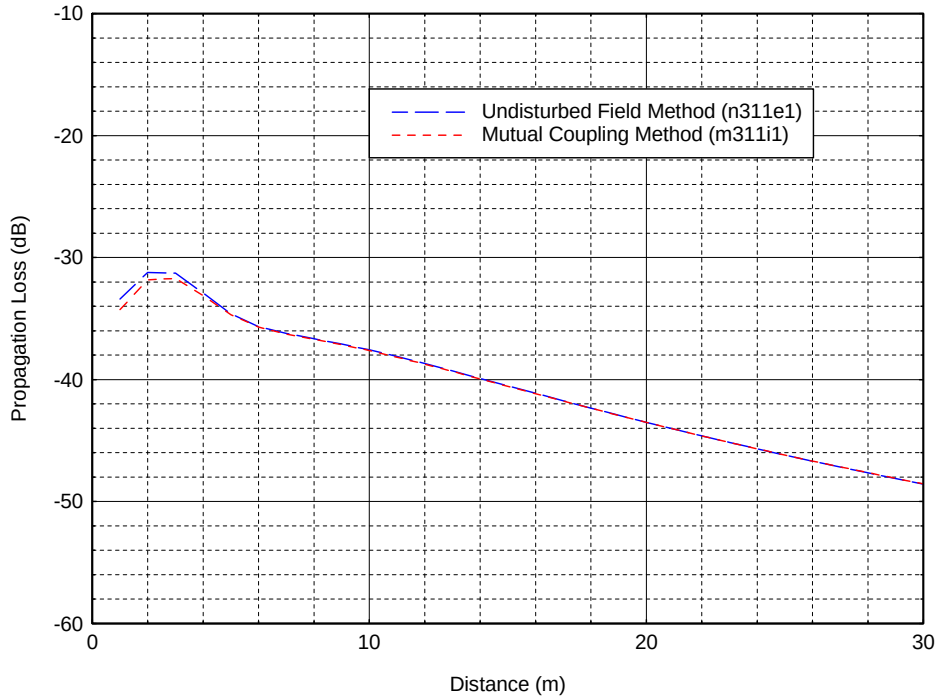


Figure D-3. Comparison of mutual-coupling method with undisturbed-field method at 150 MHz for antenna heights $h_1$=3m and $h_2$=1m.

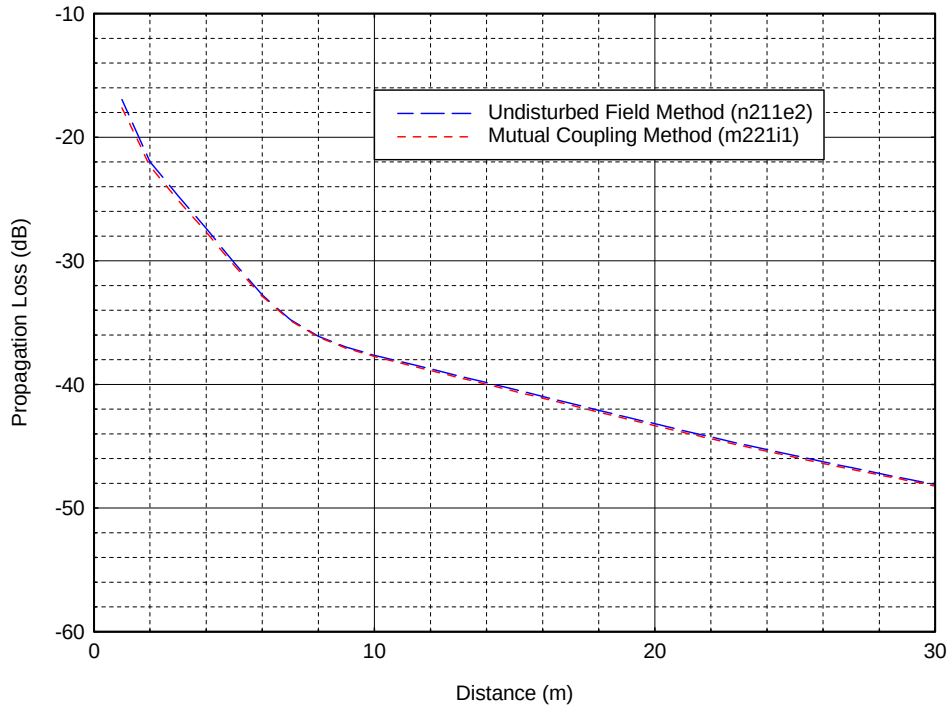


Figure D-4. Comparison of mutual-coupling method with undisturbed-field method at 150 MHz for antenna heights $h_1$=2m and $h_2$=2m.

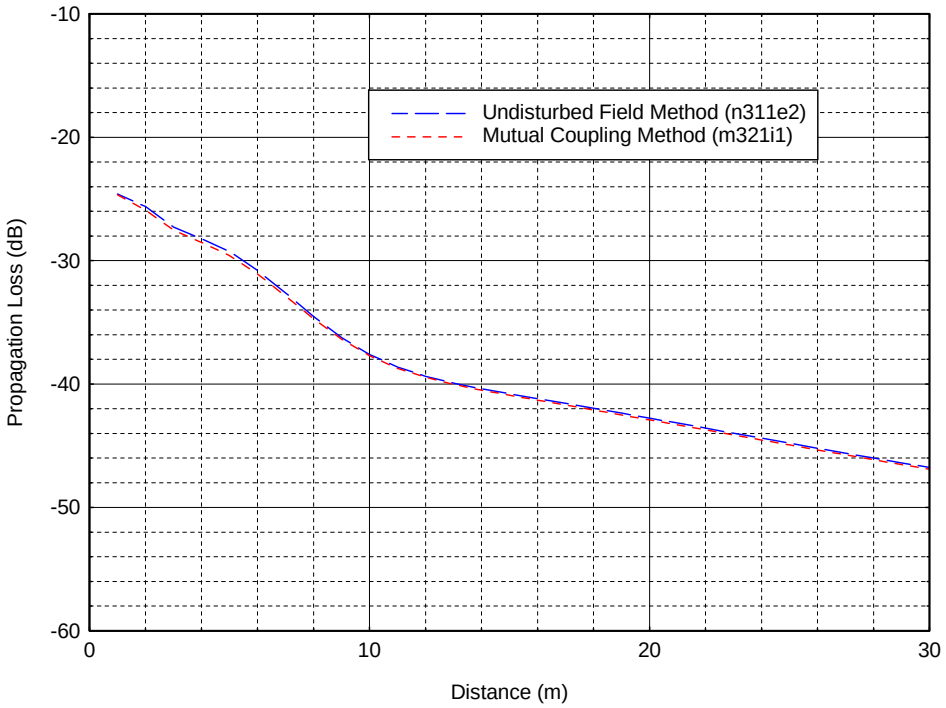


Figure D-5. Comparison of mutual-coupling method with undisturbed-field method at 150 MHz for antenna heights $h_1$=3m and $h_2$=2m.

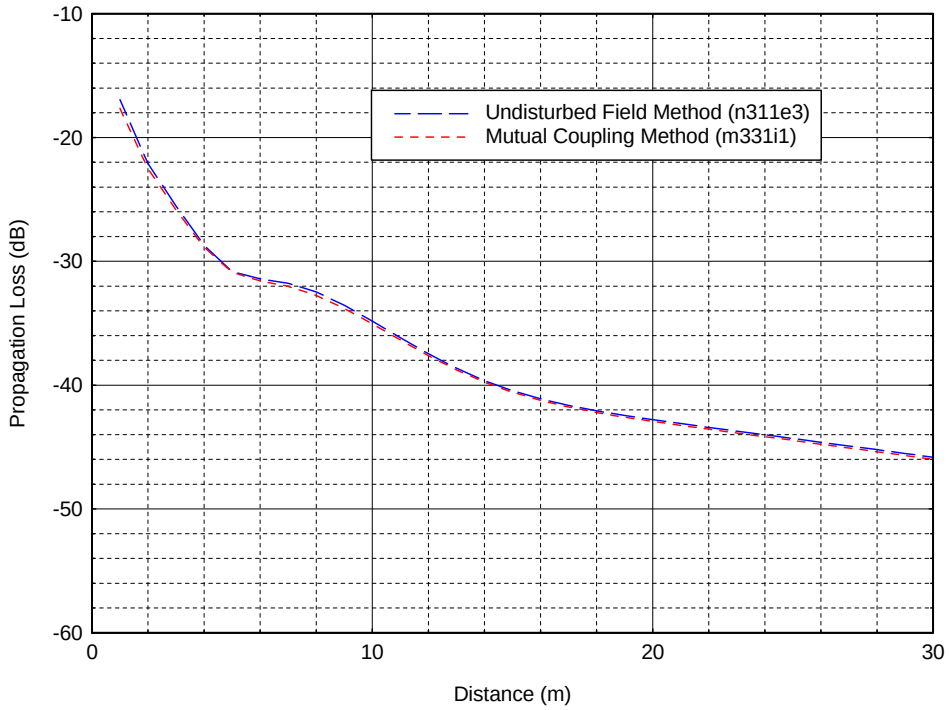


Figure D-6. Comparison of mutual-coupling method with undisturbed-field method at 150 MHz for antenna heights $h_1$=3m and $h_2$=3m.

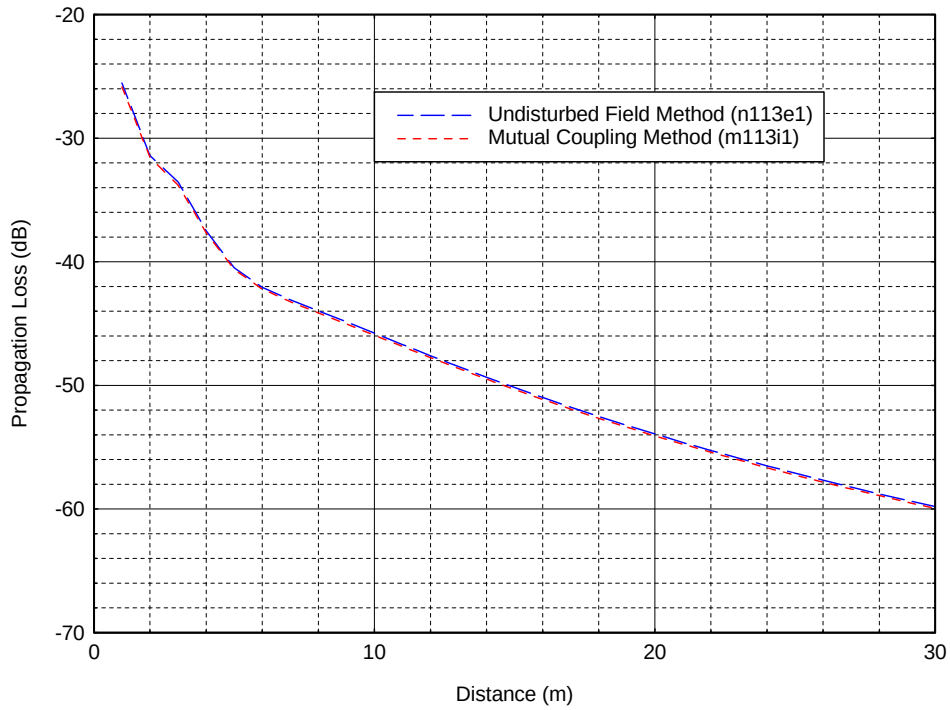


Figure D-7. Comparison of mutual-coupling method with undisturbed-field method at 450 MHz for antenna heights $h_1$=1m and $h_2$=1m.

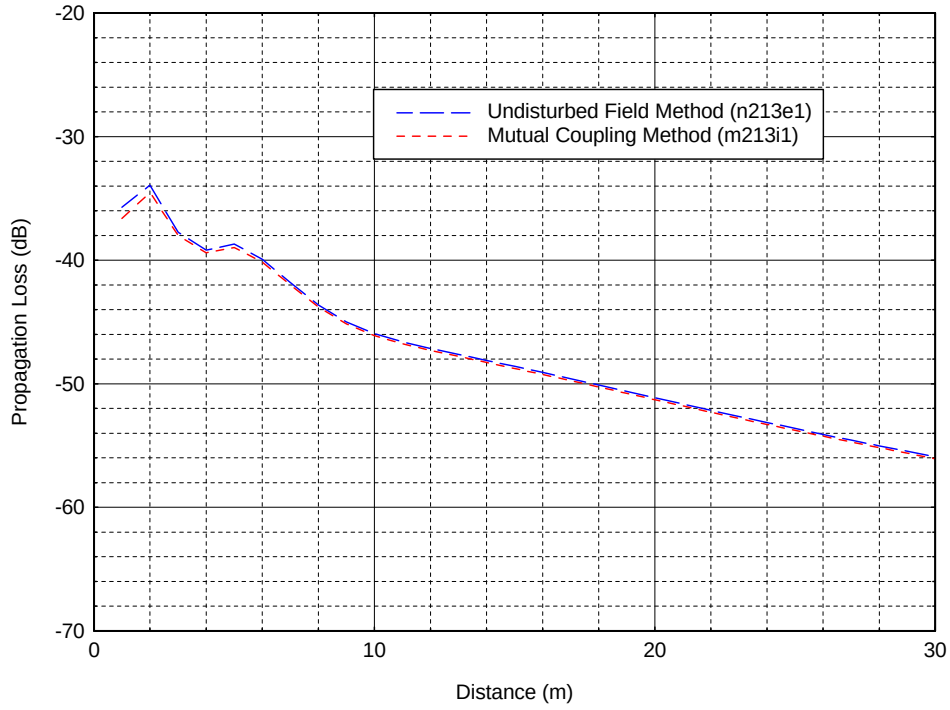


Figure D-8. Comparison of mutual-coupling method with undisturbed-field method at 450 MHz for antenna heights $h_1$=2m and $h_2$=1m.

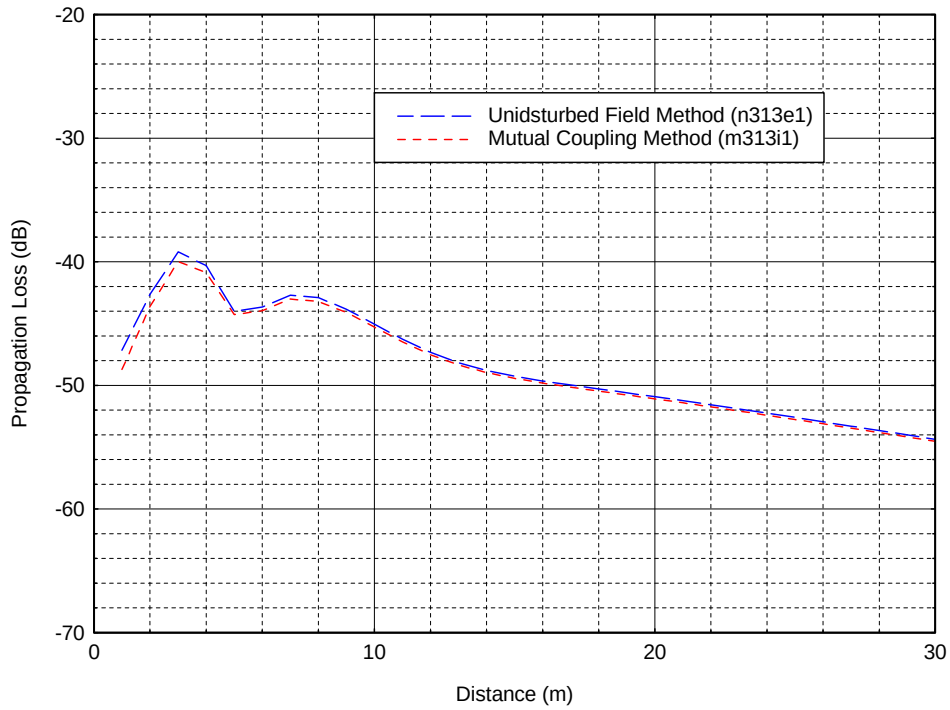


Figure D-9. Comparison of mutual-coupling method with undisturbed-field method at 450 MHz for antenna heights $h_1$=3m and $h_2$ = 1m.

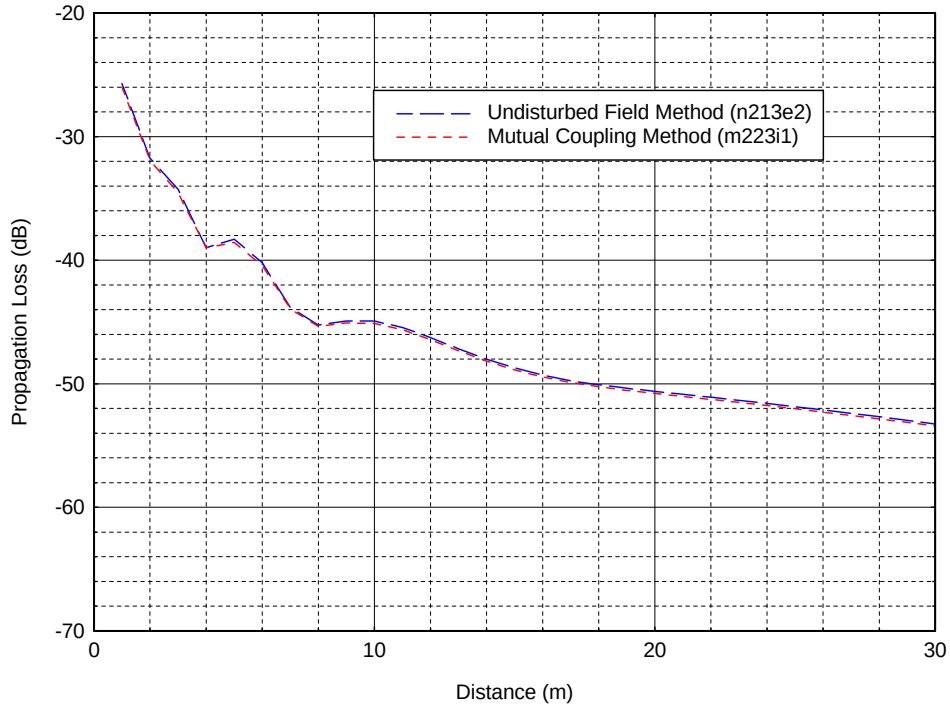


Figure D-10. Comparison of mutual-coupling method with undisturbed-field method at 450 MHz for antenna heights $h_1$=2m and $h_2$=2m.

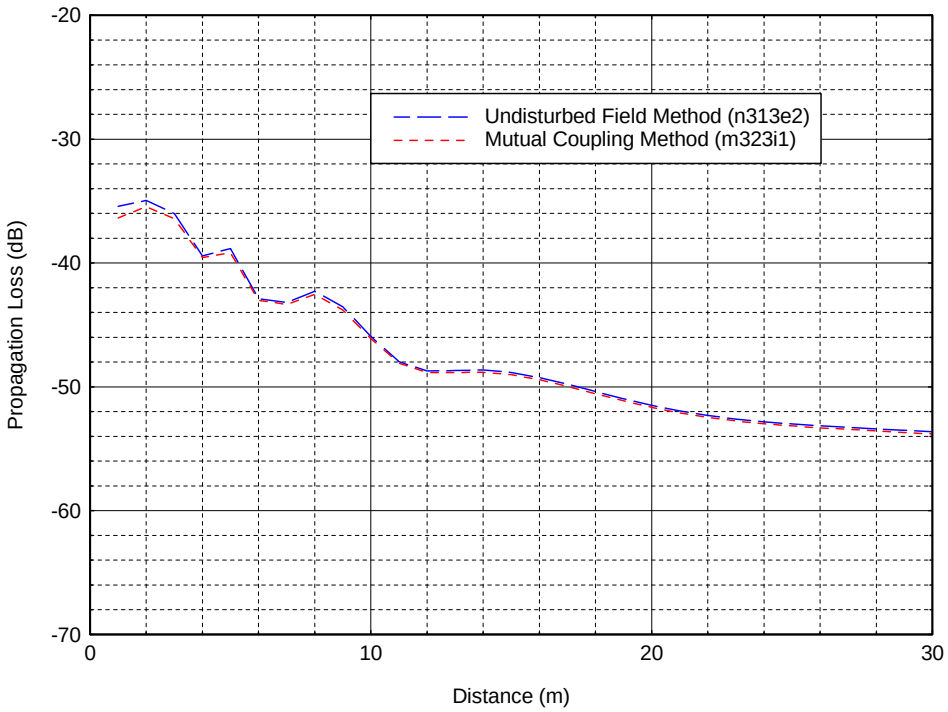


Figure D-11. Comparison of mutual-coupling method with undisturbed-field method at 450 MHz for antenna heights $h_1$=3m and $h_2$=2m.

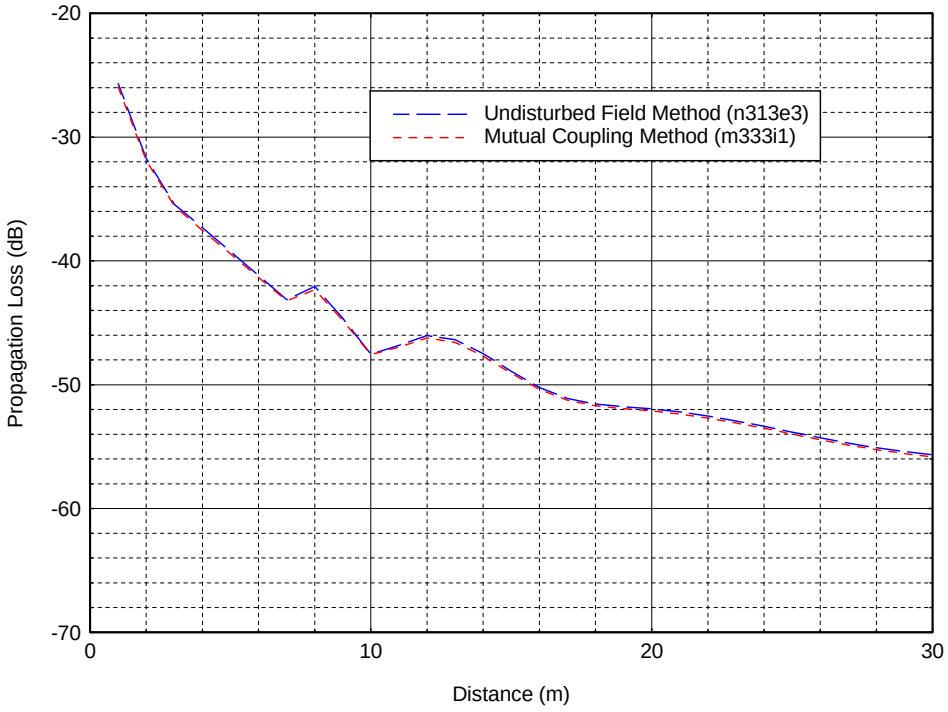


Figure D-12. Comparison of mutual-coupling method with undisturbed-field method at 450 MHz for antenna heights $h_1$=3m and $h_2$=3m.

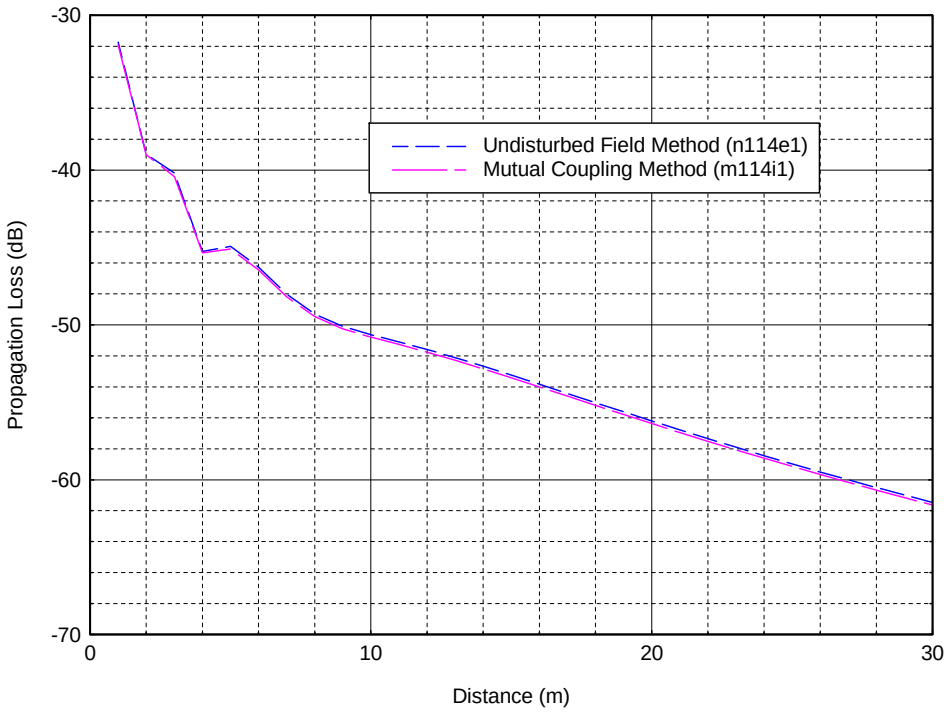


Figure D-13. Comparison of mutual-coupling method with undisturbed-field method at 900 MHz for antenna heights $h_1$=1m and $h_2$=1m.

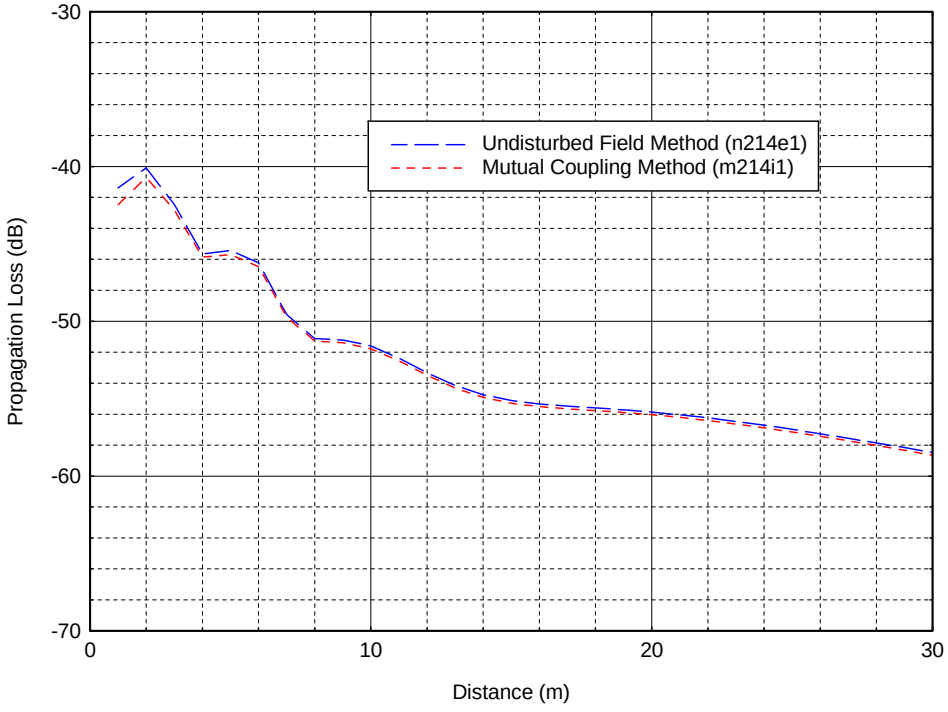


Figure D-14. Comparison of mutual-coupling method with undisturbed-field method at 900 MHz for antenna heights $h_1$=2m and $h_2$=1m.

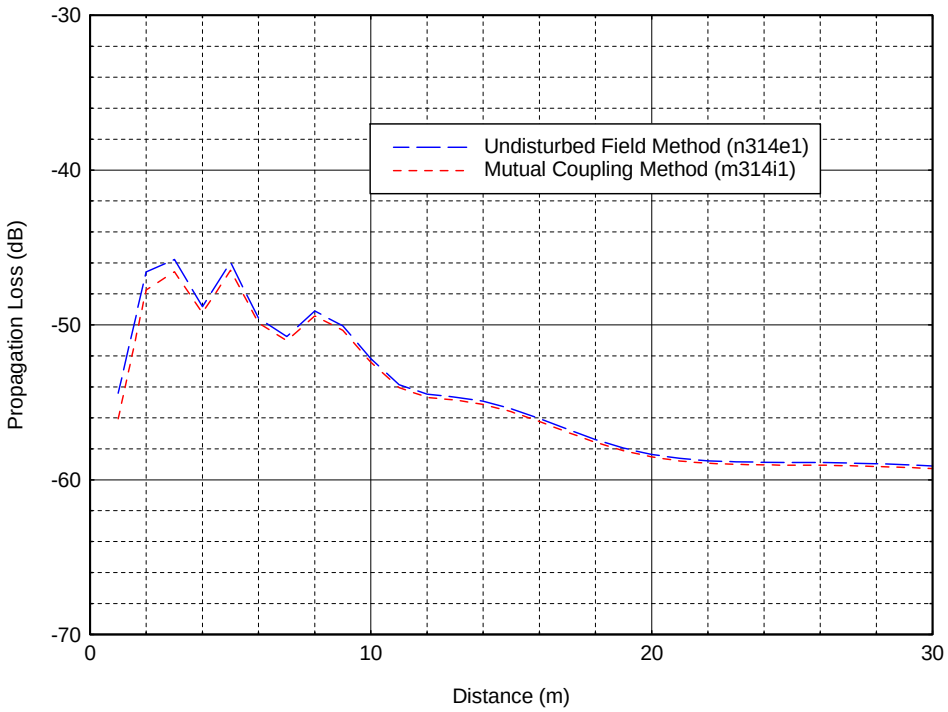


Figure D-15. Comparison of mutual-coupling method with undisturbed-field method at 900 MHz for antenna heights $h_1$=3m and $h_2$=1m.

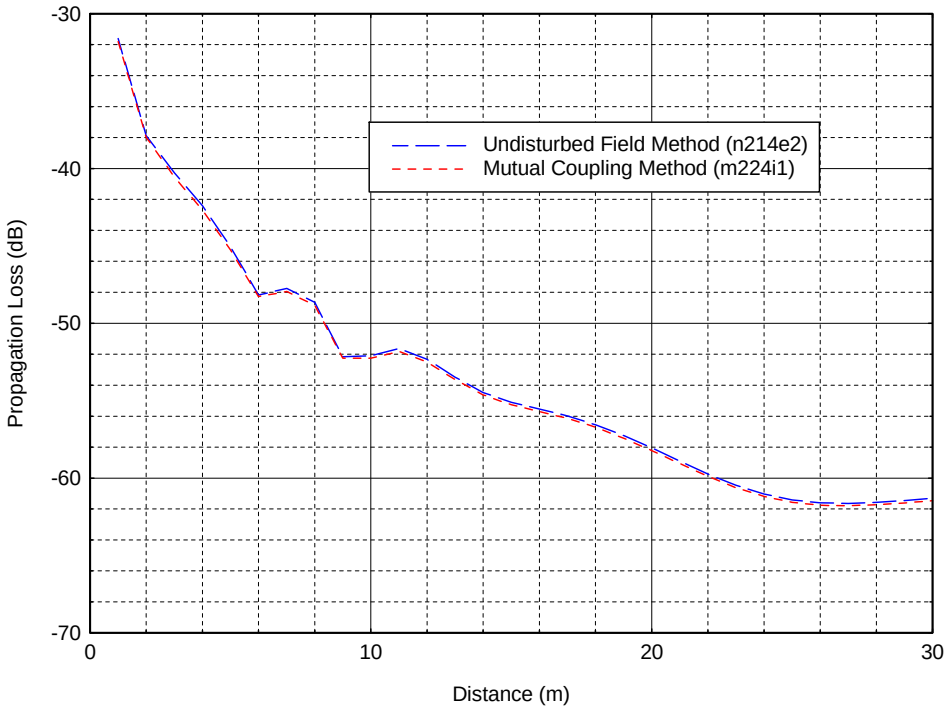


Figure D-16. Comparison of mutual-coupling method with undisturbed-field method at 900 MHz for antenna heights $h_1$=2m and $h_2$=2m.

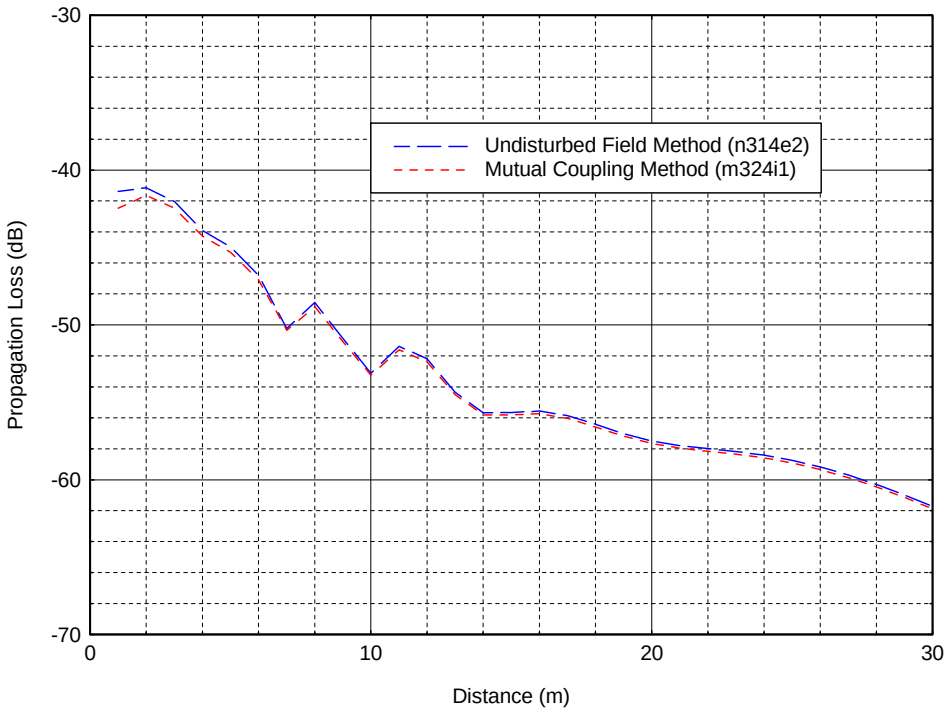


Figure D-17. Comparison of mutual-coupling method with undisturbed-field method at 900 MHz for antenna heights $h_1$=3m and $h_2$=2m.

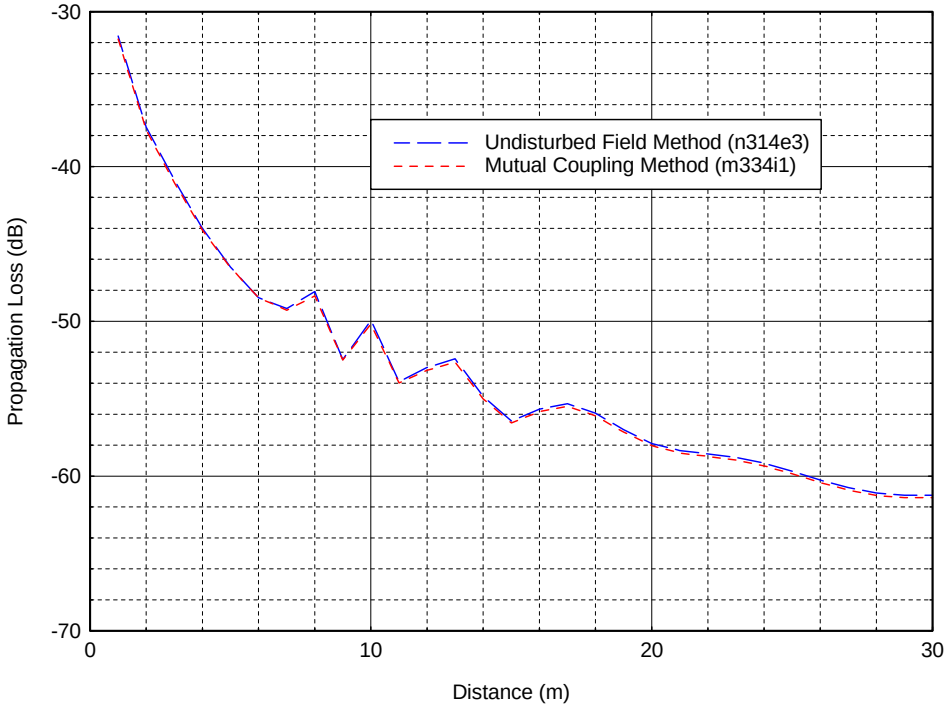


Figure D-18. Comparison of mutual-coupling method with undisturbed-field method at 900 MHz for antenna heights $h_1$=3m and $h_2$=3m.

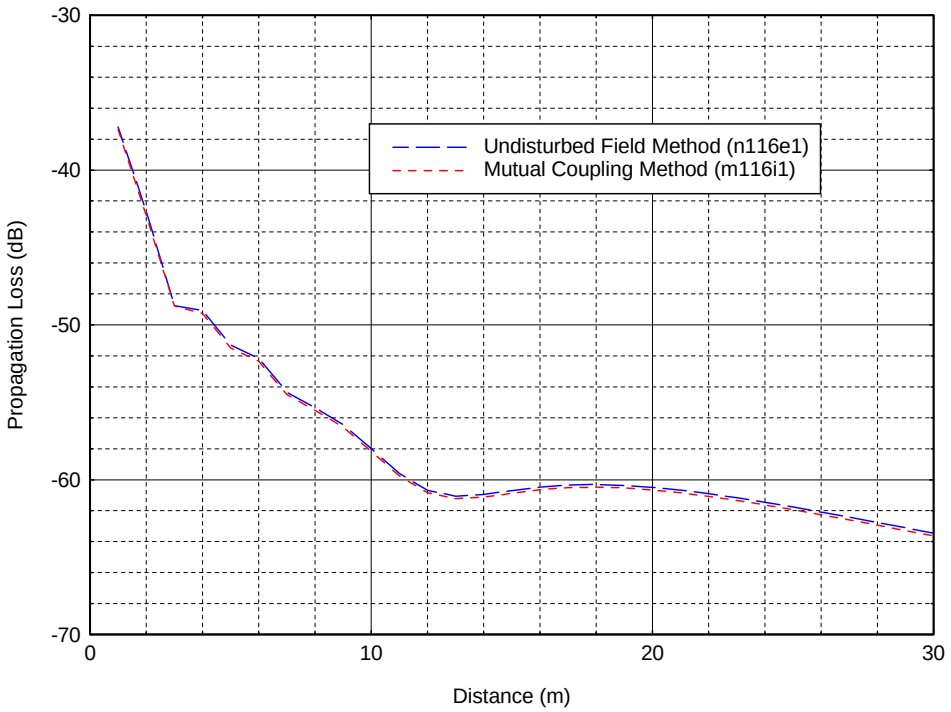


Figure D-19. Comparison of mutual-coupling method with undisturbed-field method at 1750 MHz for antenna heights $h_1$=1m and $h_2$=1m.

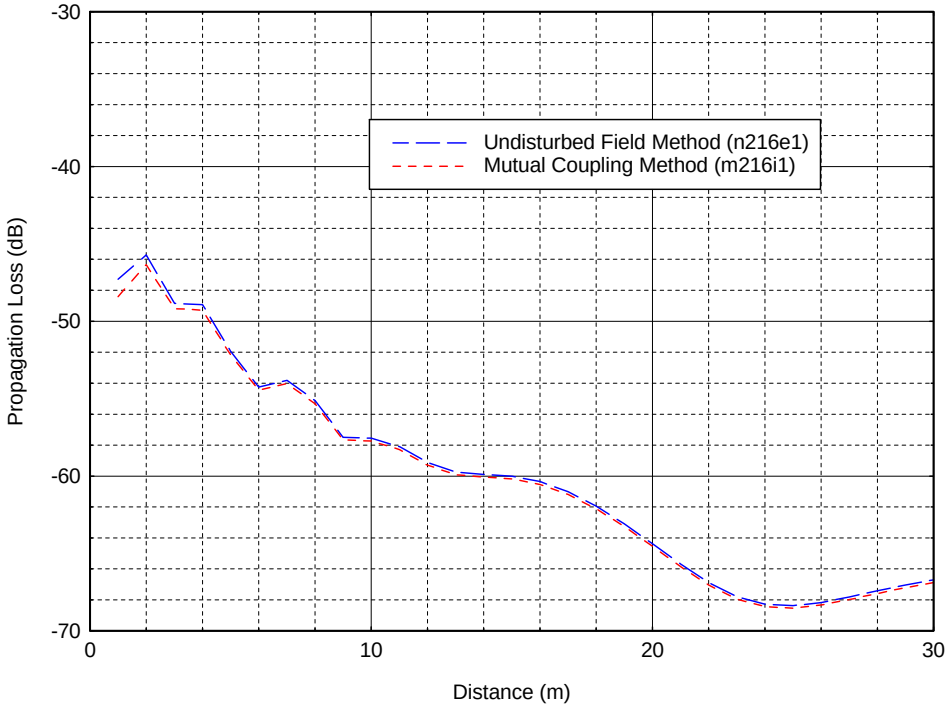


Figure D-20. Comparison of mutual-coupling method with undisturbed-field method at 1750 MHz for antenna heights $h_1$=2m and $h_2$=1m.

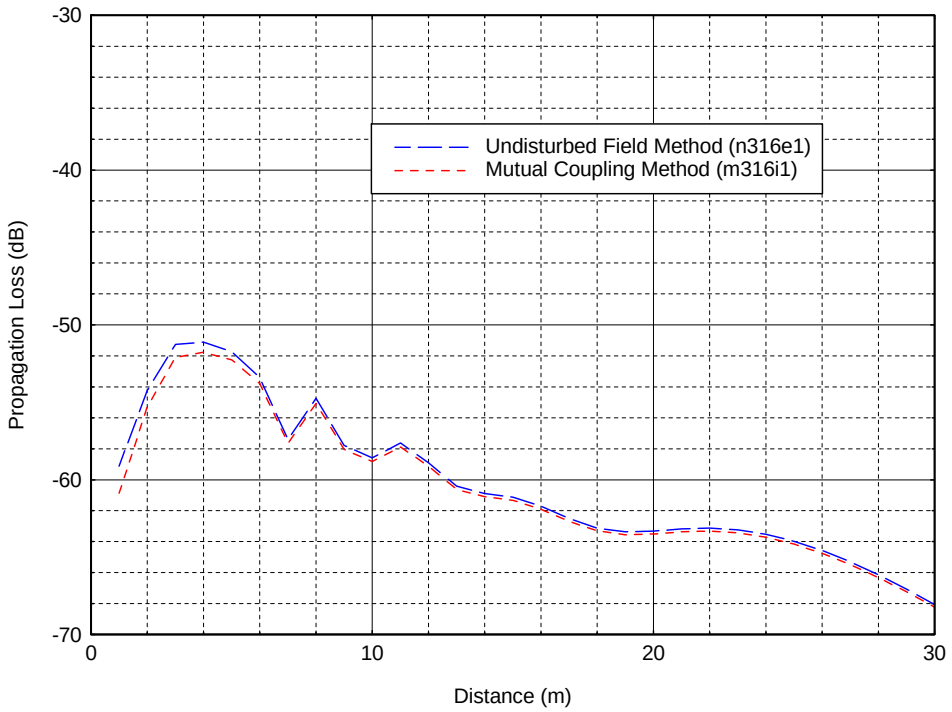


Figure D-21. Comparison of mutual-coupling method with undisturbed-field method at 1750 MHz for antenna heights $h_1$=3m and $h_2$=1m.

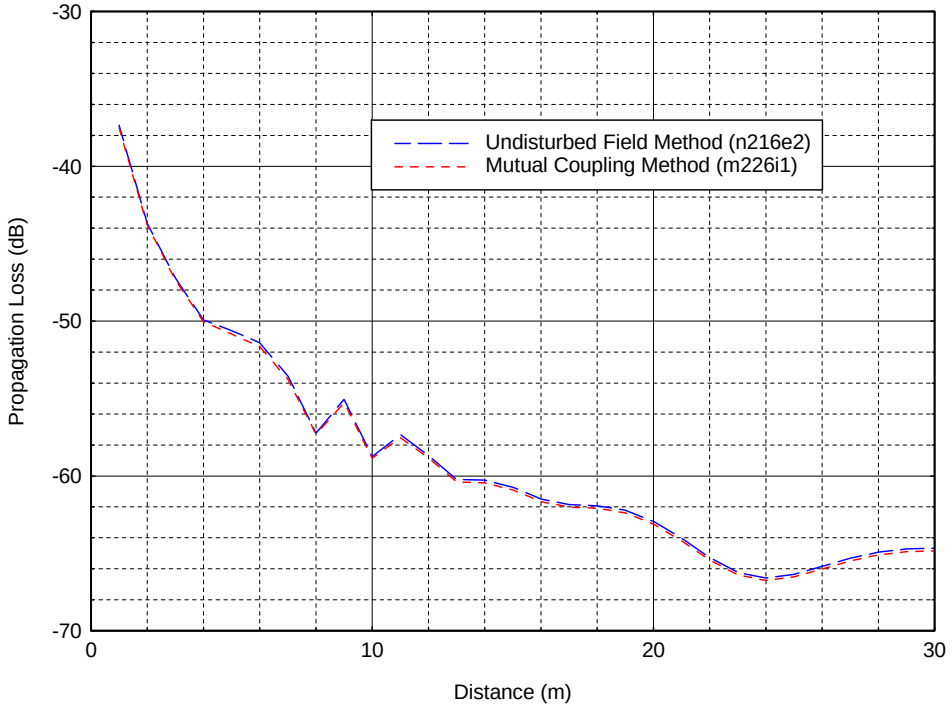


Figure D-22. Comparison of mutual-coupling method with undisturbed-field method at 1750 MHz for antenna heights $h_1$=2m and $h_2$=2m.

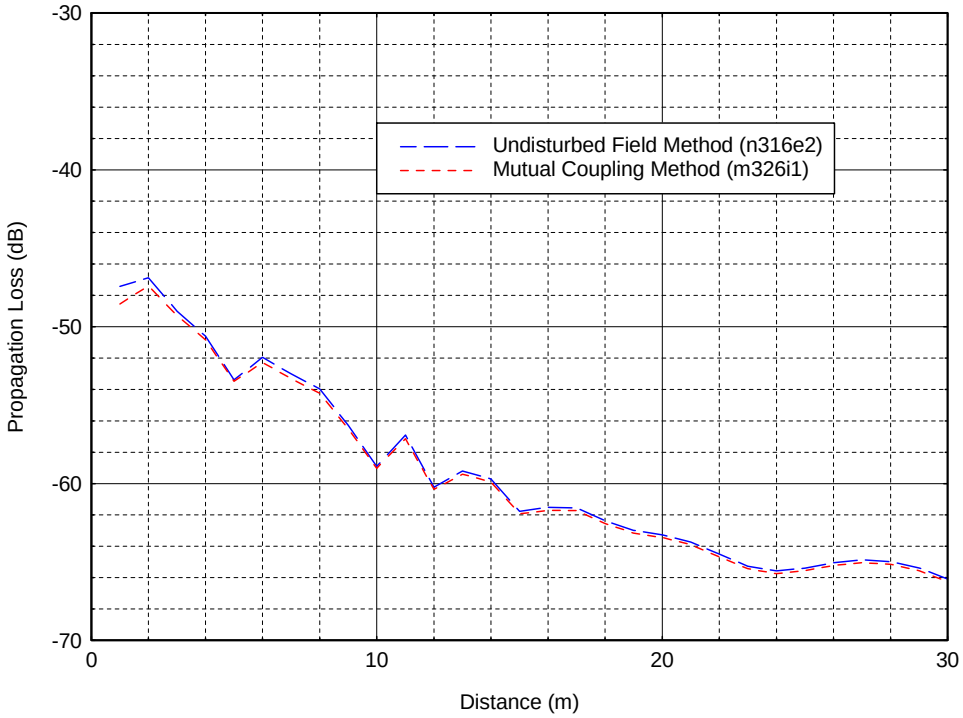


Figure D-23. Comparison of mutual-coupling method with undisturbed-field method at 1750 MHz for antenna heights $h_1$=3m and $h_2$=2m.

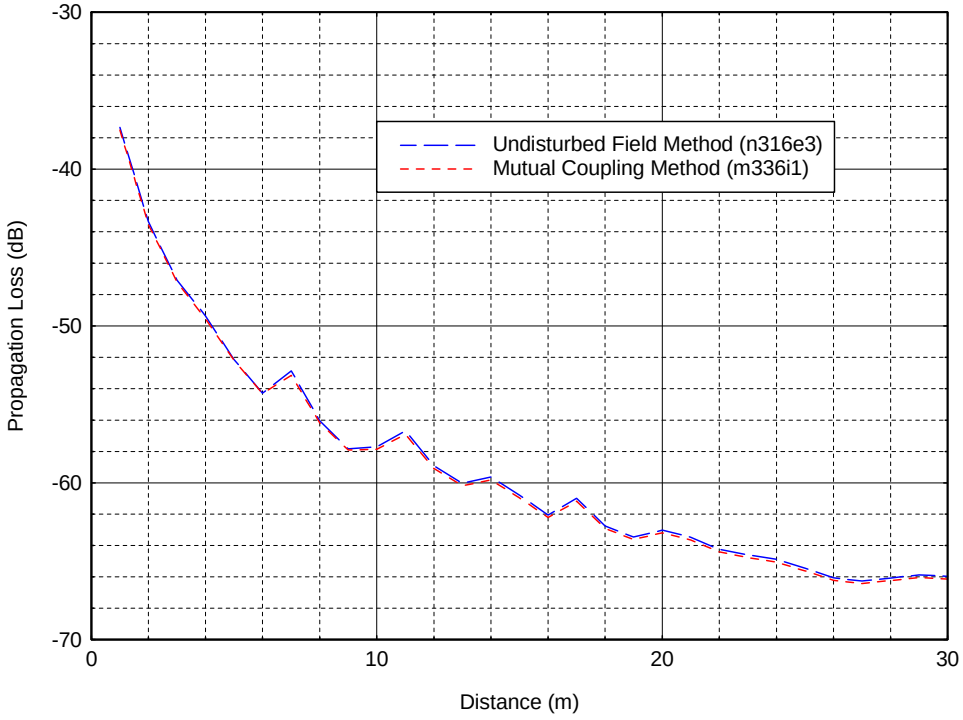


Figure D-24. Comparison of mutual-coupling method with undisturbed-field method at 1750 MHz for antenna heights $h_1$=3m and $h_2$=3m.

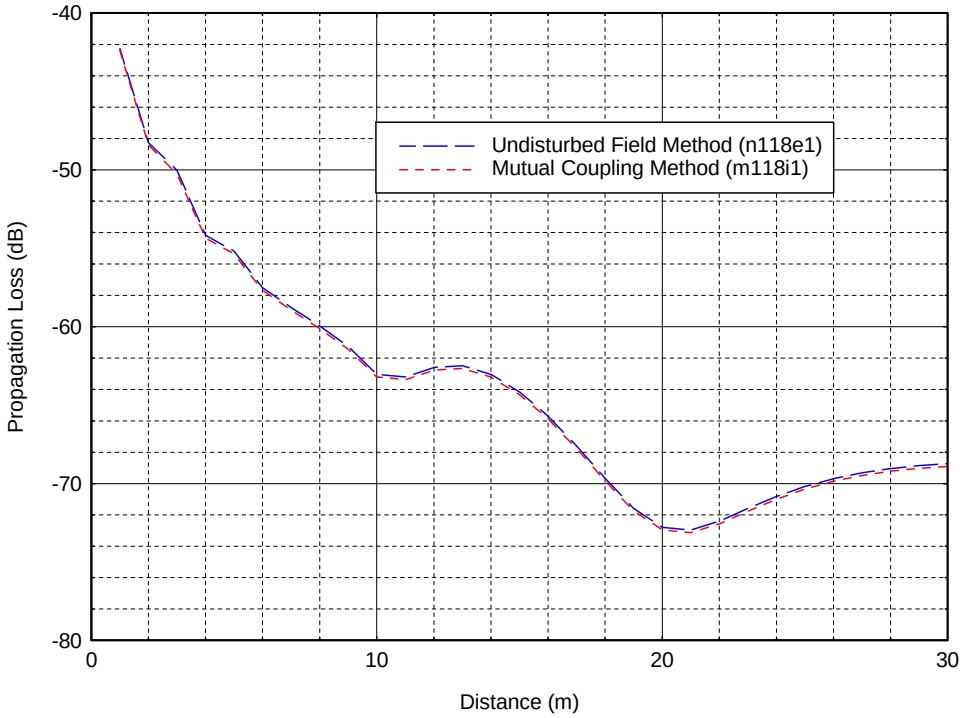


Figure D-25. Comparison of mutual-coupling method with undisturbed-field method at 3000 MHz for antenna heights $h_1$=1m and $h_2$=1m.

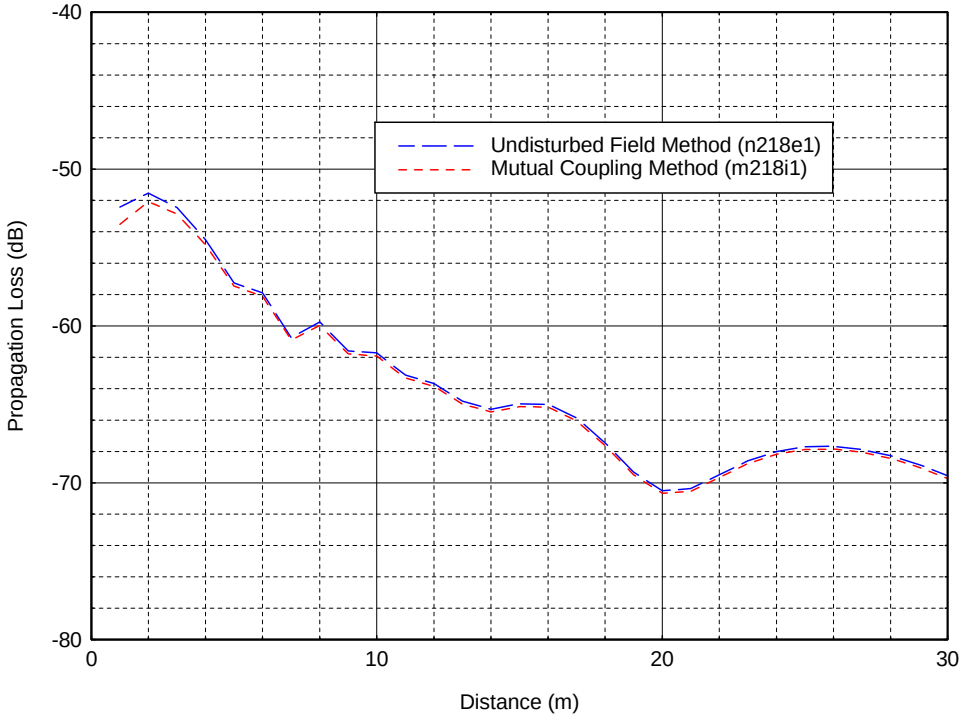


Figure D-26. Comparison of mutual-coupling method with undisturbed-field method at 3000 MHz for antenna heights $h_1$=2m and $h_2$=1m.

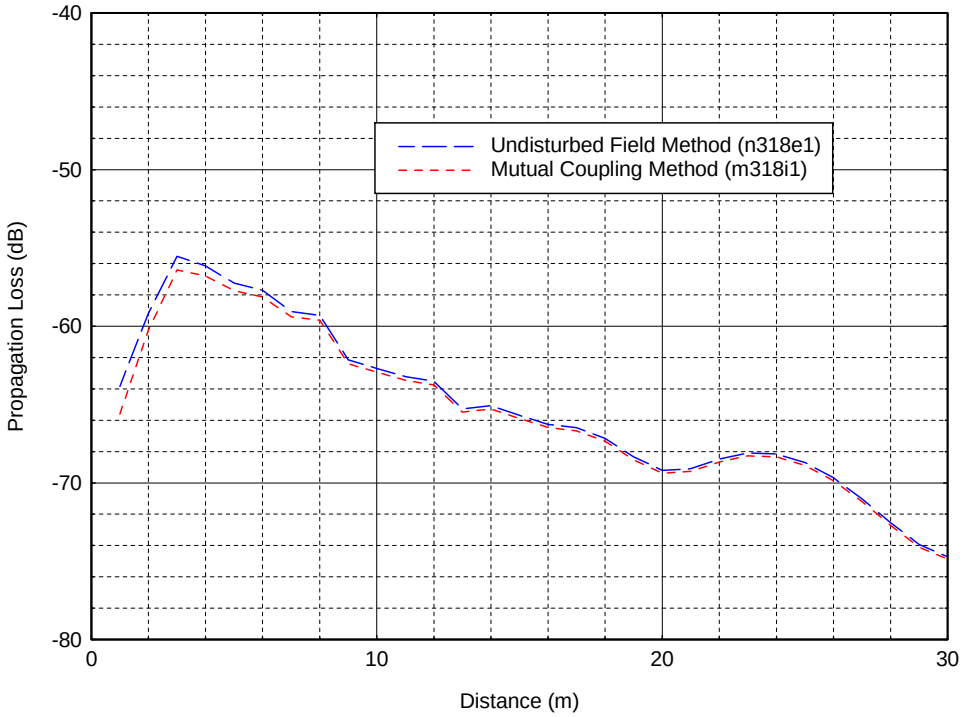


Figure D-27. Comparison of mutual-coupling method with undisturbed-field method at 3000 MHz for antenna heights $h_1$=3m and $h_2$=1m.

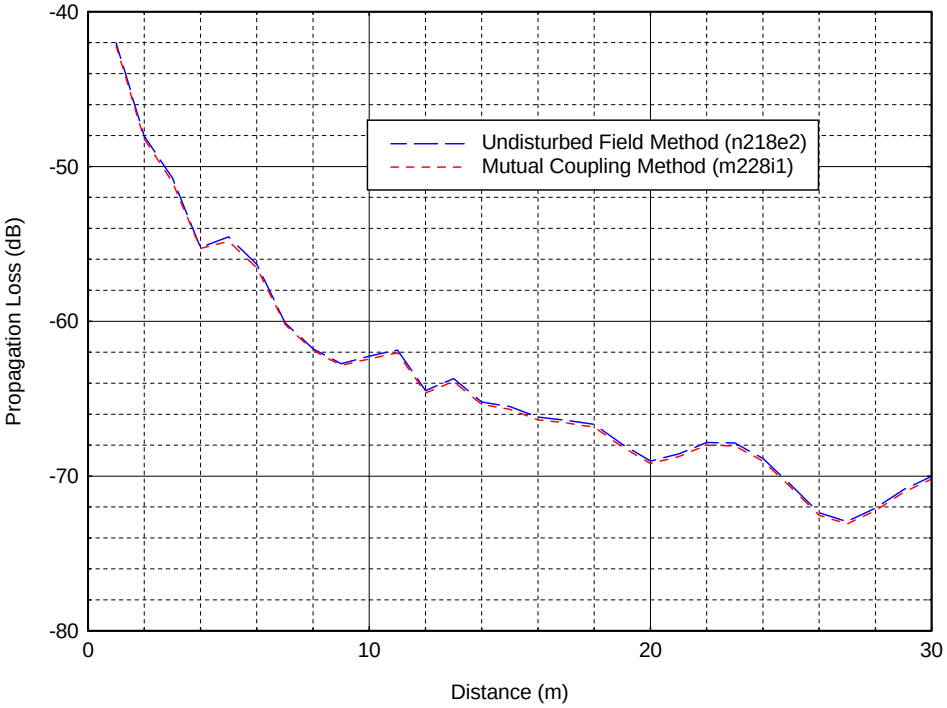


Figure D-28. Comparison of mutual-coupling method with undisturbed-field method at 3000 MHz for antenna heights $h_1$=2m and $h_2$=2m.

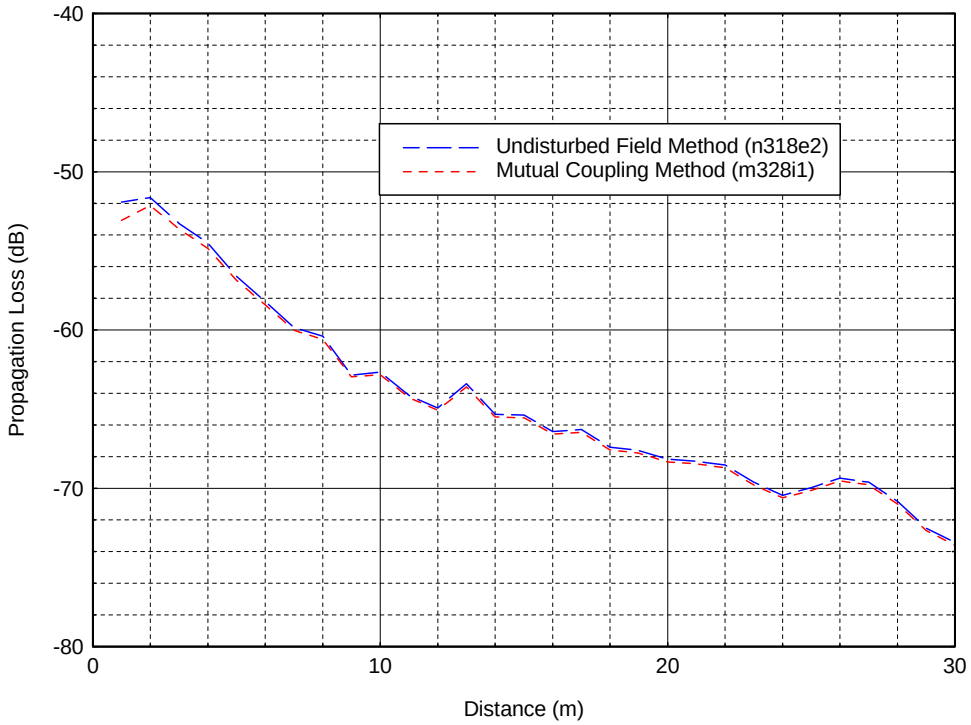


Figure D-29. Comparison of mutual-coupling method with undisturbed-field method at 3000 MHz for antenna heights $h_1$=3m and $h_2$=2 m.

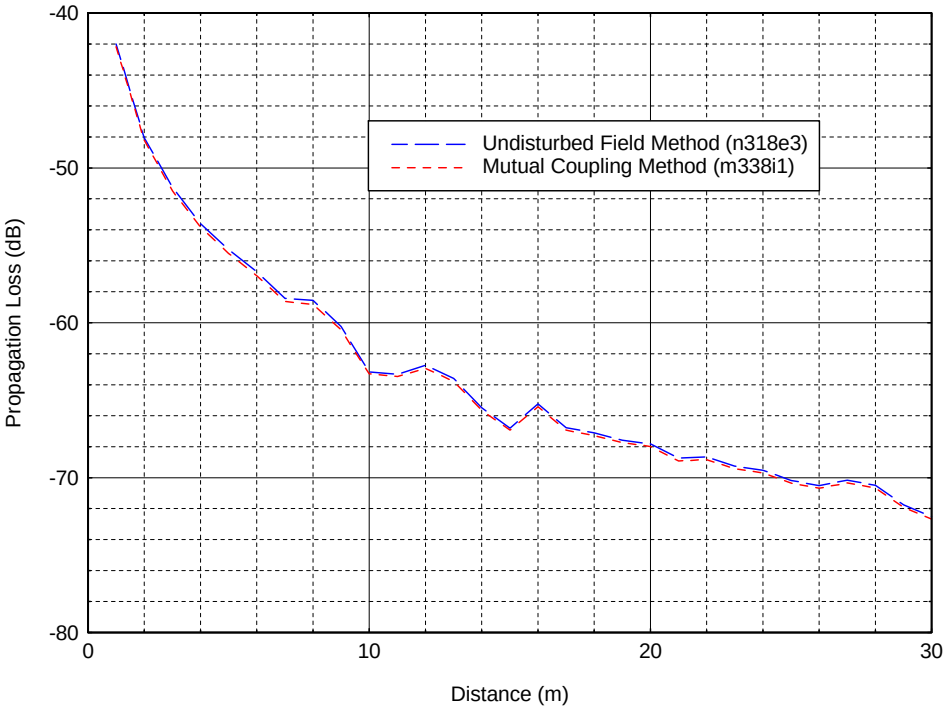


Figure D-30. Comparison of mutual-coupling method with undisturbed-field method at 3000 MHz for antenna heights $h_1$=3m and $h_2$=3m.

## APPENDIX E: COMPARISON OF THE UNDISTURBED-FIELD METHOD WITH OTHER METHODS

Appendices E and F contain a large number of figures that are referred to in the main body of the report, and it would be inappropriate to integrate this many figures into the corresponding section of the report. Appendices E and F are referred to in Section 3.3 and contain plots of predicted propagation loss versus distance for six different frequencies and six combinations of antenna heights that compare four different propagation loss prediction methods: the free-space loss method, two versions of the complex two-ray method, and the undisturbed-field method. Appendix E plots contain the predicted loss out to 30 meters and Appendix F plots contain the predicted loss out to 10 meters with an expanded distance scale to provide more detail of the short-range behavior of the different propagation prediction methods. These plots are the results of analytic computations described in Section 3.3. These plots show how poorly the free-space propagation loss represents the actual propagation loss predicted by the undisturbed-field method. The undisturbed-field method is the most accurate method.

Also shown on these plots are situations where the complex two-ray method can be used to save computation time for different combinations of antenna heights, frequencies, and distances. For all combinations of antenna heights and frequencies the complex two-ray model achieves accurate propagation loss predictions for distances greater than 20 meters. The complex two-ray method is a faster and easier computation than the undisturbed field method, but there are combinations of antenna heights, frequencies, and distances shown by these plots where the undisturbed-field method is the best method to use for computation.

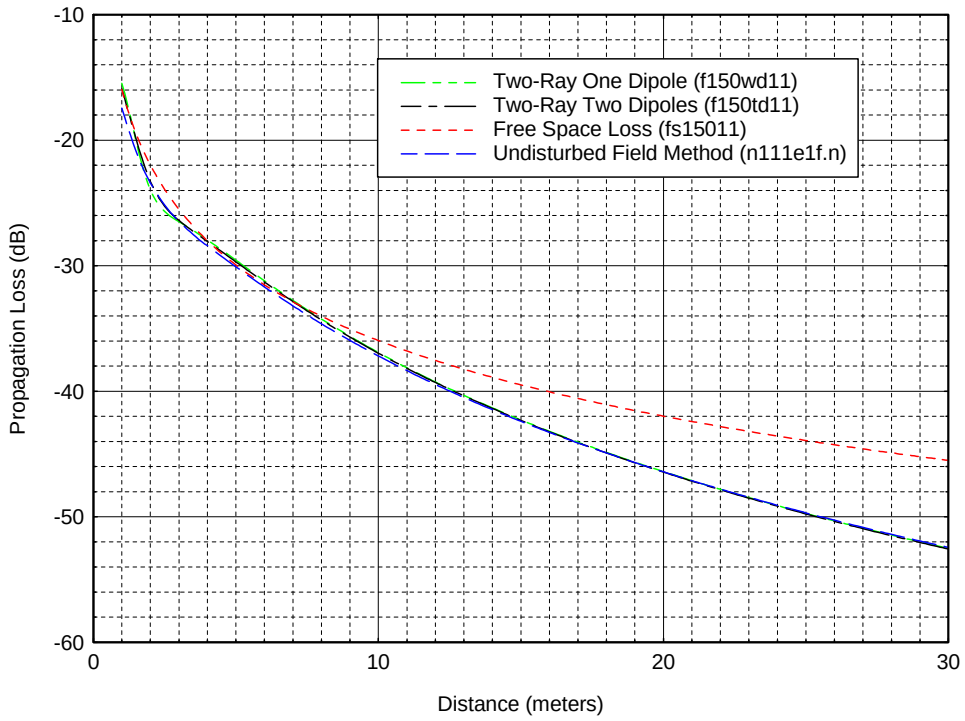


Figure E-1. Comparison of the undisturbed-field method with other methods at 150 MHz for antenna heights $h_1$=1m and $h_2$=1m.

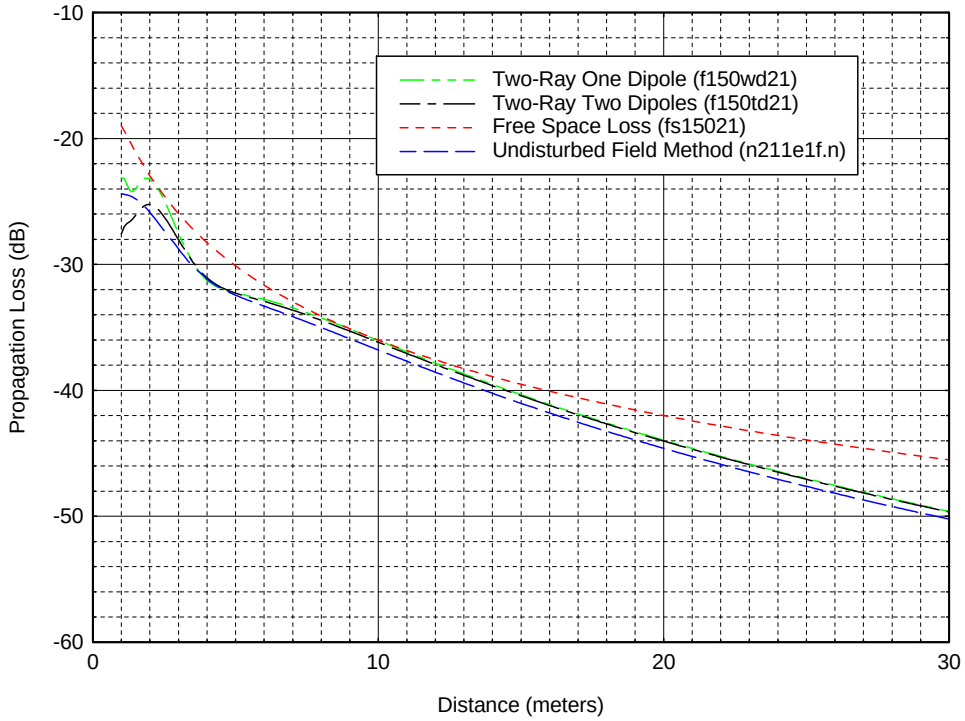


Figure E-2. Comparison of the undisturbed-field method with other methods at 150 MHz for antenna heights $h_1$=2m and $h_2$=1m.

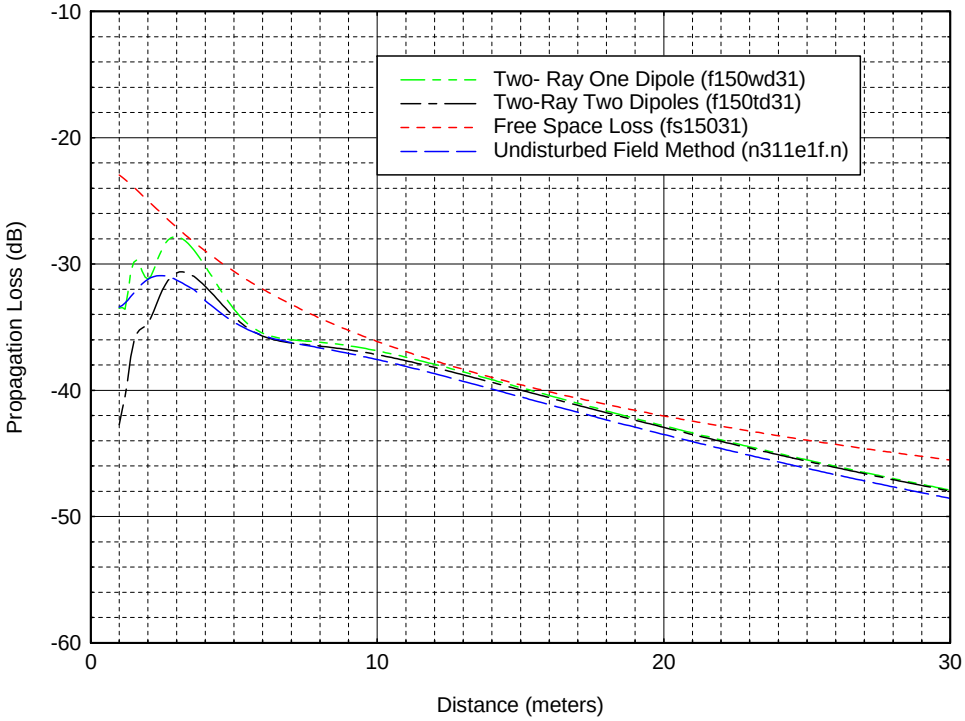


Figure E-3. Comparison of the undisturbed-field method with other methods at 150 MHz for antenna heights $h_1$=3m and $h_2$=1m.

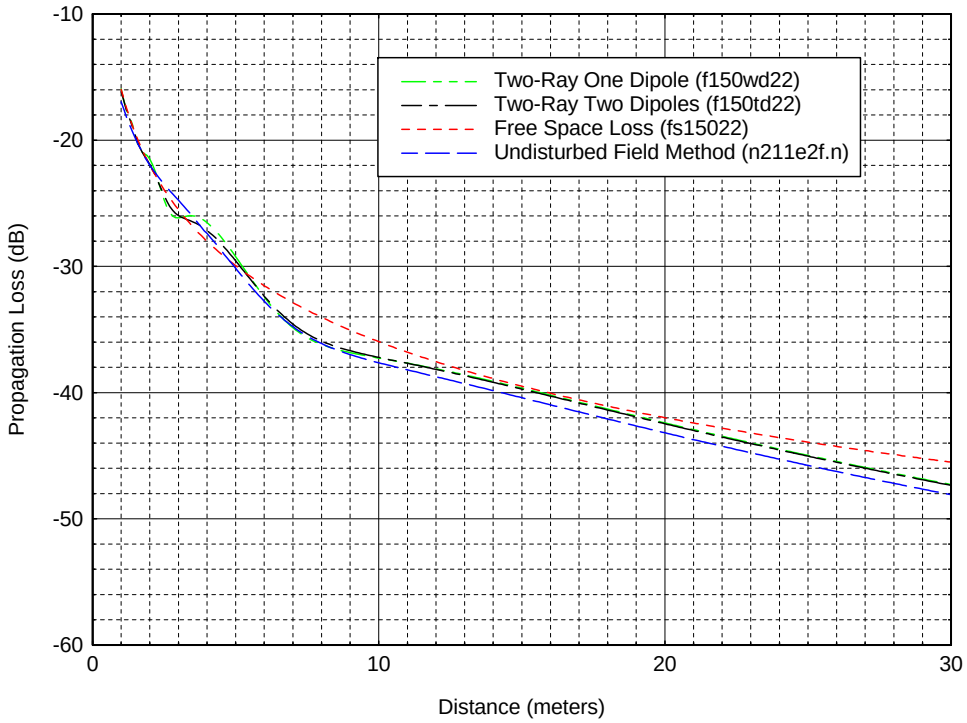


Figure E-4. Comparison of the undisturbed-field method with other methods at 150 MHz for antenna heights $h_1$=2m and $h_2$=2m.

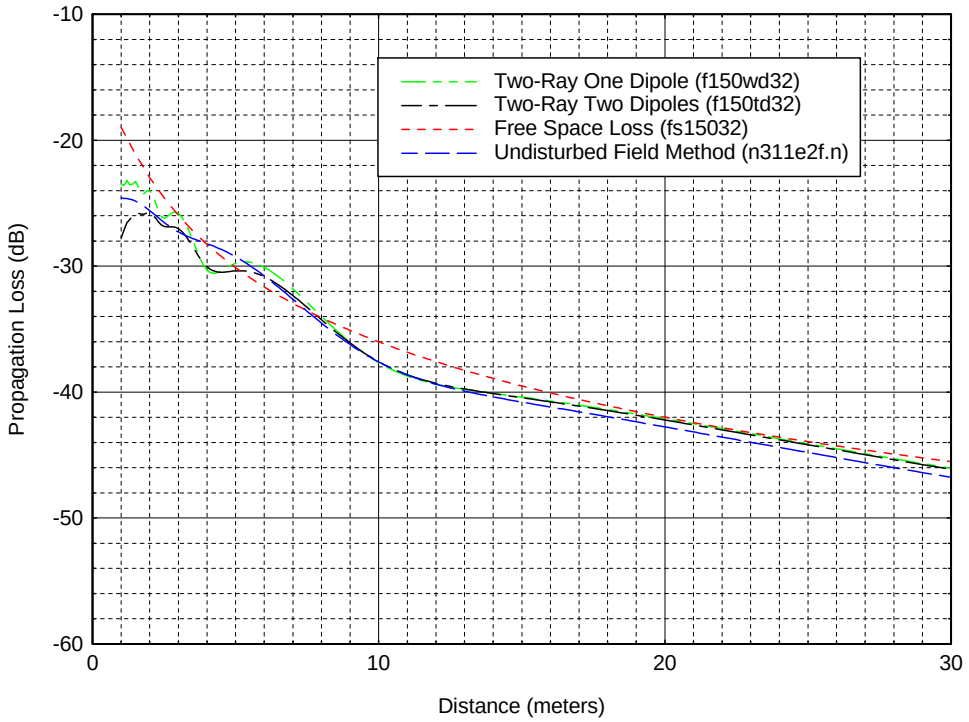


Figure E-5. Comparison of the undisturbed-field method with other methods at 150 MHz for antenna heights $h_1$=3m and $h_2$=2m.

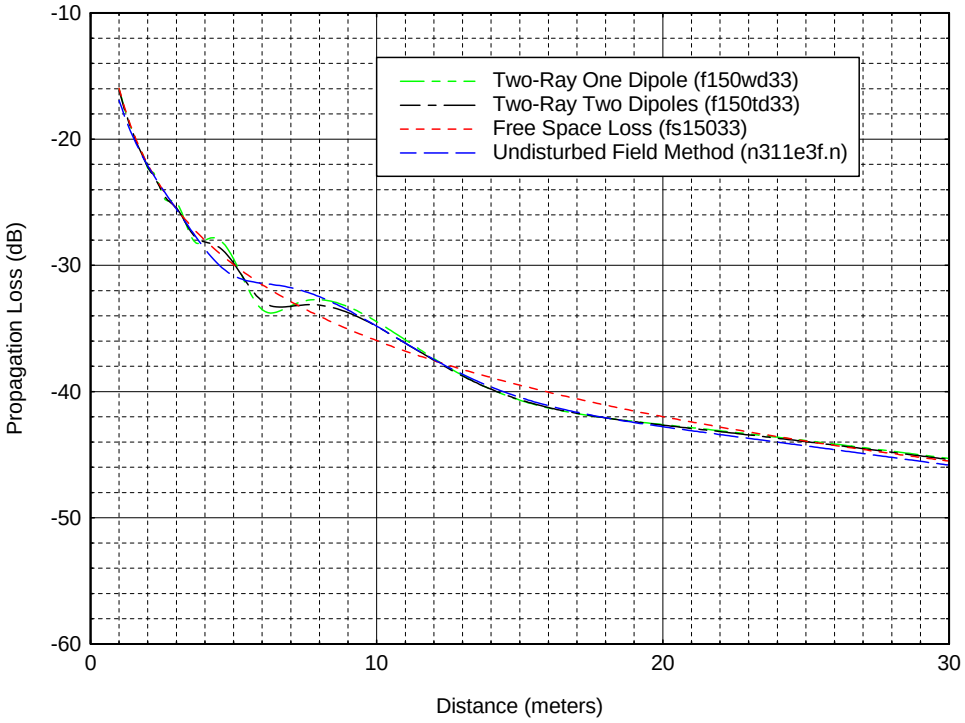


Figure E-6. Comparison of the undisturbed-field method with other methods at 150 MHz for antenna heights $h_1$=3m and $h_2$=3m.

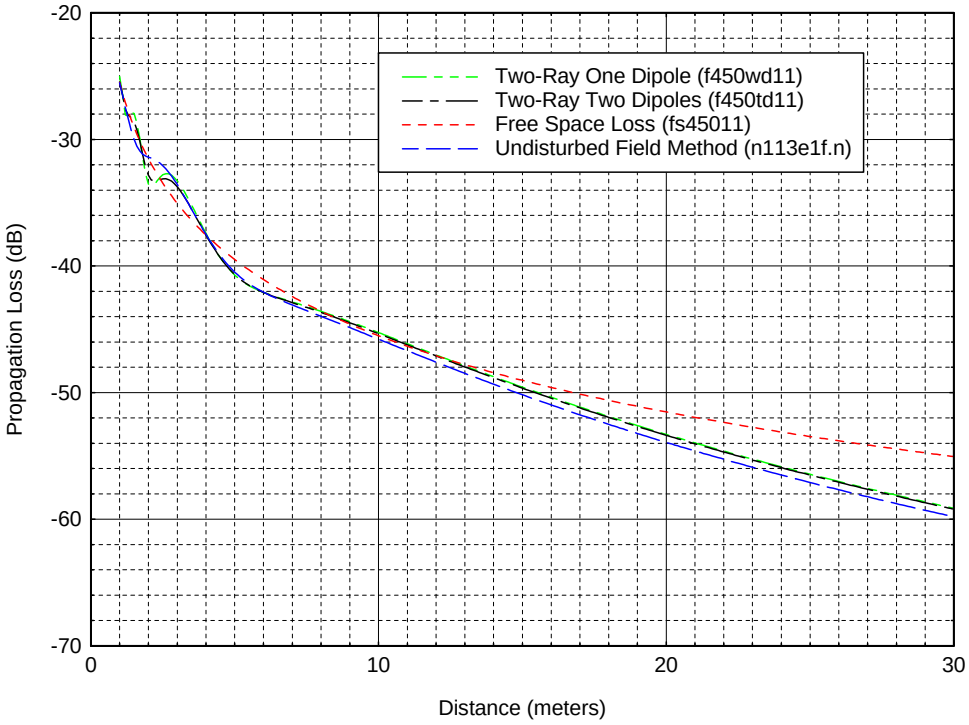


Figure E-7. Comparison of the undisturbed-field method with other methods at 450 MHz for antenna heights $h_1$=1m and $h_2$=1m.

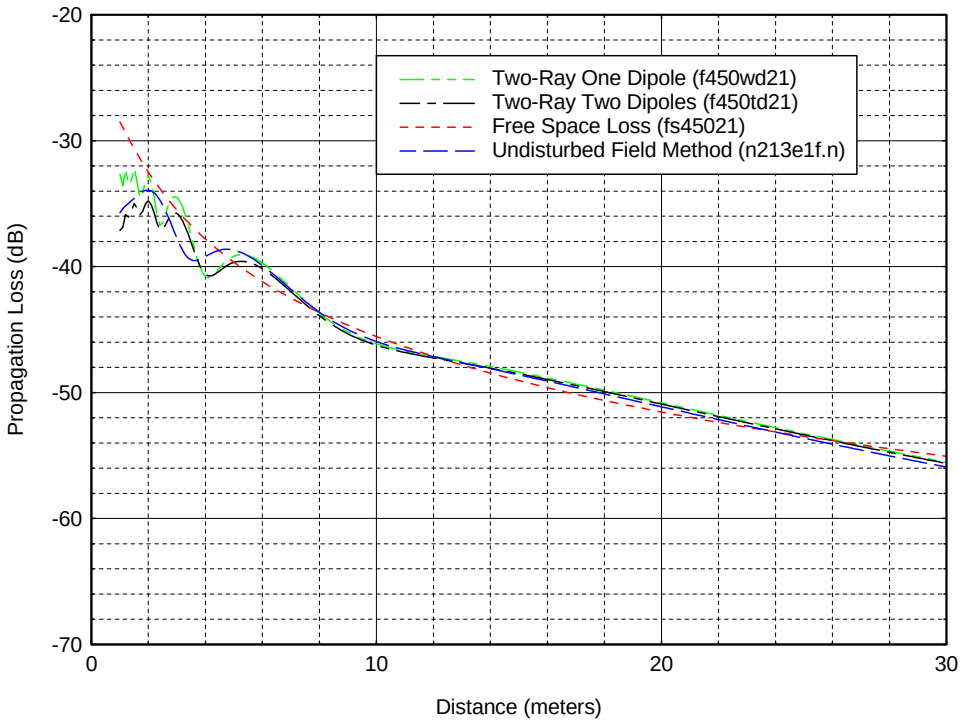


Figure E-8. Comparison of the undisturbed-field method with other methods at 450 MHz for antenna heights $h_1$=2m and $h_2$=1m.

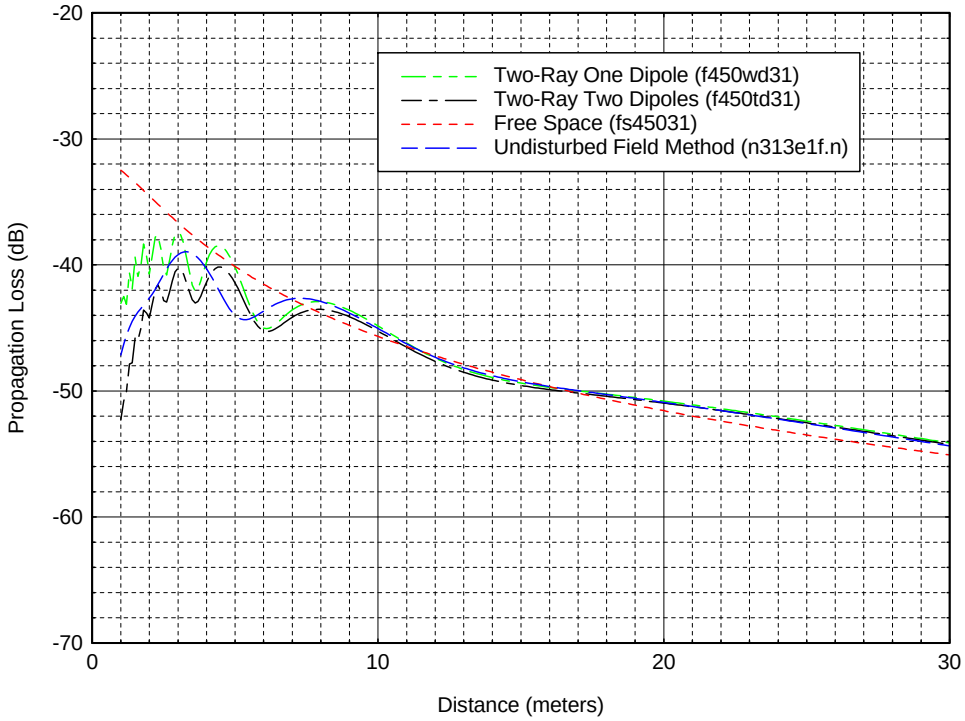


Figure E-9. Comparison of the undisturbed-field method with other methods at 150 MHz for antenna heights $h_1$=3m and $h_2$=1m.

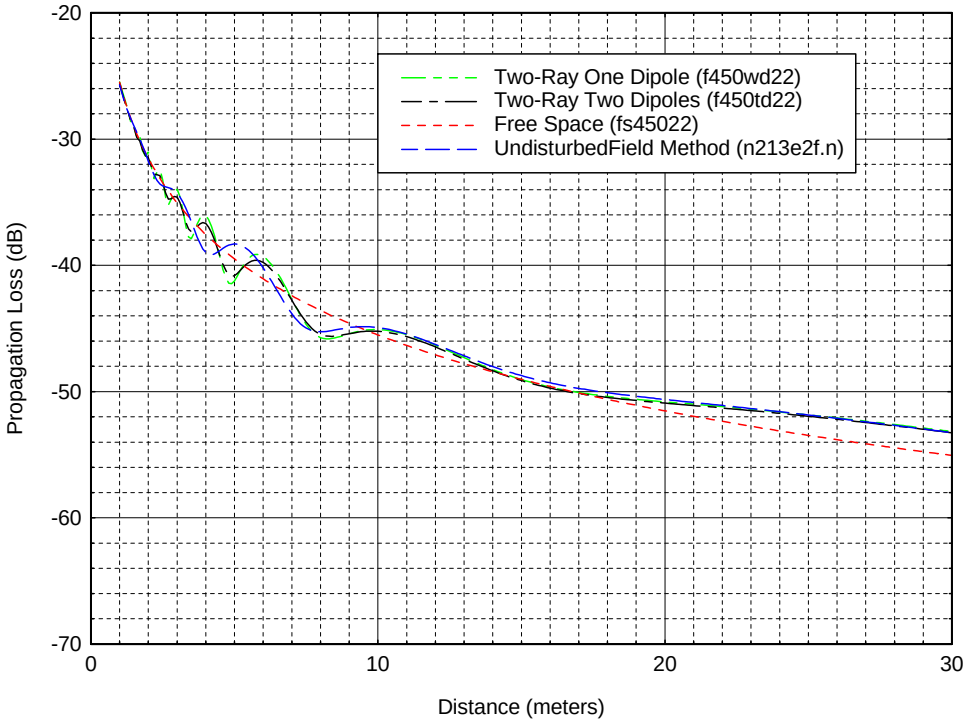


Figure E-10. Comparison of the undisturbed-field method with other methods at 450 MHz for antenna heights $h_1$=2m and $h_2$=2m.

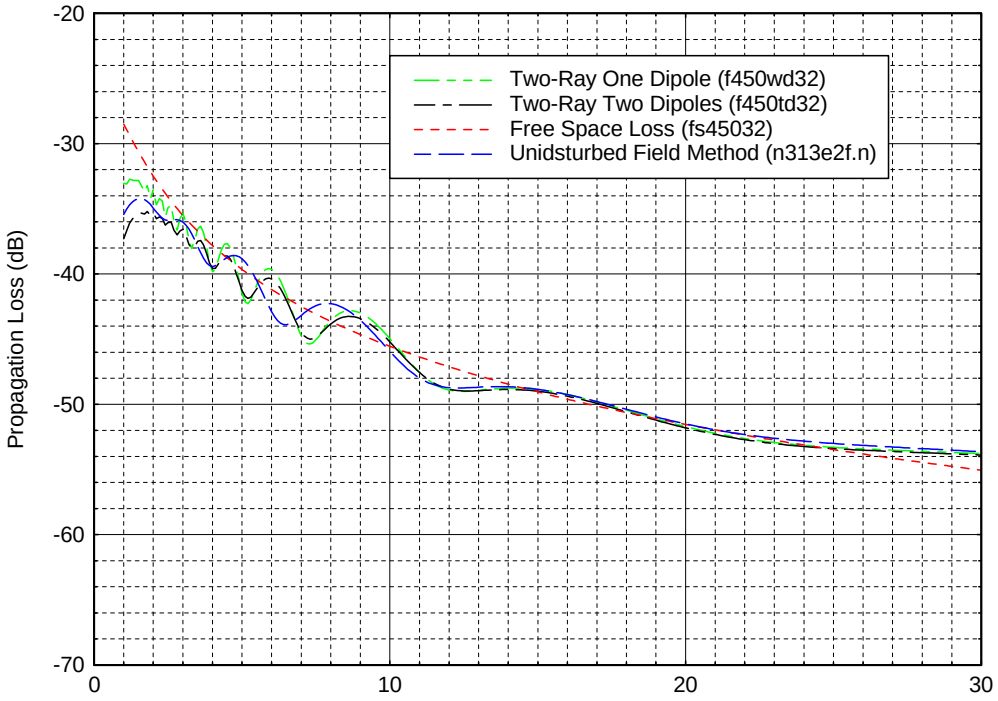


Figure E-11. Comparison of the undisturbed-field method with other methods at 450 MHz for antenna heights $h_1$=3m and $h_2$=2m.

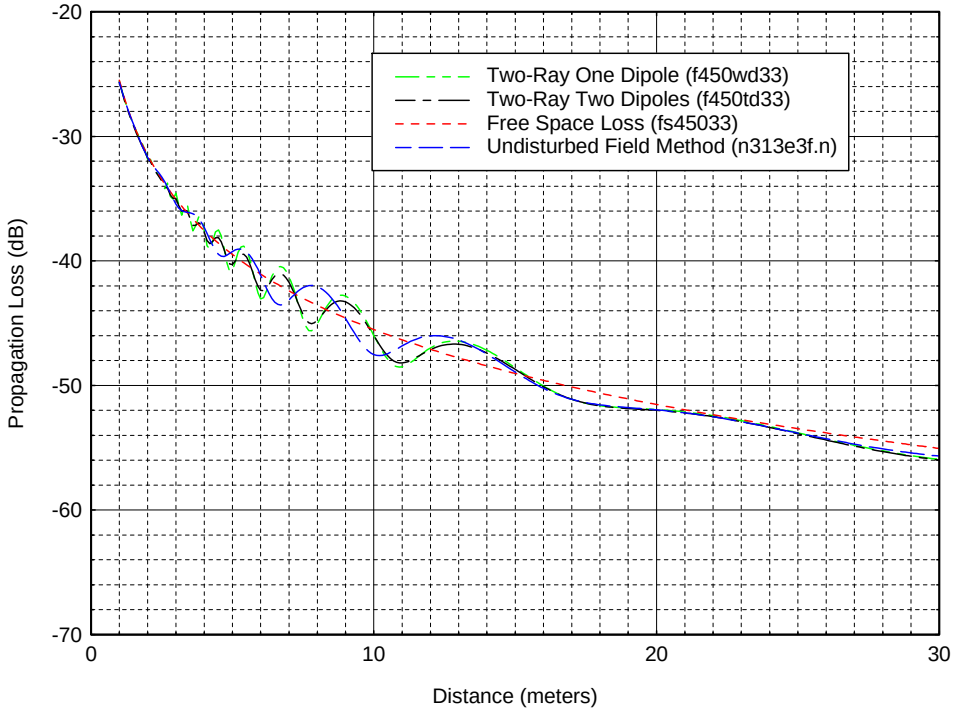


Figure E-12. Comparison of the undisturbed-field method with other methods at 450 MHz for antenna heights $h_1$=3m and $h_2$=3m.

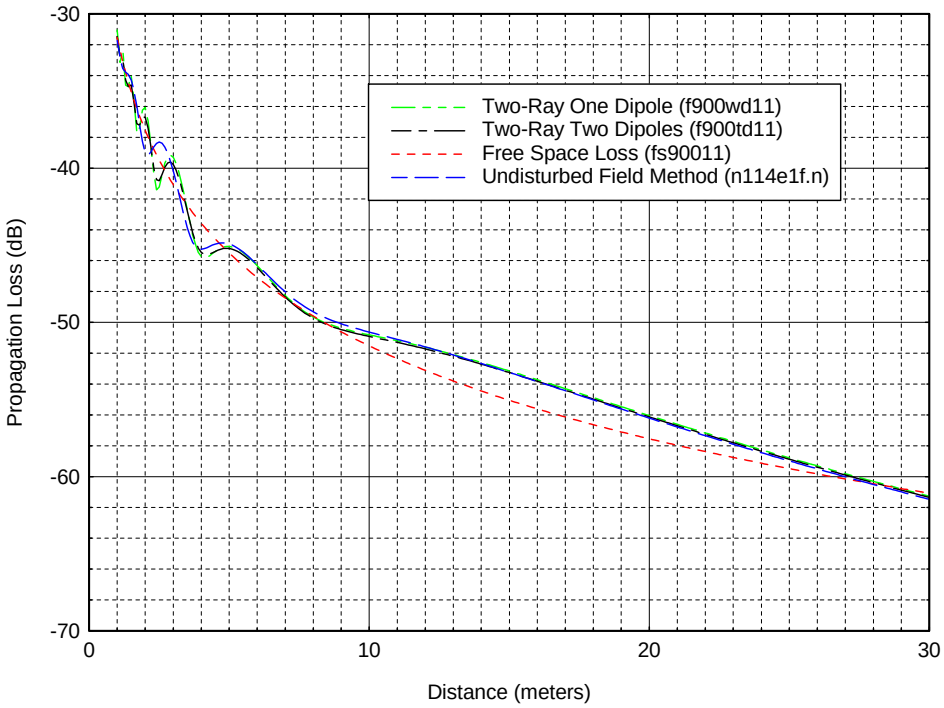


Figure E-13. Comparison of the undisturbed-field method with other methods at 900 MHz for antenna heights $h_1$=1m and $h_2$=1m.

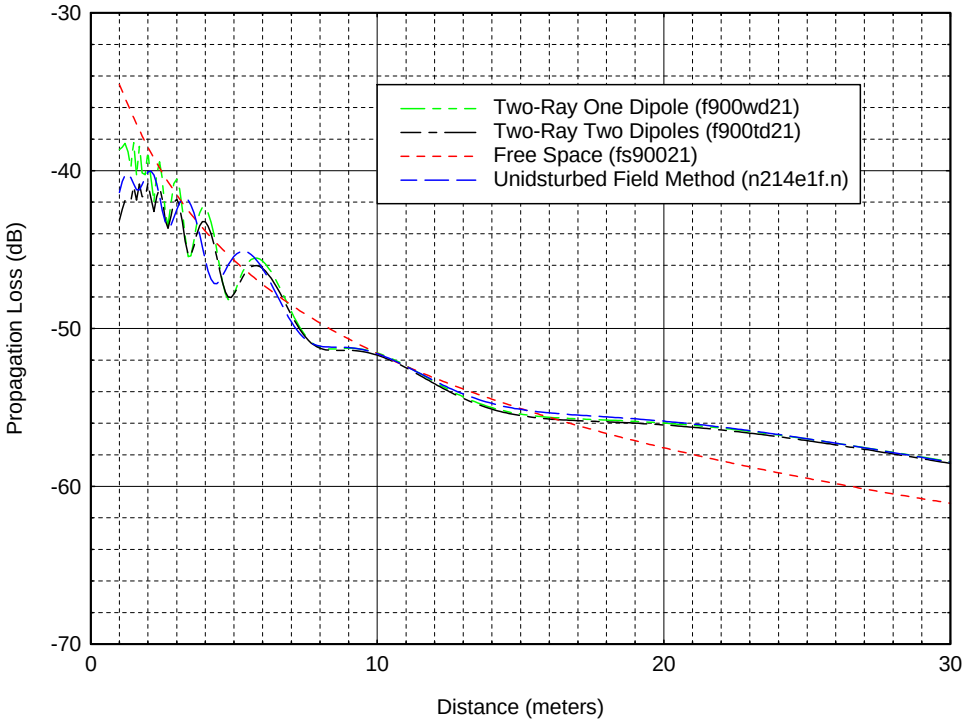


Figure E-14. Comparison of the undisturbed-field method with other methods at 900 MHz for antenna heights $h_1$=2m and $h_2$=1m.

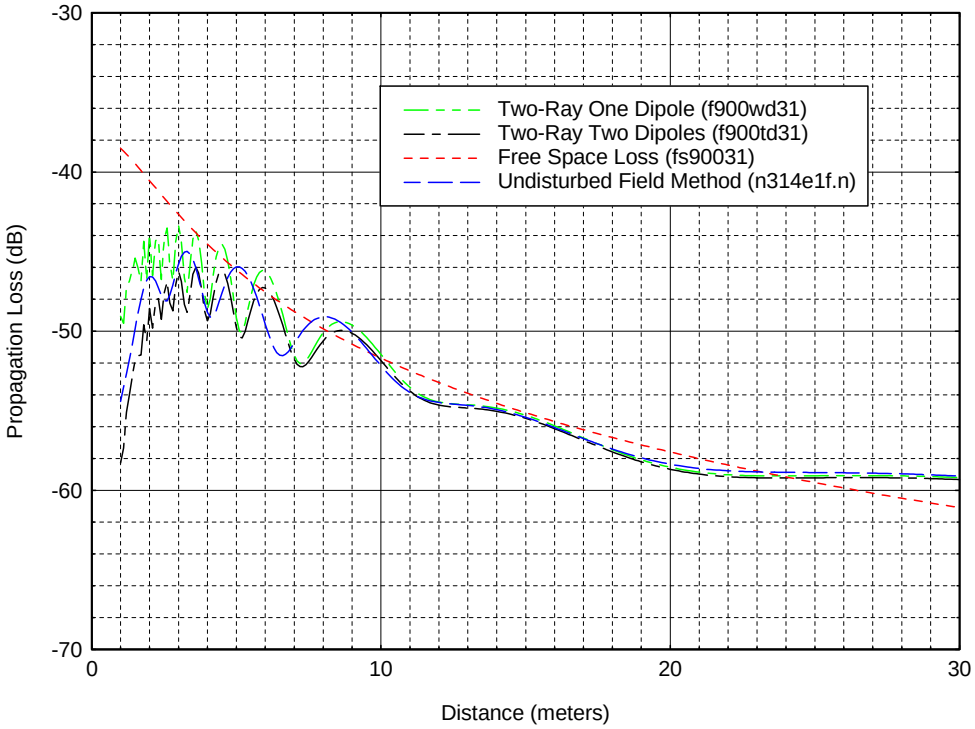


Figure E-15. Comparison of the undisturbed-field method with other methods at 900 MHz for antenna heights $h_1$=3m and $h_2$=1m.

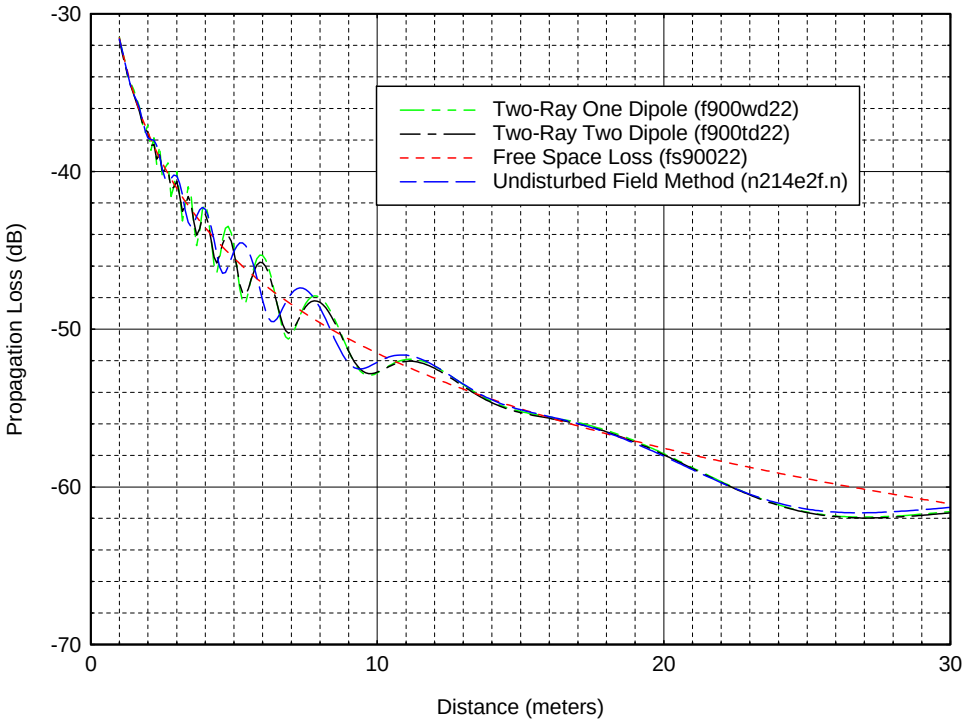


Figure E-16. Comparison of the undisturbed-field method with other methods at 900 MHz for antenna heights $h_1$=2m and $h_2$=2m.

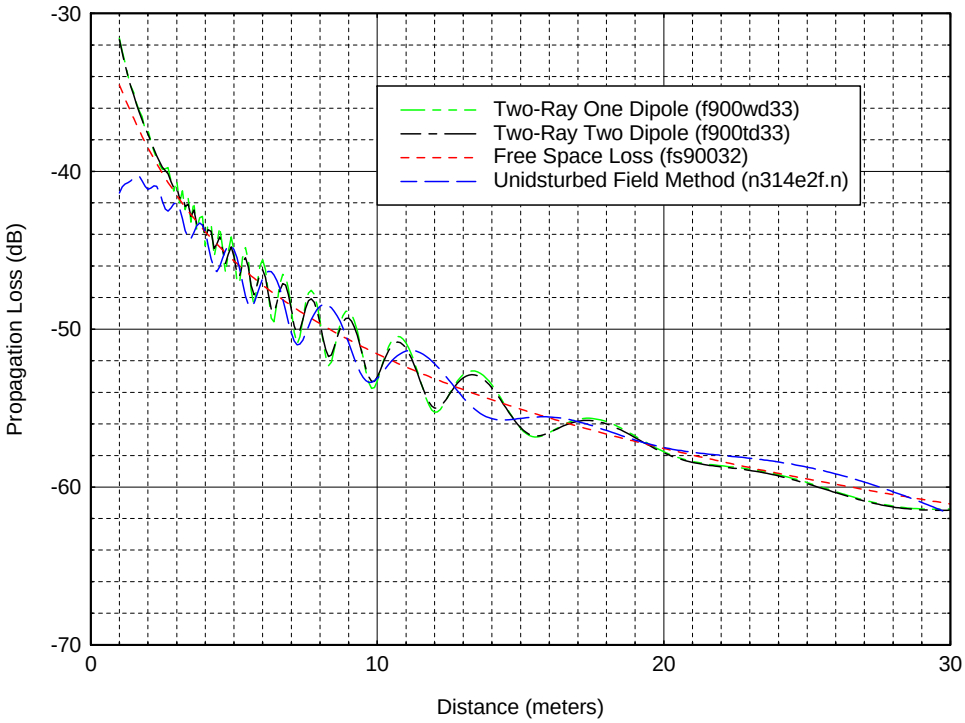


Figure E-17. Comparison of the undisturbed-field method with other methods at 900 MHz for antenna heights $h_1$=3m and $h_2$=2m.

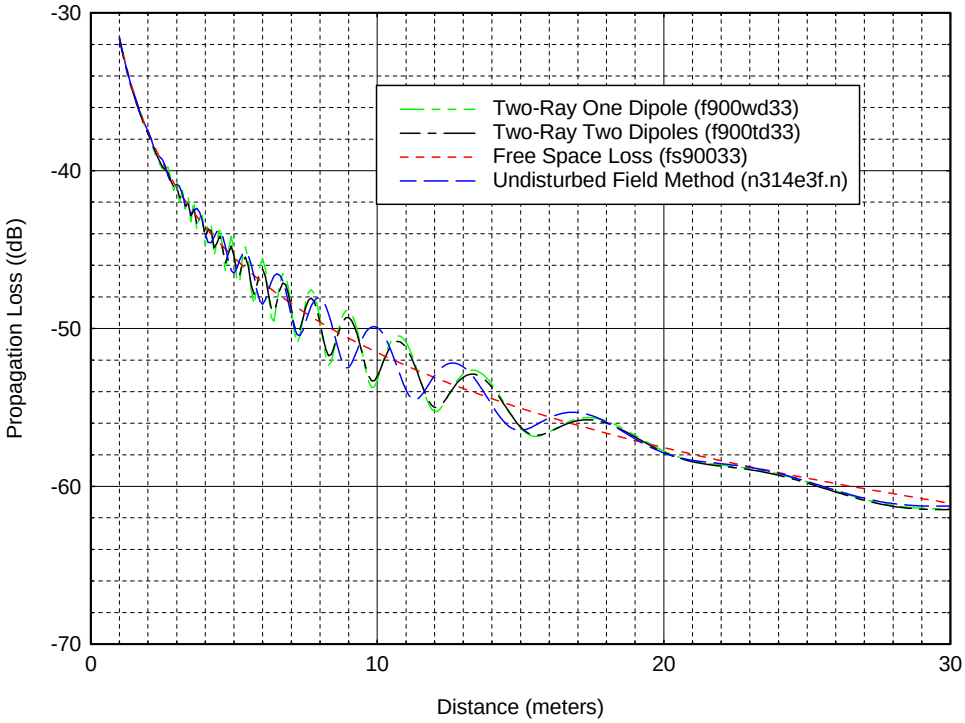


Figure E-18. Comparison of the undisturbed-field method with other methods at 900 MHz for antenna heights $h_1$=3m and $h_2$=3m.

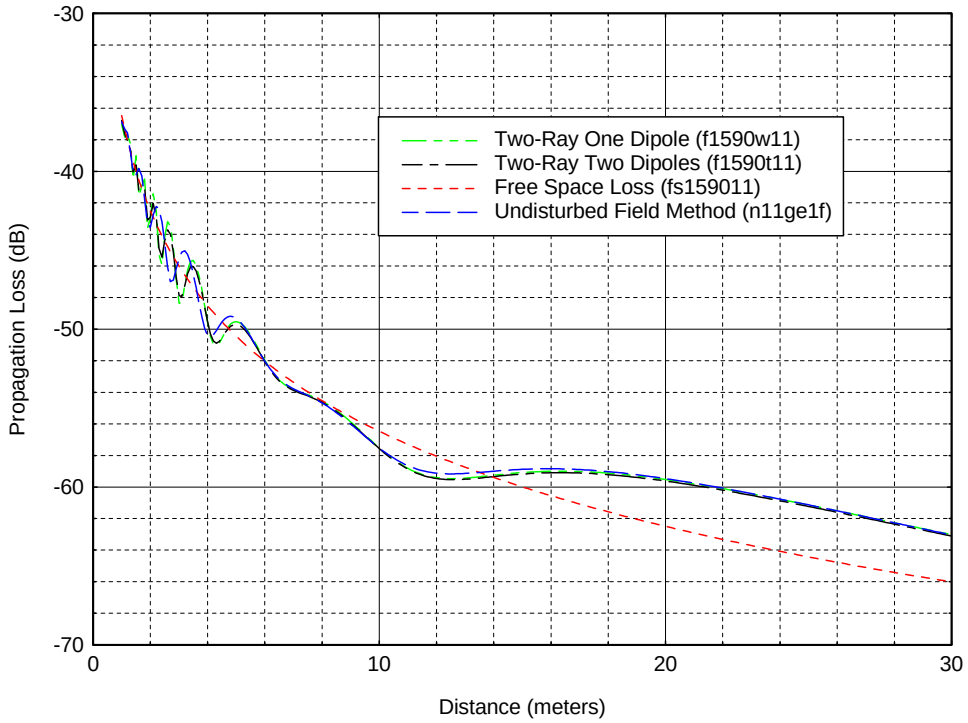


Figure E-19. Comparison of the undisturbed-field method with other methods at 1590 MHz for antenna heights $h_1$=1m and $h_2$=1m.

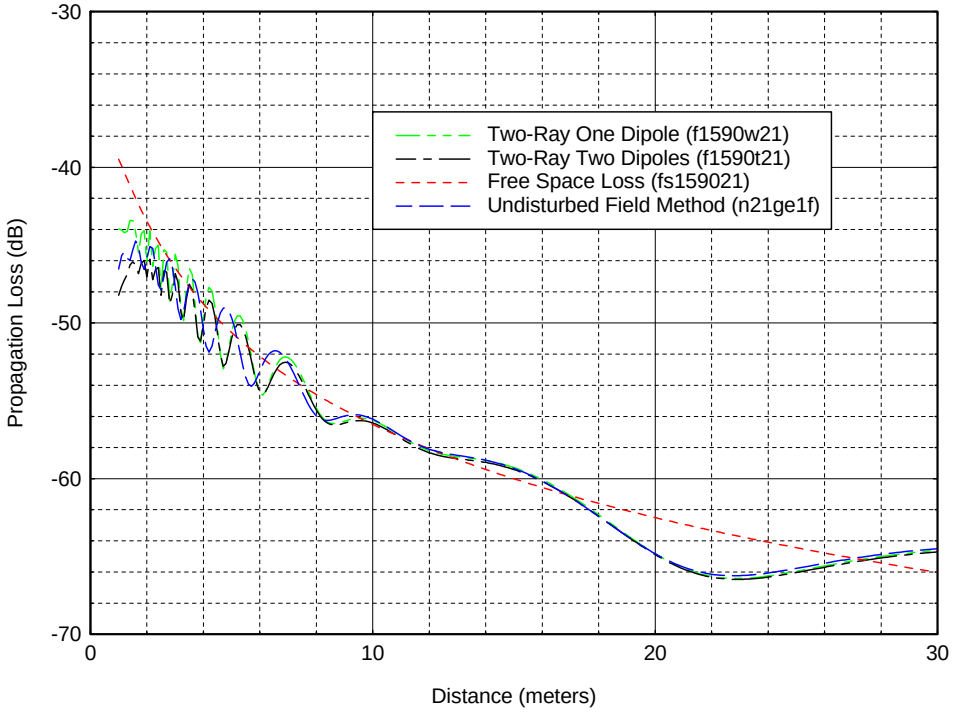


Figure E-20. Comparison of the undisturbed-field method with other methods at 1590 MHz for antenna heights $h_1$=2m and $h_2$=1m.

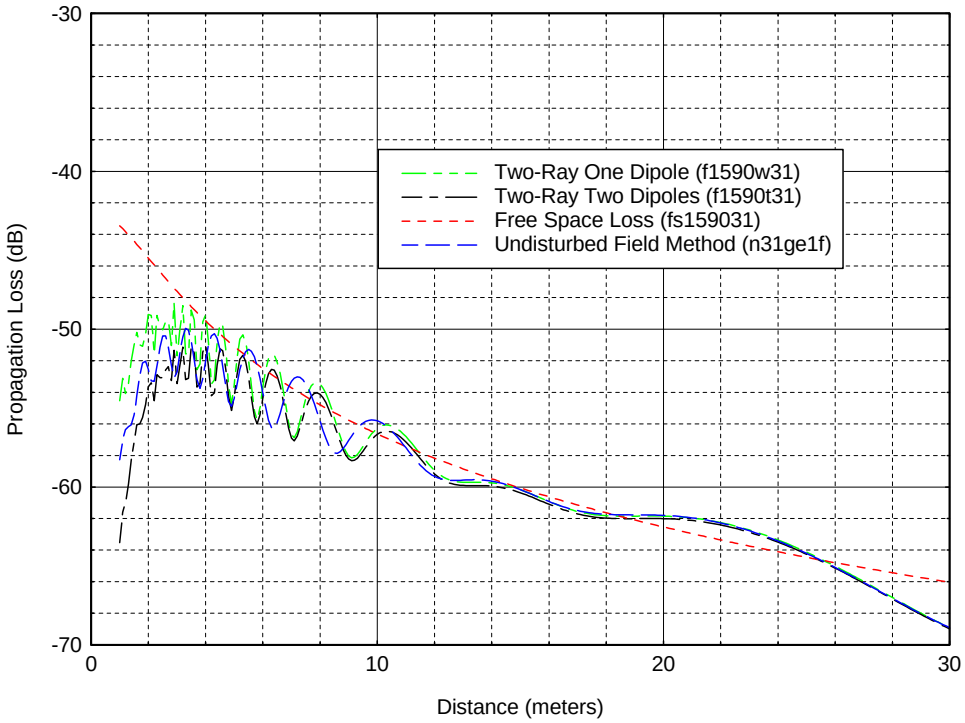


Figure E-21. Comparison of the undisturbed-field method with other methods at 1590 MHz for antenna heights $h_1$=3m and $h_2$=1m.

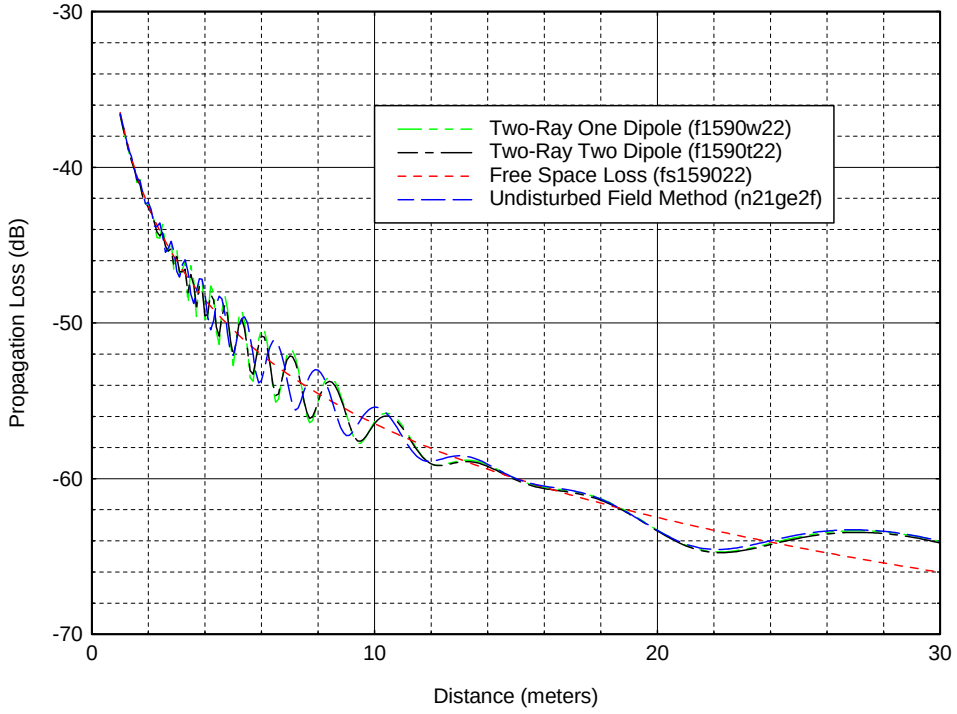


Figure E-22. Comparison of the undisturbed-field method with other methods at 1590 MHz for antenna heights $h_1$=2m and $h_2$=2m.

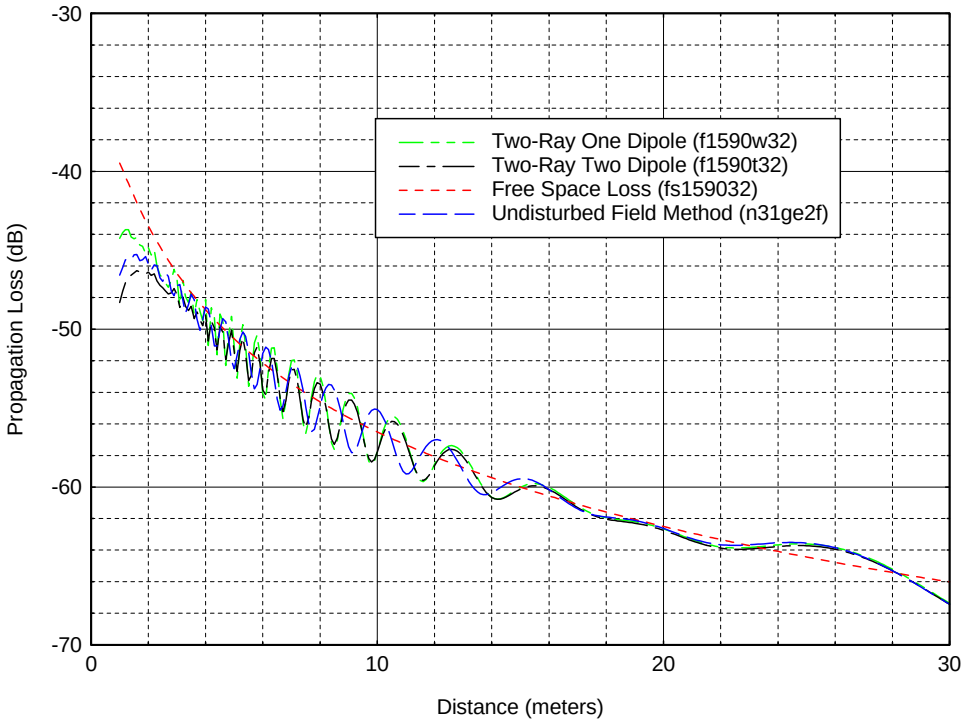


Figure E-23. Comparison of the undisturbed-field method with other methods at 1590 MHz for antenna heights $h_1$=3m and $h_2$=2m.

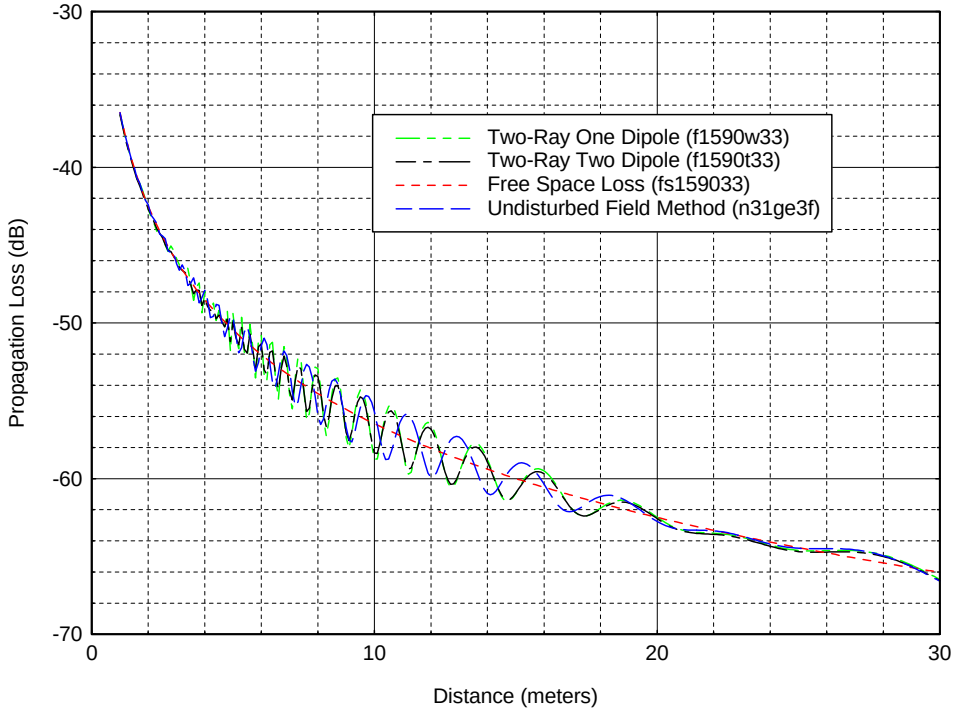


Figure E-24. Comparison of the undisturbed-field method with other methods at 1590 MHz for antenna heights $h_1$=3m and $h_2$=3m.

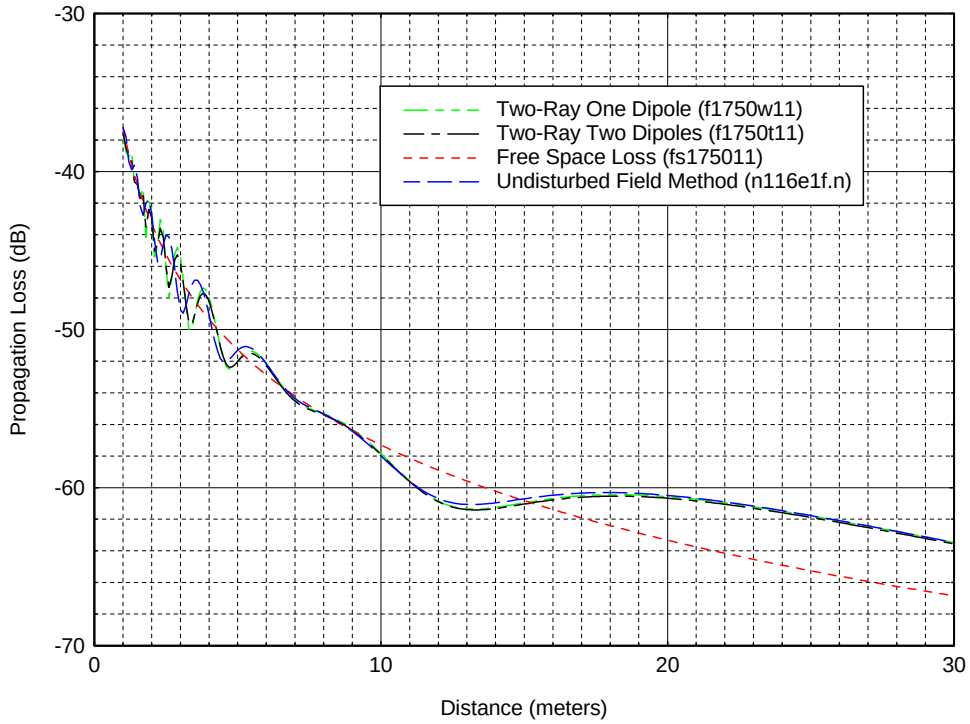


Figure E-25. Comparison of the undisturbed-field method with other methods at 1750 MHz for antenna heights $h_1$=1m and $h_2$=1m.

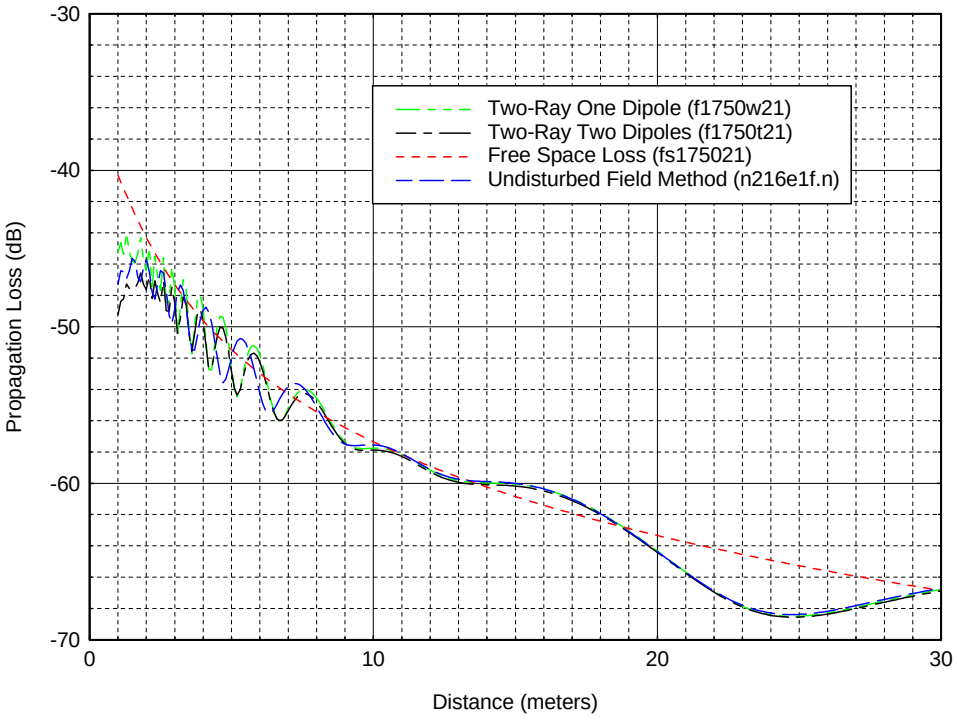


Figure E-26. Comparison of the undisturbed-field method with other methods at 1750 MHz for antenna heights $h_1$=2m and $h_2$=1m.

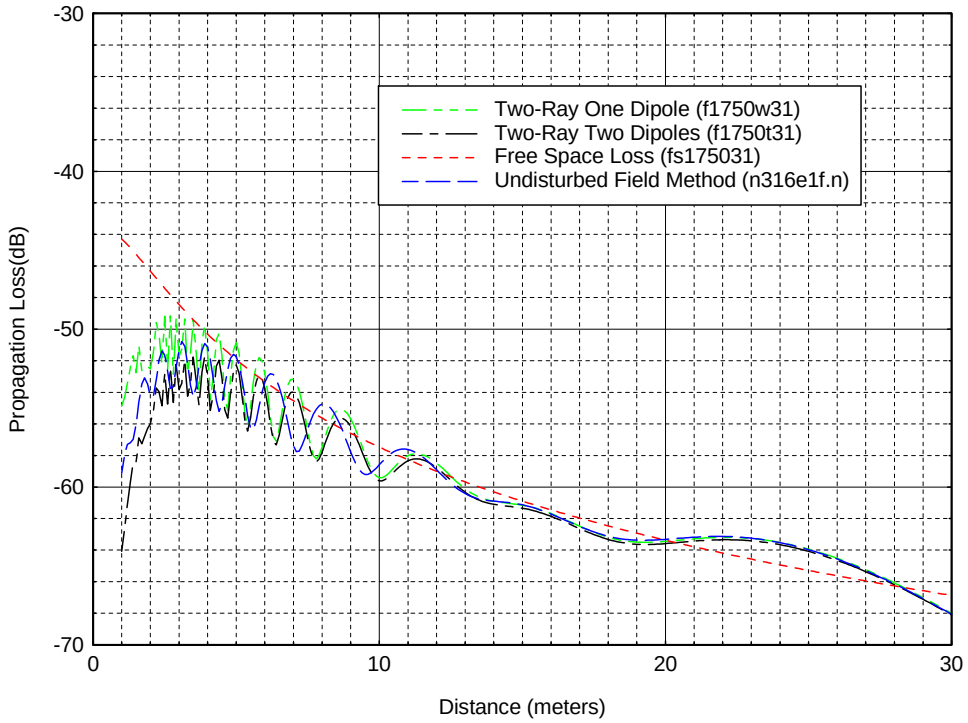


Figure E-27. Comparison of the undisturbed-field method with other methods at 1750 MHz for antenna heights $h_1$=3m and $h_2$=1m.

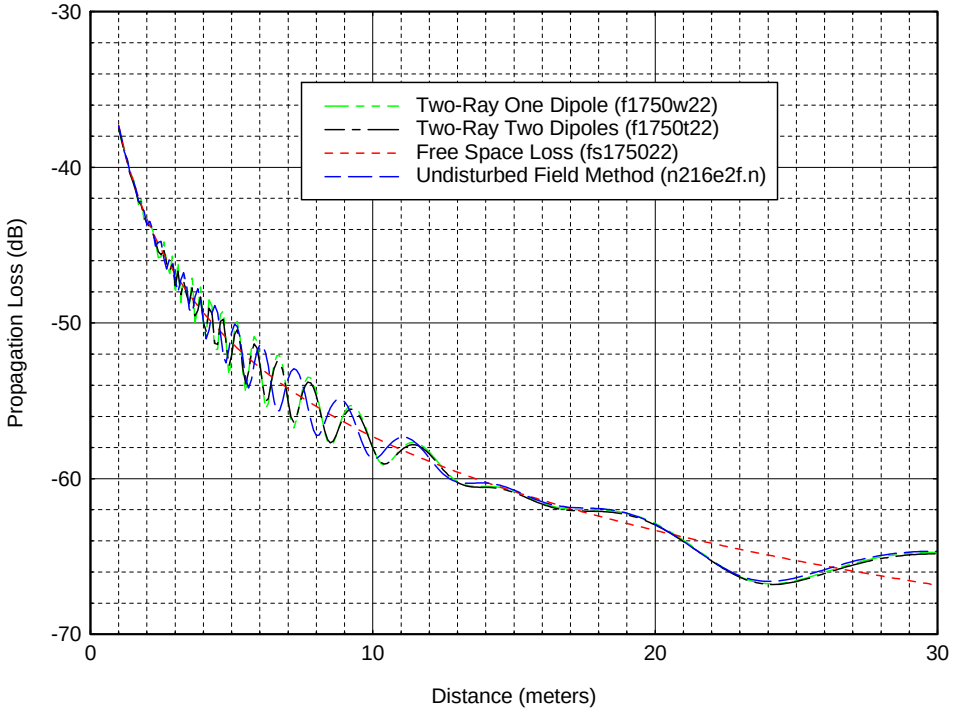


Figure E-28. Comparison of the undisturbed-field method with other methods at 1750 MHz for antenna heights $h_1$=2m and $h_2$=2m.

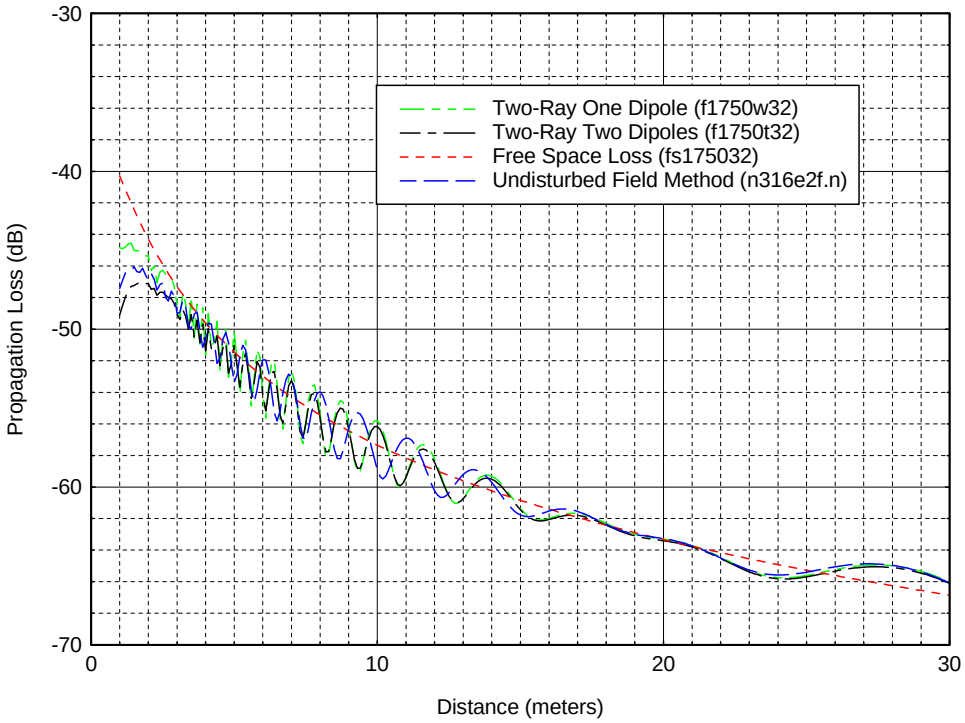


Figure E-29. Comparison of the undisturbed-field method with other methods at 1750 MHz for antenna heights $h_1$=3m and $h_2$=2m.

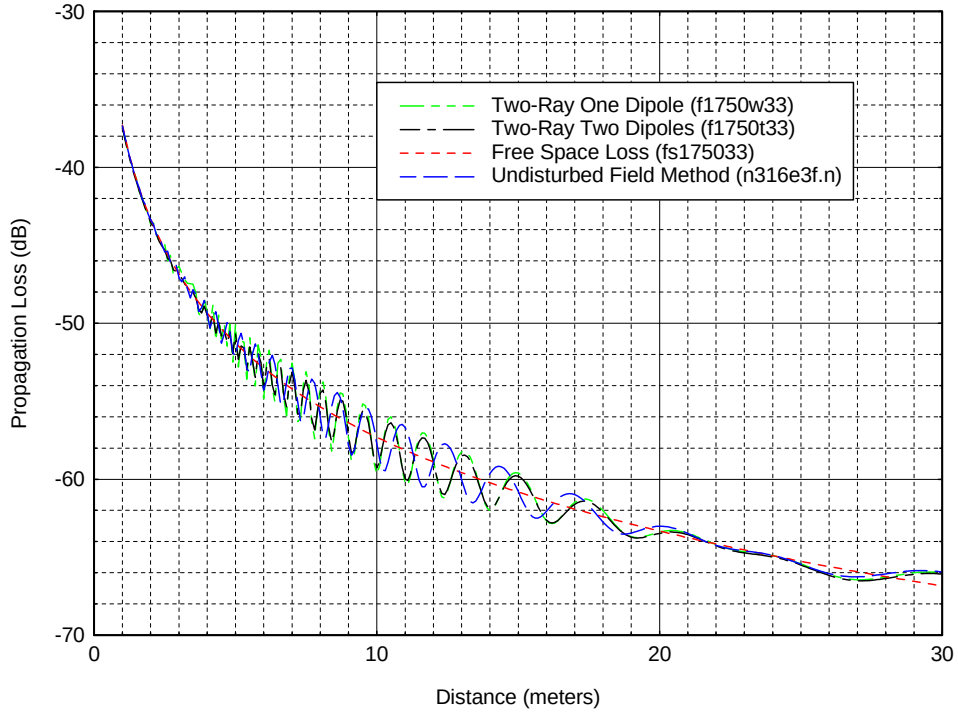


Figure E-30. Comparison of the undisturbed-field method with other methods at 1750 MHz for antenna heights $h_1$=3m and $h_2$=3m.

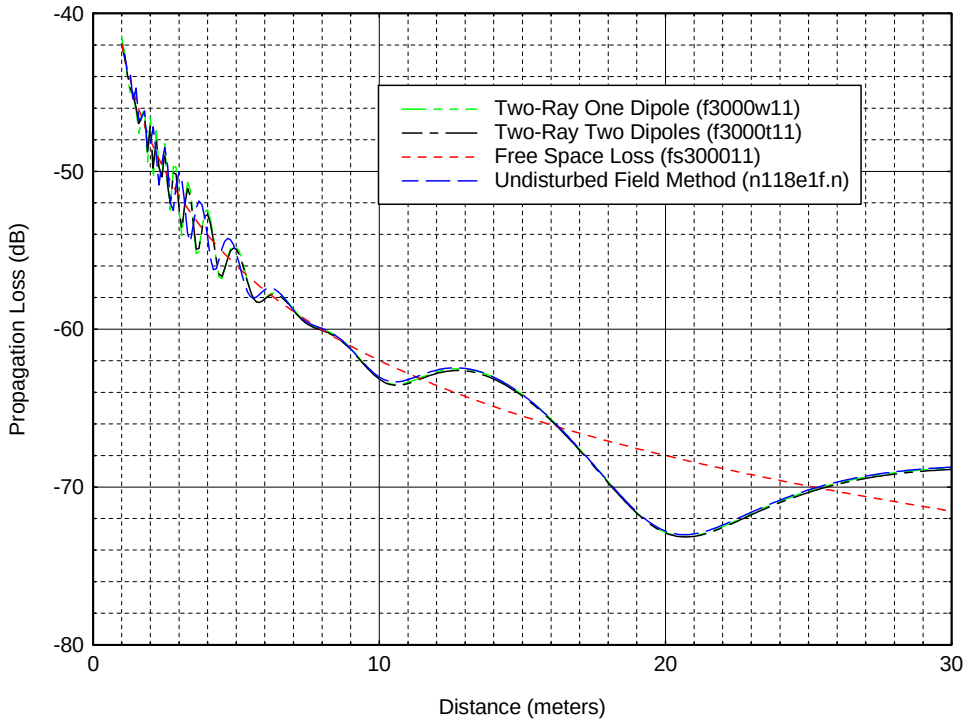


Figure E-31. Comparison of the undisturbed-field method with other methods at 3000 MHz for antenna heights $h_1$=1m and $h_2$=1m.

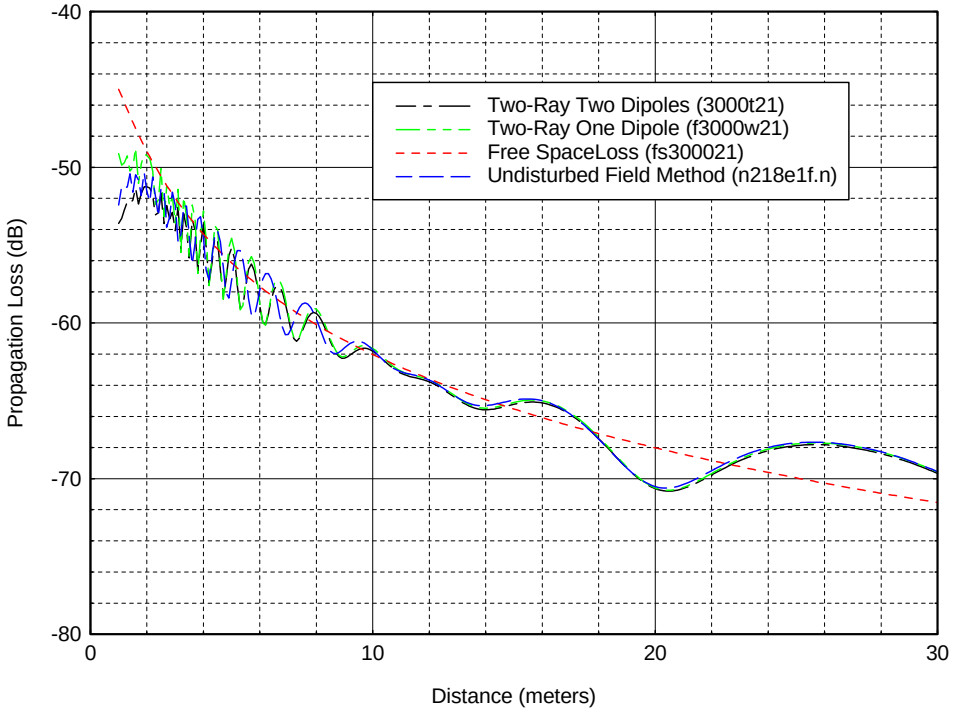


Figure E-32. Comparison of the undisturbed-field method with other methods at 3000 MHz for antenna heights $h_1$=2m and $h_2$=1m.

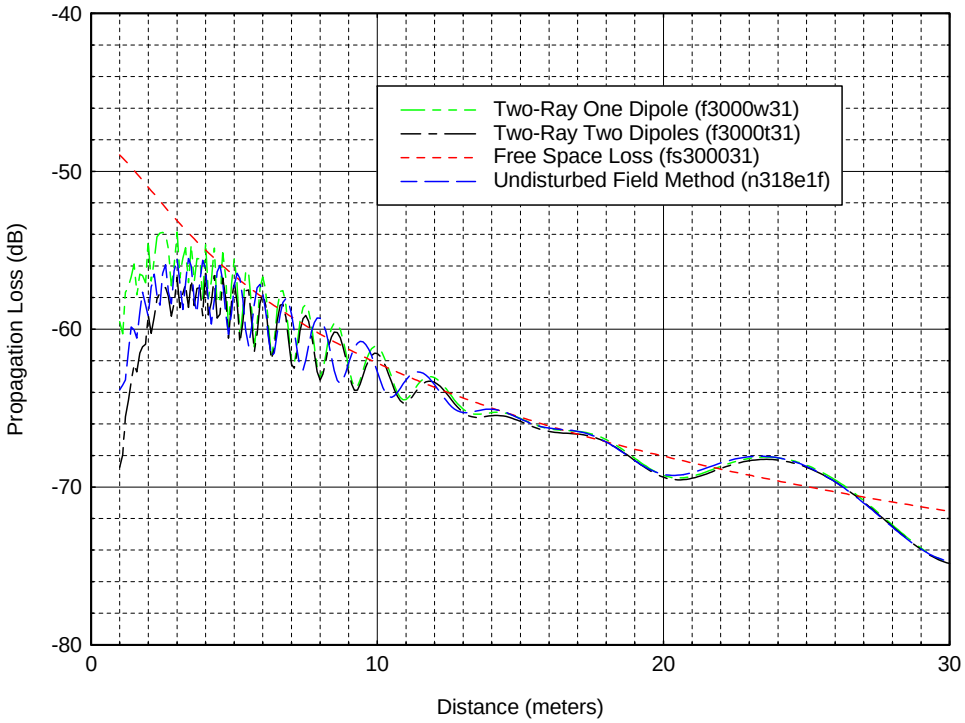


Figure E-33. Comparison of the undisturbed-field method with other methods at 3000 MHz for antenna heights $h_1$=3m and $h_2$=1m.

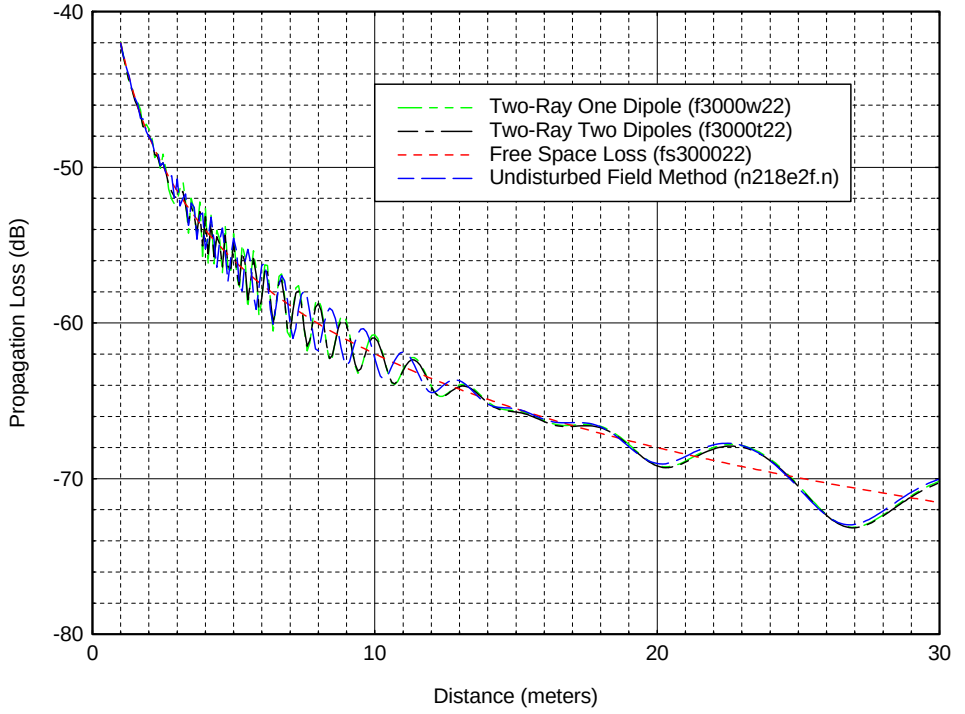


Figure E-34. Comparison of the undisturbed-field method with other methods at 3000 MHz for antenna heights $h_1$=2m and $h_2$=2m.

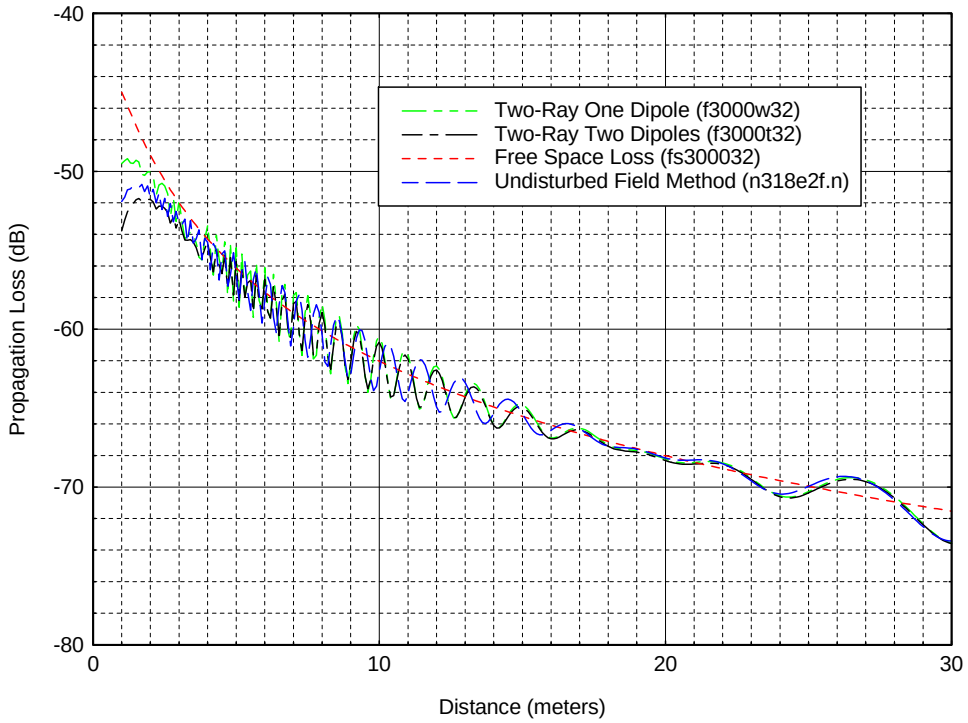


Figure E-35. Comparison of the undisturbed-field method with other methods at 3000 MHz for antenna heights $h_1$=3m and $h_2$=2m.

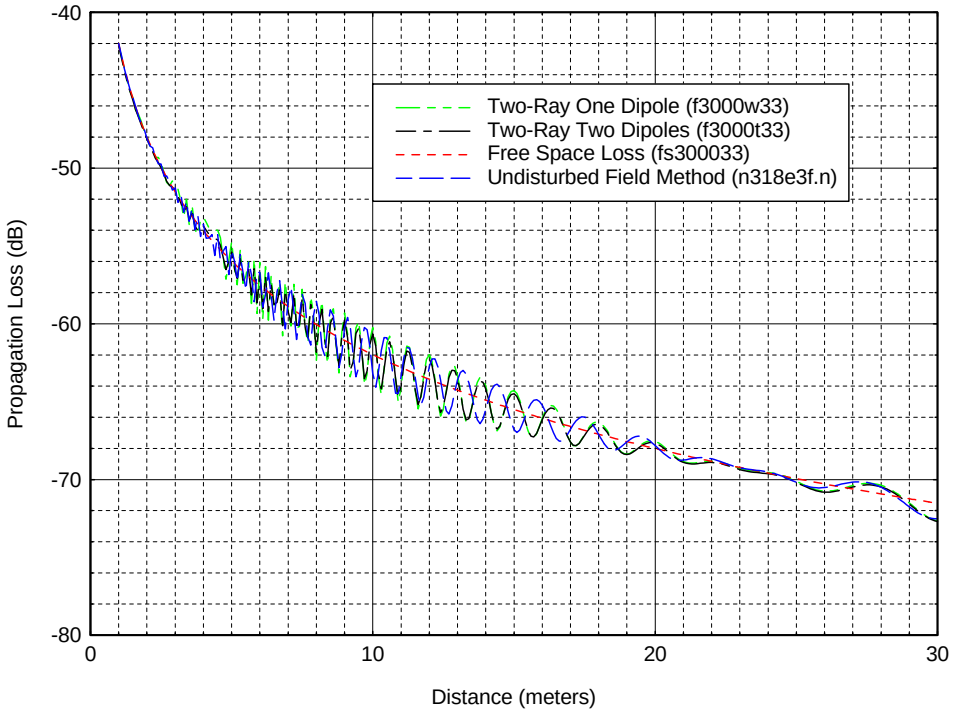


Figure E-36. Comparison of the undisturbed-field method with other methods at 3000 MHz for antenna heights $h_1$=3m and $h_2$=3m

## APPENDIX F: COMPARISON OF THE UNDISTURBED-FIELD METHOD WITH OTHER METHODS (EXPANDED SCALES)

Appendices E and F contain a large number of figures that are referred to in the main body of the report, and it would be inappropriate to integrate this many figures into the corresponding section of the report. Appendices E and F are referred to in Section 3.3 and contain plots of predicted propagation loss versus distance for six different frequencies and six combinations of antenna heights that compare four different propagation loss prediction methods: the free-space loss method, two versions of the complex two-ray method, and the undisturbed-field method. Appendix E plots contain the predicted loss out to 30 meters and Appendix F plots contain the predicted loss out to 10 meters with an expanded distance scale to provide more detail of the short-range behavior of the different propagation prediction methods. These plots are the results of analytic computations described in Section 3.3. These plots show how poorly the free-space propagation loss represents the actual propagation loss predicted by the undisturbed-field method. The undisturbed-field method is the most accurate method.

Also shown on these plots are situations where the complex two-ray method can be used to save computation time for different combinations of antenna heights, frequencies, and distances. For all combinations of antenna heights and frequencies the complex two-ray model achieves accurate propagation loss predictions for distances greater than 20 meters. The complex two-ray method is a faster and easier computation than the undisturbed field method, but there are combinations of antenna heights, frequencies, and distances shown by these plots where the undisturbed-field method is the best method to use for computation.

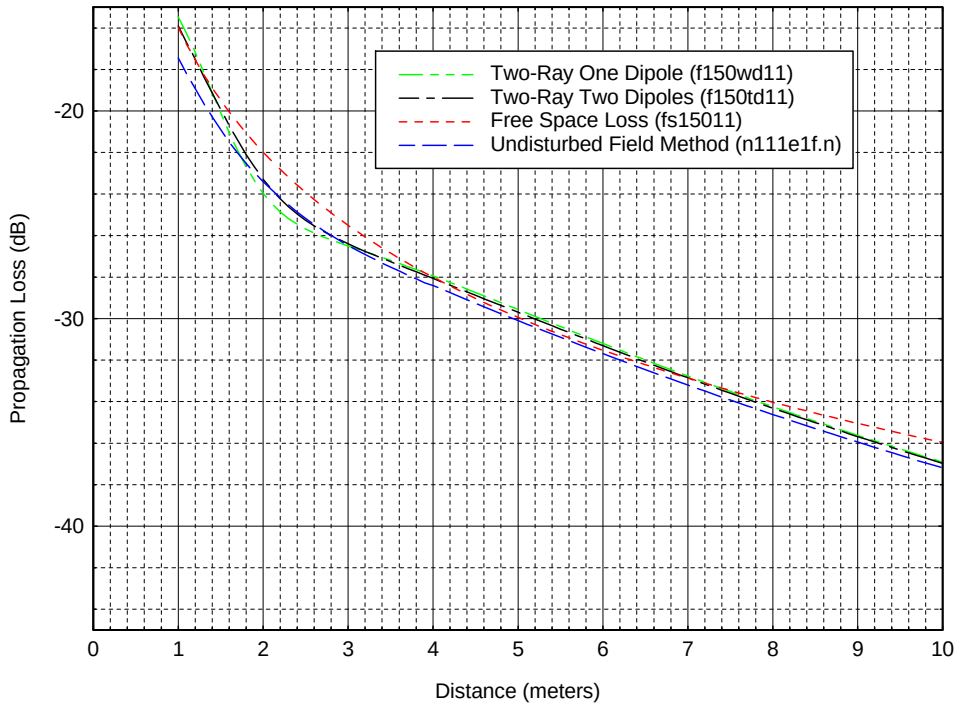


Figure F-1. Comparison of the undisturbed-field method with other methods at 150 MHz for antenna heights $h_1$=1m and $h_2$=1m.

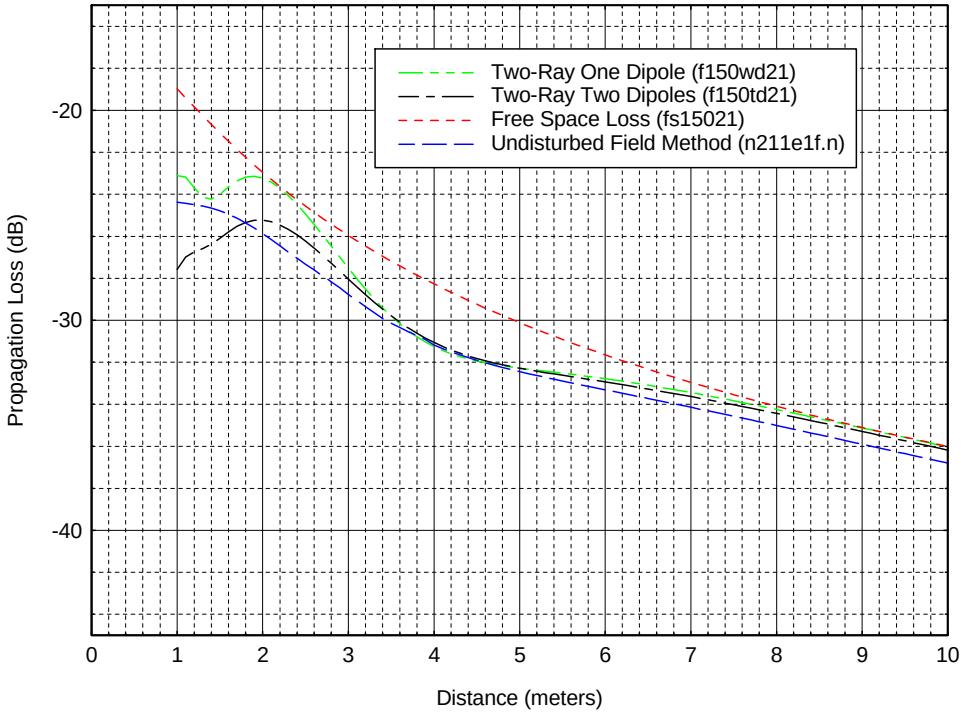


Figure F-2. Comparison of the undisturbed-field method with other methods at 150 MHz for antenna heights $h_1$=2m and $h_2$=1m.

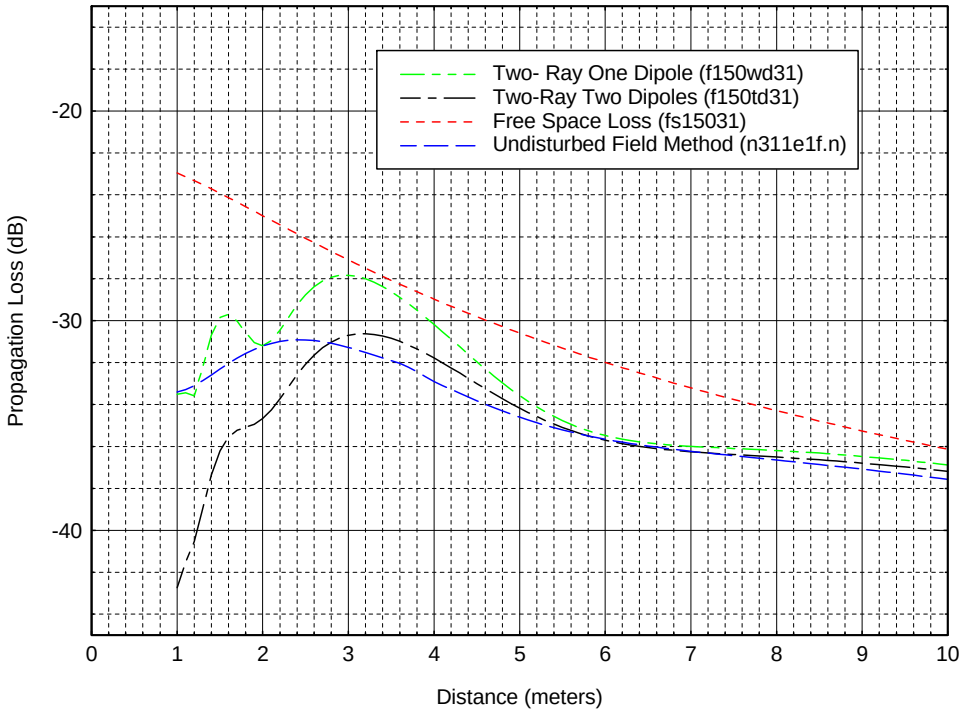


Figure F-3. Comparison of the undisturbed-field method with other methods at 150 MHz for antenna heights $h_1$=2m and $h_2$=1m.

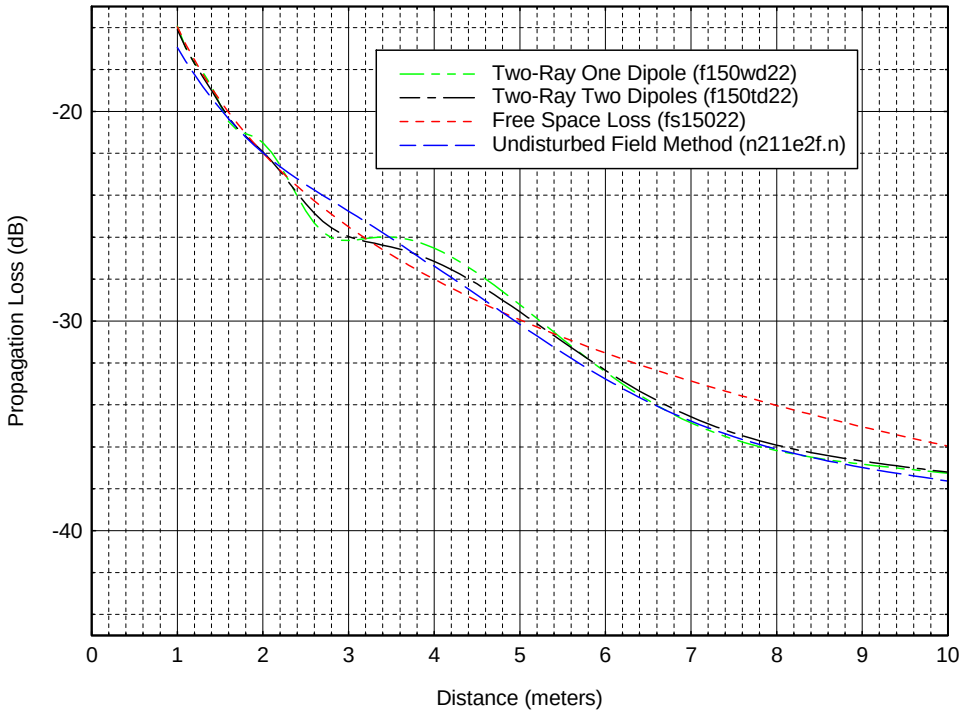


Figure F-4. Comparison of the undisturbed-field method with other methods at 150 MHz for antenna heights $h_1$=2m and $h_2$=2m.

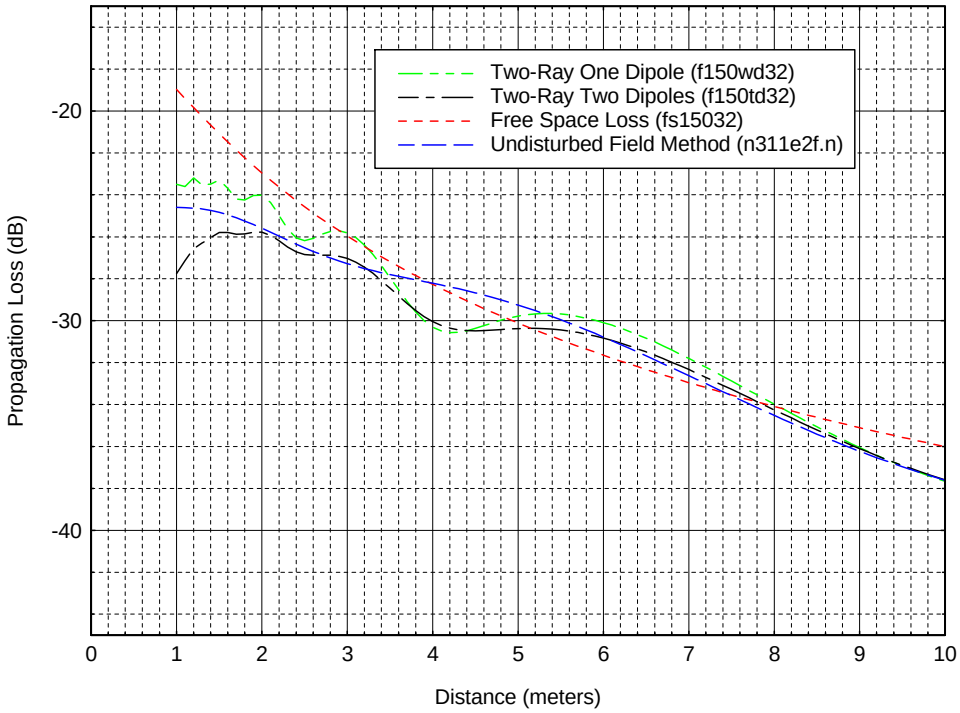


Figure F-5. Comparison of the undisturbed-field method with other methods at 150 MHz for antenna heights $h_1$=3m and $h_2$=2m.

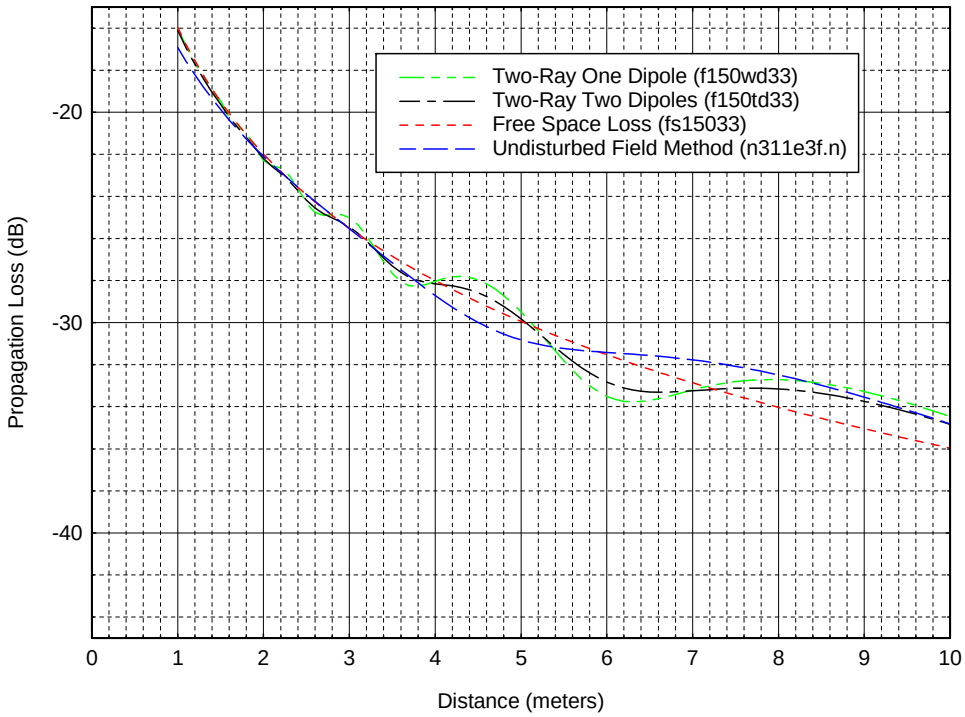


Figure F-6. Comparison of the undisturbed-field method with other methods at 150 MHz for antenna heights $h_1$=3m and $h_2$=3m.

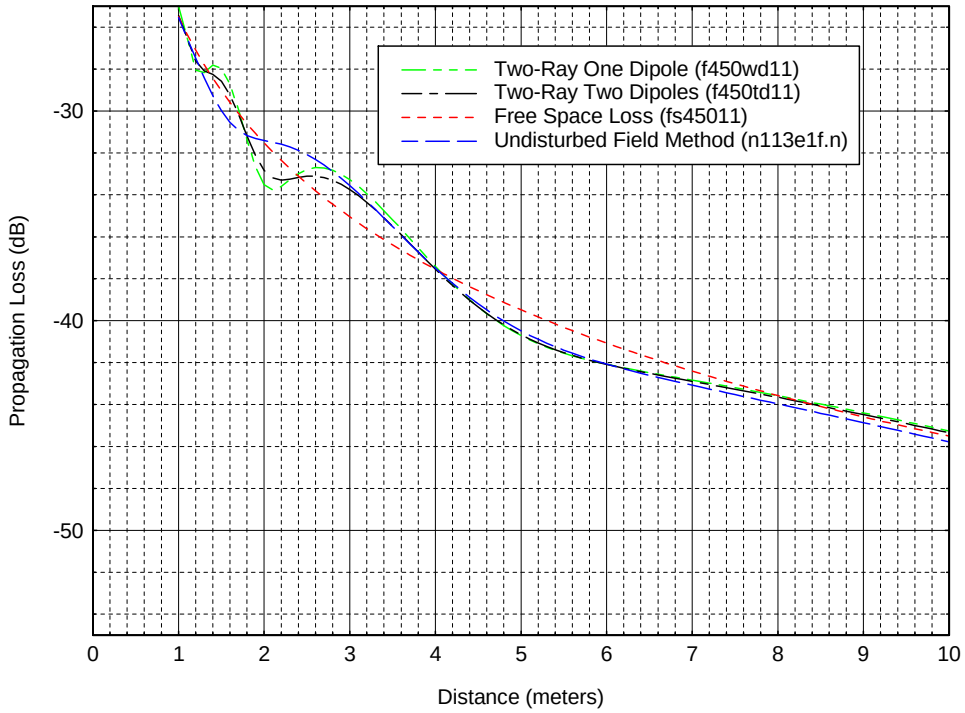


Figure F-7. Comparison of the undisturbed-field method with other methods at 450 MHz for antenna heights $h_1$=1m and $h_2$=1m.

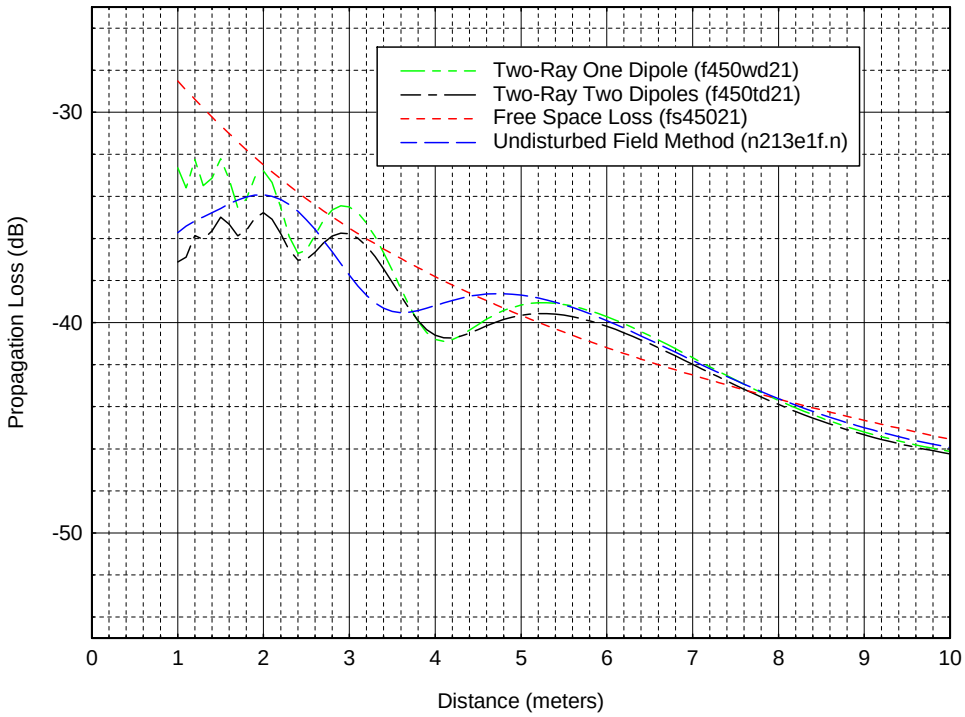


Figure F-8. Comparison of the undisturbed-field method with other methods at 450 MHz for antenna heights $h_1$=2m and $h_2$=1m.

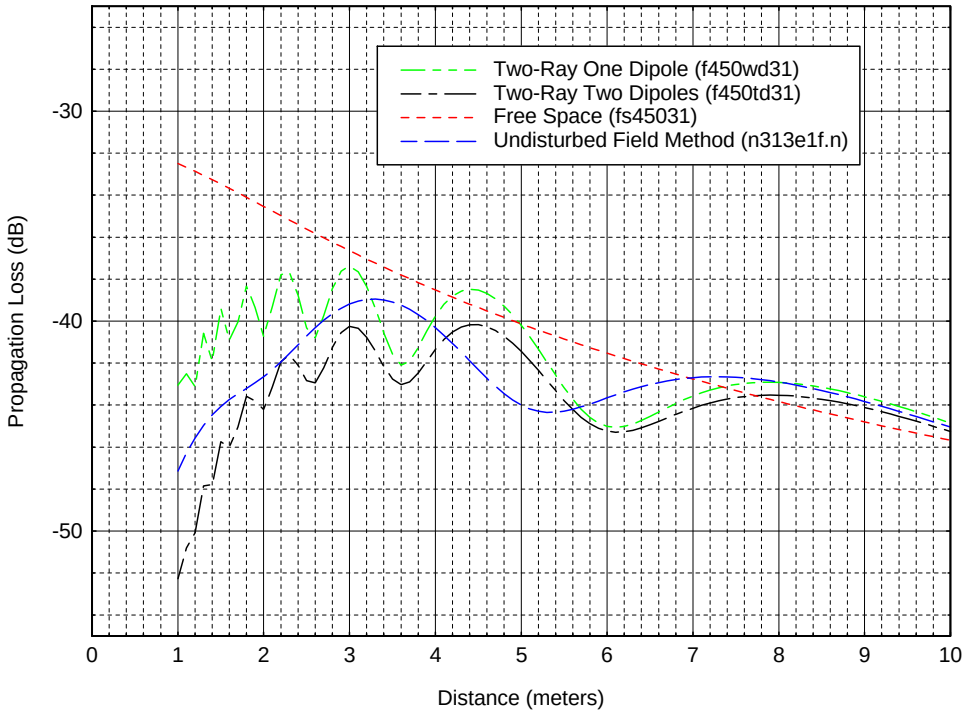


Figure F-9. Comparison of the undisturbed-field method with other methods at 450 MHz for antenna heights $h_1$=2m and $h_2$=1m.

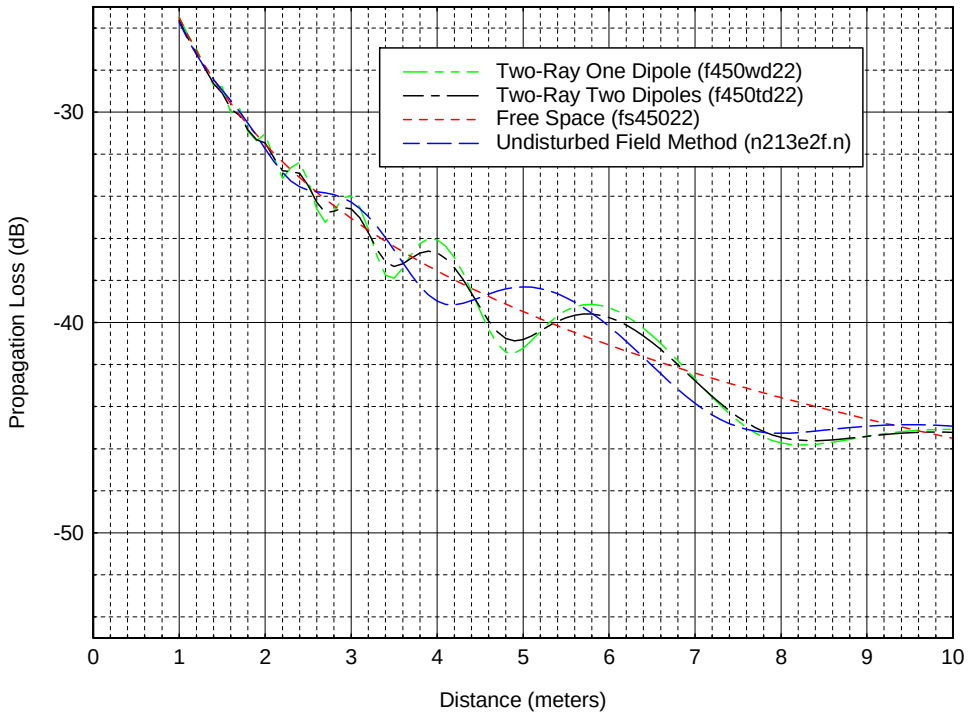


Figure F-10. Comparison of the undisturbed-field method with other methods at 450 MHz for antenna heights $h_1$=2m and $h_2$=2m.

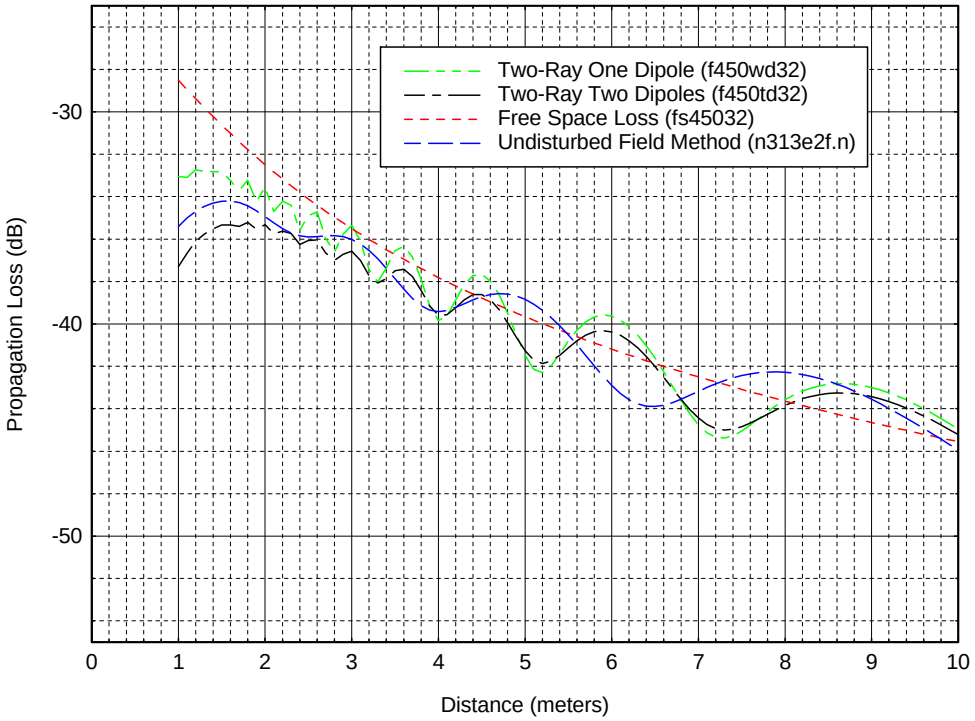


Figure F-11. Comparison of the undisturbed-field method with other methods at 450 MHz for antenna heights $h_1$=3m and $h_2$=2m.

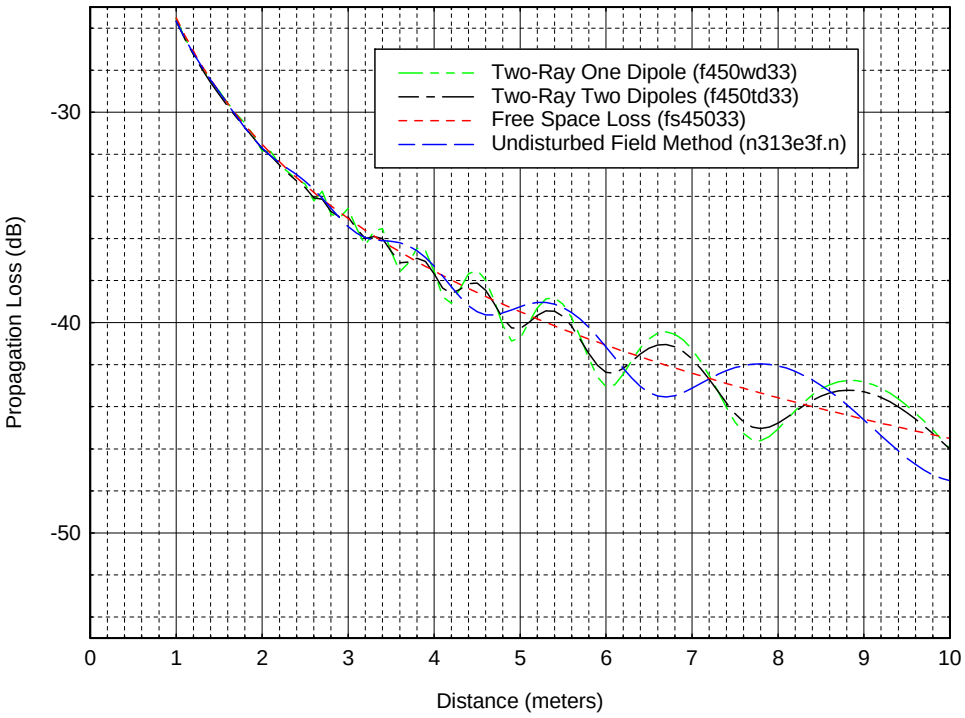


Figure F-12. Comparison of the undisturbed-field method with other methods at 450 MHz for antenna heights $h_1$=3m and $h_2$=3m.

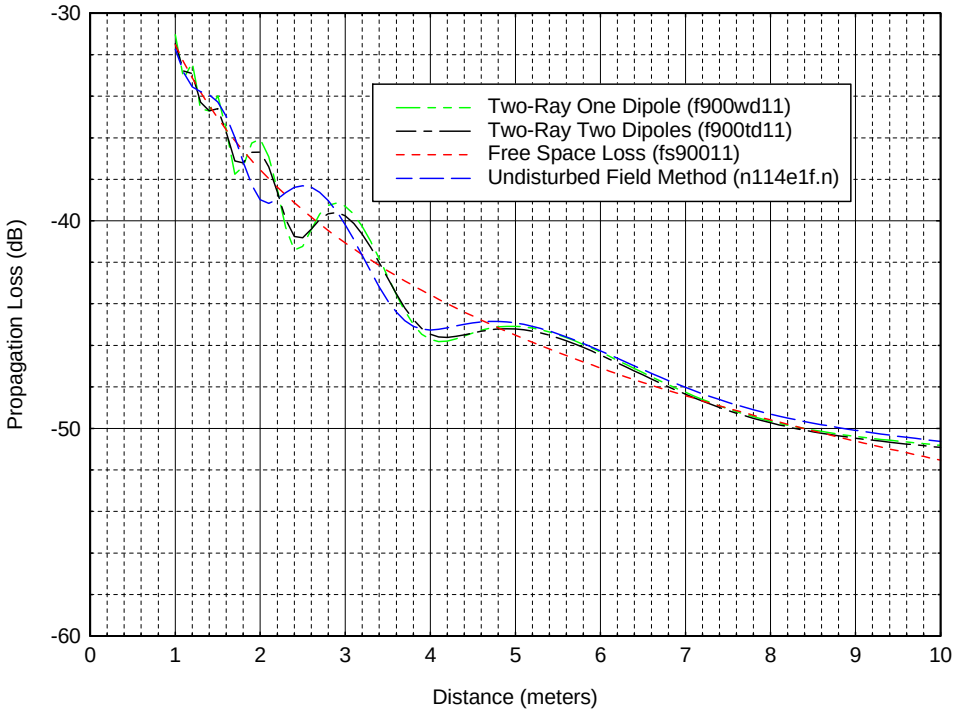


Figure F-13. Comparison of the undisturbed-field method with other methods at 900 MHz for antenna heights $h_1$=1m and $h_2$=1m.

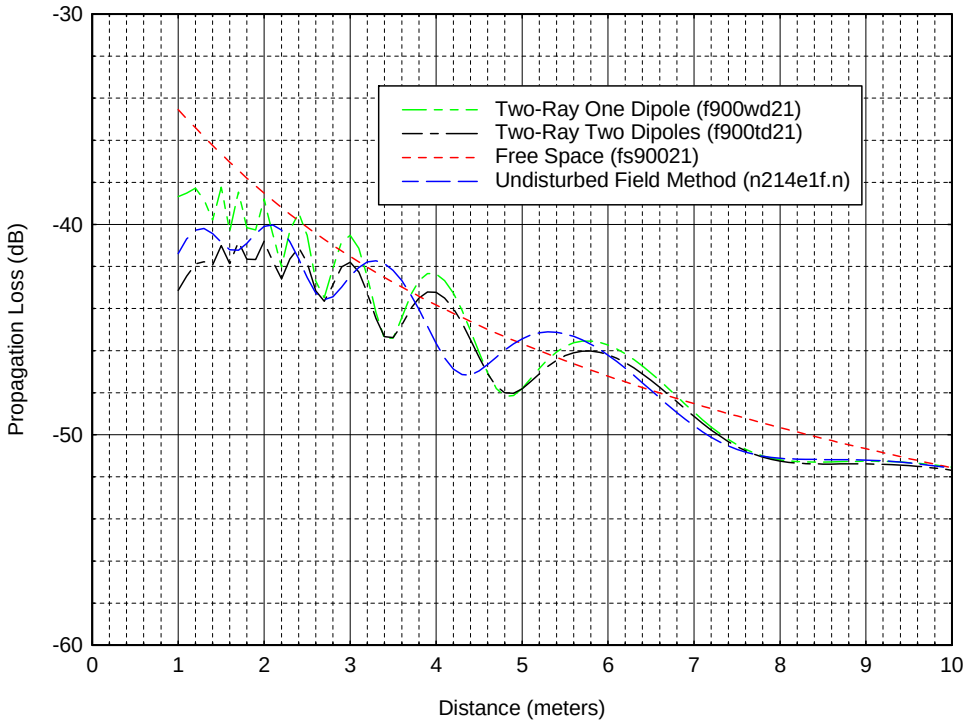


Figure F-14. Comparison of the undisturbed-field method with other methods at 900 MHz for antenna heights $h_1$=2m and $h_2$=1m.

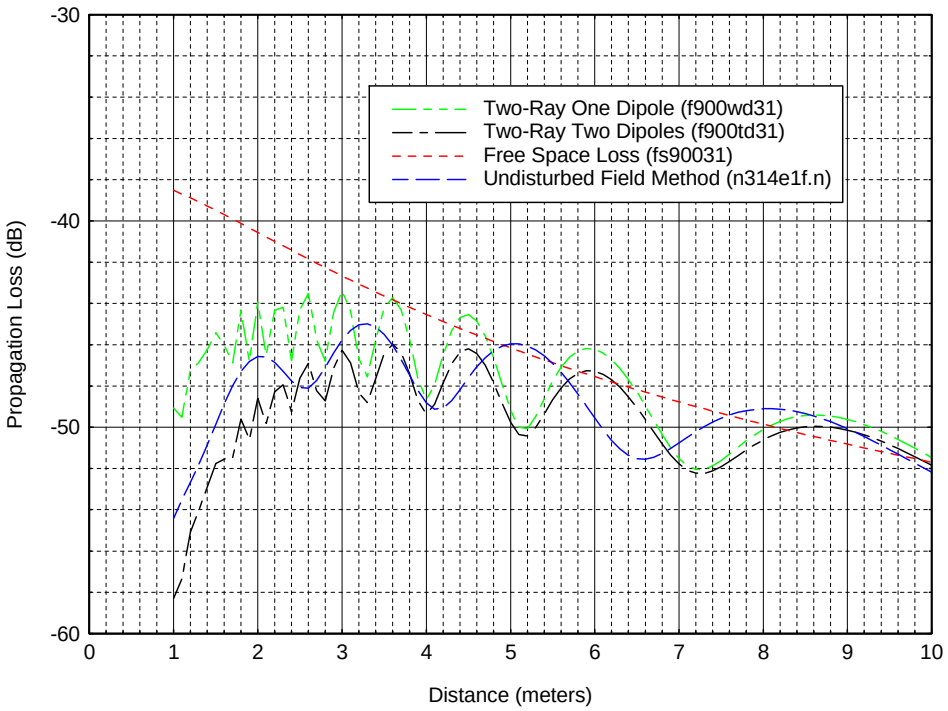


Figure F-15. Comparison of the undisturbed-field method with other methods at 900 MHz for antenna heights $h_1$=3m and $h_2$=1m.

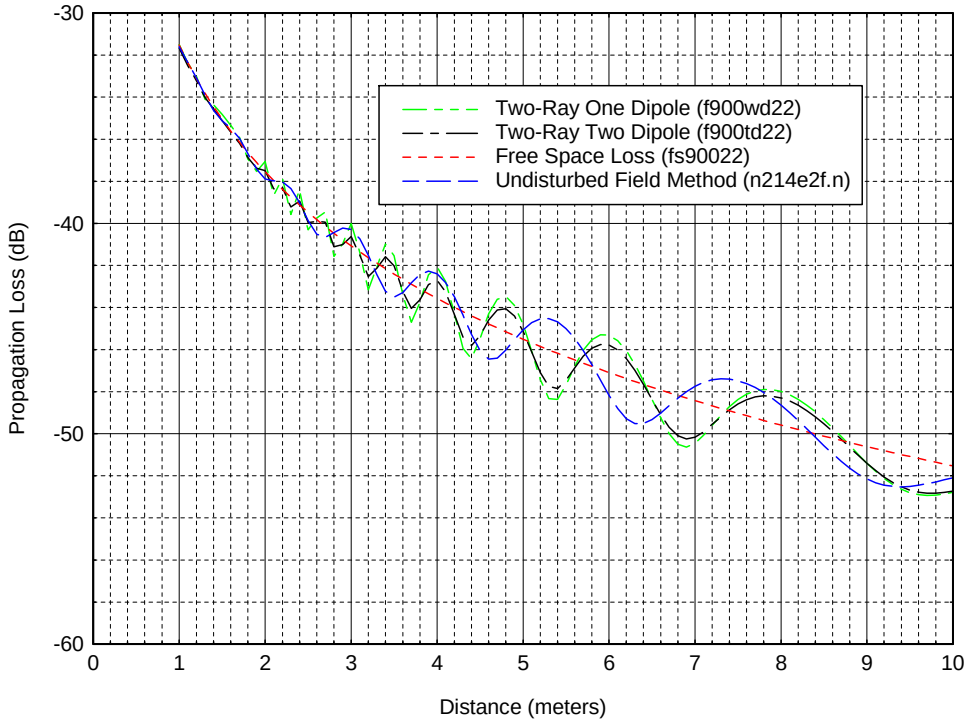


Figure F-16. Comparison of the undisturbed-field method with other methods at 900 MHz for antenna heights $h_1$=2m and $h_2$=2m.

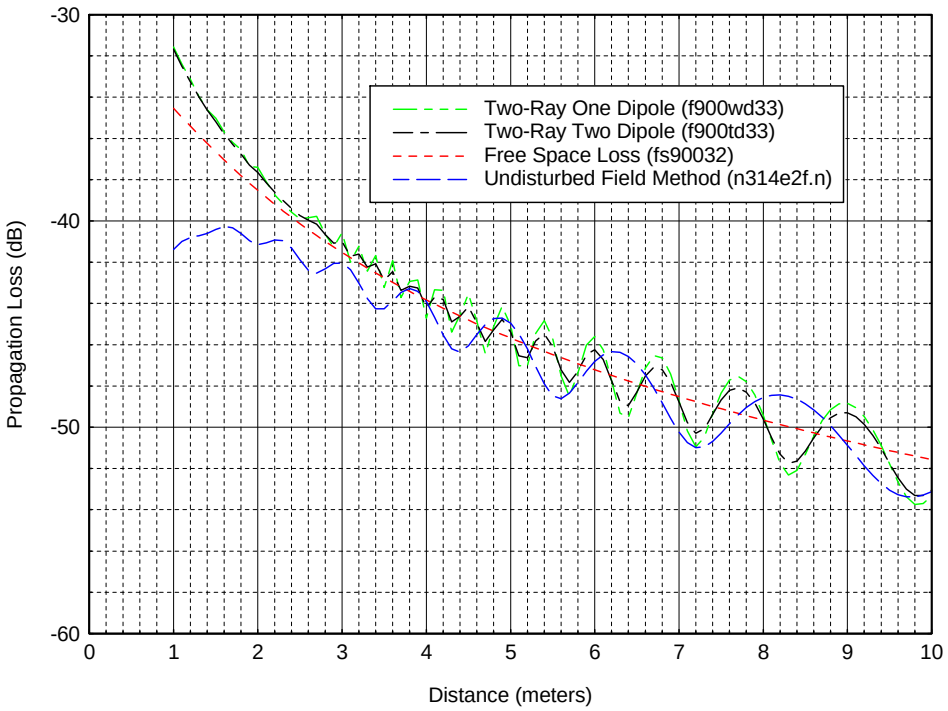


Figure F-17. Comparison of the undisturbed-field method with other methods at 900 MHz for antenna heights $h_1$=3m and $h_2$=2m.

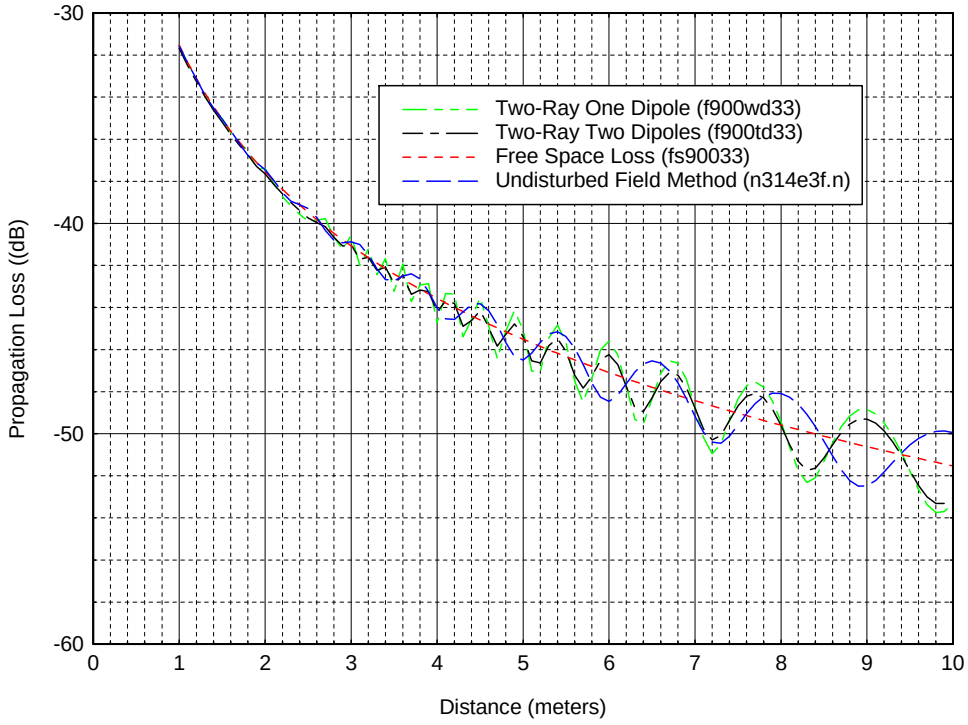


Figure F-18. Comparison of the undisturbed-field method with other methods at 900 MHz for antenna heights $h_1$=3m and $h_2$=3m.

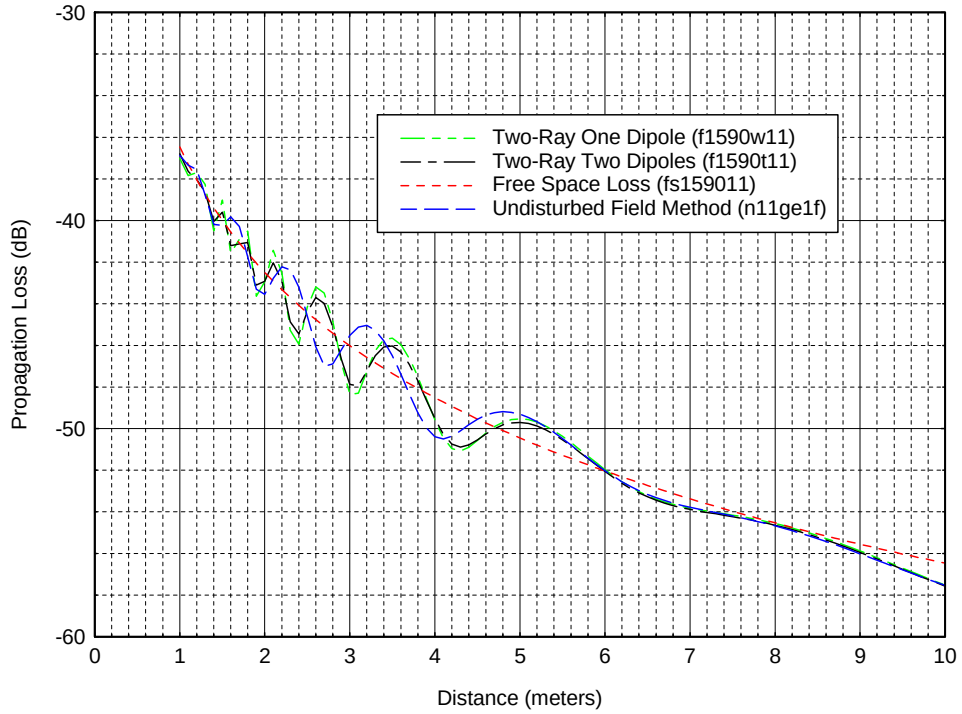


Figure F-19. Comparison of the undisturbed-field method with other methods at 1590 MHz for antenna heights $h_1$=1m and $h_2$=1m.

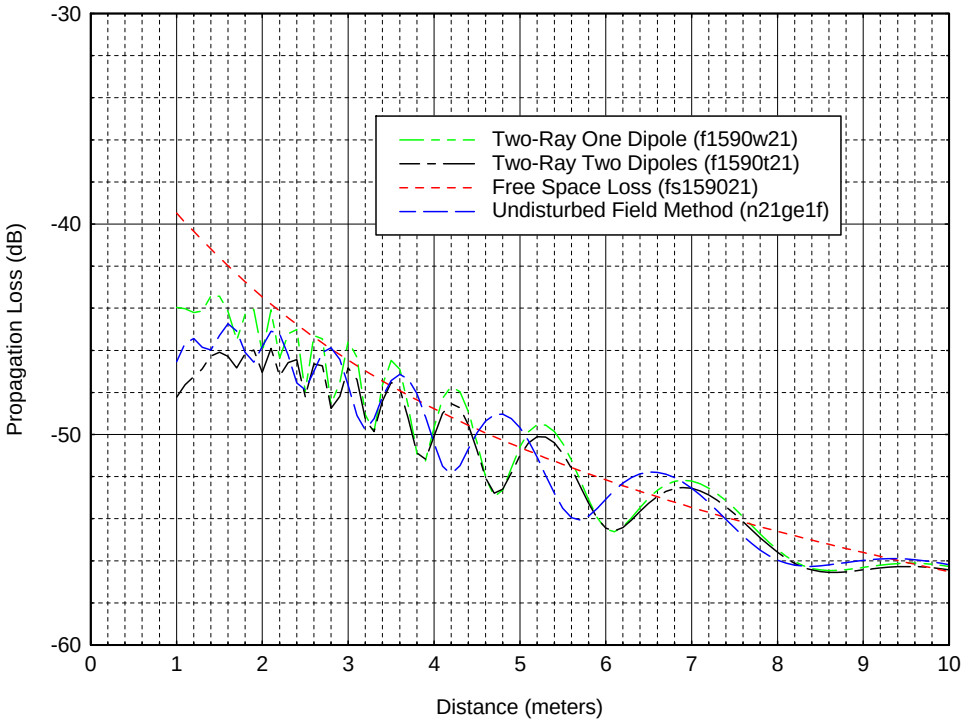


Figure F-20. Comparison of the undisturbed-field method with other methods at 1590 MHz for antenna heights $h_1$=2m and $h_2$=1m.

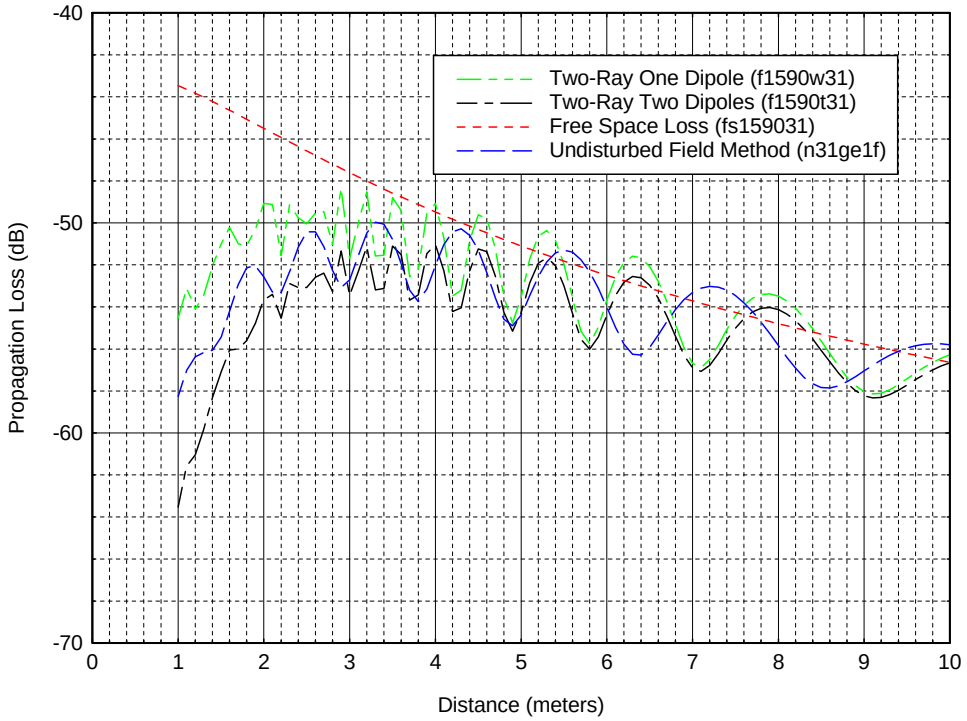


Figure F-21. Comparison of the undisturbed-field method with other methods at 1590 MHz for antenna heights $h_1$=3m and $h_2$=1m.

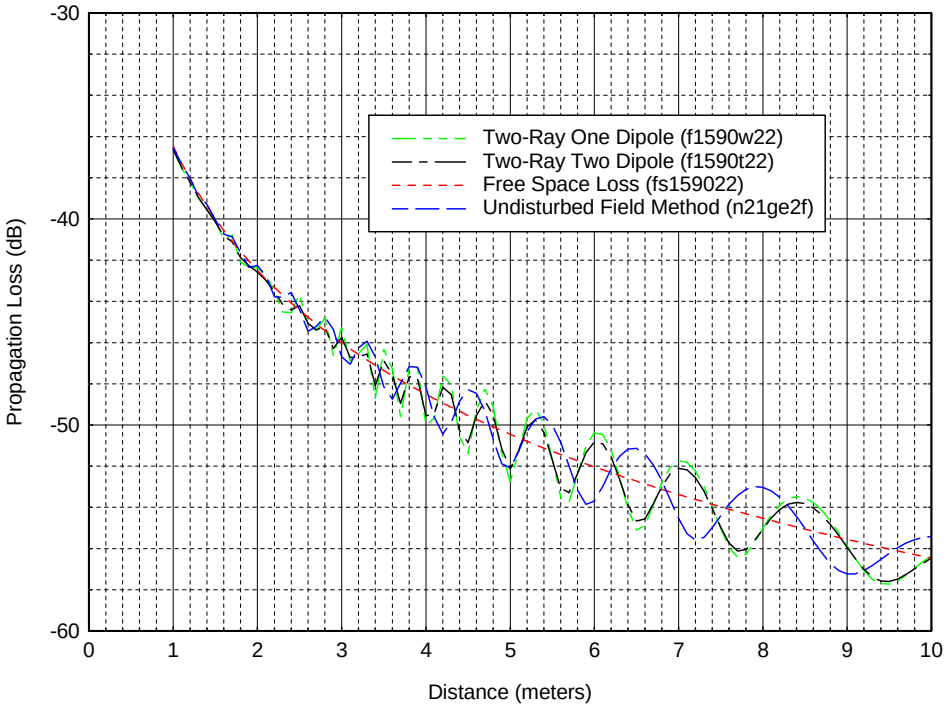


Figure F-22. Comparison of the undisturbed-field method with other methods at 1590 MHz for antenna heights $h_1$=2m and $h_2$=2m.

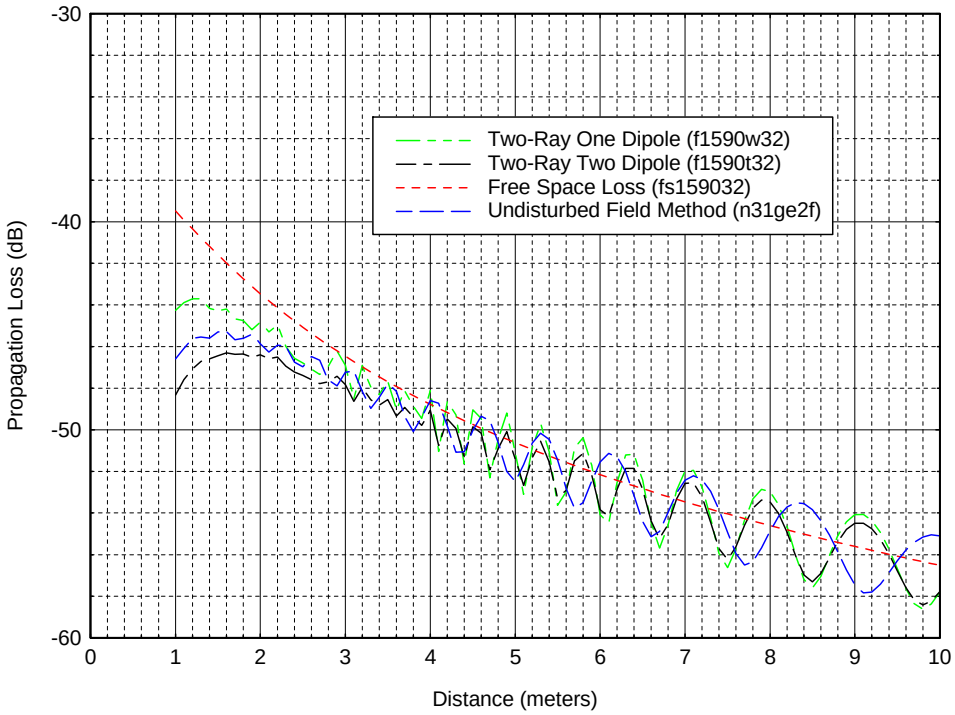


Figure F-23. Comparison of the undisturbed-field method with other methods at 1590 MHz for antenna heights $h_1$=3m and $h_2$=2m.

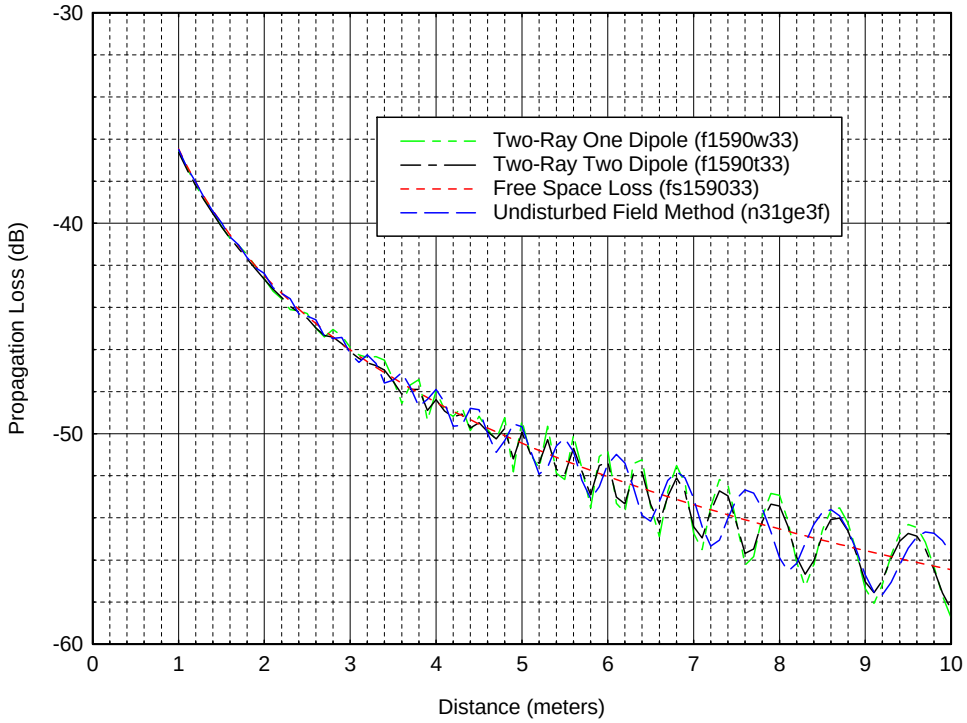


Figure F-24. Comparison of the undisturbed-field method with other methods at 1590 MHz for antenna heights $h_1$=3m and $h_2$=3m.

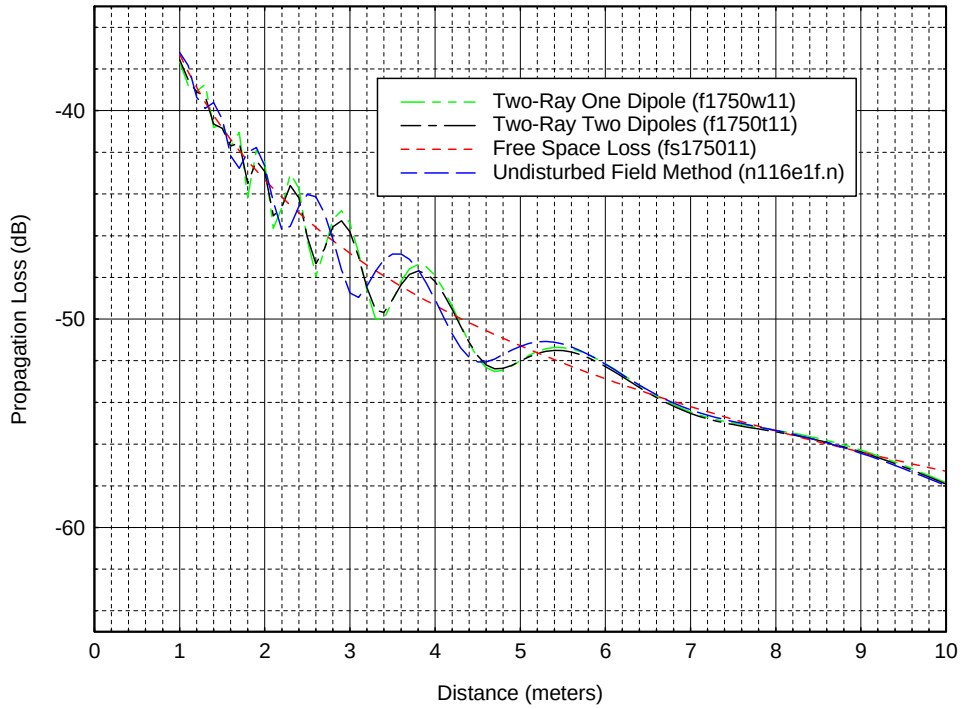


Figure F-25. Comparison of the undisturbed-field method with other methods at 1750 MHz for antenna heights $h_1$=1m and $h_2$=1m.

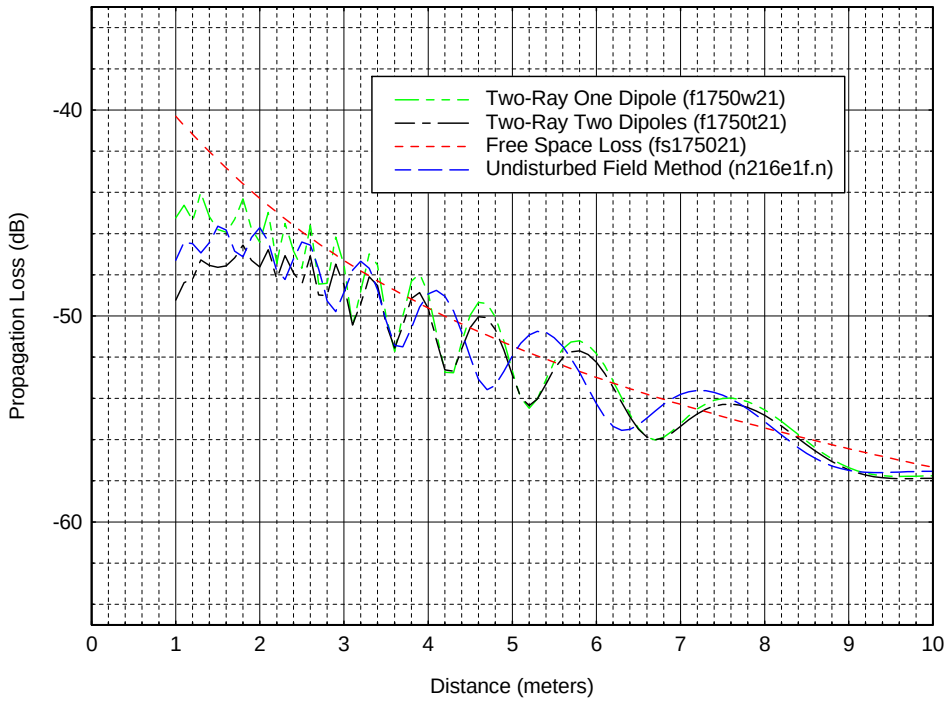


Figure F-26. Comparison of the undisturbed-field method with other methods at 1750 MHz for antenna heights $h_1$=2m and $h_2$=1m.

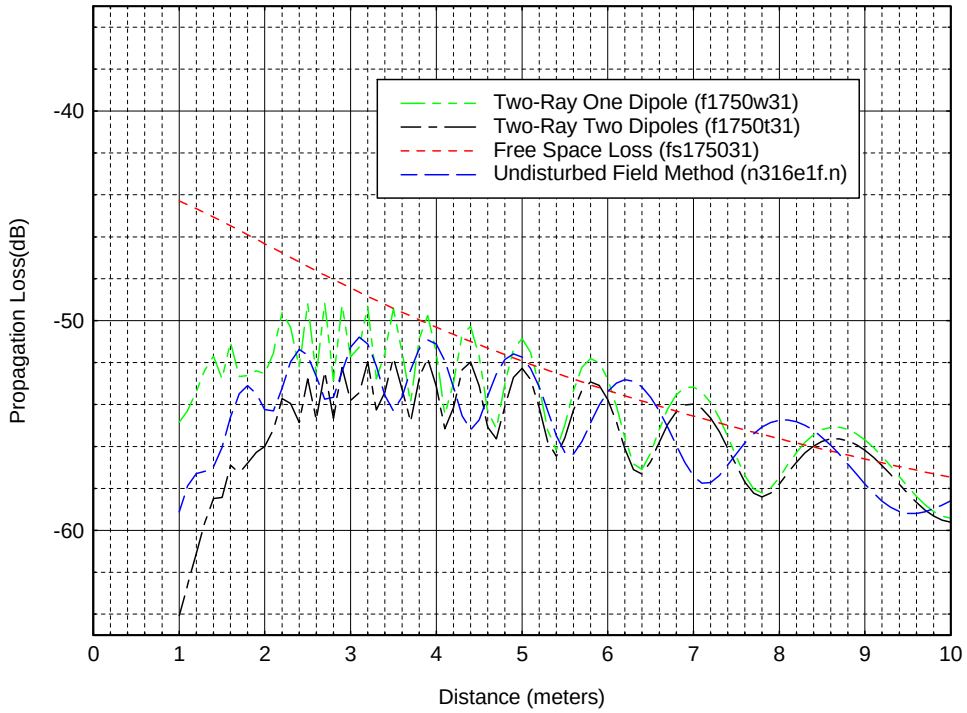


Figure F-27. Comparison of the undisturbed-field method with other methods at 1750 MHz for antenna heights $h_1$=3m and $h_2$=1m.

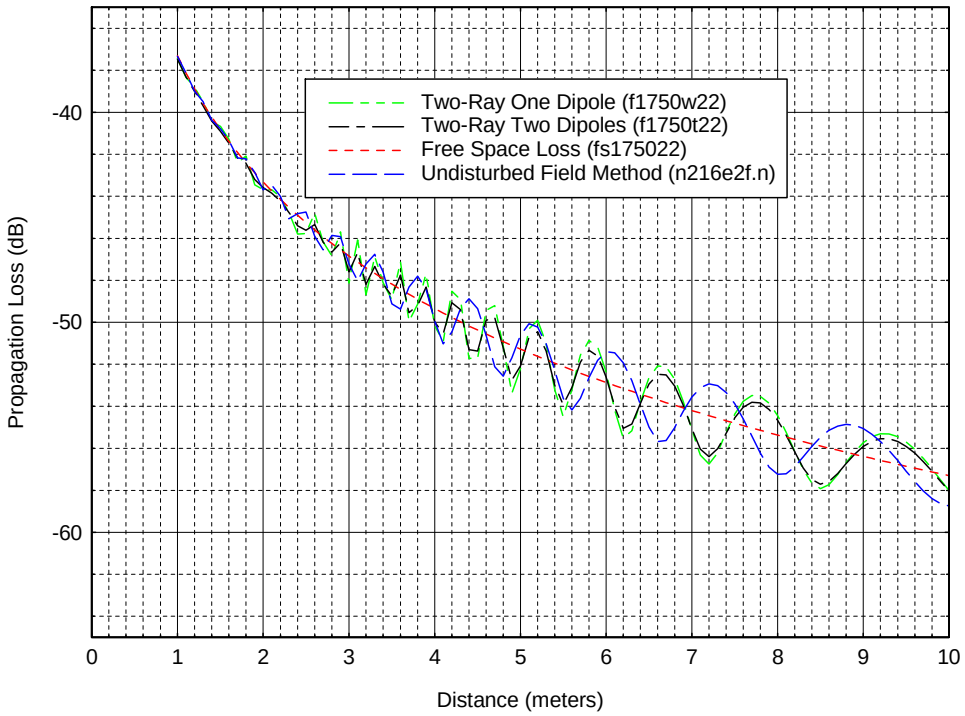


Figure F-28. Comparison of the undisturbed-field method with other methods at 1750 MHz for antenna heights $h_1$=2m and $h_2$=2m.

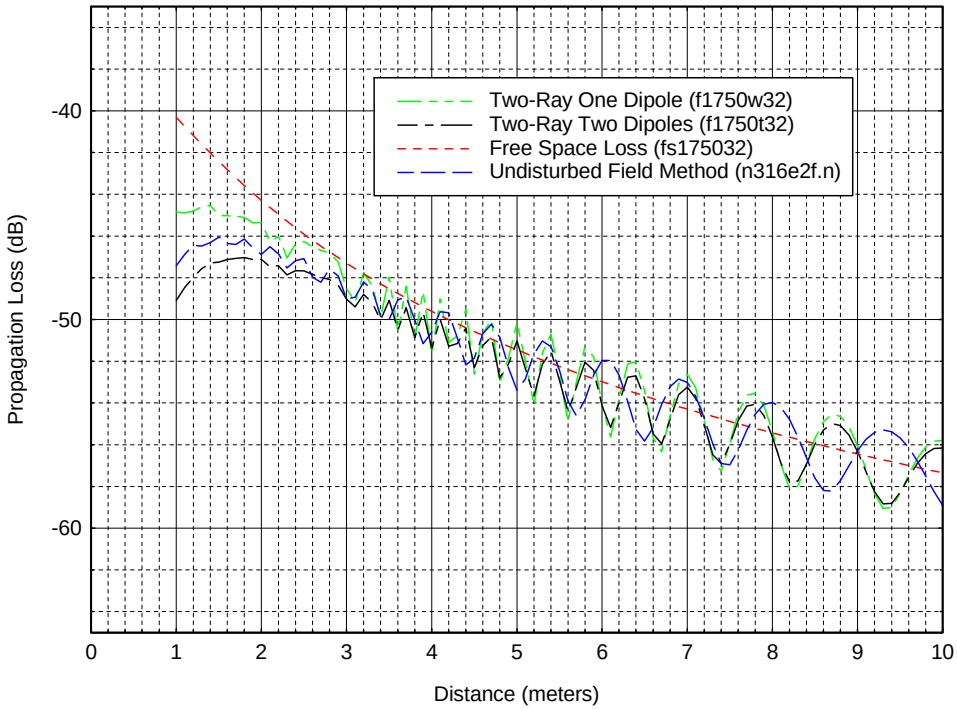


Figure F-29. Comparison of the undisturbed-field method with other methods at 1750 MHz for antenna heights $h_1$=3m and $h_2$=2m.

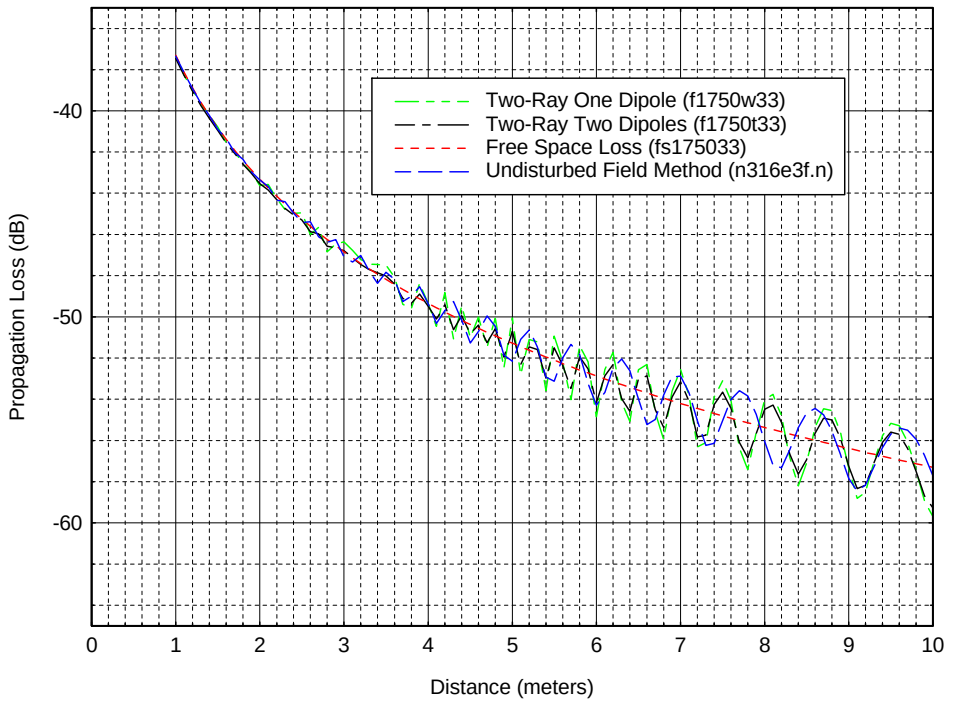


Figure F-30. Comparison of the undisturbed-field method with other methods at 1750 MHz for antenna heights $h_1$=3m and $h_2$=3m.

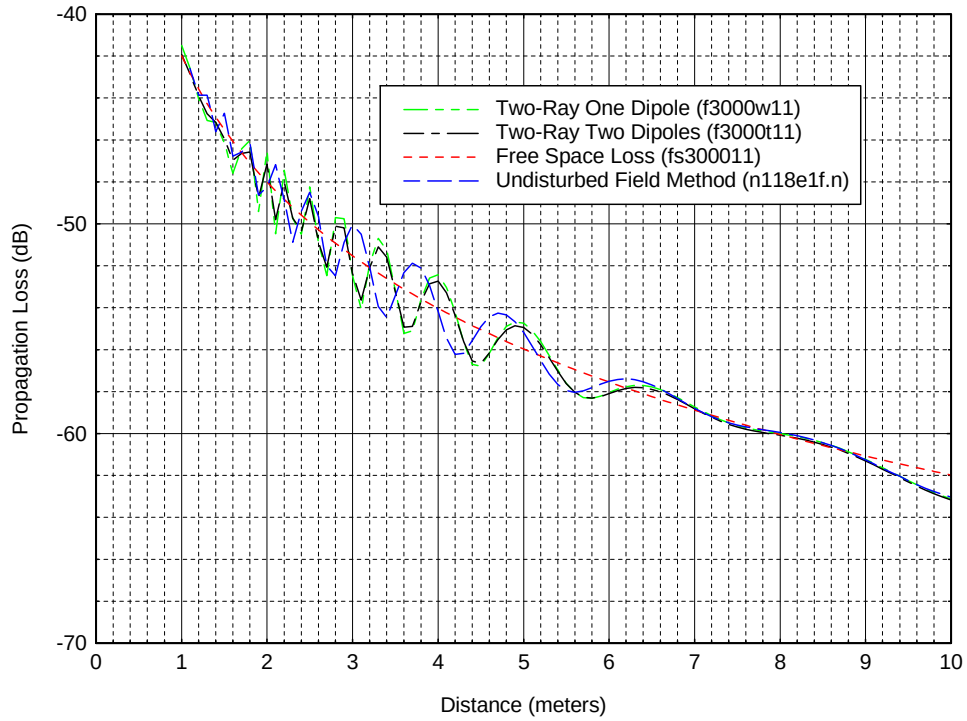


Figure F-31. Comparison of the undisturbed-field method with other methods at 3000 MHz for antenna heights $h_1$=1m and $h_2$=1m.

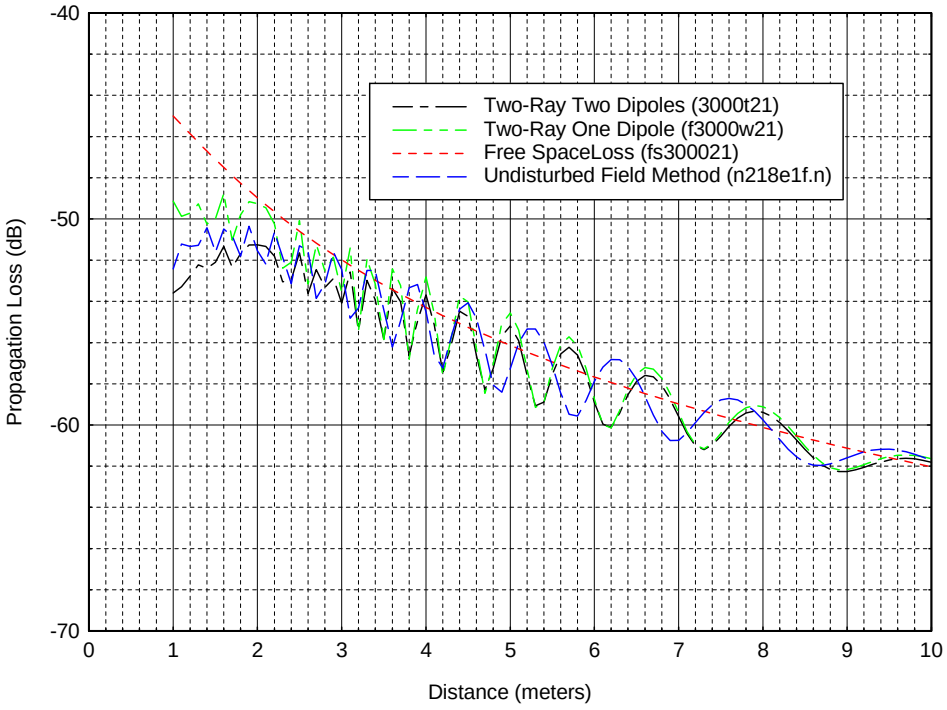


Figure F-32. Comparison of the undisturbed-field method with other methods at 3000 MHz for antenna heights $h_1$=2m and $h_2$=1m.

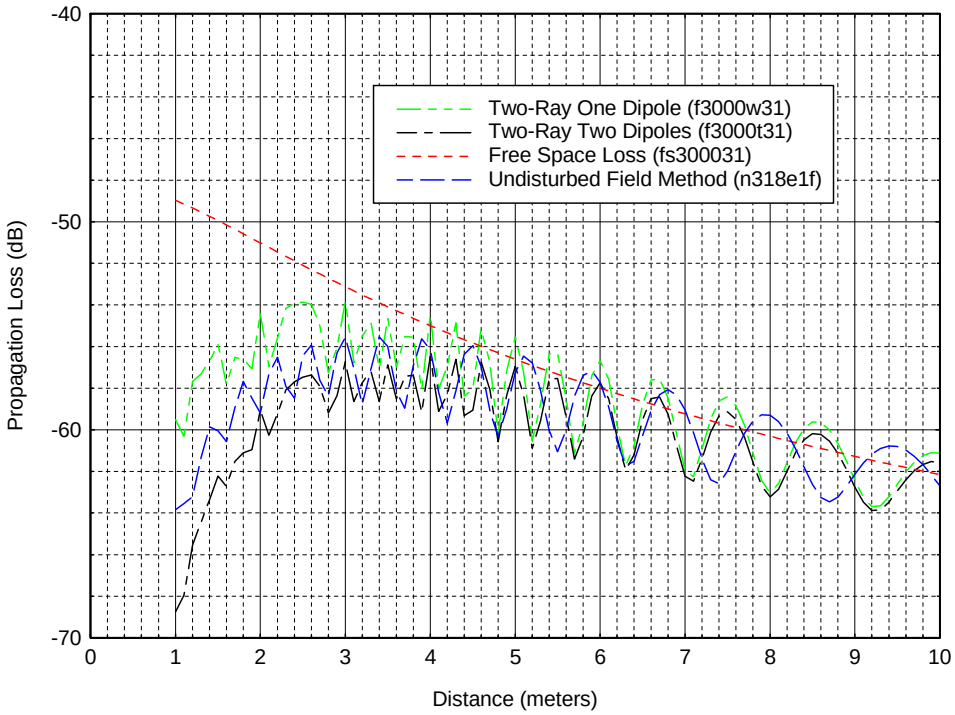


Figure F-33. Comparison of the undisturbed-field method with other methods at 3000 MHz for antenna heights $h_1$=3m and $h_2$=1m.

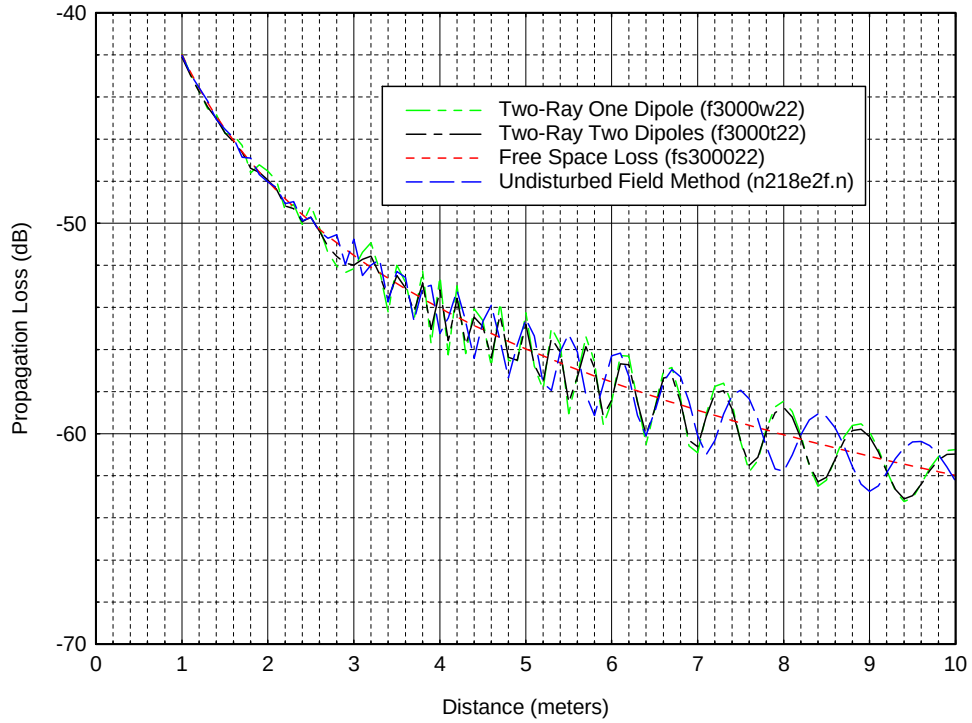


Figure F-34. Comparison of the undisturbed-field method with other methods at 3000 MHz for antenna heights $h_1$=2m and $h_2$=2m.

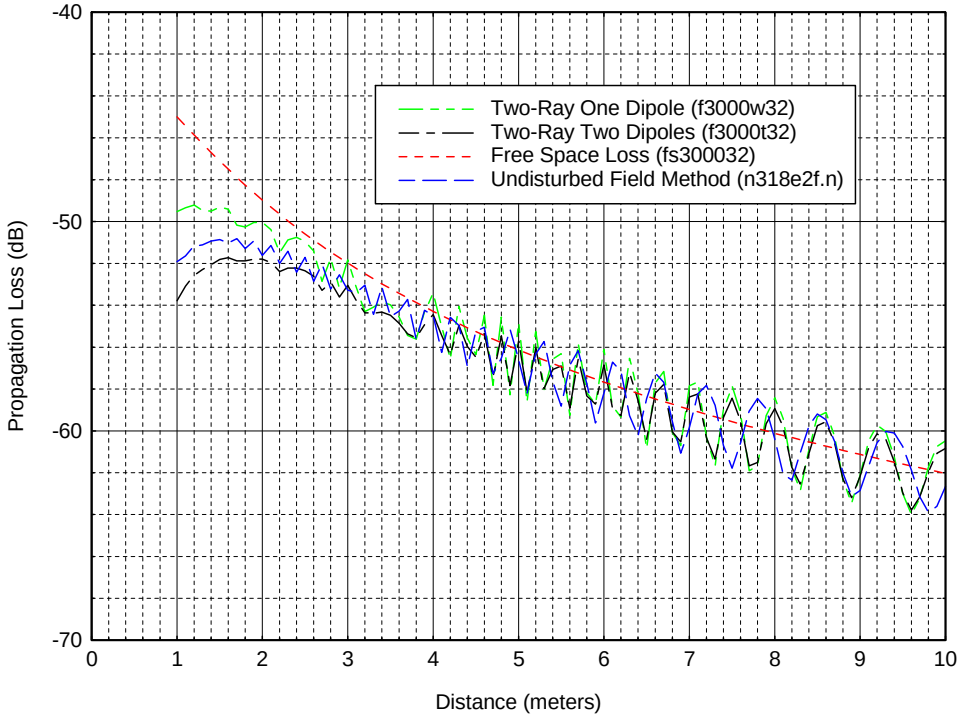


Figure F-35. Comparison of the undisturbed-field method with other methods at 3000 MHz for antenna heights $h_1$=3m and $h_2$=2m.

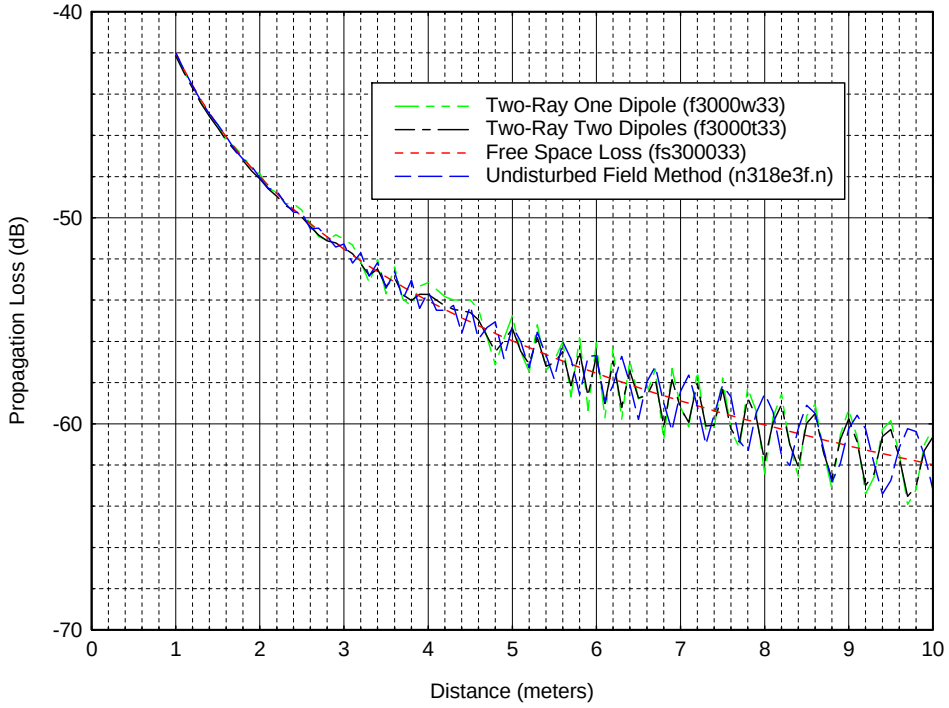


Figure F-36. Comparison of the undisturbed-field method with other methods at 3000 MHz for antenna heights $h_1$=3m and $h_2$=3.

FORM **NTIA-29** U.S. DEPARTMENT OF COMMERCE
(4-80) NAT'L. TELECOMMUNICATIONS AND INFORMATION ADMINISTRATION

# BIBLIOGRAPHIC DATA SHEET

| 1. PUBLICATION NO.<br>TR-07-449 | 2. Government Accession No. | 3. Recipient's Accession No. |
|---|---|---|
| 4. TITLE AND SUBTITLE<br><br>Propagation Loss Prediction Consideratons for Close-In Distances and Low Antenna Height Applications | | 5. Publication Date<br>May 2005<br>6. Performing Organization Code |
| 7. AUTHOR(S)<br>Nicholas DeMinco | | 9. Project/Task/Work Unit No.<br><br>6496000-200 |
| 8. PERFORMING ORGANIZATION NAME AND ADDRESS<br>Institute for Telecommunication Sciences<br>National Telecommunications & Information Administration<br>U.S. Department of Commerce<br>325 Broadway<br>Boulder, CO 80305 | | 10. Contract/Grant No. |
| 11. Sponsoring Organization Name and Address<br>National Telecommunications & Information Administration<br>Herbert C. Hoover Building<br>14th & Constitution Ave., NW<br>Washington, DC 20230 | | 12. Type of Report and Period Covered |

14. SUPPLEMENTARY NOTES

15. ABSTRACT (A 200-word or less factual summary of most significant information. If document includes a significant bibliography or literature survey, mention it here.)

An investigation of different propagation modeling methods to meet the special requirements of a short-range propagation model with low antenna heights was performed, and has resulted in the development of approaches to be taken to accurately model radio-wave propagation loss for these types of scenarios. The basic requirements for the Short-Range Mobile-to-Mobile Propagation Model include: separation distances between the transmitter and receiver from one meter to two kilometers, a frequency range of 150 MHz to 3000 MHz, and antenna heights of one to three meters for both transmitter and receiver sites. It is necessary to develop alternative methods for accurate predictions of propagation loss to provide a propagation model that will simultaneously meet all of these requirements.

16. Key Words (Alphabetical order, separated by semicolons)
antennas; low antenna heights; mobile communications; mutual coupling; propagation modeling; radio-wave propagation

| 17. AVAILABILITY STATEMENT | 18. Security Class. (This report) | 20. Number of pages |
|---|---|---|
| ☐ UNLIMITED. | Unclassified | 142 |
| | 19. Security Class. (This page)<br><br>Unclassified | 21. Price: |

# NTIA FORMAL PUBLICATION SERIES

## NTIA MONOGRAPH (MG)

A scholarly, professionally oriented publication dealing with state-of-the-art research or an authoritative treatment of a broad area. Expected to have long-lasting value.

## NTIA SPECIAL PUBLICATION (SP)

Conference proceedings, bibliographies, selected speeches, course and instructional materials, directories, and major studies mandated by Congress.

## NTIA REPORT (TR)

Important contributions to existing knowledge of less breadth than a monograph, such as results of completed projects and major activities. Subsets of this series include:

### NTIA RESTRICTED REPORT (RR)

Contributions that are limited in distribution because of national security classification or Departmental constraints.

### NTIA CONTRACTOR REPORT (CR)

Information generated under an NTIA contract or grant, written by the contractor, and considered an important contribution to existing knowledge.

### JOINT NTIA/OTHER-AGENCY REPORT (JR)

This report receives both local NTIA and other agency review. Both agencies' logos and report series numbering appear on the cover.

## NTIA SOFTWARE & DATA PRODUCTS (SD)

Software such as programs, test data, and sound/video files. This series can be used to transfer technology to U.S. industry.

## NTIA HANDBOOK (HB)

Information pertaining to technical procedures, reference and data guides, and formal user's manuals that are expected to be pertinent for a long time.

## NTIA TECHNICAL MEMORANDUM (TM)

Technical information typically of less breadth than an NTIA Report. The series includes data, preliminary project results, and information for a specific, limited audience.

For information about NTIA publications, contact the NTIA/ITS Technical Publications Office at 325 Broadway, Boulder, CO, 80305 Tel. (303) 497-3572 or e-mail info@its.bldrdoc.gov.

*This report is for sale by the National Technical Information Service, 5285 Port Royal Road, Springfield, VA 22161,Tel. (800) 553-6847.*